Mild Arylboration of Cyclic Enones via Cooperative Copper/Palladium Catalysis

by Kian Mansour

Thesis Supervisor: Stephen G. Newman

A thesis submitted in partial fulfillment

of the requirements for the Master's degree in Chemistry

Department of Chemistry and Biomolecular Sciences

Faculty of Science

University of Ottawa

Abstract

Cyclic enones are abundant building blocks with diverse applications in the synthesis of complex organic molecules. As such, a variety of methodologies for enone functionalization have been developed, with conjugate addition of cuprates and enolate trapping sequences serving as a dominant strategy. While robust, these approaches are limited by their cryogenic conditions, the need for stoichiometric organometallics, and a narrow range of functional groups which are compatible. Modern advancements in cyclic enone functionalization aim to move away from cuprate chemistry and towards more mild, catalytic conditions which can install a breadth of functionalities. Catalytic methods for cyclic enone mono-functionalization are plentiful, including copper-catalyzed conjugate borylation, the Mizoroki–Heck reaction, Pd-catalyzed α-arylation and rhodium-catalyzed conjugate arylation. Surprisingly, only a handful of direct catalytic difunctionalization reactions have been reported for cyclic enones, while the difunctionalization of other alkenes has been extensively explored in recent years. Alkene arylboration via cooperative Cu/Pd catalysis has emerged as a particularly powerful method for the difunctionalization of a range of alkene classes, but this has never been applied to cyclic enones. Chapter 1 of this thesis provides a literature overview of the existing methods for cyclic enone functionalization, as well as an introduction to alkene arylboration. In Chapter 2, these insights are applied towards the discovery, optimization, and application of a Cu/Pd co-catalyzed method for achieving the anti-selective arylboration of cyclic enones under mild conditions. At the outset of the project, it was hypothesized that trapping of transient copper enolate intermediates with palladium complexes would be challenging, and that in-situ degradation would lead to an undesired conjugate borylation side product. Kinetic reasoning suggested that high Pd:Cu ratio would be required to ensure efficient interception of transient enolate intermediates and enable the desired reaction. High-throughput screening identified an initial hit for the arylboration reaction in 10% yield, which was subsequently optimized to provide room-temperature conditions affording enone arylboration products in moderate yields of around 50%. The optimization results suggest that high Pd:Cu ratio is ideal, as predicted by our mechanistic hypothesis, and that a JohnPhos-Pd catalyst is uniquely privileged for trapping transient enolates. A variety of aryl triflates and hetero-aryl bromides are tolerated in the reaction, along with examples of alkenyl triflates and an allyl carbonate. Diastereoselectivity generally favours the anti products in dr between 5:1 and 8:1, with ortho-

substituted aryl triflates providing exclusively anti products (dr > 20:1); this suggests that the diastereo-determining step must be sensitive to sterics. The scope of cyclic enones is shown to be more limited, with reduced yields observed on smaller-ring substrates, and reactions failing entirely with enones bearing α or β substituents. Facial selectivity based on existing bulky groups on the enone substrate was shown to be possible. The reaction can easily be scaled up to 1 mmol with no significant impact on yield. The products of enone arylboration are readily functionalized at the B(pin), ketone, and ring, providing access to a variety of complex carbocycles with high stereochemical control. Mechanistic experiments suggest that the conjugate borylation side product is not a competent intermediate and must be forming in-situ through degradation with an unknown proton source. No evidence of in-situ product epimerization is seen, suggesting a stereo-determining transmetallation or reductive elimination event. An attempt was made to render the reaction asymmetric through use of a chiral NHC ligand for copper, affording an ee of 10%. Though low, this result suggests that the development of an asymmetric cyclic enone arylboration reaction may be possible with further exploration.

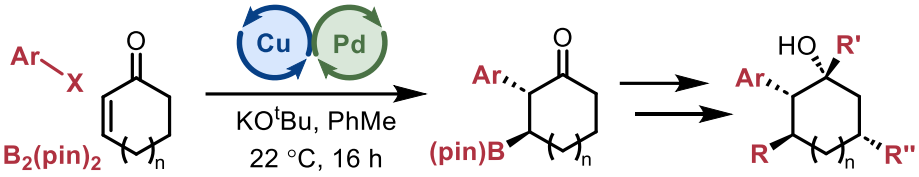

mild arylboration of cyclic enones - diversification at B(pin) and ketone

Acknowledgements

First and foremost, I want to thank my supervisor, Dr. Stephen Newman, for his exceptional guidance and support throughout this degree. Thank you, Steve, for taking me on, for believing in me, and for granting me the freedom to explore my interests in this project. I am forever grateful for your kindness and advice over the past few years!

I want to thank Dr. Louis Barriault for accommodating me in his lab during the difficult and uncertain health circumstances I experienced in 2022 before I started my Master's. Your help during this period was incredibly generous, and my time in your group was full of joy and learning. Thank you so much for everything you have done for me! Furthermore, I want to express my appreciation for both Dr. Louis Barriault and Dr. André Beauchemin for serving on my thesis advisory committee, for their excellent feedback, for their wonderful ideas on experiments to run to strengthen the project, and for making the time to evaluate my thesis. Additionally, I want to thank Dr. Jeffrey Keillor for his exceptional contribution to my growth and development as a chemist and person during my time in his group as an Honour's student, and Dr. Derek Pratt for inspiring me to pursue organic chemistry through his teaching in Organic 3 and Phys-Org. I also want to thank Dr. Paul Mayer for introducing me to research in the first place, and thank you to the Zoom algorithm for pairing me up with my future wife in Paul's communications class!

To all the current and former members of the Newman lab who I shared time with, thank you for making the lab environment a blast to be a part of. Thank you to Lukas Dellermann for being a wonderful hard-working student, a quick learner, a great friend, and for helping me out with the enone scope. Wish you the best in Germany, we miss you here! Thanks to Piyas Saha for helping me out with the aryl bromide scope and for being such an uplifting and entertaining lab mate. This project would not have been possible without you both, Lukas & Piyas! I want to thank Aisha Kassymbek, Eric Isbrandt, and Adam Cook for welcoming me into the group, for their mentorship and help with experiments, and for pushing me to work harder. I am also extremely grateful for Zichuan Chen, for being such a happy presence in the lab, for teaching me how to run the inventory system, and for leaving me plenty of aryl triflates to work with! Thanks to Piers St-Onge, Kostya Prystupa, and Aref Vaezghaemi for all the helpful discussions and endless jokes. I wish you all the best! Thank you to Shajia Khan and Hana Nugraha for being so kind and thoughtful in organizing gifts and surprises for group birthdays and events, and for being so

welcoming. Thank you to Fran Troyano and Isuru Mudiyanselage for hosting the succulent brisket BBQ, and for the amazing advice and post-doc expertise (along with Mario Martinez!) over the years whenever I had doubts or fears about an experiment. I will miss all of you, and all our memories together from the lab will be cherished!

As for other students in the department, I want to thank Soufian Tibouti, Chad Normandin, and Sherif Meshref for all their insightful discussions, their inspirational passion for chemistry, and their motivation which kept me working hard in the lab and in the gym. I will miss you guys! I also want to thank Chris Wicks, who mentored me during my time in the Barriault lab. Thank you, Chris, for teaching me a ton of chemistry, for always having my back, and for being an amazing mentor. I hope Edmonton is treating you well!

I want to thank the entire uOttawa Powerlifting club, and everyone who has been a part of uOPower throughout the past seven years, for giving me the opportunity to be your coach, for always being there for me, and for providing an energetic team environment which helped tremendously in blowing off some steam at the end of every week or whenever experiments were not working.

Words cannot begin to describe how grateful I am for my parents and their endless love and support over the past few years. Thank you for everything.

Lastly, I want to thank my fiancé, Stasa Skorupan. Thank you for all your kindness, for pushing me to grow, and for changing my life.

Table of Contents

List of Tables

List of Figures

List of Schemes

Statement of Contribution

The project described in Chapter 2 was done in collaboration with Piyas Saha, a PhD candidate in the Newman lab, and Lukas Dellermann, a visiting Mitacs student from Würzburg, Germany. All experiments presented herein were designed and performed by me unless otherwise specified. Piyas performed the synthesis, purification, and characterization of arylboration products **3r** and **3t-3w**, and screened most of the unsuccessful aryl and heteroaryl bromide coupling partners. Lukas performed the synthesis, purification, and characterization of arylboration products **3ac** and **3ad**, and screened most of the unsuccessful enones and unsaturated esters.

Abbreviations

µL	microlitre
µm	micrometre
Å	angstrom
Ac	acetyl
acac	acetonyl acetonate
Ar	general aromatic group
BINAP	2,2'-bis(diphenylphosphino)-1,1'-binaphthyl
Boc	*tert*-butyloxycarbonyl
BQ	1,4-benzoquinone
brsm	yield based on recovered starting material
calcd	calculated
cat	general catalyst or (catecholato)
cm	centimetre
COD	1,5-cyclooctadiene
COSY	2-dimentional homonuclear (^{1}H) correlation spectroscopy
Cp	cyclopentadienyl
Cy	cyclohexyl
DABCO	1,4-diazabicyclo[2.2.2]octane
dba	dibenzylideneacetone
DCM	dichloromethane
DFT	density functional theory
DIPEA	N,N-diisopropylethylamine
DMA	N,N-dimethylacetamide
DME	dimethyl ether
DMF	N,N-dimethylformamide
dppbz	1,2-bis(diphenylphosphino)benzene
dppf	1,1'-bis(diphenylphosphino)ferrocene
dr	diastereomeric ratio
dtbpy	4,4′-di-*tert*-butyl-2,2′-dipyridyl

E^+	general electrophile
ee	enantiomeric excess
EI	electron impact ionization
equiv	equivalents
er	enantiomeric ratio
Et	ethyl
G3	Grubb's generation 3 Pd pre-catalyst
GC	gas chromatography
GC-FID	gas chromatography, flame ionization detector
GC-MS	gas chromatography, mass spectrometry
h	hour(s)
HMPA	hexamethylphosphoramide
HTE	high throughput experimentation
Hz	Hertz
^{i}Bu	iso-butyl
^{i}Pr	iso-propyl
J	coupling constant
LDA	lithium di-isopropyl amide
L-selectride	lithium tri-sec-butylborohydride
M	molar, or general metal
m/z	mass-to-charge ratio
Me	methyl
mg	milligram(s)
MHz	megahertz
min	minute(s)
mL	millilitre(s)
mm	millimetre(s)
mmol	millimole(s)
mol%	amount of reagent expressed as percentage of moles relative to limiting reactant
nBu	n-butyl
NHC	N-heterocyclic carbene

nm	nanometre
NMR	nuclear magnetic resonance spectroscopy
nOe	nuclear Overhause effect
NOESY	nuclear Overhauser effect spectroscopy
Nuc^-	general nucleophile
NR_3	general tertiary amine
OTf	Triflate
Ph	phenyl
pin	pinacolato
ppm	parts per million
PR_3	general tertiary phosphine
R	general organic group
Rf	retention factor
RPM	rotations per minute
rr	regioisomer ratio
Selectfluor	1-chloromethyl-4-fluoro-1,4-diazoniabicyclo[2.2.2]octane bis(tetrafluoroborate)
SFC	supercritical fluid chromatography
SPS	solvent purification system
^{t}Amyl	*tert*-amyl
TBS	*tert*-butyldimethylsilyl
^{t}Bu	*tert*-butyl
TFA	trifluoroacetic acid
TFT	α,α,α-trifluorotoluene
THF	tetrahydrofuran
TLC	thin-layer chromatography
TMP	2,2,6,6-Tetramethylpiperidine
TMS	trimethylsilyl
UV	ultraviolet
X	general halide, pseudo-halide, or electronegative atom

Chapter 1: Cyclic enone functionalization and alkene carboboration

1.1: Cyclic enone functionalization

1.1.1: Cyclic enones as starting materials in chemical synthesis

Cyclic enones are abundant chemical building blocks used often as starting materials for the synthesis of pharmaceuticals and natural products. For example, 2-cyclohexene-1-one is commercially available for less than a dollar per gram ($72 for 100 g from Enamine),[1] and has been used in large quantities for the syntheses of bioactive molecules such as (+)-Phomactin A,[2] a platelet-activating-factor receptor antagonist, and Taxol,[3] a billion-dollar cancer drug (Scheme 1). To access these and other complex molecules from simple cyclic enone starting materials, chemists have devoted extensive effort towards the development of synthetic methods for installing new carbon–carbon bonds and various other functional groups onto the enone framework. While some methods are known for functionalization at γ or α' positions through deprotonation with strong bases,[4–6] and reactions at the ketone group itself are commonplace, the polarized alkene moiety is the most typical site of reactivity for cyclic enones. The highly electrophilic β-carbon and pro-nucleophilic α-carbon (through the corresponding enolate)[7] are poised for reactions with a variety of nucleophilic and electrophilic partners, respectively. A range of both classical and modern reactions for functionalizing cyclic enones through taking advantage of electronic properties of the polarized alkene are discussed in the following sections.

Scheme 1. Cyclohexenone as a representative cyclic enone for complex molecule syntheses.

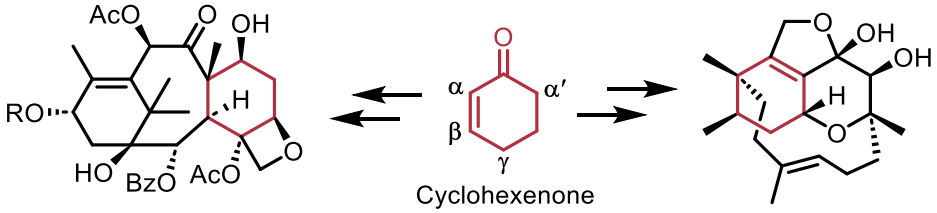

Taxol
Baran, 2012

(+)-Phomactin A
Sarpong, 2020

1.1.2: Classical methods for cyclic enone mono-functionalization

Cuprate conjugate additions and the Morita–Baylis–Hillman reaction are two classical transformations for installing one new substituent, achieving a mono-functionalization, on cyclic enone frameworks. These reactions have become staples in organic chemistry, and are introduced briefly in this section.

1.1.2.1: Organocuprate conjugate additions

Discovered by Gilman in 1952,[8] organocuprates are soft nucleophiles ideal for conjugate addition into unsaturated systems.[9] Organocuprates are often synthesized through reaction between copper(I) salts and organolithiums, which are themselves typically made by lithium-halogen exchange from organohalides.[10] Conjugate addition to a cyclic enone at the β position results in rapid insertion, forging a new carbon–carbon bond, and leaving a copper enolate which may be protonated to restore the ketone upon workup (Scheme 2). A diverse array of organocuprates can be prepared, including sp^3,[11] sp^2,[12] and sp-hybridized carbons.[13] Though cuprate conjugate addition chemistry is robust, several limitations exist. The reaction must generally be performed at cryogenic temperatures and with stoichiometric copper, hampering scalability. Proceeding through harsh organolithiums may pose challenges for functional group compatibility on the nucleophile. Furthermore, some aliphatic cuprates may be susceptible to degradation via β-hydride elimination.[14] Nevertheless, cuprate chemistry remains one of the most predominant strategies for cyclic enone functionalization.[10,11,13]

Scheme 2. General synthesis of organocuprate and use in conjugate addition.

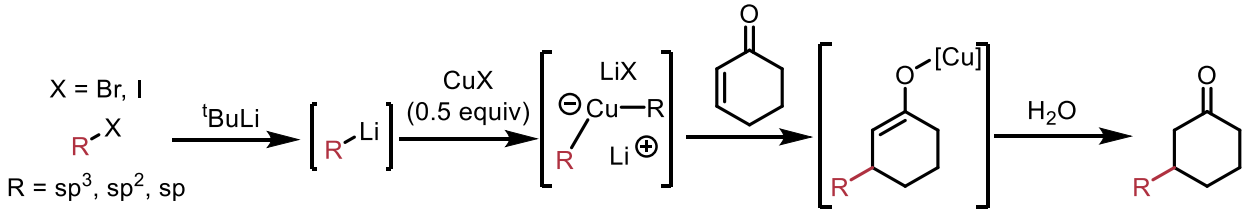

1.1.2.2: The Morita–Baylis–Hillman reaction

The Morita–Baylis–Hillman reaction[15,16] achieves α-functionalization of a cyclic enone through utilizing the intrinsic pro-nucleophilicity of this position to capture a reactive aldehyde. A nucleophile, usually either a tertiary amine or phosphine, serves as the catalyst. Conjugate addition of the catalyst forms a nucleophilic enolate intermediate which is trapped at the α position by an

aldehyde in an aldol-like addition. Elimination of the catalyst unveils the desired product (Scheme 3).[17] The novelty introduced by this transformation is the ability to directly form a carbon–carbon bond at the α position of an enone system, while preserving the unsaturation. Examples of Morita–Baylis–Hillman reactions and their applications in the syntheses of complex molecules have been reviewed extensively.[18]

Scheme 3. General mechanism for phosphine (or amine) catalyzed Morita–Baylis–Hillman reaction between aldehyde and cyclic enone.

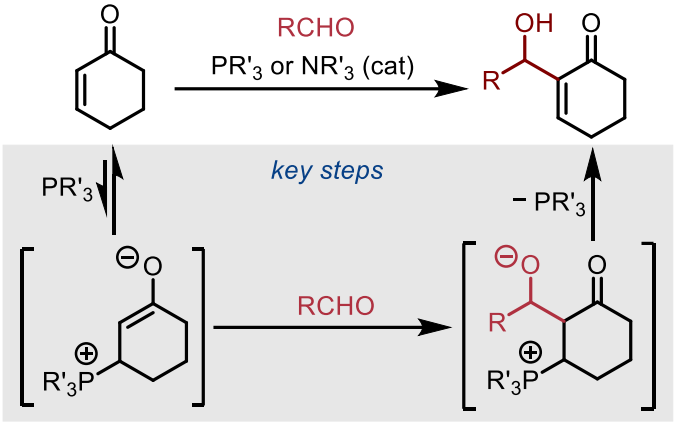

1.1.3: Modern, catalytic methods for cyclic enone mono-functionalization

Beyond the classical transformations of the cuprate conjugate addition and the Morita–Baylis–Hillman reaction, modern research efforts have aimed to develop more mild, catalytic reactions for directly installing a broader range of functional groups at either the α or β position of cyclic enones. Four of these such modern, catalytic strategies for cyclic enone mono-functionalization are highlighted in this section, with an emphasis on common transition metal catalysts and broad mechanistic patterns.

1.1.3.1: The Mizoroki–Heck reaction

The Mizoroki–Heck reaction is a common cross-coupling of an organo(pseudo)halide and an alkene. Its catalytic step sequence includes oxidative addition of a palladium catalyst into the organohalide, insertion into the alkene (also called carbopalladation), β-hydride elimination to form product, and reductive elimination to restore the catalyst. While conjugated alkenes such as acrylates and acrylonitrile are common substrates for the Mizoroki–Heck reaction,[19] the reliable involvement of cyclic enones in this chemistry remained an unsolved challenge. Recent contributions from our group led to the development of a robust Mizoroki–Heck reaction between

cyclic enones and heteroaryl-bromides through judicious choice of BippyPhos-Pd catalyst (Scheme 4).[20] Though initial assumptions suggested that Mizoroki–Heck reactions on cyclic enones are difficult due to the need for an anti β-hydride elimination,[21] mechanistic studies demonstrate rapid β-hydride elimination (likely through prior epimerization via C-bound and O-bound metal enolates)[22] and a rate-determining migratory insertion.

Scheme 4. β-arylation of cyclic enones through Mizoroki–Heck reaction.

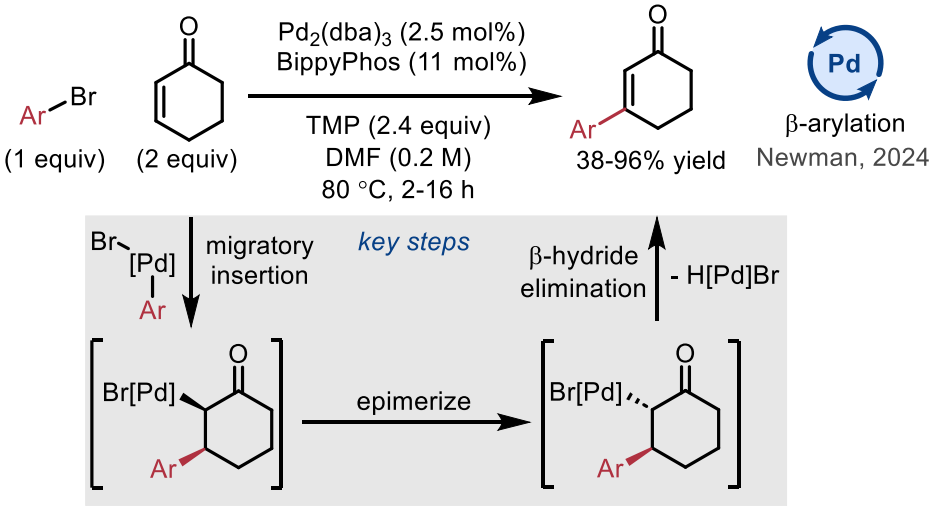

1.1.3.2: Conjugate arylation

Similarly to the Mizoroki–Heck reaction, catalytic conjugate arylation forms a new carbon–carbon bond to an aromatic group in the β position of cyclic enones. Here, the key aryl-metal species is typically accessed through transmetallation with an aryl boronic acid. Following carbon–carbon bond formation in the initial migratory insertion, rather than reforming the alkene via β-hydride elimination, hydrolysis provides the conjugate addition product. Contributions in this field over the past 30 years have been reviewed.[23] Rhodium catalysis has historically been most prevalent in this area, allowing for catalytic enantioselective conjugate addition of aryl boronic acids into cyclic enones (Scheme 5).[24] More recently, other metals such as palladium have been employed for this purpose.[25]

Scheme 5. Conjugate arylation of cyclic enone via rhodium catalysis.

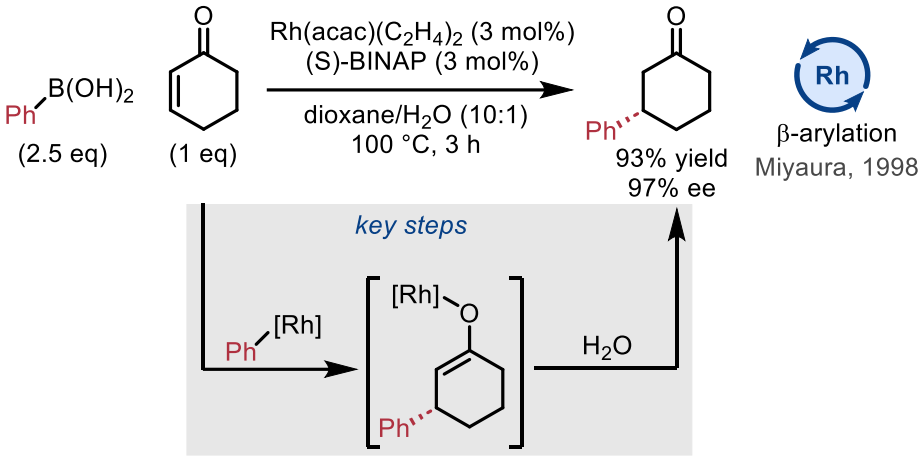

1.1.3.3: Conjugate borylation

Though it is not a carbon–carbon bond-forming process, conjugate borylation of cyclic enones has recently become a mainstay in synthesis due to its ease of operation and the versatility of organoboron compounds.[26] Initially reported separately by Hosomi[27] and Miyaura[28] in 2000, this copper-catalyzed process has been subject to extensive study over the past 25 years. Simply mixing a copper(I) salt, a phosphine ligand, a base co-catalyst, $B_2(pin)_2$, and solvent at room temperature provides β-borylation in high yield (Scheme 6).[29] Mechanistically, the base catalyst activates $B_2(pin)_2$, polarizing the boron-boron bond, rendering it more nucleophilic towards copper, and facilitating the formation of a boryl copper intermediate. Insertion of the boryl copper into the enone unsaturation forms the desired bond, and the resulting copper enolate can be converted to product via in situ protonolysis with methanol. This in situ protonolysis also turns over the free copper catalyst.

Scheme 6. Conjugate borylation of cyclic enones by copper-phosphine catalysis.

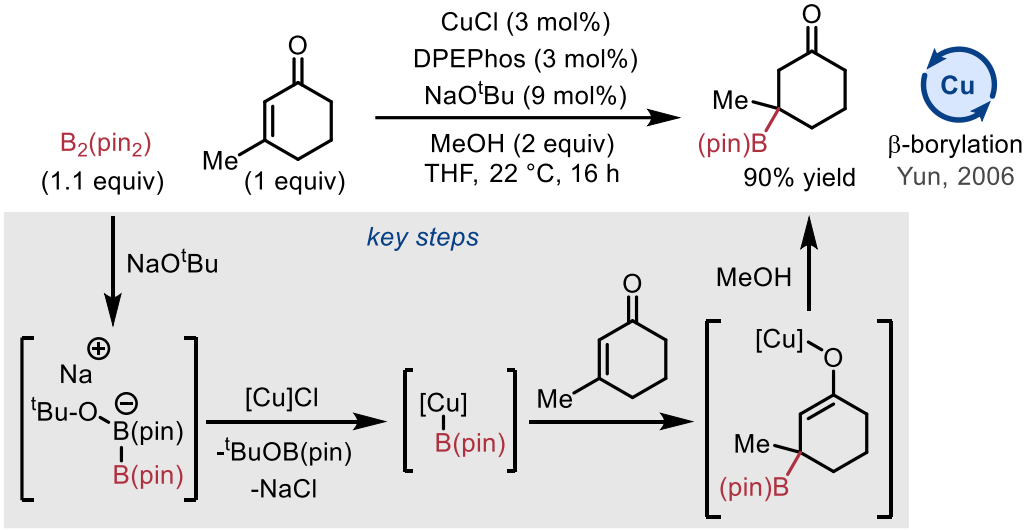

Though copper-phosphine catalysts are most common in conjugate borylation chemistry, some copper-NHC systems are known,[30,31] and the Hoveyda group has replaced copper entirely with NHC salts.[32] In their studies, the Hoveyda group reported that both the NHC-catalyzed and copper-NHC-catalyzed reactions do not require MeOH for turnover, as the strongly electron-donating NHC ligand increases the reactivity of the intermediate enolate, allowing for a direct σ-methesis reaction between the enolate and $B_2(pin)_2$. This provides boron enolates that are quenched upon workup to give rise to the desired conjugate borylation products (Scheme 7).[32] More recently, enantioselective variants of cyclic enone conjugate borylation have been reported using chiral ligands, [33,34] and di-enone desymmetrization[35] reactions have been developed and applied in the total synthesis of Vitamin D analogs.[36]

Scheme 7. Conjugate borylation of cyclic enones by copper-NHC catalysis.

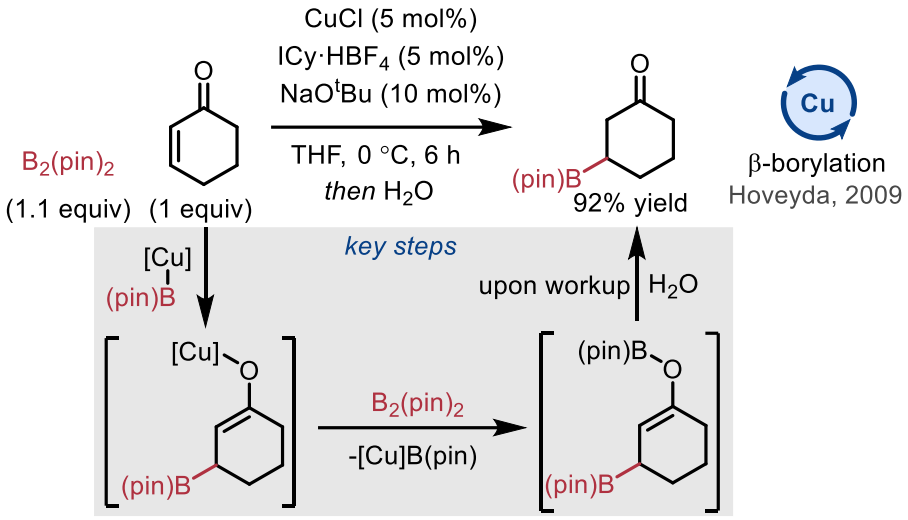

1.1.3.4: α-Arylation

Despite extensive progress in modern catalytic methods for the β-functionalization of cyclic enones, direct methods for carbon–carbon bond-forming α-functionalization remain scarce, other than the classical Morita–Baylis–Hillman reaction which is limited to aldehyde partners. Our group has explored this area and recently reported a direct α-arylation of cyclic enones with aryl triflates through a Pd-catalyzed pathway inspired by the Morita–Baylis–Hillman reaction (Scheme 8).[37] High-throughput screening unveiled a palladium catalyst system compatible with DABCO, a common nucleophilic catalyst in Morita–Baylis–Hillman transformations. Mechanistically, the reaction commences with attack of DABCO to form the key enolate intermediate that is nucleophilic at the α carbon. This enolate can then be effectively trapped by an oxidative addition complex (ArPdX), which then yields the desired carbon–carbon bond after reductive elimination. Finally, the product forms through elimination of the nucleophilic catalyst. This creative approach opens the door to direct catalytic α-functionalization reactions of cyclic enones, and the transient enolate concept may prove applicable to future methodologies.

Scheme 8. Direct catalytic α-arylation of cyclic enones via Morita–Baylis–Hillman-inspired Pd-catalysis.

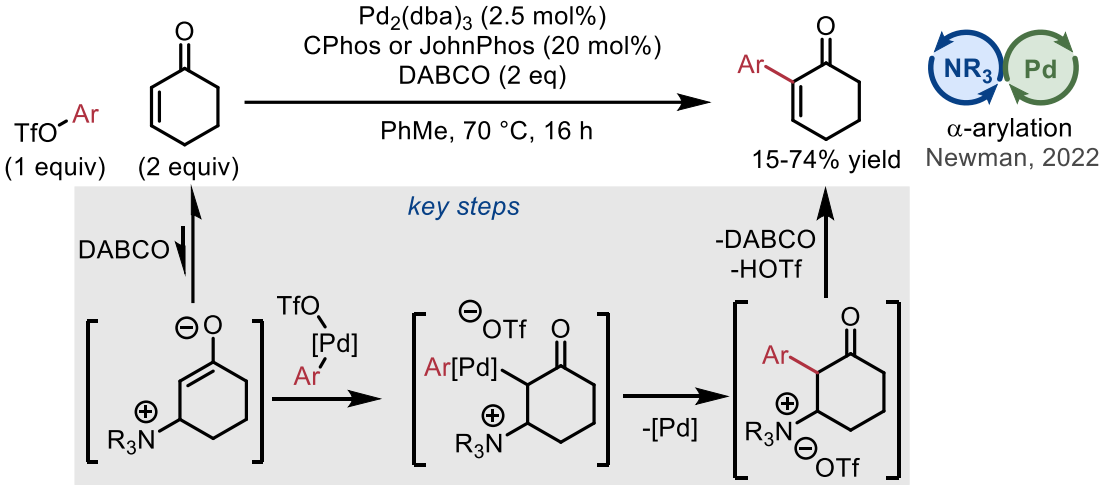

1.1.4: Stoichiometric difunctionalization of cyclic enones via cuprate trapping

Instead of simply installing one new functional group onto the cyclic enone, it is possible to form two new bonds across the alkene through direct difunctionalization, enabling efficient access to complex molecules. Conjugate addition of a nucleophile to react with the electrophilic β-carbon, followed by trapping of the resultant enolate with an electrophilic reagent, easily achieves this goal (Scheme 9).

Scheme 9. General mechanism for cyclic enone difunctionalization via conjugate addition and enolate trapping.

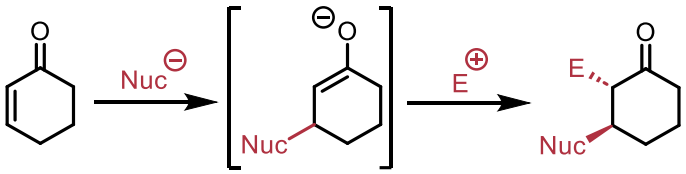

The classic, time-tested method for difunctionalization of cyclic enones is via cuprate conjugate addition and electrophilic trapping. This field bloomed in the late 20th century (1970s and 1980s) due to applications in the synthesis of the prostaglandins and other highly-functionalized carbocyclic natural products, and has been reviewed.[38] An example of this strategy is shown in Scheme 10.[39] An alkenyl iodide is converted to an organolithium through lithium-halogen exchange, then copper is added to afford the desired organocuprate. Facile conjugate addition into the cyclic enone follows, but the subsequent enolate trapping with an allylic iodide proved challenging. The authors noted a lack of reactivity with the electrophile, instead reporting

side reactions such as alkene shifts. Successful difunctionalization was only achieved through the addition of stoichiometric triphenyltin chloride as an additive.

Scheme 10. Classical cuprate conjugate addition and enolate trapping with SN2-reactive electrophile.

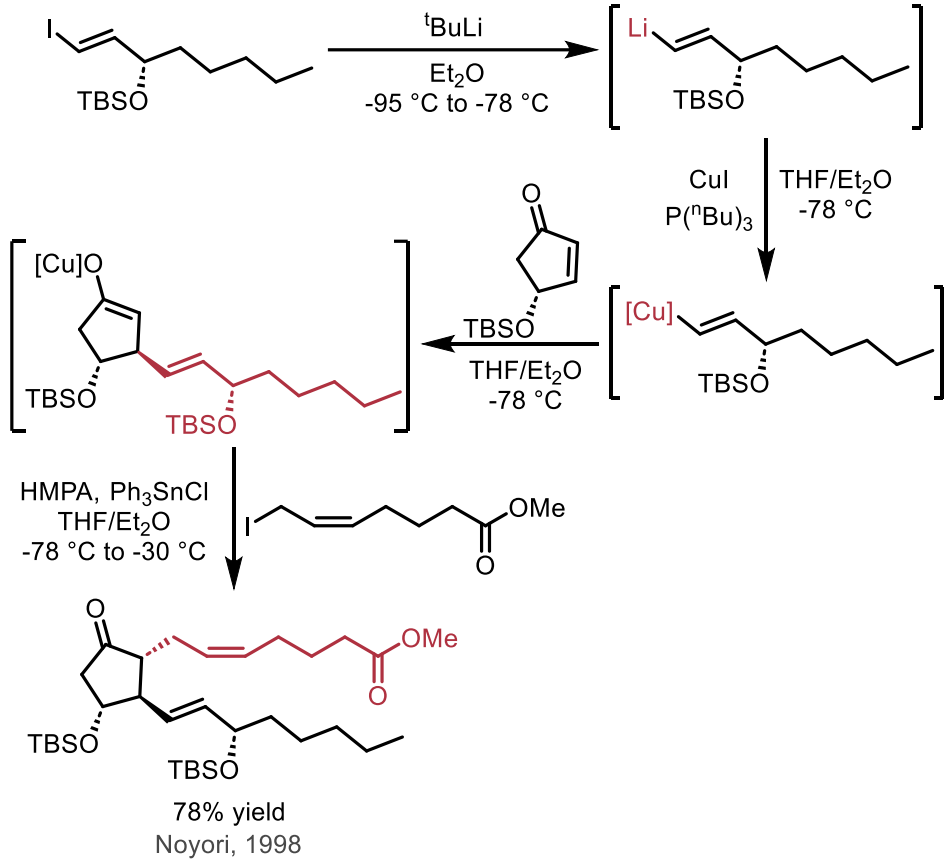

The main strength of the cuprate conjugate addition and enolate trapping approaches is the breadth of compatible nucleophiles and electrophiles. Virtually any carbon-based nucleophile can be used, and the range of electrophiles includes alkyl halides, acyl halides,[40] aldehydes,[41] enones as Michael acceptors,[42] and sulfur-based electrophiles.[43] Though robust, these methods come with the same limitations as standard cuprate chemistry as discussed in Section 1.1.2.1, namely the need for careful control of cryogenic temperatures, stoichiometric metals, and the handling of pyrophoric organolithiums, all of which limit scalability. Furthermore, while broad carbon-based nucleophiles are tolerated, heteroatoms cannot be installed at the β position via cuprate chemistry. Similarly, only highly reactive electrophiles are compatible, while less activated alkylating reagents often lead to loss of regioselectivity via enolate equilibration and the formation of undesired side products. High-yielding copper enolate trapping can also be finnicky

experimentally, requiring testing of various co-solvent combinations or solvent swaps, and even with these modifications, outcomes are substrate-dependent.[38,44] Furthermore, α-arylation remains inaccessible. Modern advances, such as hypervalent iodine chemistry (Scheme 11)[45] have opened the doors to β-alkylation, α-arylation. The need to synthesize the hypervalent iodine reagent for each aromatic group, however, adds a barrier to entry and complexifies the reaction even further. Nonetheless, this method was used in the total synthesis of meroterpenoids from *Psoralea coryliforia*.[46] Despite the strong history of cuprate conjugate additions and enolate trapping sequences, the cryogenic conditions, stoichiometric nature, and limited range of coupling partners leave more to be desired in the realm of cyclic enone difunctionalization.

Scheme 11. Modern cuprate conjugate addition and enolate trapping with hypervalent iodine reagent for α-arylation.

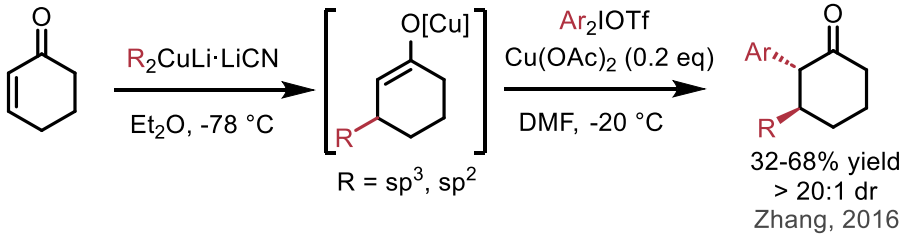

1.1.5: Modern, catalytic methods for cyclic enone difunctionalization

Given the limitations associated with cuprate conjugate addition and enolate trapping sequences, modern research has aimed to develop more mild, catalytic methods for cyclic enone difunctionalization methods. Compared to alkene difunctionalization however, which is extensively developed and reviewed,[47–49] cyclic enone difunctionalization remains tremendously underexplored and underreported. It has been hypothesized that this could be due to challenges associated with dynamic tautomerization between C-bound and O-bound metal enolates (Scheme 12)[22,50–52] which may interfere with the desired bond formations at the α carbon or lead to undesired reactivity. In other words, trapping transient metal-bound enolates with catalytic metals likely proves difficult. Despite this challenge, a handful of groups have been successful in developing methods for fully catalytic cyclic enone difunctionalization, discussed below.

Scheme 12. Tautomerization between C-bound and O-bound metal enolates.

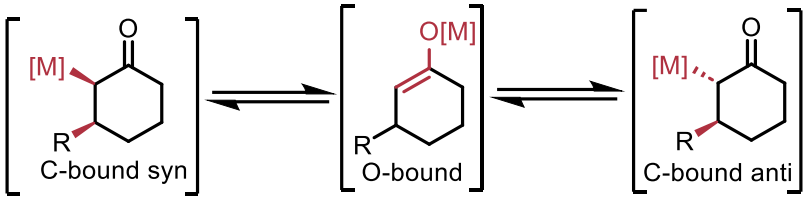

1.1.5.1: Conjugate borylation, tandem aldol

In 2009, the Hoveyda group reported a method achieving a conjugate borylation, tandem aldol for catalytic cyclic enone difunctionalization (Scheme 13).[32] This reaction makes use of NHC-catalyzed, copper-free conjugate borylation chemistry discussed in Section 1.1.3.3, but traps the transient boron enolate in situ with a reactive aldehyde through an aldol reaction. The result is a mild reaction which easily delivers a complex product in high yield and diastereoselectivity. The Riant group expanded on this finding in their 2012 report of copper-catalyzed tandem conjugate borylation-aldol chemistry.[53] Though limited in scope to reactive aldehydes, these works lay strong precedent for in situ enolate trapping after a catalytic nucleophile addition.

Scheme 13. Catalytic cyclic enone difunctionalization by conjugate borylation, tandem aldol.

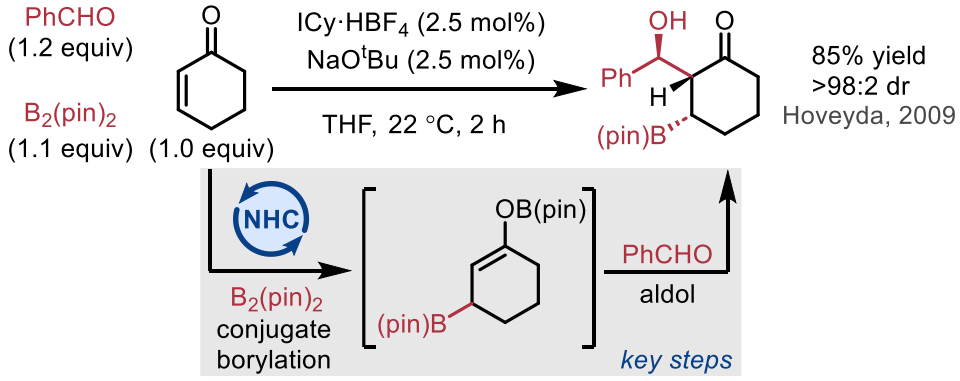

1.1.5.2: Conjugate reduction, α-allylation

The Riant group reported a conjugate reduction, α-allylation of cyclic enones in 2013 (Scheme 14).[54] Cooperative NHC-copper and phosphino-oxazoline-palladium catalysis is employed, along with a silane reagent as the nucleophile and an electrophilic allyl carbonate. A copper hydride formed in situ undergoes migratory insertion into the enone, providing a copper enolate. Separately, oxidative addition of palladium into the allyl carbonate yields an oxidative addition complex. Transmetallation between the organocopper and organopalladium species restores the copper salt, while providing a palladium enolate. Finally, reductive elimination

furnishes the desired product. Control experiments showed that a conjugate reduction side product forms via hydrolysis of an off-cycle silyl enol ether. Separate synthesis of the silyl enol ether shows that it is incompetent as an intermediate in the absence of copper. Though the net reaction is not a difunctionalization, the mechanistic pathway of conjugate addition and enolate trapping is reminiscent of both cuprate chemistry (discussed in Section 1.1.4) and the conjugate borylation, tandem aldol reaction (discussed in Section 1.1.5.1). Furthermore, both the nucleophilic and electrophilic reagents, the silane and allyl carbonate, respectively, are activated in situ by transition metal catalysts. This combination of cooperative copper and palladium catalysis to separate the nucleophilic and electrophilic components introduces a valuable concept for more developments in catalytic cyclic enone difunctionalization.

Scheme 14. Catalytic cyclic enone difunctionalization by conjugate reduction, α-allylation.

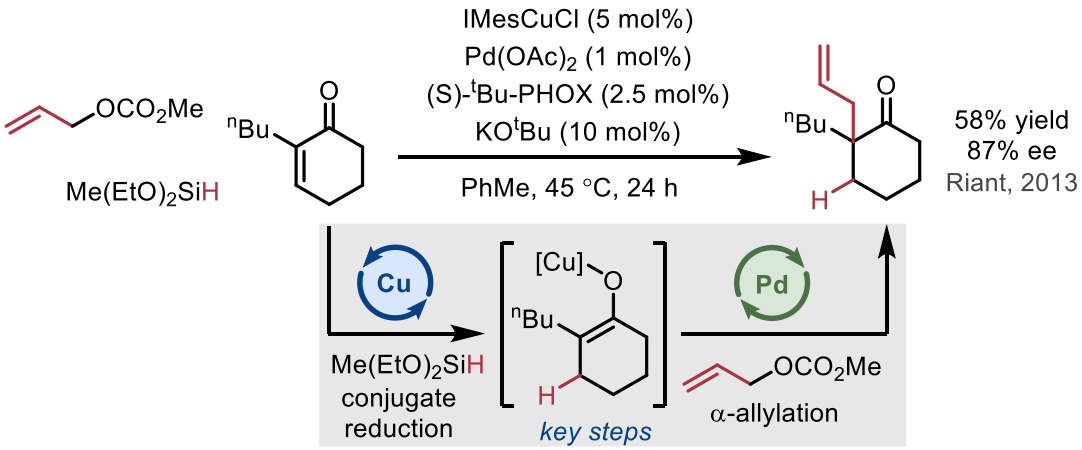

1.1.5.3: Conjugate arylation, α-allylation

In a closely related report from 2023, the Lundgren group achieved β-arylation, α-allylation through cooperative rhodium-iridium catalysis (Scheme 15).[55] The mechanism commences with conjugate arylation via rhodium catalysis, as discussed in Section 1.1.3.2, but is intercepted with an iridium cycle to furnish difunctionalization. Mild room temperature conditions, low catalyst loadings, high yields, incredible enantio- and diastereoselectivity, and the production of three contiguous stereocentres and two new carbon–carbon bonds make this work incredibly impressive. Nevertheless, this report only tackles a narrow range of the vast possibilities in cyclic enone difunctionalization, as there is no way of introducing aromatic groups at the α position or heteroatoms at the β position. In a related work, a similar β-arylation, α-allylation was achieved through dual palladium-palladium catalysis, but cyclic enones were found to perform much worse

(under 40% yield) than acyclic ones.[56] Despite this great advance, more cyclic enone difunctionalization methods are needed.

Scheme 15. Catalytic cyclic enone difunctionalization by conjugate arylation, α-allylation.

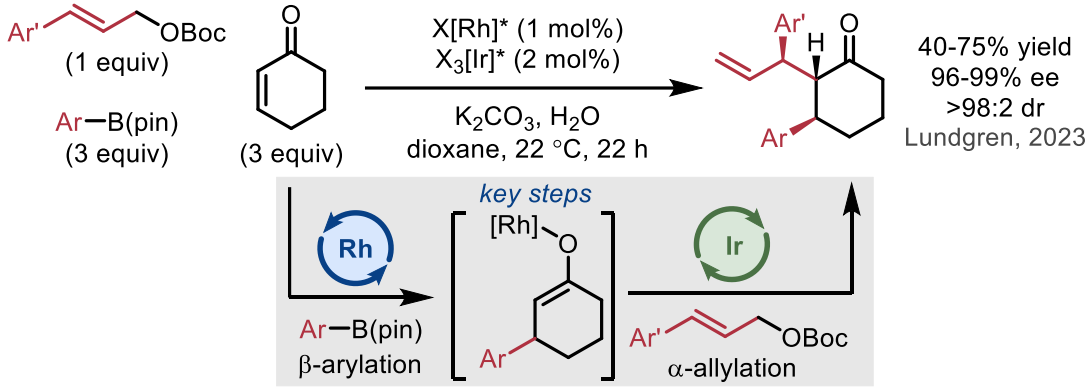

1.1.5.4: Photoredox-catalyzed β-alkylation, α-arylation

Proceeding through a different reactivity paradigm compared to the other transformations discussed in this section, a photoredox method for β-alkylation, α-arylation was reported by the Molander group in 2021. Most of their reaction scope focuses on acyclic unsaturated esters, but one example with a cyclic enone is reported in rather high yield (Scheme 16).[57] Although the overall mechanism involves radical intermediates and electron transfer steps with nickel and photocatalysts, the key bond-forming steps follow a similar pattern to other common types of enone chemistry. The carbon–hydrogen bond α to the alcohol is first converted to a nucleophilic radical, which adds into the cyclic enone at the electrophilic β position. This provides an α-keto radical that behaves somewhat like an enolate, and this is trapped by the nickel catalyst to ultimately give rise to the α-arylated product. This report nicely compliments the Lundgren groups work (Section 1.1.5.3), as access to a different substitution pattern is enabled, with an aromatic group at the α position. Once again however, this example is only one piece of the vast cyclic enone difunctionalization puzzle, as only tertiary alkyl C-H bonds α to oxygen can serve as the nucleophilic partner, and there is no way of introducing heteroatoms or other groups in the β position.

Scheme 16. Catalytic cyclic enone difunctionalization by photoredox method.

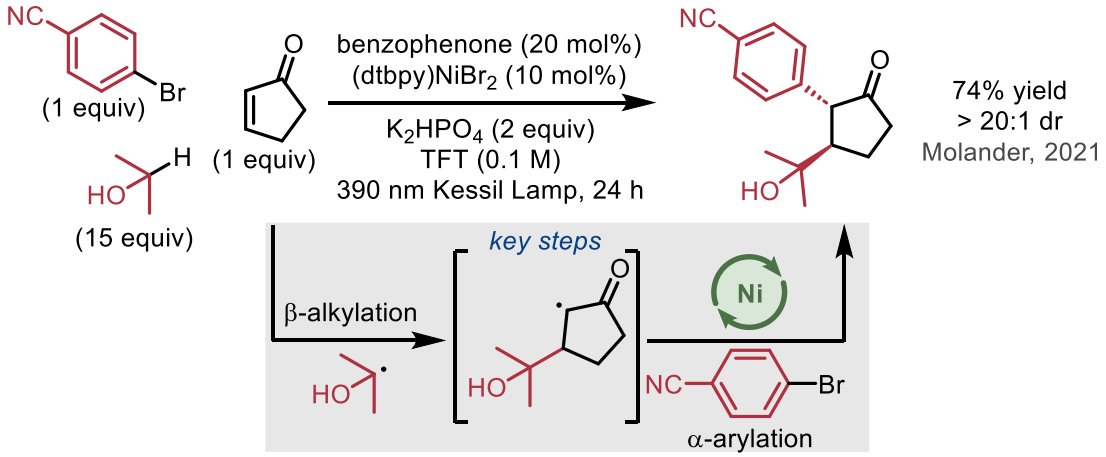

Though there have been a handful of modern, catalytic, and mild methods reported for cyclic enone difunctionalization, the range of accessible product substitution patterns remains narrow. There is thus a need to expand this range through developing new methods. Given the breadth of reactions developed for the difunctionalization of alkenes,[58,59] it is worth looking into existing alkene difunctionalization methods to seek inspiration for applications to cyclic enone chemistry.

1.2: Alkene arylboration

Arylboration is a particularly powerful method of catalytic alkene difunctionalization which has received a great deal of attention in the past decade.[60–63] An alkene, an aryl halide, and a boron reagent (all of which are common and accessible building blocks) are combined in a three-component coupling reaction, rapidly generating molecularly complexity (Scheme 17). A major strength of arylboration chemistry is the diversity of products accessible based on the various transformations possible using the boronate ester moiety in subsequent product functionalization reactions (discussed in Section 1.2.1). Another strength is that the reaction occurs under mild, simple, and redox-neutral transition metal-catalyzed conditions. Common catalytic manifolds for these types of transformations include palladium catalysis, nickel catalysis, and cooperative copper-palladium catalysis; the corresponding mechanisms of these pathways, along with their strengths and weaknesses, are discussed in Section 1.2.2. Though plentiful research into arylboration chemistry has been conducted and a wide array of alkenes have been employed, the substrate scope of tolerated alkenes, discussed in Section 1.2.3, could be expanded further.

Scheme 17. Transition metal-catalyzed alkene arylboration.

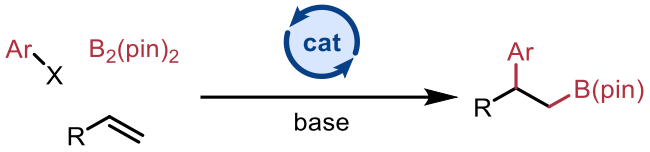

1.2.1: Utility of boronate ester for further functionalization

The utility of arylboration chemistry is strengthened by the diversity of possible functional groups that are accessible through modification of the boronate ester group (Scheme 18). A wide array of stereospecific transformations of boronate esters have been developed over the years,[26] and application of these to the products of arylboration allow for access to a broad range of functionalities. Heteroatoms can be easily installed through oxidation,[64] amination,[65] and fluorination[66–68] of the B(pin) group. The boronate ester may also be converted into a trifluoroborate salt through a simple reaction,[64] and deuteration is also possible.[69] Furthermore, carbon–carbon bond formation can be done by classical Matteson homologation[35] and Zwiefel[33] chemistry. Lastly, modern cross-coupling[35] and metallaphotoredox[70] methods may be employed for direct arylation of the boronate ester. Though these boronate transformations add an additional step after arylboration, they provide access to a breadth of functionalities which would be difficult to install otherwise. Effectively, different difunctionalization patterns are accessible from the initial arylboration product, precluding the need to develop multiple reaction types, and expanding the range of alkene difunctionalization products accessible from one simple arylboration.

Scheme 18. Examples of possible arylboration product functionalization reactions through transformations involving the boronate ester.

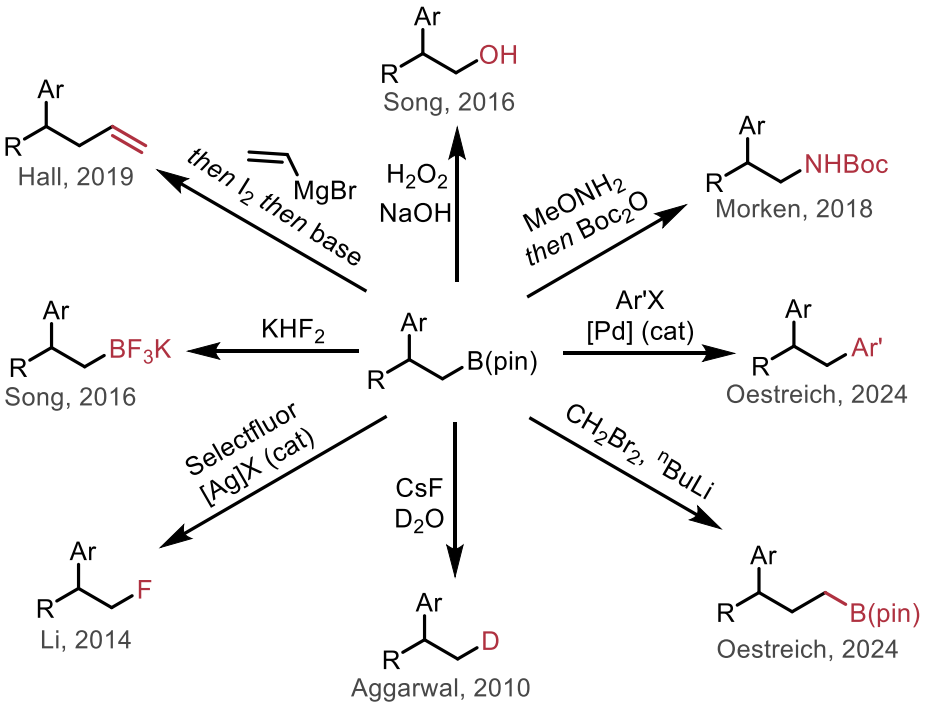

1.2.2: Common catalytic manifolds for alkene arylboration

As mentioned previously, the most common alkene arylboration catalysts include palladium, nickel, and cooperative copper-palladium systems. Challenges associated with each, along with their mechanisms, are discussed in this section.

1.2.2.1: Palladium-catalyzed alkene arylboration

Alkene arylboration can be achieved through palladium catalysis through a simple Mizoroki–Heck-type pathway. Unfortunately, alkyl palladium intermediates are often susceptible to rapid β-hydride elimination and reinsertion, resulting in chain walking (Scheme 19) that often leads to unpredictable and low regioselectivity in these reactions.

Scheme 19. Chain walking of alkyl palladium intermediates through β-hydride elimination and reinsertion.

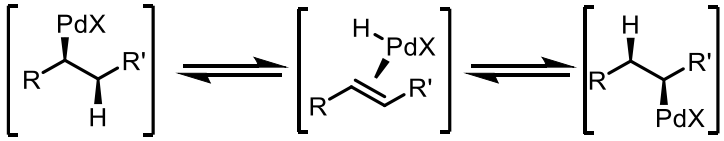

A report from the Toste group in 2015 demonstrates this concept (Scheme 20).[71] Following oxidative addition into an aryl diazonium salt, the aryl palladium-(II) complex inserts into a terminal alkene with good regioselectivity. However, chain walking provides the thermodynamic benzyl palladium intermediate, which after transmetallation with $B_2(pin)_2$ and reductive elimination, yields a 1,1-arylboration product. Though this product may be desirable in some instances, the mechanistic challenge of chain walking proves to be a recurring problem in palladium-catalyzed arylboration reactions which often reduces yields and gives side products.

Scheme 20. Palladium-catalyzed 1,1-arylboration of alkene through chain walking.

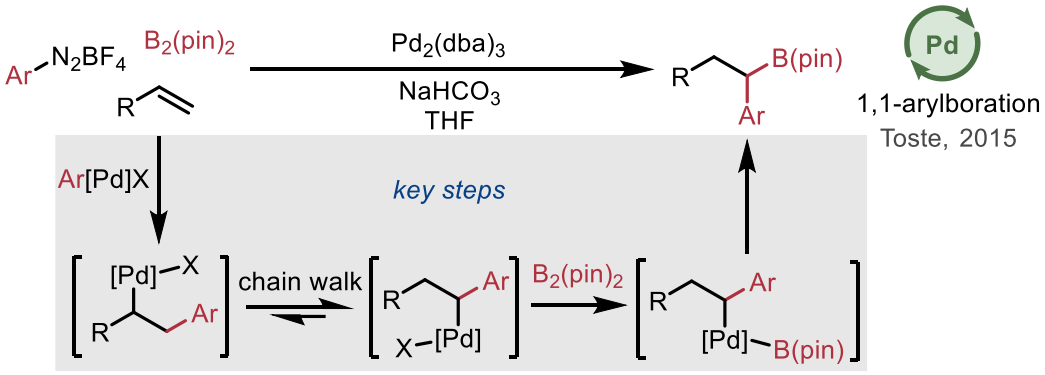

The Engle lab introduced a technique for overcoming chain walking and enhancing regioselectivity in palladium-catalyzed arylboration through use of an amino-quinoline directing group (Scheme 21).[72] The mechanism of this transformation is similar to that discussed in Scheme 20, but with one key difference; the strongly-coordinating directing group in this case forms a metallacycle with the alkyl palladium intermediate, preventing β-hydride elimination, avoiding chain-walking, and forcing the desired 1,2 regioselectivity. While this solves the chain walking problem, the need for a directing group both limits the scope of alkene substrates that can be used in this chemistry and adds a synthetic burden due to the need to introduce and then remove the directing group itself. This challenge of chain walking and unpredictable regioselectivity prevents palladium catalysis from being the first choice for new methods development in arylboration.

Scheme 21. Regioselective Pd-catalyzed alkene 1,2-arylboration through directing group.

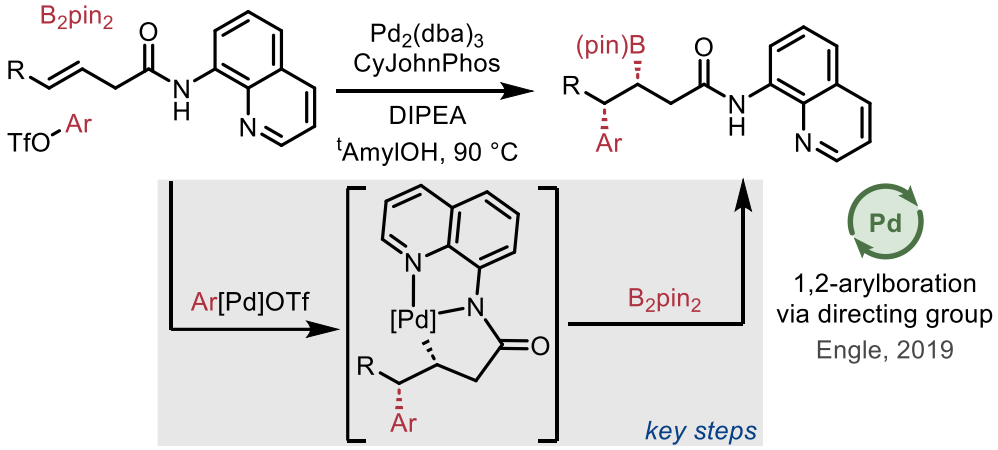

1.2.2.2: Nickel-catalyzed alkene arylboration

Nickel catalysis has been more successful than palladium in arylboration chemistry due to more facile ligand-control over chain walking rather than the substrate control present in palladium systems. GuoYin Yin's group has taken advantage of chain walking to achieve regiodivergent 1,1 and 1,3 (remote) arylboration (Scheme 22).[73] The mechanism of this transformation is similar to the palladium pathway, but in the opposite order. A nickel-(I) boryl complex first inserts the alkene, then chain walking to either the benzylic or α-boryl position occurs depending on the choice of bidentate amine ligand. Oxidative addition with the aryl chloride to nickel-(III), followed by reductive elimination, furnishes the products. While the regioselectivities obtained are often >20:1, some products can be contaminated with up to 10% of the undesired regioisomer, which can be very difficult to remove by common purification methods.

Scheme 22. Ligand-controlled nickel-catalyzed regiodivergent arylboration.

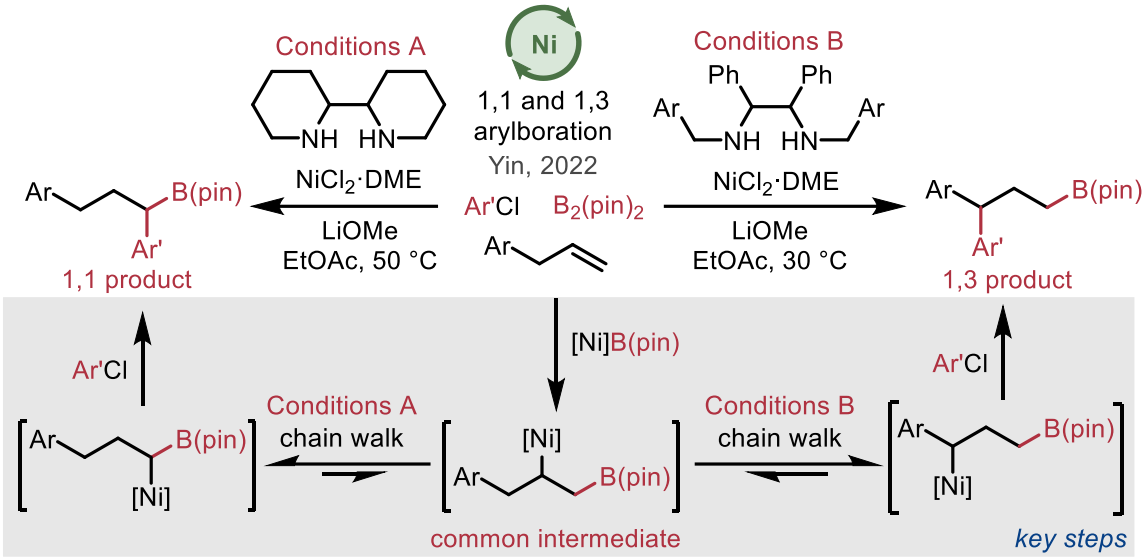

In contrast, Kevin Brown's research group has developed nickel catalytic systems which suppress β-hydride elimination and avoid chain walking to afford 1,2 arylboration of alkenes.[74–76] Interestingly, ligand-free conditions provide the 1,2 arylboration product in high selectivity (Scheme 23),[76] albeit still contaminated with around 5% of the 1,1 arylboration product derived from chain walking pathways. While nickel-catalyzed arylboration reactions are more extensively developed than those with palladium, they are not as common or explored as the cooperative catalytic options.

Scheme 23. Nickel catalyzed 1,2-arylboration.

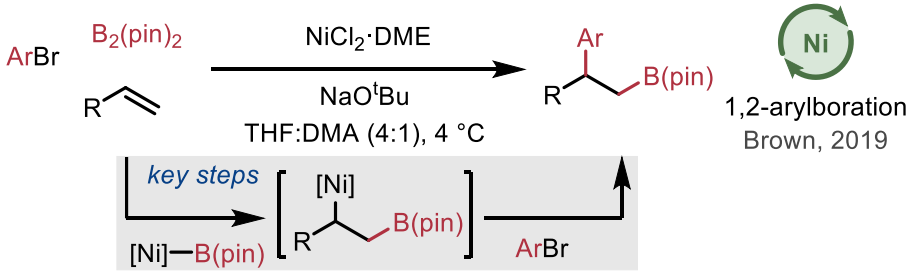

1.2.2.3: Copper/palladium-catalyzed alkene arylboration

Cooperative copper/palladium catalysis is by far the most developed system for alkene arylboration.[63] This is likely due to the robustness of alkyl copper intermediates against undesired β-hydride elimination, along with the complementary reactivities of copper and palladium for

engaging the boron and ArX coupling partners, respectively. Initially reported in 2014 by Semba and Nakao,[58] as well as the Brown group,[77] dozens of examples of this reactivity for a broad range of alkene substrate classes have appeared in the past decade,[78–81] including enantioselective variants which use chiral NHC ligands for copper.[80,82–86]

A representative example of a copper-palladium cooperative catalytic system for alkene arylboration is presented in Scheme 24.[87] As is most common, a copper-NHC catalyst and palladium-monophosphine are combined with an alkoxide base in a polar aprotic solvent at room temperature, in the presence of the alkene, aryl halide, and boron reagent, to achieve the desired arylboration. The sequence of elementary steps involves an initial migratory insertion of a boryl copper intermediate into the alkene, forging the key carbon–boron bond, and providing an alkyl copper species which is resistant to β-hydride elimination. A separately-formed aryl palladium halide oxidative addition complex then transmetallates with this organocopper, providing an alkyl palladium intermediate, which quickly undergoes reductive elimination to afford the arylboration product. Interestingly, the key copper-to-palladium transmetallation can be either stereoretentive, providing syn product, or stereoinvertive, providing the anti product. In this work, the Brown group managed to provide stereodivergent arylboration pathways, both with high yield and diastereoselectivity, through altering the palladium ligand as the main contributor to diastereoselectivity. No traces of any other arylboration regioisomers, such as those expected from chain walking, were detected. This work is but one of many which demonstrates the strength of Cu/Pd catalysis for achieving highly selective arylboration under mild conditions.

Scheme 24. Ligand-controlled stereodivergent alkene arylboration by Cu/Pd catalysis.

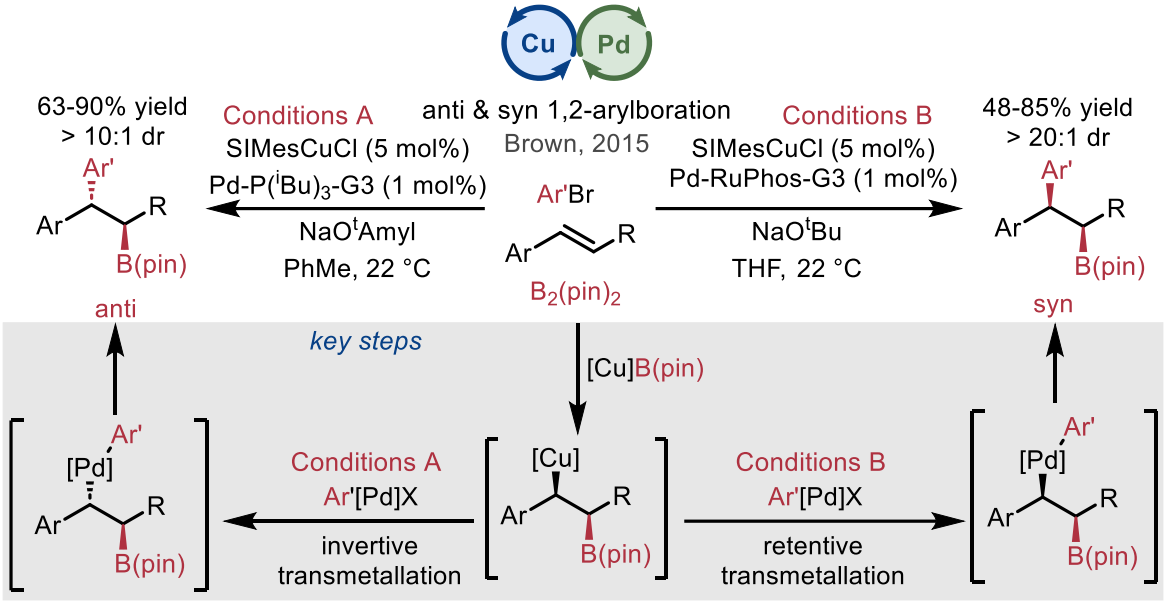

Though arylboration regioisomers are usually not observed in Cu/Pd-catalysis and this overcomes some of the challenges experienced in Ni and Pd chemistry, cooperative-catalyzed arylboration reactions still produce a range of common side products (Scheme 25). Optimization campaigns in the literature usually report observations of aryl-aryl homodimers via reductive homocoupling, as well as aryl boronate ester side products derived from palladium-catalyzed Miyaura borylation of the aryl halide.[77] Furthermore, hydroboration side products are often obtained, likely through proto-decupration (protonolysis) of organocopper intermediates.[58,88,89] Both of these undesired pathways detract from the yield and efficiency of Cu/Pd-catalyzed arylboration chemistry, though fortunately, optimization efforts can usually suppress their formation, and this methodology for alkene difunctionalization remains strong and impactful given its high regioselectivity, predictable reactivity pattern, and diversity of alkene substrates tolerated.

Scheme 25. Common side products observed in Cu/Pd-catalyzed alkene arylboration.

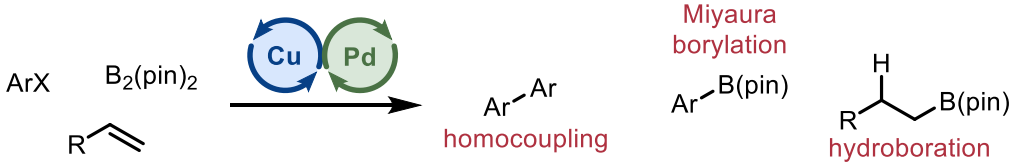

1.2.3: Substrate scope of alkenes tolerated in current arylboration chemistry

As discussed above, a major strength of arylboration as a difunctionalization technology is the breadth of alkene substrates which are tolerated. Shown in Scheme 26 is an overarching set of

alkene classes with known and reported arylboration reactions. Styrenes and other vinylarenes of various substitution patterns are by far the most common substrates in arylboration,[58,77,90] likely due to the ease of achieving regioselectivity given the differences in reactivity of the benzylic and homobenzylic carbons. Aliphatic terminal alkenes,[91] as well as symmetrical carbocyclic alkenes,[74] are also well-behaving substrates. Dienes pose unique challenges to regioselectivity but have been tamed[88] predictably. Several niche examples of arylboration on vinylsilane and vinylborane substrates have also been reported,[92] adding to the vast range of alkenes tolerated in this chemistry.

Scheme 26. Range of alkenes tolerated in known arylboration chemistry.

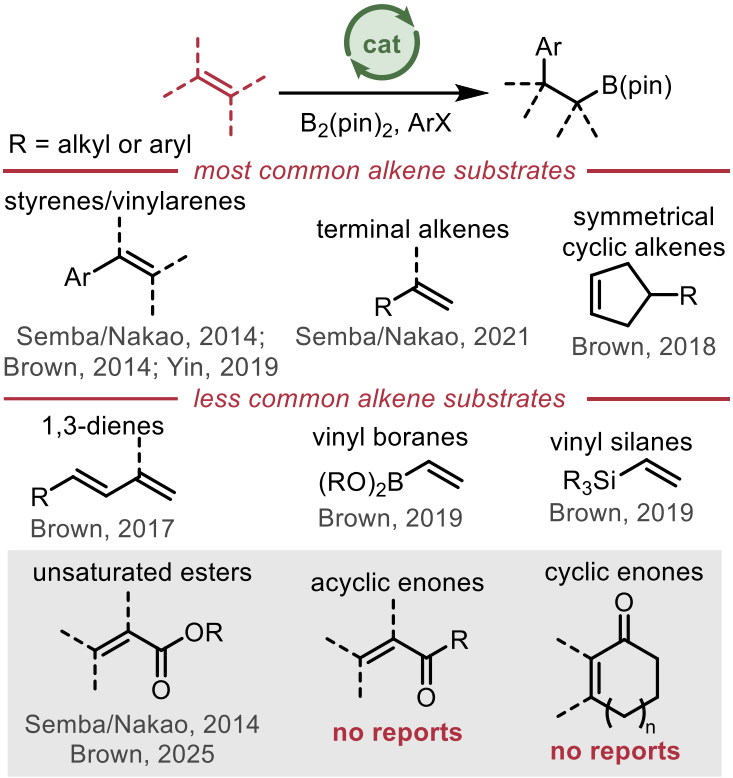

Surprisingly, however, electron-deficient alkenes, such as those in unsaturated esters or enones, remain nearly absent in the arylboration literature. To the best of our knowledge as of September 2023 (at the beginning of this thesis project), only one example of such a reaction was known at the time; β-methyl methacrylate was reported by Semba and Nakao in 2014 to undergo Cu/Pd-catalyzed arylboration in 66% yield and 4:1 dr (Scheme 27).[58] Typically, unsaturated esters give no product at all in other arylboration systems such as with Ni catalysts.[90] Thus, incorporating these and other electron-deficient alkenes into arylboration chemistry remains an unsolved challenge, and developing new methods which function on enones or unsaturated esters would be of great impact in expanding the applications of arylboration chemistry. During the preparation of

this thesis, the Brown group published (pre-print made available online on March 27, 2025) a Cu/Pd co-catalyzed method for the anti-selective arylboration of acyclic unsaturated esters, filling a key gap in this area.[93] Even with this recent advancement, there are still no known examples of arylboration on cyclic or acyclic enones, and this gap remains to be filled.

Scheme 27. Arylboration of an unsaturated ester substrate.

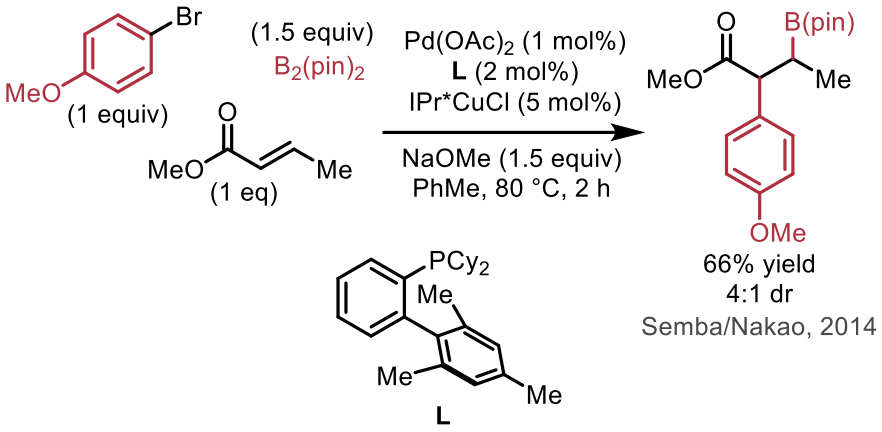

1.3: Research goals

As described in Section 1.1, cyclic enones are abundant and cheap building blocks for assembling complex molecules. Although cuprate methods are time-tested and robust for achieving mono- and difunctionalization of cyclic enones (discussed in Section 1.1.2.1 and Section 1.1.4), they come with the inconvenience of cryogenic temperatures, require stoichiometric organometallic reagents, and can be limited in the range of functional groups which can be installed. Modern research efforts have led to the development of many new mild, catalytic organic transformations for mono-functionalization of cyclic enones at either the α or β position, and some of these approaches were outlined in Section 1.1.3. Unfortunately, developments in the direct, catalytic difunctionalization of cyclic enones have lagged behind, with only a few known examples being reported (Section 1.1.5). These existing methods only provide access to a narrow range of all the desired enone difunctionalization substitution patterns, and there remains plenty of room for the development of more methods for efficient access to complex products from simple enones.

In contrast, alkene difunctionalization is extensively developed, with arylboration emerging as a particularly powerful technique due to the versatility of the boronate ester moiety in subsequent transformations that may provide a plethora of various functional groups (Section 1.2.1). While palladium and nickel catalysis are functional in arylboration chemistry, cooperative

Cu/Pd catalysis dominates this field due to its ability to overcome and suppress undesired chain walking (Section 1.2.2). Surprisingly, electron-poor conjugated alkenes remain nearly absent in arylboration literature (Section 1.2.3), and there are no known examples of cyclic enones undergoing this mode of reactivity.

Given the shortage of catalytic cyclic enone difunctionalization methods, the absence of cyclic enone substrates in arylboration literature, and the utility of boronate esters, the current work aims to develop a mild, catalytic method for the arylboration of cyclic enones (Scheme 28, and developed fully in Chapter 2). A Cu/Pd cooperative catalytic system is hypothesized to be ideal for this endeavour (explained in Section 2.1.3), based on the strength of Cu/Pd catalysis in alkene arylboration (Section 1.2.2.3), as well as the mechanistic precedent provided by copper-catalyzed enone conjugate borylation (Section 1.1.3.3) and palladium-catalyzed enone α-arylation (Section 1.1.3.4). The targeted transformation would efficiently convert cheap cyclic enones into complex 1,2,3-trisubstituted building blocks which would otherwise require several synthetic steps to access (see Section 2.1.2). There is also potential for producing an enantioselective enone arylboration reaction given the precedent in both asymmetric alkene arylboration and enone conjugate borylation with chiral copper catalysts. The products of arylboration also present opportunities for further functionalization at both the ketone and boronate ester moieties (see Section 2.1.1.1), increasing the diversity of carbocyclic scaffolds accessible, and opening doors towards expediting the synthesis of bioactive molecules (see Section 2.1.1.2) with the proposed enone arylboration as an enabling and productive key step.

Scheme 28. Proposed cyclic enone arylboration via copper-palladium catalysis.

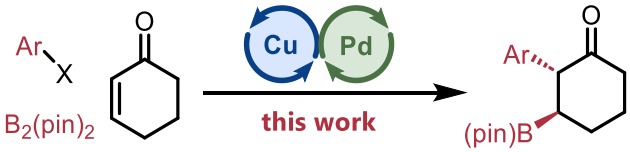

Chapter 2: Mild arylboration of cyclic enones via cooperative copper-palladium catalysis

2.1: Background

Before embarking on the campaign towards the experimental discovery of a method for cyclic enone arylboration, the utility of the resulting difunctionalization products, as well as existing methods for accessing them, should be discussed; these are explored in Section 2.1.1 and Section 2.1.2, respectively. Furthermore, the strong literature precedent provided by Cu/Pd-catalyzed alkene arylboration (Section 1.2.2.3) and catalytic enone functionalization (Section 1.1.3) can be used to propose a hypothetical mechanism for the desired transformation (discussed in Section 2.1.3) and to predict the expected side products (detailed in Section 2.1.4). All of these concepts provide key insights for how to carry out the discovery and development of the desired cyclic enone arylboration, and are thus crucial to consider beforehand to aid in the experimental design of this project.

2.1.1: Utility and relevance of cyclic enone arylboration products

Though boronate esters themselves are rarely a desired functional group in the end-product of a synthetic sequence, they provide a flexible entry point for further functionalization. Additionally, the ketone moiety of the proposed arylboration product provides a second functional handle for adding more molecular complexity. The possibilities for product functionalization to access highly substituted carbocyclic scaffolds are discussed in Section 2.1.1.1, and some bioactive molecules with structures that may be efficiently accessed through arylboration and subsequent functionalization are outlined in Section 2.1.1.2. The diversity of accessible scaffolds and relevance to bioactive structures enhance the potential impact of the envisioned cyclic enone arylboration reaction.

2.1.1.1: Opportunities for product functionalization

In addition to the diverse, stereospecific transformations on boronate esters which were described in Section 1.2.1, the ketone moiety of the proposed arylboration product could be leveraged to install a plethora of functional groups and substitution patterns around the carbocyclic ring (Scheme 29). Diastereoselective ketone reduction or addition of nucleophiles to the ketone is

expected to be facile and occur anti to the aromatic group,[33,94] providing a pathway for adding hydride, deuteride, and carbon nucleophiles, and allowing access to a broad range of 1,2,3-trisubstituted patterns. The range of possible substitution patterns could be expanded by converting the ketone to an imine prior to nucleophilic attack, enabling alcohols or amines to be produced. Ketone deprotonation and α-functionalization could add new groups to the other side of the ring. Additionally, the ketone could be used to furnish a desaturation. This transformation would open doors to a second difunctionalization reaction, which would be expected to occur diastereoselectively by Fürst-Plattner control.[35] These diverse product functionalization options after arylboration provide an approach for accessing a broader range of complex carbocyclic scaffolds, most of which would be challenging to synthesize otherwise.

Scheme 29. Possibilities for functionalization of arylboration products to access highly substituted and diverse carbocyclic scaffolds.

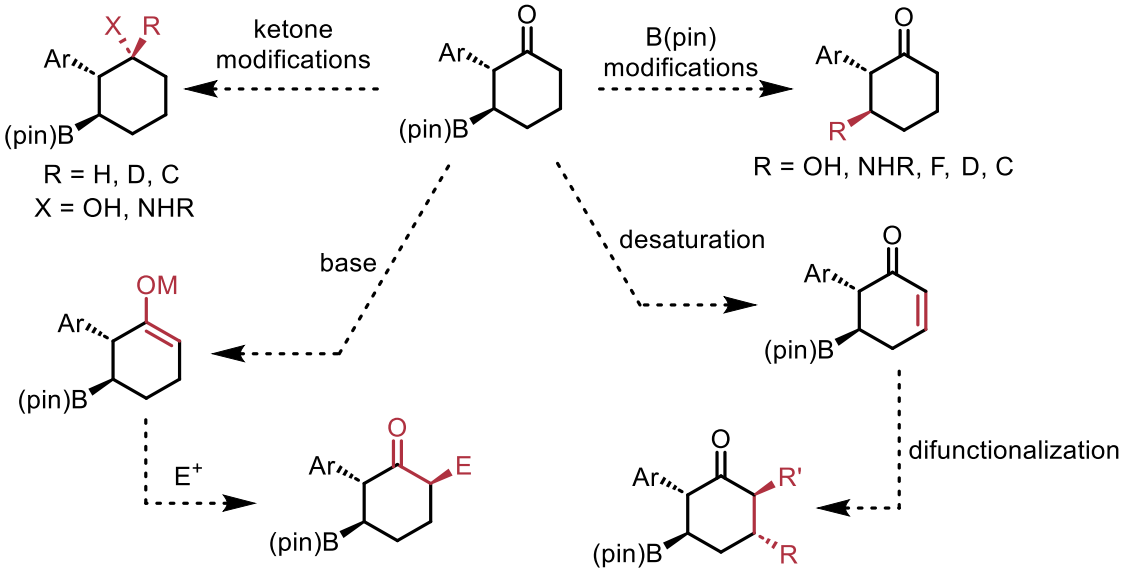

2.1.1.2: Bioactive carbocycles with mappable substitution patterns

One of the many possible carbocyclic scaffolds which could be accessed from functionalization of cyclic enone arylboration products is the 1,2,3-trisubstituted pattern shown in Scheme 30. Ketone reduction and B(pin) transformation could provide this pattern. These scaffolds are biologically relevant, as there are natural products and pharmaceuticals with this structural pattern. A meroterpene natural product, (-)-psorocorylifol G, found in the traditional medicinal plant *Psoralea corylifolia*,[46] possesses this substructure. Additionally, (+)-pancratistatin, a

naturally-occurring anti-cancer agent which inhibits topoisomerase I,[95] has been the subject of several total synthesis efforts[96–104] and displays this same 1,2,3-trisubstituted pattern. Though this α-aryl, β-substituted cyclic alcohol pattern is found in these bioactive molecules, such scaffolds remain underrepresented in pharmaceutical developments, potentially due to synthetic inefficiencies in producing them. The proposed arylboration and subsequent functionalization approach could potentially expedite synthetic access to these and other similar motifs.

Scheme 30. Bioactive natural products with structures that can map onto possible derivatives of product functionalization following arylboration of cyclic enones.

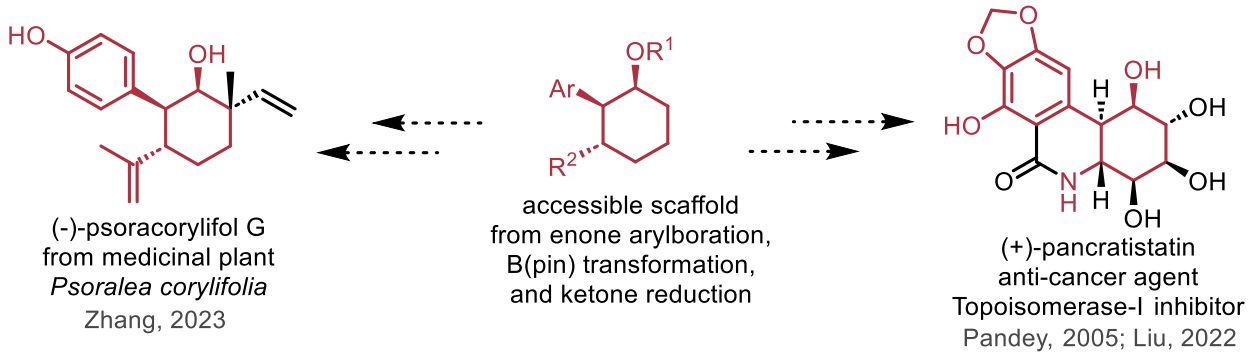

2.1.2: Existing approaches for synthesizing α-aryl, β-boryl cyclic ketones

Given the potential utility of the proposed cyclic enone arylboration products, it is worth considering alternative, known approaches for accessing them. Assessing existing routes to these products would also provide a benchmark for evaluating the gain in synthetic efficiency provided by the proposed difunctionalization reaction over classical methods. To the best of our knowledge, there is only one report for the synthesis of α-aryl, β-boryl cyclic ketones (Scheme 31).[105] The authors first stoichiometrically iodinate cyclopentenone, then subject this α-iodo cyclopentenone to a Pd-catalyzed Suzuki-Miyaura cross-coupling with an aryl boronic acid, and finally install the boronate ester through Cu-catalyzed conjugate borylation. While all steps involve robust chemistry, three synthetic steps are required in total, with plenty of reagents, and only moderate yields for each step. Overall, the final products are obtained in 3-29% yield over three steps, highlighting the difficulty in accessing these products. This sequence could potentially be shortened through bypassing the iodination-Suzuki sequence via direct α-arylation as described in Section 1.1.3.4,[37] but even this approach is clearly much less efficient than the proposed direct arylboration of the cyclic enone in one simple and catalytic synthetic step.

Scheme 31. Existing approaches for accessing α-aryl, β-boryl cyclic ketones.

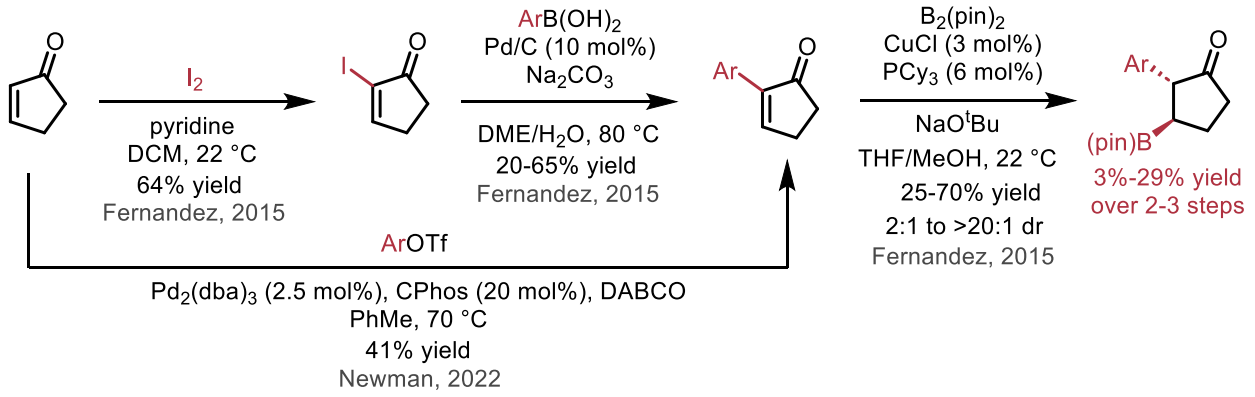

2.1.3: Proposed mechanism for Cu/Pd-catalyzed arylboration of cyclic enones

After having established the relevance of the arylboration products as well as the utility of the proposed arylboration reaction for improving synthetic efficiency (Section 2.1.2), the true challenge of developing the desired transformation awaits. Literature precedent in arylboration chemistry (Section 1.2) and catalytic cyclic enone functionalization (Section 1.1.3 and Section 1.1.5) can be used to propose a hypothetical mechanism (Scheme 32) for the desired transformation to aid in the design of discovery experiments.

First, a Cu(I) halide catalyst is expected to undergo transmetallation with a base-activated equivalent of $B_2(pin)_2$, yielding a boryl-copper intermediate.[77] This may then interact with the cyclic enone, providing migratory insertion to deliver the desired carbon–boron bond and form an O-bound copper enolate, in a manner akin to conjugate borylation.[35] Separately, a Pd(0) catalyst may perform oxidative addition with an aryl (pseudo)-halide coupling partner, providing an aryl-Pd(II) oxidative addition complex. The Cu-enolate and the Pd oxidative addition complex may then undergo transmetallation, restoring the Cu(I) halide catalyst and providing a C-bound Pd-enolate. The feasibility of this transmetallation, especially the trapping of the transient enolate, is demonstrated by successes in enone α-arylation,[37] conjugate reduction α-allylation,[54] and conjugate arylation α-allylation[55] sequences (Section 1.1.5). Though the intricate mechanistic details of this transmetallation and the dynamic nature of the tautomerization of C-bound and O-bound metal enolates are hard to understand and predict,[50,51] the O-bound Cu-enolate to C-bound Pd-enolate transmetallation is expected to occur as shown based on precedent in the trapping of copper enolates,[45] and is predicted to provide the C-bound palladium enolate in an anti stereochemical relationship with the bulky B(pin) moiety due to approach of the oxidative addition

complex from the less hindered face. Lastly, stereo-retentive reductive elimination from this Pd-enolate will hopefully provide the desired anti arylboration product while restoring the Pd(0) catalyst. It is also worth noting that this proposal is only one of several possible mechanisms, with the most significant alternative pathway involving contributions from O-bound Pd-enolates, fast equilibration between syn and anti epimers of the Pd-enolate, and stereo-determining reductive elimination. Though this transformation is a complex and ambitious cyclic enone difunctionalization reaction with many moving parts, the proposed mechanism is believed to be reasonable based on the strong precedent in related chemistry, and the Cu/Pd cooperative catalytic system seems ideal for achieving this goal.

Scheme 32. Proposed mechanism for the Cu/Pd-catalyzed arylboration of cyclic enones.

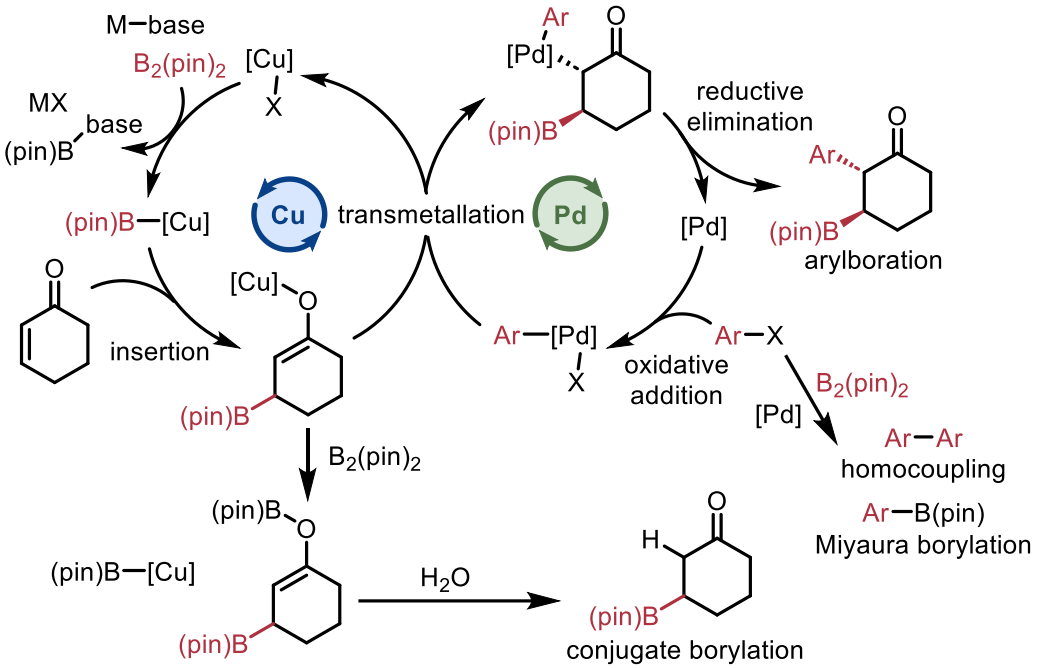

2.1.4: Expected side products in cyclic enone arylboration

Despite the strong precedent for the proposed mechanism and foreseen success of this Cu/Pd-catalyzed cyclic enone arylboration, several potentially problematic side products are expected (Scheme 32), and these may pose challenges in the discovery and optimization. Numerous alkene arylboration reports detail the observation of aryl boronate ester side products,[58,64,77] which presumably form by Pd-catalyzed Miyaura borylation of the aryl halide with $B_2(pin)_2$. The same side product can be expected in our arylboration project. Along with this, one may hypothesize that homocoupling of the aryl halide partner could occur, either by direct

reductive coupling, or through a subsequent Suzuki coupling of the aryl boronate formed by Miyaura borylation with another equivalent of aryl halide. Although both the Miyaura borylation and reductive homocoupling side products are likely to detract from product yield by eating up equivalents of aryl halide, optimization of the catalytic system is expected to overcome these challenges, as they have been conquered in previously reported arylboration reactions[58,64,77] which achieve the desired three-component coupling over the undesired two-component pathways (Section 1.2.2.3).

The principal challenge which is expected to hinder enone arylboration is the undesired conjugate borylation pathway. Given the extensive precedent in Cu-catalyzed conjugate borylation of cyclic enones (see Section 1.1.3.3) and the rapid kinetics of this reaction (often complete in a few hours at room temperature), achieving arylboration over conjugate borylation is expected to be difficult. Mechanistic studies from the Hoveyda group on their conjugate borylation system demonstrate that Cu-enolates formed from NHC-Cu catalysts can undergo rapid transmetallation with $B_2(pin)_2$ to yield boron enolates.[32] These boron enolates might be inactive and off-cycle in our desired transformation, preventing trapping with Pd oxidative addition complexes, and leading only to conjugate borylation side products upon hydrolysis. Although hydroboration side products are occasionally observed in alkene arylboration chemistry via protodecupration of alkyl-Cu species,[58,88,89] the conjugate borylation side product expected in enone arylboration is believed to be much more problematic given the affinity between oxygen and boron. More specifically, transmetallation (σ-methathesis) between a diboron compound and an O-bound Cu-enolate has been shown computationally by Marder (Figure 1) to possess a much lower kinetic barrier (10.2 kcal/mol) than the corresponding reaction with the C-bound form (24.2 kcal/mol barrier).[106] Thus, this undesired pathway is easily accessible for the Cu-enolate intermediates expected in enone arylboration, but is likely not relevant in alkene arylboration. This phenomenon explains why alkene diboration is not usually seen in reported arylboration chemistry, and could provide a possible reason for why the arylboration of cyclic enones has not yet been reported. Overcoming the undesired conjugate borylation pathway may be an incredibly difficult problem to solve in our discovery and optimization efforts towards a successful cyclic enone arylboration reaction.

Figure 1. DFT computations by Marder comparing barriers for σ-metathesis of O-bound and C-bound Cu-enolates with a diboron reagent.

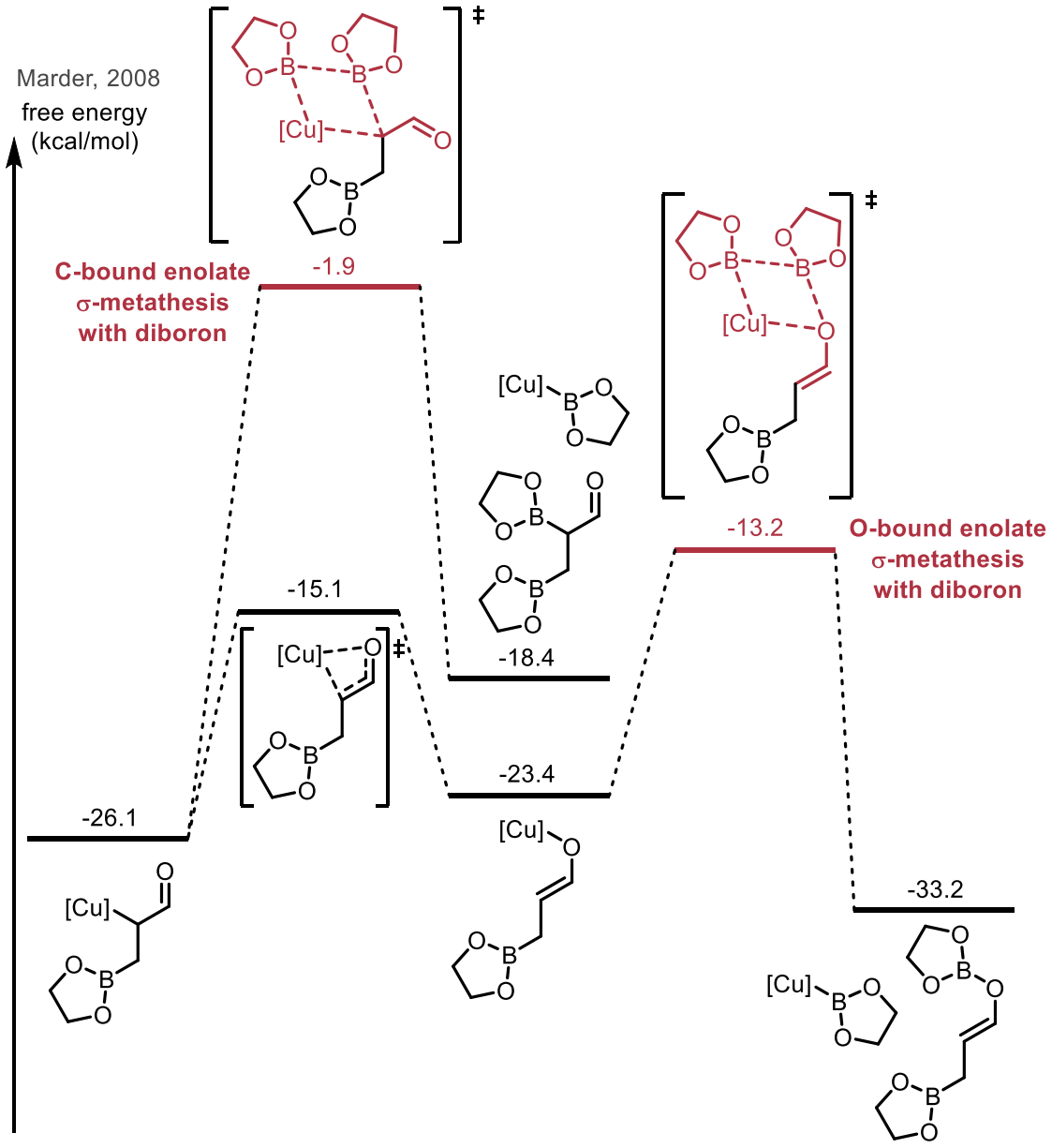

2.2: Results and discussion

2.2.1: Reaction discovery

With the hypothesized mechanism (Section 2.1.3) and the expected side products in mind (Section 2.1.4), some simple experimental parameters can be rationally selected to maximize the odds of discovering a functional catalytic system for enone arylboration. Since the formation of the conjugate borylation side product is expected to be the most significant hindrance to the desired arylboration, steps can be taken to minimize the contribution of this pathway. Looking at the proposed mechanism in Scheme 32, once the copper enolate forms, there is expected to be a kinetic competition for transmetallation with either $B_2(pin)_2$ to yield the undesired conjugate borylation, or with aryl-Pd-halide oxidative addition complex to eventually give rise to the desired arylboration product. Logically, to maximize arylboration over conjugate borylation, the rate of transmetallation with the oxidative addition complex must be high enough to out-compete the undesired pathway. Ideally, all equivalents of this copper enolate are consumed through transmetallation with the Pd oxidative addition complex as fast as they are formed. This means that high concentrations of oxidative addition complex are desirable, while Cu-enolate concentrations should be kept low in situ. Thus, it becomes evident that a successful arylboration reaction would likely benefit from keeping concentrations of the Cu catalyst low, while providing a relatively larger quantity of the Pd catalyst. This would ensure that plenty of oxidative addition complex is available for trapping copper enolates as soon as they form, and hopefully out-compete the undesired $B_2(pin)_2$ metathesis. Looking at established literature conditions for Cu/Pd-catalyzed alkene arylboration reactions, it is obvious that there is a heavy bias towards moderate Cu loadings (5 to 10 mol%) but with rather low relative Pd loadings (often between 0.5 to 2 mol%);[77,79,80,84,85,87,88,91,92] these catalyst loadings could explain why current conditions fail to provide arylboration of cyclic enones, and why electron-poor conjugated alkenes remain nearly absent in arylboration literature in general (see Section 1.2.3). We propose that the opposite ratio, with low Cu catalyst levels and high Pd loadings, would be much better suited for the arylboration of cyclic enones given the need to trap transient copper enolates before they react in undesired pathways.

Hence, for our enone arylboration discovery efforts, Cu loadings were kept at a moderate 5 mol%, while Pd levels were set at a rather high 10 mol%. Other key variables which are

hypothesized to play critical roles in maximizing the rate of transmetallation between the Cu-enolate and Pd oxidative addition complex include ligands for both metals, solvents, and bases. As it is rather difficult to predict a priori how these variables will impact the reaction, we turned towards high-throughput screening, a tool which is used often by our group for discovery campaigns.[107,108] Phosphine ligands are most commonly used for Pd in alkene arylboration, so a diverse array of six phosphines with various steric properties, electronics, and denticities were selected for screening. While most Cu/Pd-catalyzed systems for alkene arylboration use NHC ligands for copper,[58,77,78,86,87,91,109] some reports use phosphine ligands.[81,89,110] Therefore, two Cu sources were selected for analysis: a pre-formed NHC-Cu complex (IMesCuCl) and free CuCl with no added ligand, so that phosphine complexes would be formed with the same ligands added for the Pd catalyst. Importantly, ligand loadings were adjusted for this experimental setup. For reactions with IMesCuCl, bidentate phosphine ligands were added in a stoichiometrically equivalent ratio with the palladium catalyst (10 mol%), while monodentate phosphine ligand loadings were doubled (20 mol%). For reactions in which free CuCl was the copper source, all of the phosphine ligand loadings were doubled to 20 mol% and 40 mol% accordingly. Additionally, four bases and two solvents with vastly different properties were selected to broaden the overall chemical space explored in our initial high-throughput discovery screen. To complete our discovery system, cyclohex-2-ene-1-one **1a** was selected as the enone substrate, along with bromobenzene **2** as our aryl halide, with $B_2(pin)_2$, and $Pd_2(dba)_3 \cdot CHCl_3$ in a reaction at 80 °C. Results from this screen are shown in Figure 2.

Figure 2. High-throughput screening for cyclic enone arylboration reaction discovery.

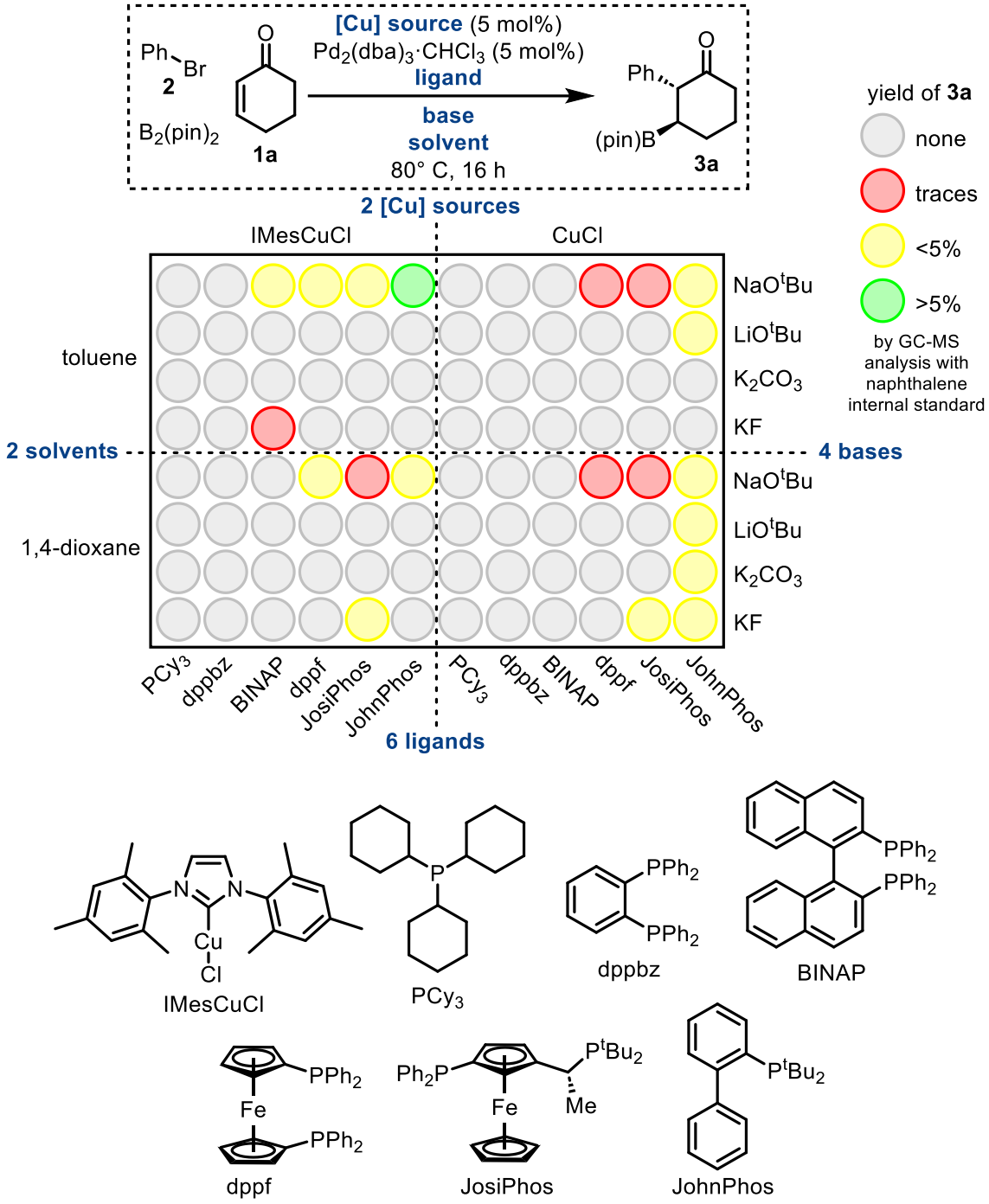

To our delight, the discovery plate was successful, and the desired arylboration product was detected in several reaction wells. Expectedly, all the predicted side products of two-component coupling (see Section 2.1.4 and Scheme 32) were also observed. Most reactions showed moderate amounts of both the reductive homocoupling and Miyaura borylation side

products. Conjugate borylation was widespread in high levels throughout nearly every set of reaction conditions screened. This demonstrates the efficient and rapid nature of conjugate borylation chemistry, while also outlining how difficult it is to trap Cu-enolates in situ and deliver successful arylboration. Even though conjugate borylation is a common occurrence and seems to occur irrespective of ligands, solvents, or bases, arylboration is a highly sensitive and challenging transformation to achieve, requiring careful matching of all key reaction variables. Notably, only one set of conditions provides an arylboration yield above 5%. This reaction involves a catalytic system using IMesCuCl as the Cu source, toluene as solvent, NaO^{t}Bu as the base, and JohnPhos as the ligand for Pd. Any slight deviation away from this combination of ligand, base, and solvent results in a rapid decline in yield or shuts down reactivity entirely. Scale-up and product isolation of this initial hit provides a 10% isolated yield of the desired arylboration product as the anti diastereomer **3a**, along with a 23% yield of conjugate borylation side product **4** (Scheme 33). Traces of the syn arylboration diastereomer were also detected upon GC-MS and GC-FID analysis of the crude reaction mixture, and the crude dr can be estimated as a 7:1 ratio of anti/syn isomers. The predominance of the anti diastereomer matches the mechanistic hypothesis (see Section 2.1.3) that the aryl-Pd-halide complex approaches the face opposite the boronate ester. Purification proved rather difficult, as the arylboration and conjugate borylation products have overlapping spots on TLC and tend to co-elute on silica gel columns. Although this initial hit is rather low yielding in the arylboration product **3a**, and the conjugate borylation pathway towards **4** seems to be both detrimental for yield and highly problematic for purification, the discovery high-throughput plate was successful, as this hit serves as a reasonable starting point for further reaction optimization.

Scheme 33. Scale-up and isolation of initial arylboration hit.

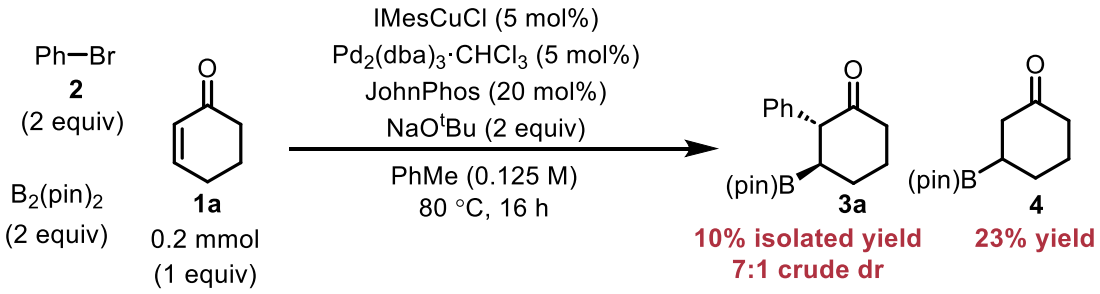

2.2.2: Reaction optimization

With the initial arylboration hit in hand, optimization of the reaction conditions was commenced. The yield of conjugate borylation side product **4** was tracked alongside the arylboration product **3a** throughout the optimization to gain insight into the effectiveness of transient Cu-enolate trapping with Pd, and in hopes of suppressing this side product to make chromatographic purifications easier to perform.

While the initial hit reaction was found through a discovery plate run at 80 °C and many reported alkene arylboration reactions require elevated temperatures,[58,109,111] a plethora of Cu/Pd-catalyzed alkene arylboration reactions[77,87,92] and enone conjugate borylation reactions[29,36,112] occur readily at room temperature. Thus, we reasoned that it may be possible to reduce the reaction temperature without much impact on arylboration yield.

Table 1. Screening of reaction temperatures.

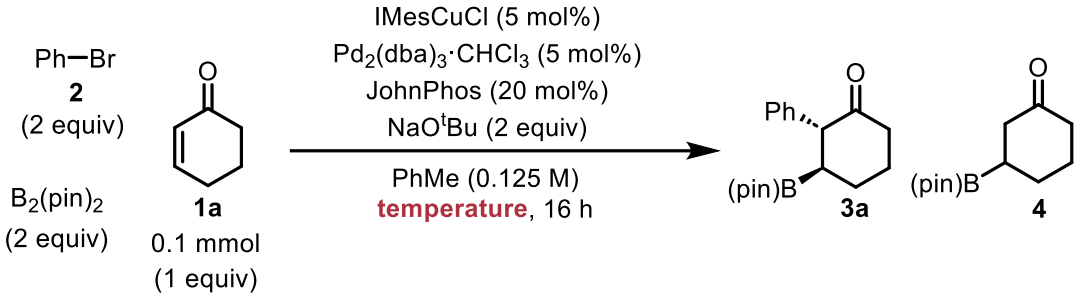

entry	temperature (°C)	yield **3a** (%)	yield **4** (%)
1	80	11	25
2	50	9	20
3	22	11	22
4	5	6	29
5	-17	5	17

GC-MS yields with naphthalene as internal standard

Surprisingly, reaction temperature seems to have no significant impact on arylboration or conjugate borylation yield between 80 °C and 22 ºC, with similar yields being found throughout this range (Table 1, entries 1-3). Somehow, the relative rates of competing pathways seem not to be affected. Running the reaction inside a standard lab fridge (entry 4) or freezer (entry 5),

however, results in reduction in arylboration yield. Based on these results, room temperature (22 ºC) was selected as the optimal temperature to carry forward given its mildness, good yields and experimental convenience.

Since the initial discovery plate (Figure 2) demonstrates that ligand choice is crucial for the success of the arylboration reaction, ligands for palladium were screened next. The discovery plate showed that JohnPhos, a Buchwald phosphine ligand, out-performs bidentate and monodentate phosphines. Thus, focus was placed on screening other Buchwald ligands, along with an uncommon 1,5-Diaza-3,7-diphosphacyclooctane (P_2N_2) ligand used by our group in other transformations which Buchwald ligands are typically used for.[113–116]

Table 2. Screening of ligands for palladium.

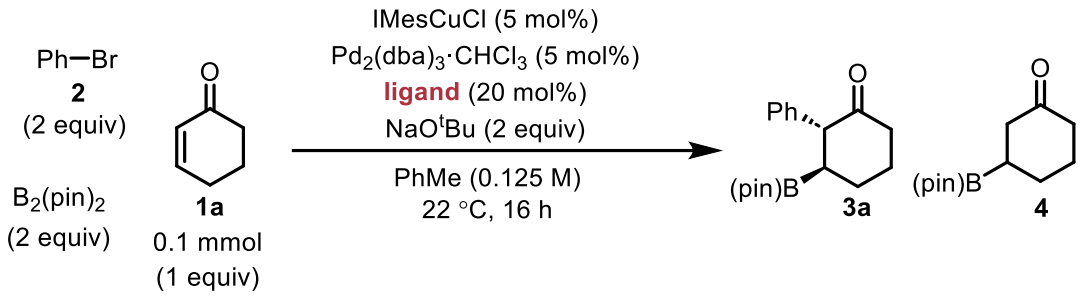

entry	ligand	yield **3a** (%)	yield **4** (%)
1	JohnPhos	12	21
2	XPhos	5	19
3	CyJohnPhos	1	30
4	DavePhos	1	28
5	^{t}BuXPhos	4	33
6	SPhos	0	35
7	$(P^{Ph}N^{ArCF3})_2$	0	33
8	dppf	2	27

GC-MS yields with naphthalene as internal standard

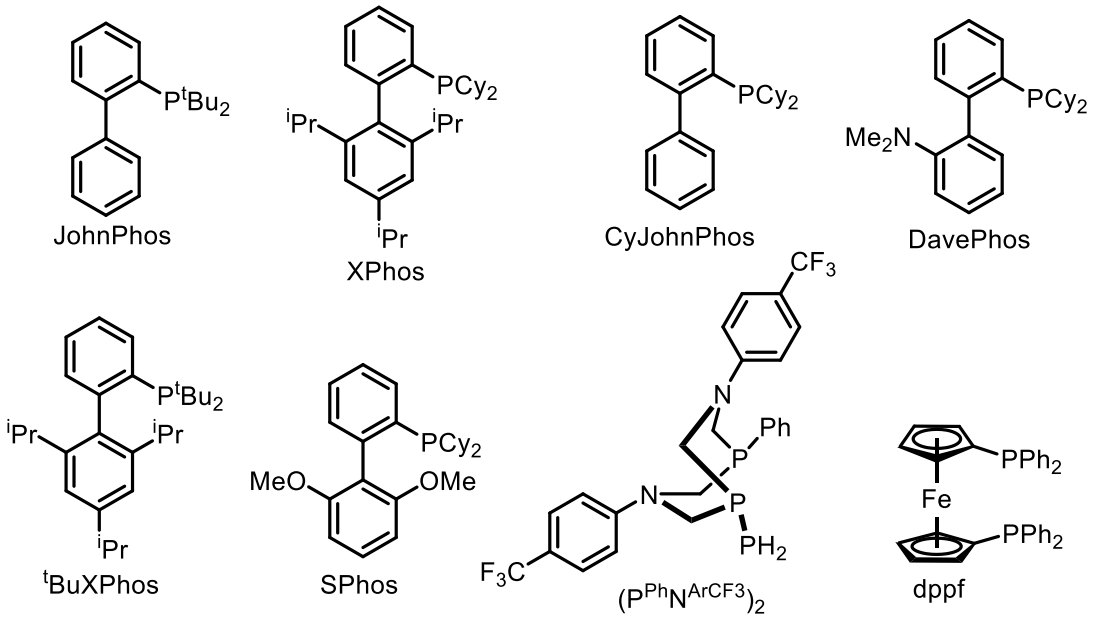

Surprisingly, the initial hit ligand, JohnPhos, remained as the best Pd ligand for this transformation based on the results in Table 2. Most other ligands screened give only trace amounts of product, highlighting the sensitivity of this challenging reaction system to any changes. JohnPhos was also the optimal ligand in our lab's Morita–Baylis–Hillman-inspired Pd-catalyzed enone α-arylation (Section 1.1.3.4),[37] demonstrating the strength of this particular ligand in imparting the necessary properties onto Pd for the trapping of transient enolate intermediates.

Pd pre-catalysts were screened next (Table 3). Most of the pre-catalysts screened provide arylboration yields which are likely within experimental error, and no big changes are observed. At this point, it was becoming increasingly clear that modifications to the palladium catalytic system would likely not result in major improvements in reaction yield. However, the allyl chloride dimer pre-catalyst seemed to show the most consistent and reproducible results out of all the palladium sources screened, so this was selected for further study.

Table 3. Screening of palladium pre-catalysts.

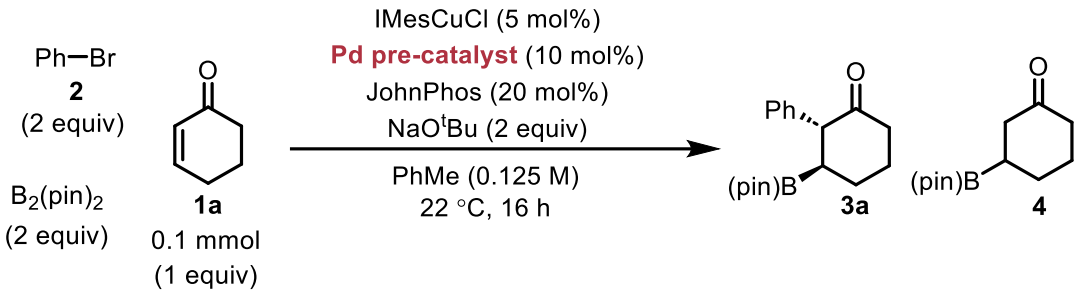

entry	Pd pre-catalyst	yield **3a** (%)	yield **4** (%)
1	$Pd_2(dba)_3 \cdot CHCl_3$	12	24
2	Pd(cinnamyl)Cp	10	28
3	$Pd(OAc)_2$	13	26
4	Pd-JohnPhos-G3 + 10 mol% JohnPhos	8	31
5	$[Pd(cinnamyl)Cl]_2$	11	27
6	$[Pd(allyl)Cl]_2$	15	23

GC-MS yields with naphthalene as internal standard

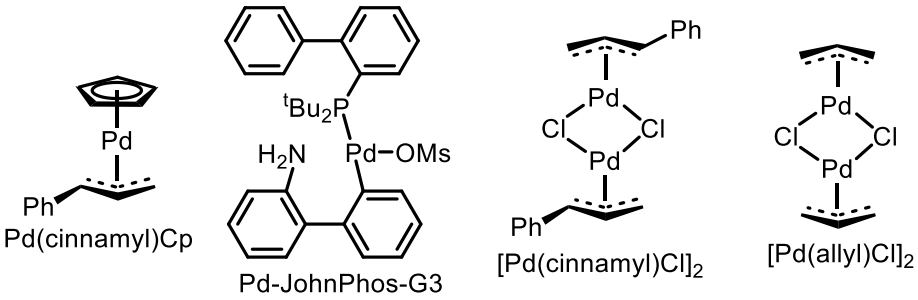

The rate of oxidative addition into an aryl halide, as well as the electrophilicity of the resulting oxidative addition complex, is known to be influenced by the identity of the halide. Typically, weaker carbon-halogen bonds result in faster oxidative addition, and also provide more cationic oxidative addition complexes since the resulting halide counterion is less coordinating.[117] Based on this, it can be expected that the halide identity would have an impact on arylboration yield. One may predict that faster oxidative addition and a more cationic oxidative addition complex is desirable in this chemistry, since this would maximize the rate of formation of oxidative addition complexes and improve their reactivity towards trapping with copper enolates. Halides

that form weaker bonds to carbon and which are less coordinating are expected to give higher yields. Thus, a range of common aryl halides and pseudo-halides were screened (Table 4).

Table 4. Screening of aryl (pseudo)halides.

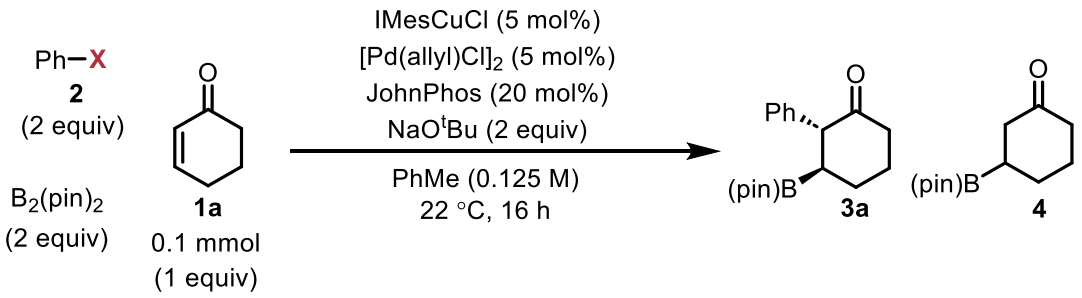

entry	Phenyl (pseudo)halide	yield **3a** (%)	yield **4** (%)
1	Chloride	10	34
2	Bromide	14	25
3	Iodide	7	21
4	Triflate	23	24

GC-MS yields with naphthalene as internal standard

Interestingly, the trend in yield upon changing the halide portion of the aryl halide is not fully clear. Iodides and triflates are expected to give higher arylboration yields than bromides since they form weaker bonds to the aromatic group, would result in faster oxidative addition, and give more cationic complexes; this is not observed, as the iodide underperforms relative to both the bromide and triflate. It is unclear why this is the case. Nevertheless, there is a clear and significant improvement in yield upon switching from aryl bromide to aryl triflate, so optimization was continued with the triflate. After struggling to improve yields by a significant margin up to this point, the improvement up to over 20% yield proved exciting, and hope in this reaction was restored.

Subsequently, attention was turned to screening various solvents and bases for the arylboration reaction. It was hypothesized that interdependencies may be present in the solvent and base systems, since solubility of bases in various solvents may affect their abilities to operate as effective activators for $B_2(pin)_2$. For this reason, a high-throughput screening plate for the

optimization of solvent and base was conducted. A series of 12 bases and 8 solvents were chosen and screened as shown in Figure 3.

Figure 3. High-throughput screening of solvents and bases.

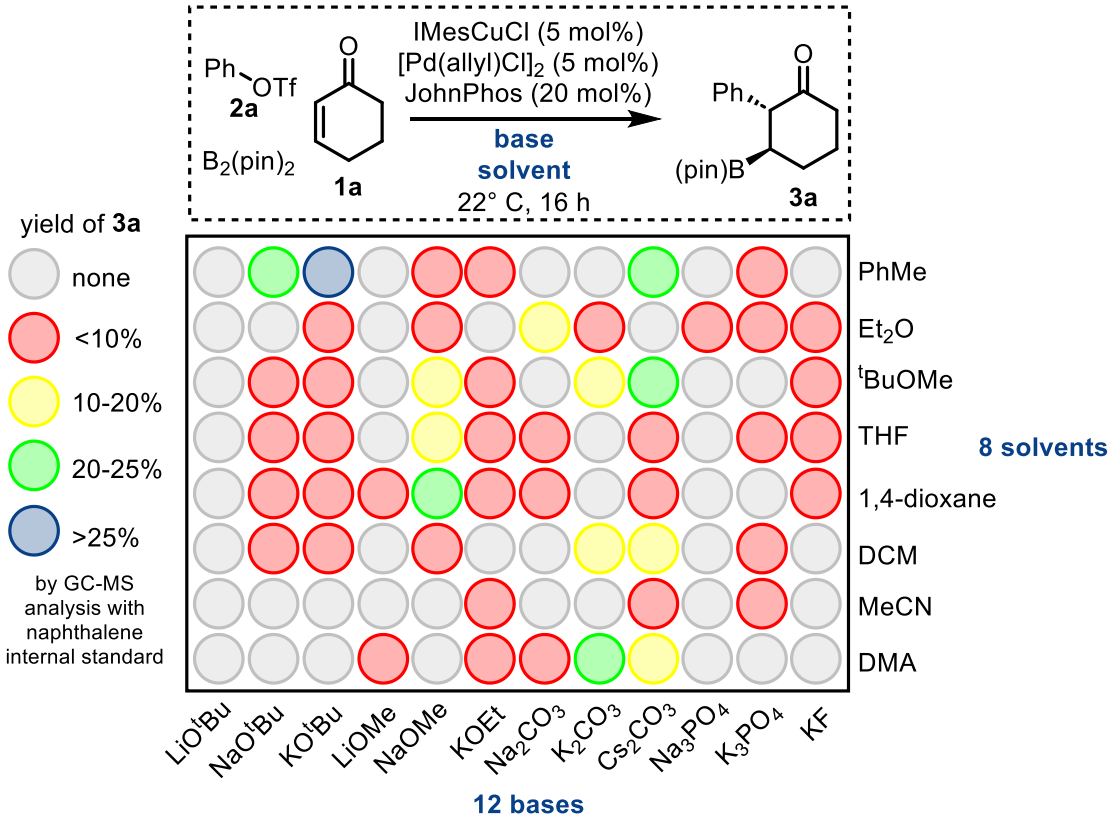

None of the solvents surveyed performed better than toluene, although some ethereal solvents like THF and dioxane provided a few hits with moderate yields when employing different bases. The difference in yield between the series of alkali metal *tert*-butoxides is quite stark, with LiO^{t}Bu failing universally, and yields rising sharply with the heaver sodium and potassium bases. Most notably, switching from sodium to potassium *tert*-butoxide provides a significant increase in yield of arylboration product **3a**, so KO^{t}Bu was carried forward.

Given the results from the initial discovery plate in Figure 2, high arylboration yield only seems to be provided by NHC ligands on copper. Since up until this point only IMes had been tested, a series of other common NHC-CuCl complexes were synthesized and evaluated as shown in Table 5.

Table 5. Screening of NHC ligands for copper.

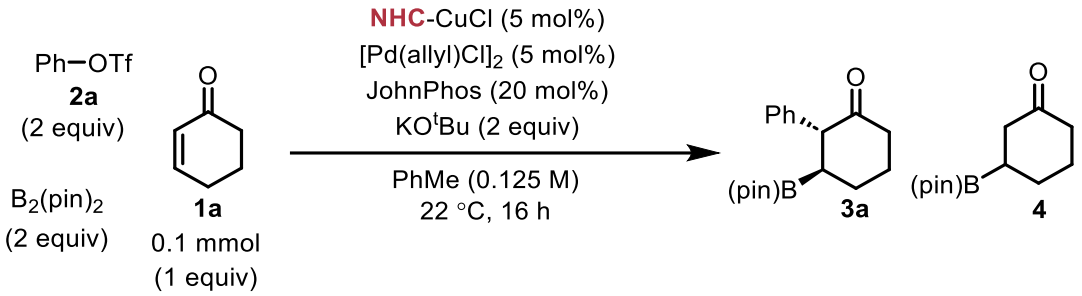

entry	NHC	yield **3a** (%)	yield **4** (%)
1	IMes	28	20
2	SIMes	31	34
3	IPr	19	12
4	SIPr	17	8
5	I^{t}Bu	17	13
6	ICy	24	23

GC-MS yields with naphthalene as internal standard

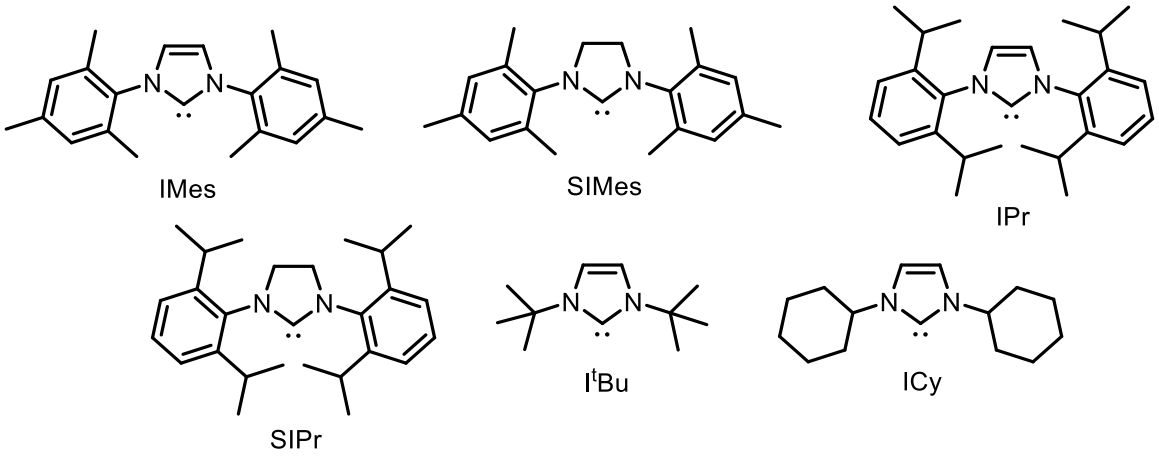

Once again, the ligand identified in the initial screen, IMes, shows the best reactivity pattern. Although SIMes shows slightly higher yield of **3a**, this may be within experimental error and is not worth the switch given the marked increase in the undesired hydroboration side product **4**.

With the major discrete variables optimized and set in stone, the equivalents of each reagent were manipulated next. Given the known Lewis acid-base interaction between *tert*-butoxide bases

and $B_2(pin)_2$ and the importance of this activation in conjugate borylation chemistry (Scheme 6 and Section 1.1.3.3),[32] it was expected that the ratio between the amount of base and boron reagent would be highly impactful on our arylboration outcome. This is explored below in Table 6.

Table 6. Screening of equivalents of KO^{t}Bu and $B_2(pin)_2$.

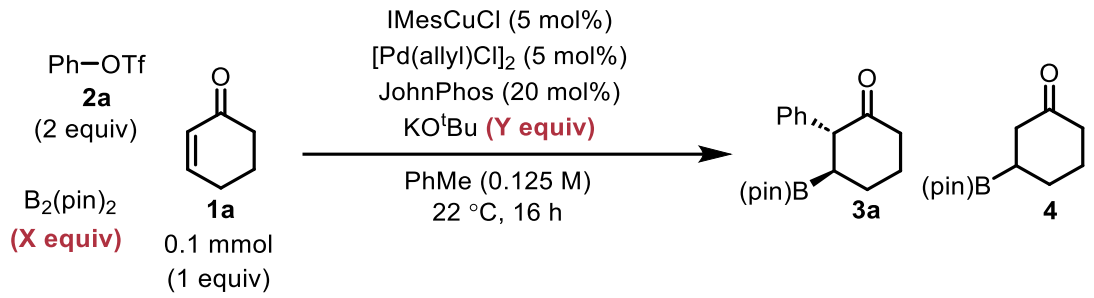

entry	**X** equiv $B_2(pin)_2$	**Y** equiv KO^{t}Bu	yield **3a** (%)	yield **4** (%)
1	2.0	1.2	26	33
2	2.0	1.5	29	28
3	2.0	1.7	33	27
4	2.0	2.0	27	22
5	2.0	2.5	14	16
6	1.7	1.5	16	15
7	2.3	1.5	29	36
8	2.4	2.0	39	34

GC-FID yields with naphthalene as internal standard

When keeping the loading of $B_2(pin)_2$ constant and varying the equivalents of KO^{t}Bu (entries 1-5), some interesting trends appear. Around 1.7 equivalents of base seems to be the sweet spot for maximizing yield of **3a**, as yields decrease as equivalents are altered in either direction. Additionally, yield of conjugate borylation side product **4** tends to increase as the equivalents of base are reduced (entries 1-5). This makes given that an excess of electrophilic boron reagent likely increases the rate of σ-metathesis between Cu-enolates and $B_2(pin)_2$, especially if there is not enough base to activate the boron reagent towards more nucleophilic reactivity. If the equivalents of KO^{t}Bu are increased to 2.5 (entry 5), the result is a sharp decline in both yield of **4** and **3a**. This suggests that if the boron reagent is saturated by interactions with KO^{t}Bu, any excess KO^{t}Bu may be detrimental to one or both of the metal catalysts. At this point, loadings of 1.7 equivalents of

KO^{t}Bu and 2.0 equivalents of $B_2(pin)_2$ seems to be an improvement. When keeping the equivalents of KO^{t}Bu set at 1.5 and changing the amount of $B_2(pin)_2$ (entries 2 and 6-7), similar trends are unraveled. With fewer equivalents of $B_2(pin)_2$, the yield of **4** is reduced as there is less of the boron reagent available, but there is also a reduction in arylboration yield. Upon increasing the equivalents of $B_2(pin)_2$ to 2.3 (entry 7), yield of **3a** is restored, yet as expected, yield of **4** increases concomitantly. Given that the best equivalents thus far were 1.7 equivalents of KO^{t}Bu and 2.0 equivalents of $B_2(pin)_2$, and that the relative ratio between these reagents heavily impacts yield and side product formation, a final experiment was run in which the ratio was kept constant (2:1.7, or 1.2:1), but the overall loading increased (entry 8). To our delight, a higher yield of arylboration product **3a** was obtained with 2 equivalents of KO^{t}Bu and 2.4 equivalents of $B_2(pin)_2$. Given the difficulty in improving the yield of this transformation, the slight increase in conjugate borylation product **4** is acceptable and inevitable in this case. Use of $B_2(cat)_2$ in place of $B_2(pin)_2$ was considered, but only gave conjugate borylation, with no trace of arylboration product.

Thus far, the cyclic enone **1a** has been held as the limiting reagent given that this is the substrate on which the difunctionalization is occurring. However, for the purpose of synthetic applications, it may be more cost-efficient to use excess enone and limiting aryl triflate, as aryl triflates are often more expensive than the cheap and accessible enone. For this reason, the equivalents of enone and aryl triflate were tested in Table 7.

Table 7. Screening of equivalents of aryl triflate and enone.

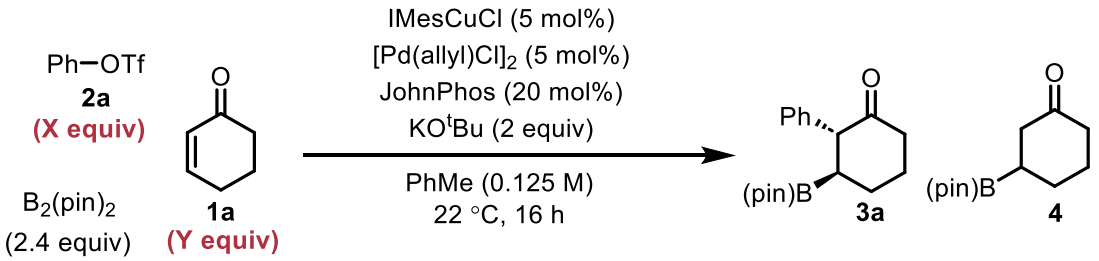

entry	**X** equiv **2a**	**Y** equiv **1a**	yield **3a** (%)	yield **4** (%)
1	2.0	1.0	35	38
2	1.5	1.0	32	43
3	1.0	1.5	40	51
4	1.0	2.0	49	54

GC-FID yields with naphthalene as internal standard. 0.1 mmol of limiting reagent in all cases.

From these results, it can be concluded that the arylboration yield of **3a** is higher when the cyclic enone **1a** is in excess and the aryl triflate **2a** is limiting, albeit with greater quantities of the conjugate borylation side product **4** forming as well. This makes sense given the fact that the undesired conjugate borylation pathway will inevitably take away from the equivalents of cyclic enone, detracting from the yield; in contrast, if there is excess enone, conjugate borylation is less consequential. With limiting aryl triflate, the relevant side products that contribute to the loss of yield are the Miyaura borylation and homocoupling products (Section 2.1.4), and these two make up most of the remaining mass balance in this case. Nevertheless, limiting the amount of conjugate borylation product and tracking its formation remains worthwhile goal given the difficulty of removing this side product in the purification.

At this point, it is worth addressing the reaction setup. Over the course of the reaction optimization, it had been observed empirically that results are more consistent when pre-mixing the Pd pre-catalyst with excess JohnPhos for 30 mins before adding it to the rest of the reaction components. This protocol had been used for all the optimization experiments up until this point. However, this adds complexity to the reaction setup and is quite inconvenient. Additionally, the necessity of the 20 mol% of JohnPhos had not been validated. An alternative catalyst option would be to form the pre-ligated (JohnPhos)Pd(allyl)Cl complex, which has been shown to be an efficient, air- and moisture-stable pre-catalyst.[118–120] This complex was tested in Table 8.

Table 8. Screening of pre-ligated palladium allyl chloride complex.

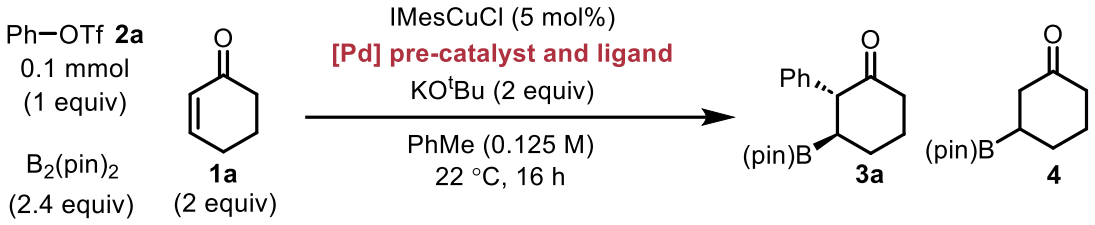

entry	[Pd] pre-catalyst and ligand	yield **3a** (%)	yield **4** (%)
1[a]	$[Pd(allyl)Cl]_2$ (5 mol%) + JohnPhos (20 mol%)	47	56
2[b]	(JohnPhos)Pd(allyl)Cl (10 mol%)	46	51
3[b]	(JohnPhos)Pd(allyl)Cl (10 mol%) + JohnPhos (10 mol%)	47	55

GC-FID yields with naphthalene as internal standard. [a]The Pd pre-catalyst and JohnPhos were pre-mixed by stirring in PhMe for 30 mins at room temperature in a glovebox prior to addition of this metal-ligand mixture to the reaction vial. [b]No pre-mixing of Pd and JohnPhos; both reagents were added directly to the reaction vial as solids.

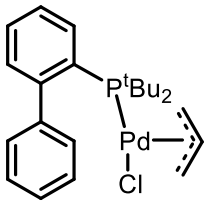

(JohnPhos)Pd(allyl)Cl

As seen from the results in Table 8, there is practically no difference in yield between the pre-mixing setup with allyl chloride dimer and excess ligand (entry 1) when compared to the pre-formed complex without any added ligand (entry 2). Additional ligand on top of the pre-formed complex (entry 3) also makes no significant difference in product yield. For the simplicity of the reaction setup, (JohnPhos)Pd(allyl)Cl was selected as the best catalyst, as it eliminates the need for any pre-mixing and reduces the number of reagents one must weigh out for the reaction.

With all the discrete variables and most of the equivalencies of reagents now tested, very few options remain possible changes to improve arylboration yields. One major component which has not been discussed up to this point is the loading of the copper and palladium catalysts. Based on the proposed mechanism for the arylboration (Section 2.1.3) and the subsequent kinetic arguments provided for the trapping of the copper enolate (Section 2.2.1), it was predicted that low

loadings of copper and high loadings of palladium would be ideal for this transformation. This is validated in Table 9.

Table 9. Screening loading of copper and palladium.

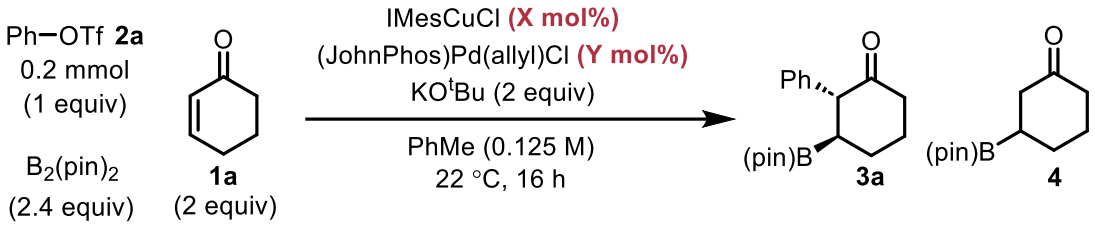

entry	[Cu] **X** mol%	[Pd] **Y** mol%	yield **3a** (%)	yield **4** (%)
1	7.5	10	43	46
2	5.0	10	44	49
3	2.5	10	57	39
4	1.0	10	51	42
5	0	10	0	0
6	2.5	7.5	27	48
7	2.5	5	21	55

GC-FID yields with naphthalene as internal standard

Reducing copper loading down from 7.5 mol% to 2.5 mol% offers an improvement in yield of **3a** (entry 1 to 3), while also reducing the amount of side product **4** that forms. This is in line with the mechanistic hypothesis that it is desirable to limit the concentration of active copper enolates in the reaction mixture to ensure that there is enough oxidative addition complex present for productive trapping. Reducing copper loadings down to 1 mol% caused a slight reduction in yield (entry 4), while removing copper altogether shuts down all arylboration and conjugate borylation chemistry (entry 5). This proves that there is no possible mechanism for background conjugate borylation chemistry under our conditions, and that both products **3a** and **4** emerge through a copper-promoted initial insertion of the boronate ester into the enone to form a copper enolate that is common to both pathways. Also in support of the mechanistic hypothesis is the fact that reducing palladium loadings at all below 10 mol% results in a marked reduction in arylboration yield, along with an increase in conjugate borylation (entries 6-7). With a reduced amount of oxidative addition complex present in solution, more of the copper enolates are directed towards the conjugate borylation pathway rather than the desired arylboration. From these

experiments, the copper and palladium loadings are optimized at 2.5 mol% and 10 mol%, respectively for our arylboration reaction.

The last continuous variable which had not been previously explored in this reaction is concentration. The results in Table 10 show that the reaction yield and side product formation are not significantly impacted by concentration between the range of 0.1 to 0.5 M. For the optimized catalytic reaction, 0.2 M was selected as a reasonable balance.

Table 10. Screening of concentration.

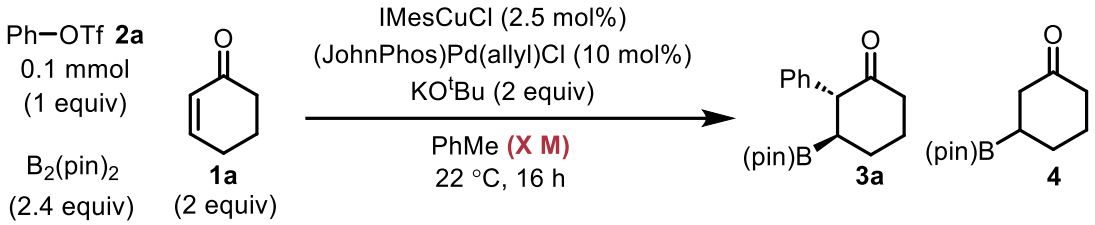

entry	concentration **X** (M)	yield **3a** (%)	yield **4** (%)
1	0.1	56	36
2	0.2	55	37
3	0.3	53	41
4	0.5	56	37

GC-FID yields with naphthalene as internal standard

With all discrete and continuous variables of the arylboration reaction now screened, we turned our attention towards attempting to assess the impact of water on the reaction outcome, with the goal of suppressing the formation of conjugate borylation product **4** and improving the yield of arylboration product **3a**. Since it is assumed that **4** arises from hydrolysis of a boron enolate (see discussion in Section 2.1.4), it was hypothesized that it may be possible to limit this pathway through vigorous removal of water from the reagents or reaction. Addition of drying agents and sieves was considered, along with using recrystallized $B_2(pin)_2$ in case it was contaminated with either water or pinacol. Purposeful addition of water was also performed as a control to confidently determine whether additional water is detrimental to the reaction.

Table 11. Assessing the impact of water.

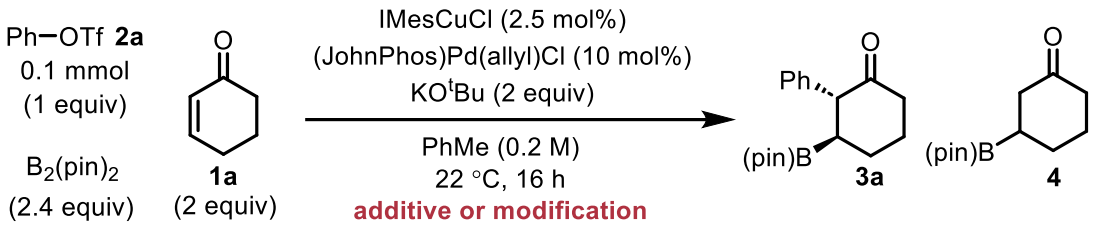

entry	additive or modification	yield **3a** (%)	yield **4** (%)
1	none	53	34
2	H_2O (2 equiv)	2	110
3	$B_2(pin)_2$ recrystallized in pentane	22	24
4	Na_2SO_4 (2 equiv)	37	27
5	$MgSO_4$ (2 equiv)	21	41
6	crushed 4 Å mol. sieves (50 mg)	34	27

GC-FID yields with naphthalene as internal standard

As shown in Table 11, the addition of water clearly shuts down the desired arylboration reactivity, while also shuttling most of the enone substrate towards conjugate borylation product **4** (entry 2). This confirms that additional water is detrimental to the reaction, and that conjugate borylation arises from the protonation of enolate intermediates. However, none of the measures taken to remove water were productive towards improving the reaction outcome, as the yields of **3a** decreased, and the production of **4** was not significantly altered (entries 3-6). It is possible that small amounts of water in the reagents may be beneficial to the reaction,[55] but this same water also necessitates the formation of the side product **4**. At this point, the proton source and mechanism of formation of **4** remain unclear.

It became evident at this point that improving the arylboration yield further would likely be quite difficult, as most of our ideas for screening had already been carried out, and the yields of **3a** remained stuck in the mid-50% range. Challenges in optimizing the reaction further likely arise from the plethora of side pathways available, and the kinetic difficulty in funneling the reaction towards the desired arylboration reaction rather than the undesired conjugate borylation, Miyaura borylation, and homocoupling side products, which are where the remainder of the mass balance

resides. Thus, we settled on the conditions in Table 11, entry 1 as our optimized conditions for the arylboration of cyclic enones with aryl triflates.

Since the optimization campaign was commenced with aryl bromides, and aryl bromides still give acceptable yields when compared to aryl triflates (Table 4), a significant amount of time was spent trying to optimize the arylboration reaction with aryl bromide substrates. The only beneficial change found was a slight modification to the loadings of copper and palladium catalysts.

Table 12. Screening loading of copper and palladium for aryl bromide substrates.

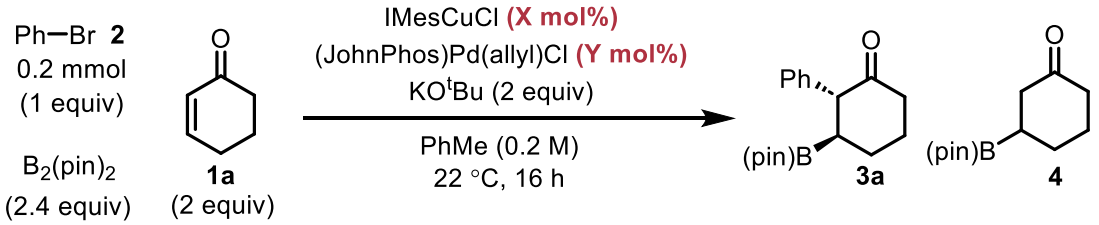

entry	[Cu] mol%	[Pd] mol%	yield **3a** (%)	yield **4** (%)
1	2.5	10	32	62
2	5.0	10	41	45
3	7.5	10	49	44
4	10	10	50	47
5	7.5	7.5	48	50
6	7.5	5.0	40	55

GC-FID yields with naphthalene as internal standard

As shown in Table 12, increasing the amount of copper to 7.5 mol% improves arylboration yield and suppresses hydroboration (entries 1-3). This effect is not understood and goes against the logical kinetic argument (enolate trapping) assumed based on the proposed mechanism, but suggests that there is a difference in the reaction kinetics between triflates and bromides. Furthermore, the palladium loading can be reduced to 7.5 mol% without much change in yield, though reducing it further to 5 results in a significant reduction (entries 5-6). Thus, a catalyst loading of 7.5 mol% was selected as optimal for both copper and palladium for arylboration reactions conducted with aryl bromide substrates.

Lastly, in efforts of improving the arylboration yield with aryl bromides even further, the addition of salt additives was considered. It is well-known that metal halide or pseudo-halide salts can strip palladium oxidative addition complexes of their bromide counterions, rendering the complex more cationic, and providing higher yields in various types of cross-coupling transformations.[113,121–124] Assuming that a more cationic Pd complex would be more reactive towards transmetallation with copper enolates and improve arylboration yields, several of these common metal halide/pseudo-halide salt additives were screened (Table 13). Unfortunately, none of the salts screened were beneficial, and most caused yields of **3a** to plumet. Thus, there remained no reasonable ideas for improving the reaction, and the optimization for both aryl bromides and triflates was completed at this point.

Table 13. Screening salt additives for aryl bromide substrates.

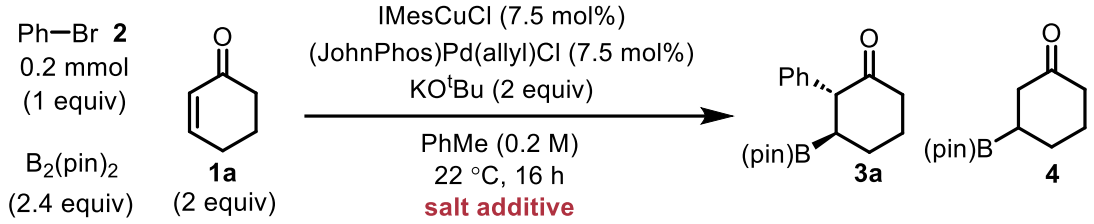

entry	salt additive (1 equiv)	yield **3a** (%)	yield **4** (%)
1	none	46	49
2	LiOTf	27	61
3	KOTf	24	41
4	LiCl	17	13
5	KI	18	16
6	NaI	18	14
7	KBr	20	19
8	$NaBF_4$	20	12
9	LiTFA	10	31
10	$LiBF_4$	6	31

GC-FID yields with naphthalene as internal standard

It is worth noting that none of the changes tested throughout the course of the optimization campaign on aryl triflates and bromides had any significant impact on the anti/syn dr of the

arylboration product **3a** (consistently 7:1 crude dr), suggesting that this feature is substrate dependent.

2.2.3: Substrate scope and large-scale reaction

With the optimized conditions in hand, the substrate scope was evaluated. The range of tolerated organo-(pseudo)halides is presented in Scheme 34, with the diversity of cyclic enones shown in Scheme 35. In general, yields are moderate, ranging in the 30% to 65% range. Though this is rather low for an optimized reaction, it is acceptable given the amount of complexity generated by this single-step enone difunctionalization, the great challenge posed by side products in this system, and the extensive effort placed into optimization. Furthermore, the yields from this one-step difunctionalization are rather enabling when compared to the existing three-step approach (iodination, Suzuki coupling, and conjugate borylation) discussed in Section 2.1.2, further justifying the utility of this new method despite its moderate yield. Diastereoselecitivies, on the other hand, are high, ranging from 5:1 to exclusive (>20:1) favouring anti products. Importantly, the reported yields are for pure isolated anti diastereomers of the arylboration products, while the diastereomer ratios shown are the crude dr by GC-FID analysis of unpurified reaction mixtures.

A range of para-substituted aryl triflates are tolerated (**3a**-**3i**) (Scheme 34). Electron-donating substituents, such as methoxy (45%, **3e**), give comparable yields to electron-withdrawing substituents, such as a methyl ester (46%, **3i**). This suggests that the reaction is not very sensitive to electronic effects on the aromatic coupling partner. Surprisingly, some sensitive or coordinating functionalities are tolerated, with moderate yields being provided by aryl triflates bearing chloro (**3f**), fluoro (**3g**), or nitro group (**3h**). Furthermore, aromatic rings with substitution at the meta and ortho positions are tolerated (**3j**-**3n**) in similar yields to their para-substituted counterparts (50% yield ortho-methoxy **3l** compared to 45% of para-methoxy **3e**). This suggests that steric hindrance also does not majorly impact yield. While the para- and meta-substituted substrates provide arylboration products in 5:1 to 9:1 crude dr (**3a**-**3k**), ortho-substituted aryl triflates provide exclusively the anti products (>20:1 in **3l**-**3n**). This confirms the notion that diastereoselectivity is substrate-controlled in this reaction, and also suggests that steric hindrance on the aromatic partner is important at the diastereo-determining step. Logically, this makes sense, as a more sterically hindered Pd centre in the oxidative addition complex would lead to a more diastereoselective transmetallation with the copper enolate, as repulsion with the boronate ester would be increased.

Scheme 34. Substrate scope of organo(pseudo)halides.[a]

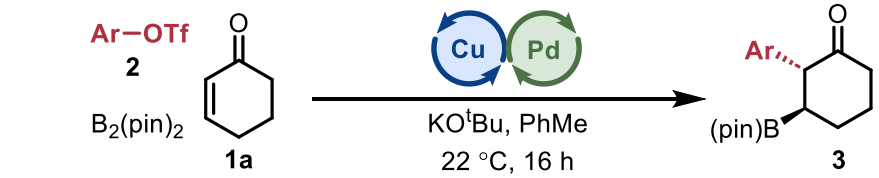

*scope of organo(pseudo)halides (with cyclohexenone **1a**)*

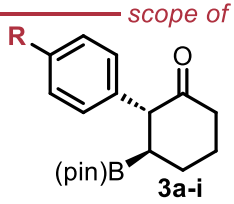

Product	R	yield	dr
3a	H	47%	7:1
3b	Ph	50%	9:1
3c	^{t}Bu	65%	7:1
3d	Me	45%	5:1
3e	OMe	53%	6:1
3f	Cl	31%	8:1
3g	F	31%	5:1
3h	NO_2	37%	9:1
3i	CO_2Me	46%	8:1

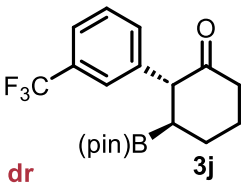

48% yield
7:1 dr

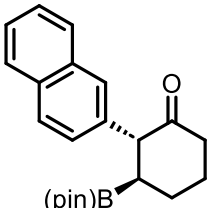

38% yield
7:1 dr

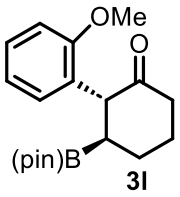

50% yield
>20:1 dr

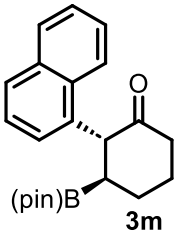

36% yield
>20:1 dr

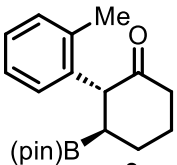

38% yield
>20:1 dr

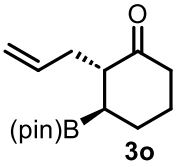

23% yield
>20:1 dr
from allyl carbonate

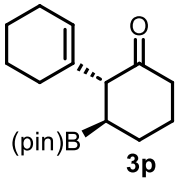

42% yield
12:1 dr
from VinylOTf

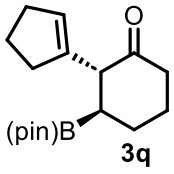

34% yield
10:1 dr
from VinylOTf

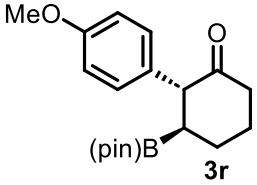

34%, 46%[b] yield
5:1 dr
from ArBr

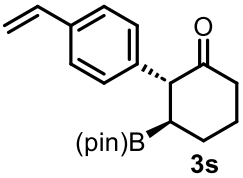

33%[b] yield
4:1 dr
from ArBr

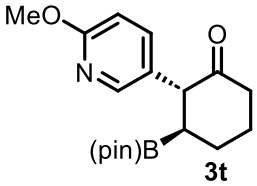

45%[b] yield
4:1 dr
from ArBr

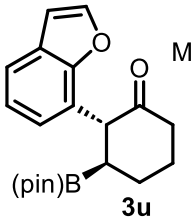

30%[b] yield
>20:1 dr
from ArBr

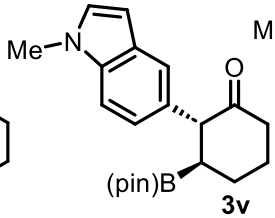

53%[b] yield
18:1 dr
from ArBr

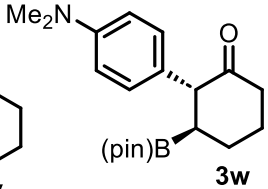

56%[b] yield
10:1 dr
from ArBr

[a]General reaction conditions: Cyclohex-2-ene-1-one **1a** (0.4 mmol), ArOTf **2** (0.2 mmol), $B_2(pin)_2$ (0.48 mmol), KO^{t}Bu (0.4 mmol), IMesCuCl (2.5 mol%), (JohnPhos)Pd(allyl)Cl (10 mol%), toluene (0.2 M), room temperature, 16 h. Isolated yields of anti **3** are shown. Crude anti/syn dr of products **3** determined by GC-FID of the crude reaction. [b]7.5 mol% copper and 7.5 mol% palladium catalysts were used.

A selection of more unique substrates, such as allyl carbonate (**3o**) and alkenyl triflates (**3p** and **3q**) also undergo arylboration in moderate yields (23-48%). It is worth noting that

cyclohexenyl triflate provides a higher dr (12:1 in **3p**) than the corresponding phenyl triflate (7:1 in **3a**), which is in accordance with the hypothesis that the steric bulk of the organohalide coupling partner influences diastereoselectivity. Several aryl and heteroaryl-bromides also provide decent yields of arylboration product (**3r**-**3w**). Using the triflate-optimal conditions of 2.5 mol% Cu and 10 mol% Pd catalysts, para-methoxy bromobenzene gives a 34% isolated yield of **3r**; however, with the bromide conditions of 7.5 mol% of both catalysts, this is improved to 46%. Additionally, 4-bromostyrene functions as a substrate, providing **3s** in 33% yield, without any detection of arylboration or hydroboration of the styrene itself. This demonstrates that our optimized conditions are selective for cyclic enones over styrene substrates, and are complementary to previous works. Some pharmaceutically relevant aryl bromides including heterocycles and nitrogen atoms provide moderate yields of arylboration products (**3t**-**3w**).

Some interesting trends are also seen in the scope of cyclic enones (Scheme 35). While the larger cyclohexenone ring provides a moderate 46% yield of product **3ab** (albeit as an inseparable 6:1 mixture of anti/syn diastereomers), switching to the smaller cyclopentenone results in a dramatic decline in yield down to 17% for **3ac**. This finding, though not understood, mirrors that reported by our group in the Morita–Baylis–Hillman-inspired enone α-arylation,[37] in which cyclopentenones were also lower-yielding substrates than cyclohexenones and cycloheptenones. A γ,γ-dimethyl substituted cyclohexenone derivative is also tolerated as a substrate in this chemistry, providing 38% yield of arylboration product **3ad**. Though this may be surprising given the hindered nature of the β-carbon due to the adjacent quaternary centre, conjugate borylation reactions on similar substrates are known.[35] Another feature of this example is that the diastereoselectivity is again favoured exclusively towards the anti arylboration adduct, with no traces of the syn material detected by GC-FID. Assuming that the boronate ester lies in an equatorial position, it is likely that the syn-facing axial methyl group hinders and fully prevents the approach of the palladium oxidative addition complex from that face, forcing it to approach from the opposite face and providing only the anti product. In the case of a γ-mono-methyl enone substrate, the all-anti arylboration product **3ae** is obtained. This suggests that the initial insertion of the boryl copper species occurs selectively on the opposite side of the methyl group. The crude material was detected as an 8:1 mixture of diastereomers, though it is not clear which stereochemical relationship is present in the minor product. A similar level of selectivity is observed in the arylboration of a γ-methyl, γ-phenyl substrate, with borylation occurring anti to

the bulkier phenyl group to ultimately give rise to **3af**. Arylboration of a 5-methyl cyclohexenone derivative also provides moderate levels of facial diastereoselectivity (6:1 dr for **3ag**), with the B(pin) insertion predominantly occurring opposite to the methyl group. This observation is best explained by conformational control through the Fürst-Plattner rule; the methyl substituent lies equatorially, and the B(pin) preferentially inserts the enone following an axial approach to provide a chair-like transition state.

Scheme 35. Substrate scope of cyclic enones.[a]

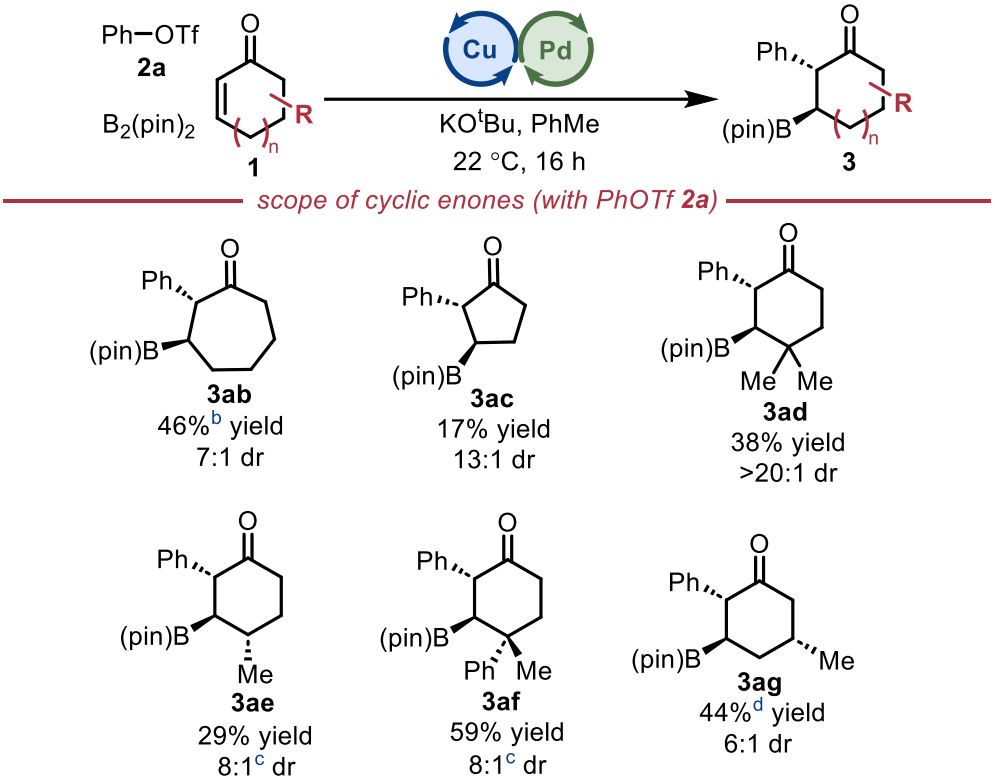

[a]General reaction conditions: Cyclic enone **1** (0.4 mmol), PhOTf **2a** (0.2 mmol), $B_2(pin)_2$ (0.48 mmol), KO^{t}Bu (0.4 mmol), IMesCuCl (2.5 mol%), (JohnPhos)Pd(allyl)Cl (10 mol%), toluene (0.2 M), room temperature, 16 h. Isolated yields of anti **3** are shown. Crude anti/syn dr of products **3** determined by GC-FID of the crude reaction. [b]Product **3ab** was isolated as an inseparable 6:1 anti/syn mixture. [c]Products **3ae** and **3af** were isolated as single diastereomers. The stereochemistry of the minor diastereomers were not determined. [d]Product **3ag** was isolated as an inseparable 4:1 mixture of diastereomers varying at the Me stereocentre.

All the scope examples discussed previously were conducted on a 0.2 mmol reaction scale, which is rather small when considering the standard scale of chemical processes in industrial syntheses. To demonstrate preliminary evidence for the scalability of this novel enone arylboration, the reaction was conducted on a 1 mmol scale, as shown in Scheme 36. The desired product (168 mg) was obtained in 48% yield, which is not significantly different from the 0.2 mmol scale reaction. This demonstrates that the reaction can be run on larger scales without any detriment.

Scheme 36. Large-scale arylboration of cyclic enone.

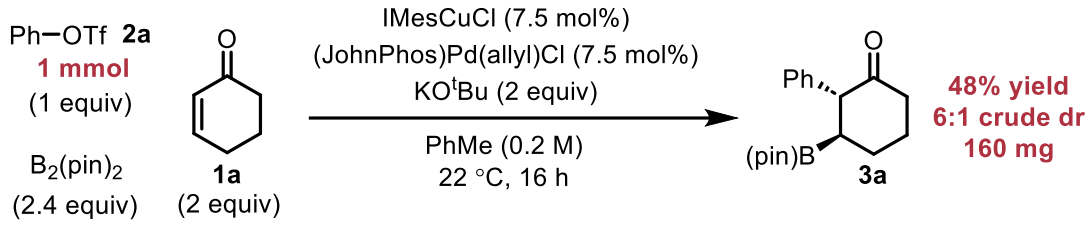

Isolated yield of anti **3a** reported. Crude dr determined by GC-FID analysis.

Aside from the obviously moderate and even low yield of this reaction, several other limitations are present in terms of substrates that are completely incompatible. A selection of failed substrates, which provide either no arylboration, trace amounts of product, or yields below 20%, are shown in Scheme 37 and Scheme 38.

We will commence with the discussion of the failed organo-(pseudo)halides. In most cases, plentiful conjugate borylation is observed along with Miyaura borylation and homocoupling products, but arylboration is unsuccessful. This suggests facile insertion of the boryl copper, but failures in the palladium side of the pathway. Some examples also leave behind leftover organo-(pseudo)halide starting material, suggesting potential palladium catalyst deactivation or failed oxidative addition. Aryl triflates with excessive steric bulk in the ortho position, such as a TMS group, tend to fail. A 2-pyridyl triflate is also incompetent. Aromatic groups functionalized with ketones or nitriles provide some arylboration, but yields are low. Aryl triflates with bromo and iodo substituents are also unsuccessful, demonstrating that there is no selectivity between these reactive carbon-halogen bonds, and side reactions dominate. An alkenyl triflate bearing a Boc-protected amine also fails, perhaps due to excessive coordination of the metal catalysts. As for the failed aryl bromides, it is seen that substrates with acidic protons tend to poison the reaction. This makes sense given that protons would be expected to quench any Cu-enolates prior to Pd-trapping; accordingly, elevated levels of conjugate borylation are seen in these cases. Heterocycles with more than two heteroatoms in the bromide-bearing aryl ring also seem to fail, potentially due to excessive coordination of palladium. Benzyl and alkenyl bromides were also unsuccessful coupling partners, demonstrating the selectivity of this protocol towards primarily aromatic groups.

Scheme 37. Unsuccessful organo(pseudo)halide substrates.

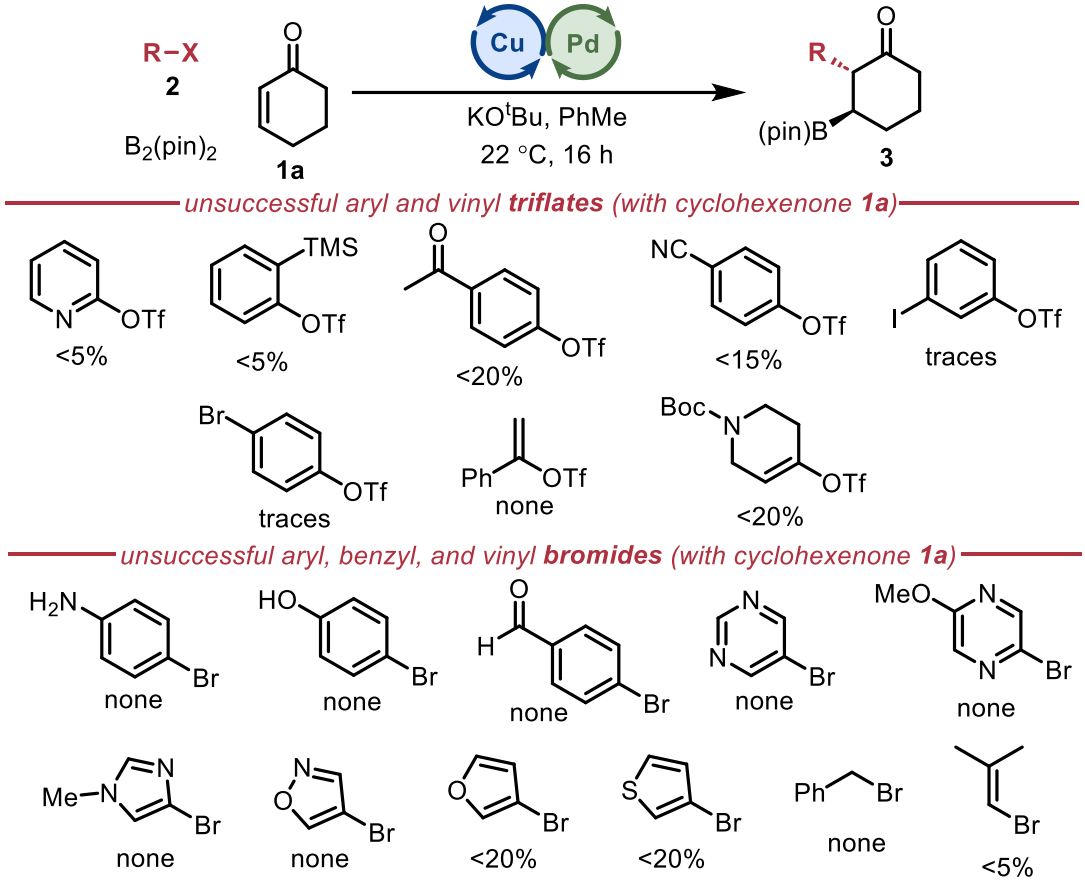

General reaction conditions: Cyclohex-2-ene-1-one **1a** (0.4 mmol), RX **2** (0.2 mmol), $B_2(pin)_2$ (0.48 mmol), KO^{t}Bu (0.4 mmol), IMesCuCl (2.5 mol%), (JohnPhos)Pd(allyl)Cl (10 mol%), toluene (0.2 M), room temperature, 16 h. Yields of the expected arylboration product **3** estimated by uncalibrated GC-MS analysis with naphthalene as internal standard by approximating the response factor of the product based on its molecular weight.

In general, the reaction is very sensitive to structural changes to the enone (Scheme 38). All α- or β-substituted cyclic enones fail, giving conjugate borylation but no arylboration. Perhaps the additional steric bulk prevents the Pd complex from approaching intermediate enolates. Ene-diones also fail, as do lactones. Acyclic substrates were universally unsuccessful; this makes sense given that the reactivities of enolates are heavily impacted by cyclization.[51,106,125] Styrene and dihydro-naphthalene only provide small amounts of arylboration, which contrasts existing arylboration reactions, and suggests that our conditions are complementary to existing protocols.

Scheme 38. Unsuccessful alkene substrates.

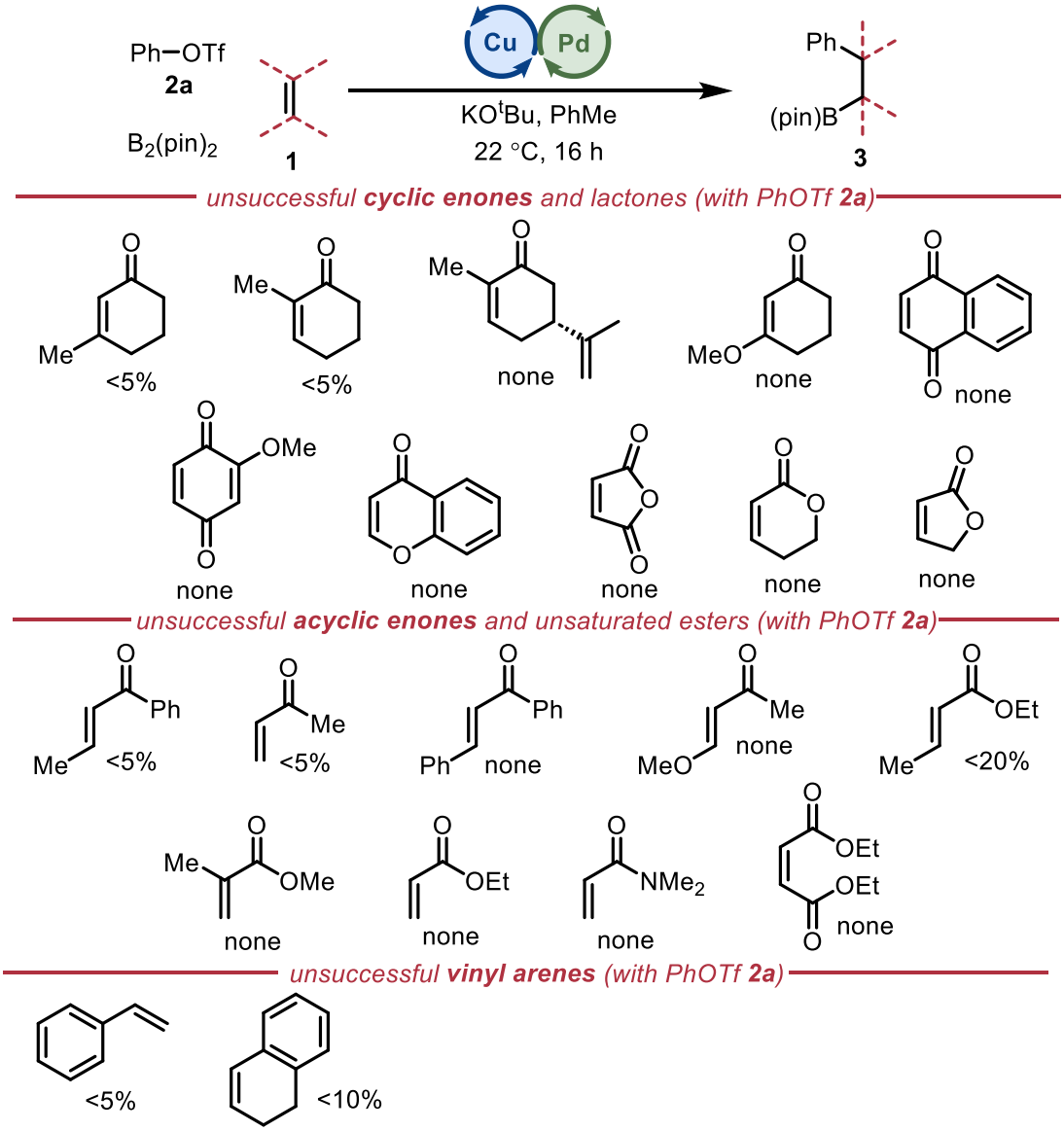

General reaction conditions: Alkene substrate **1** (0.4 mmol), PhOTf **2a** (0.2 mmol), $B_2(pin)_2$ (0.48 mmol), KO^{t}Bu (0.4 mmol), IMesCuCl (2.5 mol%), (JohnPhos)Pd(allyl)Cl (10 mol%), toluene (0.2 M), room temperature, 16 h. Yields of the expected arylboration product **3** estimated by uncalibrated GC-MS analysis with naphthalene as internal standard by approximating the response factor of the product based on its molecular weight.

2.2.4: Product functionalization

As discussed previously, one major strength of arylboration as a difunctionalization strategy is the opportunity to access various new functional groups through transformation of the boronate ester moiety. Furthermore, a hypothesized application and justification for the importance of cyclic enone arylboration is the opportunity to utilize both the B(pin) and ketone groups for further functionalization (discussed in Section 2.1.1.1). Thus, considerable effort was dedicated

towards demonstrating examples of functionalization of the arylboration products to show how this platform can be used to gain rapid access to a variety of cycloalkane scaffolds with complex and diverse substitution patterns. The results of these efforts are discussed in this section.

Successful product functionalization reactions are shown in Scheme 39. The B(pin) moiety was first easily and stereoretentively oxidized to the corresponding alcohol in high yield (89%) under mild room temperature conditions, providing a β-hydroxy, α-aryl cyclic ketone **5** in two simple steps from commercially available materials. The ketone moiety could also be used for a variety of transformations. First, a reduction with L-selectride was performed, providing the expected product **6** in 64% yield and essentially exclusive diastereoselectivity. This selectivity can be rationalized based on approach of the reductant from the opposite face of the adjacent bulky aryl ring, and is in line with previous reductions of similar substrates.[33,94] Attempts to afford the same reduction with $NaBH_4/CeCl_3$ at 0 ºC provide a 2:1 mixture of diastereomers (with the same major product). An aromatic Grignard reagent can be added along the same line of diastereoselectivity (15:1 crude dr), providing the desired tertiary alcohol **7** in 69% yield. The stereochemistry of **7** was confirmed by NOESY analysis. Addition of an aryl lithium reagent leads instead mainly to degradation of the starting material. Significant effort was dedicated towards using the ketone handle to install new functional groups at the remaining methylene carbons. Initial attempts aimed to deprotonate the less-acidic, less-hindered methylene α-proton using LDA and to trap this as the silyl enol ether, but all conditions tested resulted in low yields and poor regioselectivity of deprotonation. Referring to studies done by Corey in the 1980s, it is seen that it is rather challenging to achieve regioselective deprotonation of substrates in which the more hindered proton is also more acidic. For example, deprotonation of 1-phenyl-propan-2-one with LDA at -78 ºC, provides solely the thermodynamic enolate, and this can only be improved to a 1:1 ratio of enolates with an internal quench of TMSCl.[126] We thus turned our attention to even bulkier bases, eventually settling on 2,4,6-tri-^{t}Bu-Ph-Li.[126–128] The use of this base allowed for highly regioselective (>20:1) ketone deprotonation at the desired less hindered side, and trapping as the silyl enol ether was possible, providing **8** albeit only in 27% yield. Another 25% of the remaining mass balance was attributed to starting material, with the rest of the compound being lost through degradation. Evidently, this approach does not seem amenable to useful synthesis, and alternatives are needed. Since the intention behind deprotonation and trapping with TMS was ultimately to either functionalize α to the ketone directly, or to perform a Saegusa-Ito oxidation to give rise to

an enone, we searched for direct methods of ketone desaturation which could display a high level of regioselectivity in similar substrates. Stoichiometric desaturation with hypervalent iodine reagents such as IBX was considered, but ultimately abandoned due to reports of poor regioselectivity with functionalized cyclic ketones.[129] Stahl's palladium-catalyzed desaturation seemed to be a viable option, but was again not attempted based on its failure in differentiating protons in the case of substituted cyclic ketones. In fact, they report 3:1 selectivity towards the thermodynamic enone in the desaturation of 2-phenyl cyclohexanone,[130] which is the opposite outcome of that desired in our work. Finally, we managed to find a platinum-catalyzed desaturation method which shows high kinetic regioselectivity in the unsaturation of cyclic enones, even in cases where a strongly electron-withdrawing ester is present.[131]Application of this protocol to our substrate, the arylboration product **3e**, provides the desired enone **9** in 50% yield (78% brsm) and exclusive regioselectivity. This transformation opens an enormous breadth of possibilities for further functionalization, as we have a new enone which can be subjected to known mono- or di-functionalization chemistry. This approach would provide a rapid way of accessing highly substituted and diverse carbocycles from simple building blocks in a few mild, catalytic steps. As an initial proof-of-concept, we performed a Cu-catalyzed conjugate addition of a vinyl Grignard reagent to enone **9**,[35] and isolated Compound **10** in 43% yield. The crude dr of the addition was determined to be 11:1 by GC-FID analysis, and the stereochemistry of the major isolated product was confirmed based on ^{1}H NMR coupling constants, COSY correlations, and NOESY correlations. Next, we attempted to achieve a difunctionalization of enone **9** through performing the same Cu-catalyzed Grignard conjugate addition but quenching with iodomethane. Although the desired β-vinyl α-methyl compound was detected by GC-MS, the product was contaminated with an equal amount of Compound **10**, and these two materials were inseparable. This suggests that the cuprate addition was complete, but the enolate trapping with MeI was only partially successful. Incomplete trapping of copper enolates by alkyl halides is a common issue encountered in conjugate addition and trapping sequences, and this is assumed to be due to the slow kinetics of enolate alkylation in the solvents typically used for conjugate addition. A common way to overcome this challenge is through addition of HMPA prior to adding MeI,[38,44,132] but this resulted in degradation of our material. Ultimately, this approach was unsuccessful, and we turned our attention to catalytic ways of di-functionalizing Compound **9**. While the Rh/Ir-catalyzed β-arylation α-allylation from Lundgren (Scheme 15)[55] would be ideal for installing a different pattern

of functional groups compared to the other side of the ring, this was not practical for us given the prohibitively complex phosphoramidite ligand required for the Ir catalyst which would take at least seven steps to synthesize. Instead, we attempted Hoveyda's NHC-catalyzed conjugate borylation, tandem aldol reaction (Scheme 13)[32], but only recovered starting material **9**. Lastly, we attempted to apply our enone arylboration reaction to substrate **9**. Unfortunately, this reaction was not successful. Although crude NMR analysis displays some promising peaks which suggest that the desired product may have formed, we could not isolate this material or characterize it further, and the product m/z was not detected in crude MS analysis. Although we were not successful in achieving a difunctionalization of Compound **9**, there remains plenty of room for exploring more options such as the Rh/Ir-catalyzed β-arylation α-allylation, a broader range of alternative conditions for cuprate addition and enolate trapping, and nucleophilic epoxidation.

Scheme 39. Examples of product functionalization.

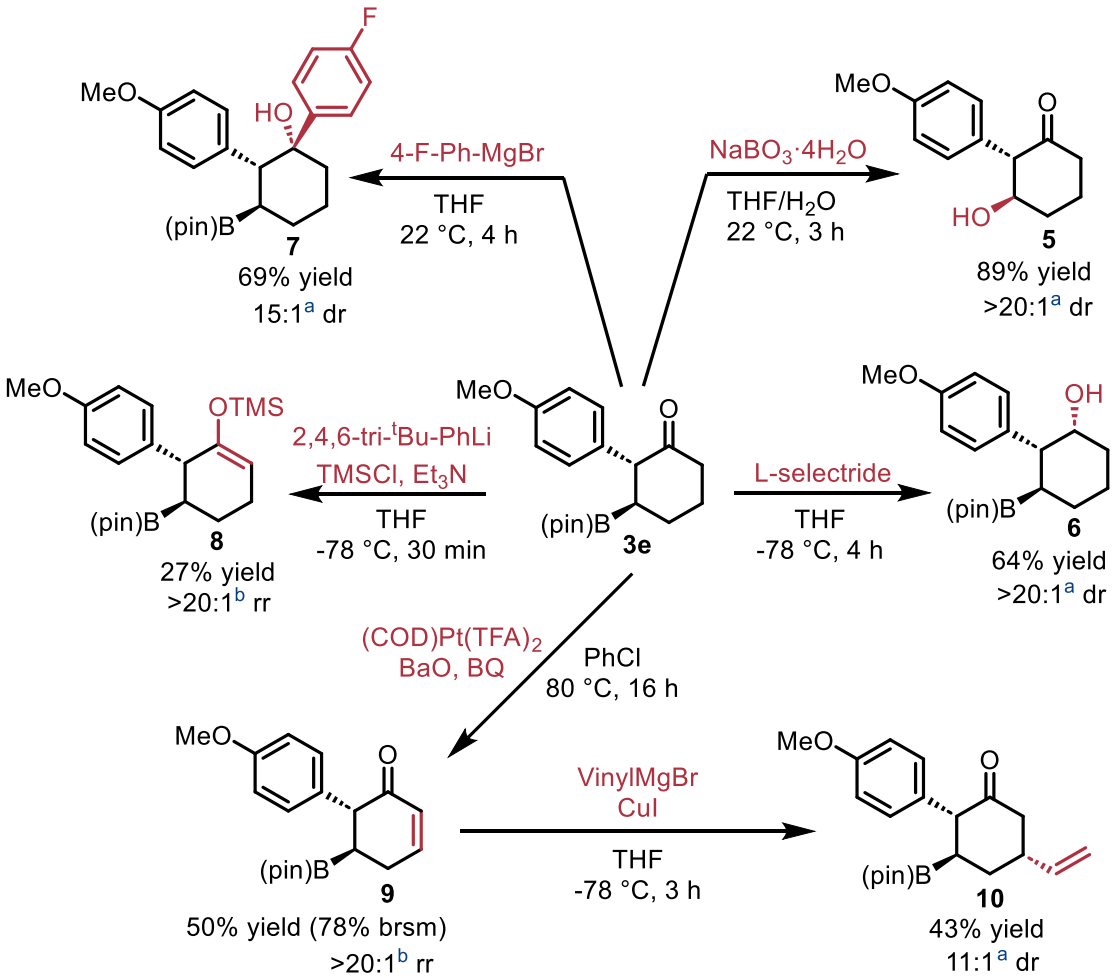

[a]Crude dr at the centre of reactivity as determined by GC-FID. Isolated yields of the single diastereomers depicted are reported. [b]Crude regioisomer ratio determined by GC-FID. Isolated yields of single isomers are reported.

Several attempts at product functionalization at the ketone or B(pin) groups of **3e** were also unsuccessful. Direct palladium-catalyzed Suzuki-Miyaura cross-coupling of the alkyl boronate ester with bromobenzene fails to provide any product, even though there is ample literature precedent for this protocol promoting the desired sp^3-sp^2 coupling on very similar β-boryl cyclic ketone substrates.[35] Additionally, attempts to convert the B(pin) group into a potassium trifluoroborate salt were unfruitful.[35] Though product formation occurred, issues with isolation prevented adequate characterization. Attempts to involve the boron group in a silver-catalyzed radical fluorination with SelectFluor also failed to deliver any of the desired product,[66] and a radical-based photoredox Ir/Ni-catalyzed cross-coupling of the alkyl B(pin) with an aryl bromide also failed to provide conversion.[70,78] Lastly, an attempt at forming an imine at the ketone was also unproductive. Though many attempts at product functionalization at the ketone and/or boron group of the arylboration product proved unsuccessful, there are still plenty of remaining opportunities for refining conditions and testing alternative methods for achieving these desired transformations. Furthermore, many transformations such as deuteration, amination, Zwiefel, and Matteson reactions were not attempted, leaving plenty of room for further developments in this area. The harsh natures of these more classical transformations would first require transient protection of the ketone as an acetal and subsequent deprotection via acidic workup, and previous efforts in this area are well-documented.[33,35,96] Application of these more synthetically demanding but robust transformations could easily expand the range of functional groups which are accessible from the B(pin)-bearing product.

2.2.5: Mechanistic experiments

Throughout the course of these studies, the mechanism of the reaction has been assumed to be that which was discussed in Section 2.1.3. However, some mechanistic questions remain, and this section outlines some simple experiments geared towards answer answering these questions, specifically regarding the origin of the conjugate borylation side product and the source of the observed diastereoselectivity in the arylboration product.

The first mechanistic question relates to the origin and stability of the conjugate borylation side product. First, we wanted to make sure that the conjugate borylation material is indeed solely a side product, and not a competent intermediate. Subjecting compound **4** to the arylboration conditions in the absence of cyclic enone (Scheme 40) did not provide any arylboration product

3e, suggesting that **4** is fully off-cycle and cannot re-enter into productive catalysis towards arylboration.

Scheme 40. Testing the competence of the conjugate borylation product.

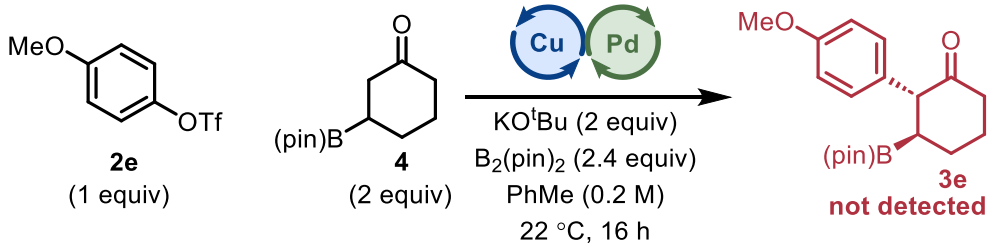

Based on our mechanistic hypothesis outlined in Section 2.1.3, conjugate borylation product **4** was believed to originate from protonolysis of Cu- or B-enolates. Given that attempts to extensively dry reagents or eliminate water from the reaction during the optimization (Table 11) had no impact on the arylboration yield or levels of conjugate borylation, it can be hypothesized that perhaps **4** does not form in situ but is only formed upon workup. This would mean that there are enolates in the reaction mixture upon completion; these would most likely be boron enolates that are incapable of reacting further with palladium oxidative addition complexes. If this were the case, then the proton source would be either the moisture in the air that the reaction is exposed to upon removal of the cap at the end, or the silica gel used to quench and filter the crude reaction mixture. This hypothesis is depicted in Scheme 41.

Scheme 41. Hypothesis for the source of conjugate borylation.

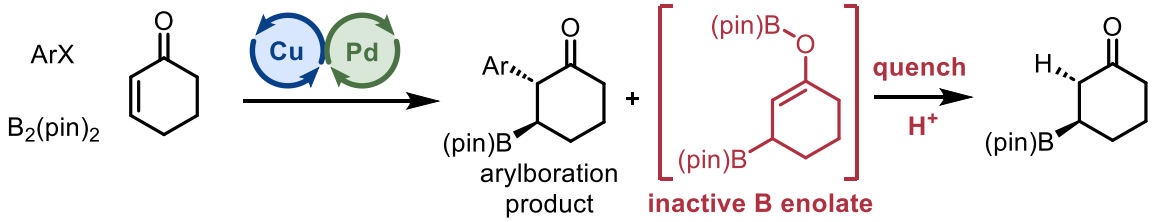

Based on these assumptions, quenching the reaction inside a nitrogen-filled glovebox with reagents that are known to react rapidly with boron enolates should provide insight into whether the conjugate borylation product results from protonation of unreacted enolates upon quenching. Thus, the experiments in Scheme 42 were conducted. Although boron enolates are known to react rapidly with both D_2O[24] and aldehydes,[53,133,134] none of the deuterated product **11** or aldol adduct **12** were detected by GC-MS when quenching with these reagents. This suggests that there are no boron (or copper) enolates present at the end of the reaction, that the conjugate borylation product

does not form upon quenching, and that it must somehow be forming in situ during the reaction progress. Since there is no copper-free pathway for generation of side product **4** (Table 9), its source must be some degradation pathway of Cu- or B-enolates with an unknown proton source that is present in the reaction.

Scheme 42. Reaction quenching with D_2O or benzaldehyde to test for leftover enolates.

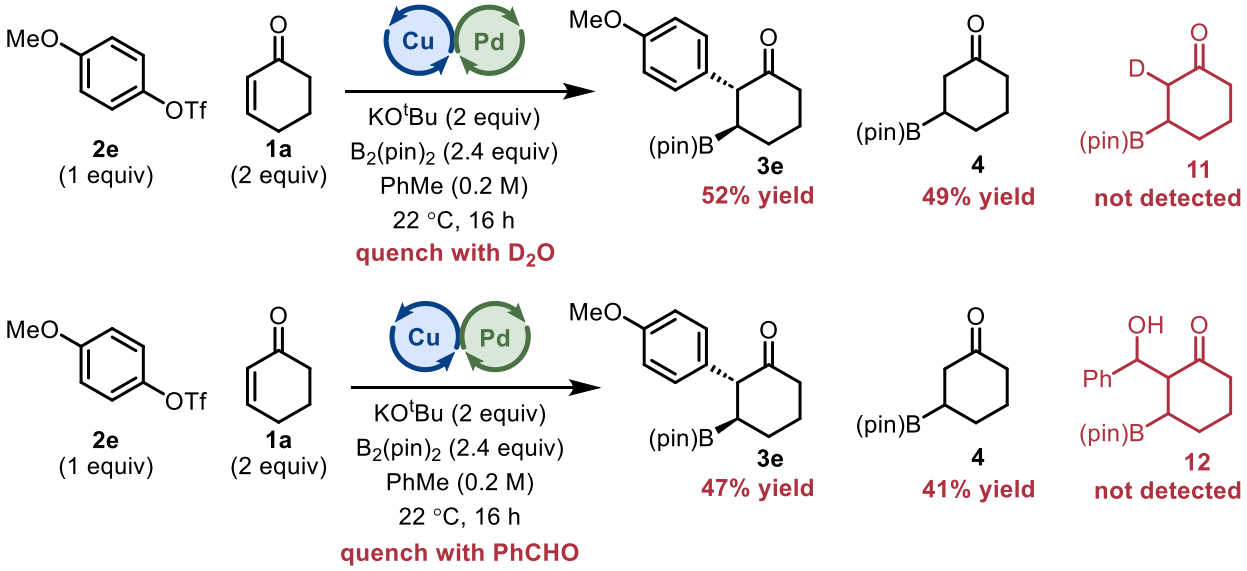

Yields of **3e** and **4** determined by GC-FID analysis with naphthalene as internal standard.

Lastly, the source of diastereoselectivity was investigated in Scheme 43. Evidence obtained during the evaluation of the reaction's scope suggests that diastereoselectivity is substrate controlled, and that steric hindrance of the aromatic group and enone influence selectivity. However, it is still possible that the arylboration itself is somewhat non-diastereoselective, but base-promoted epimerization settles the product towards the thermodynamically favoured diastereomer. The base could either be KO^{t}Bu, or alternatively, metal-bound enolate intermediates could also plausibly deprotonate the more acidic benzylic protons that are α to the ketone in the product. If this were the case, the mysterious proton source which is proposed to lead to the production of conjugate borylation products would be the arylboration product's benzylic proton! To refute this possibility, the syn diastereomer of the arylboration product, compound **13**, was independently synthesized, then subjected to the reaction conditions with a different aryl triflate. Analysis of the crude mixture by GC-FID indicates that the syn starting material retains its diastereomeric purity, with no epimerization observed. Re-isolation of the syn material and NMR analysis further confirm this. Arylboration product **3e** also forms in typical yield and dr. This experiment demonstrates that there is no epimerization of the arylboration product under the

reaction conditions, that diastereoselectivity must be a result of the reaction mechanism rather than simply thermodynamic equilibration, and that metal-bound enolate intermediates are not quenched by deprotonation of the product's benzylic proton.

Scheme 43. Investigating the source of diastereoselectivity through an epimerization control.

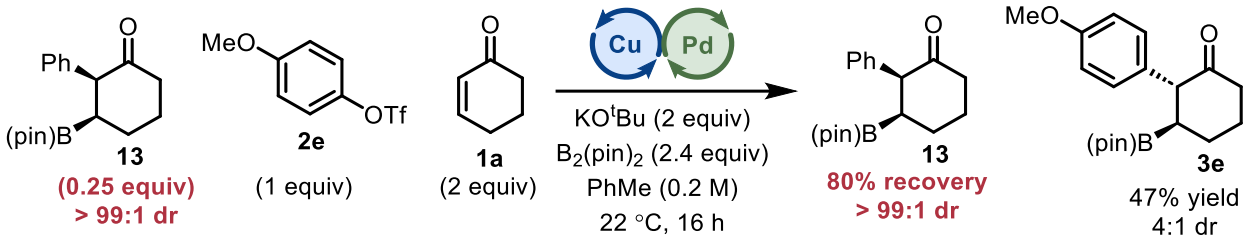

Recovery, yield, and dr of **13** and **3e** determined by GC-FID analysis with naphthalene as internal standard.

One final mechanistic question remains unanswered; it is unknown whether the proposed boron enolate is a competent intermediate for transmetallation with palladium to ultimately give rise to the arylboration product, or whether this intermediate is purely off-cycle and only the copper enolate is productive. Several attempts were made to probe the competency of the boron enolate, albeit with no success. In theory, it should be possible to form the proposed boron enolate in situ through conjugate borylation in the absence of the aryl halide and palladium catalyst, to detect the quantitative formation of this boron enolate by NMR, and lastly to add the palladium catalyst and aryl halide to see whether arylboration product forms. However, all attempts at forming the boron enolate and detecting it by NMR proved unfruitful. To the best of our knowledge, there is only one literature example demonstrating the detection of a cyclic enone boron enolate by NMR,[135] and that system involved Rh-catalyzed addition of an aryl 9BBN reagent across an enone, which is quite different from the copper and $B_2(pin)_2$ system studied herein. It is possible that the enolate derived from B(pin) is too unstable to detect, and that it degrades rapidly under our reaction conditions upon forming. The absence of detected boron enolates by NMR supports the notion that this species somehow degrades to form the conjugate borylation product rapidly in situ, complementing our earlier findings.

Overall, the mechanistic picture outlined in Section 2.1.3 seems reasonable given these experimental results, though the proton source involved in boron/copper enolate degradation remains a mystery, and the competence of the boron enolate is unknown. While the origin of diastereoselectivity is believed to be facial selection in the approach of the palladium oxidative addition complex to the diastereotopic copper enolate, influences from epimerization of Pd

enolates cannot be ruled out.[22] Another possible mechanism exists in which the O-bound Cu enolate transmetallates with Pd to form an O-bound Pd enolate, and that the subsequent O-to-C tautomerization of the Pd enolate is rapid and equilibrates between anti and syn forms prior to reductive elimination. In this case, either the tautomerization from O-to-C Pd-enolates, the syn/anti Pd-enolate equilibrium, or the subsequent reductive elimination could be the stereo-determining step. Nevertheless, precedent in related metal enolate trapping reactions suggests that transmetallation and facial approach of the electrophile is the stereo-determining step.[45,55] Our best insights regarding this reaction mechanism are summarized in Scheme 44, but it is crucial to note that we cannot experimentally rule out the alternative mechanism.

Scheme 44. Mechanistic insights in the Cu/Pd catalyzed enone arylboration.

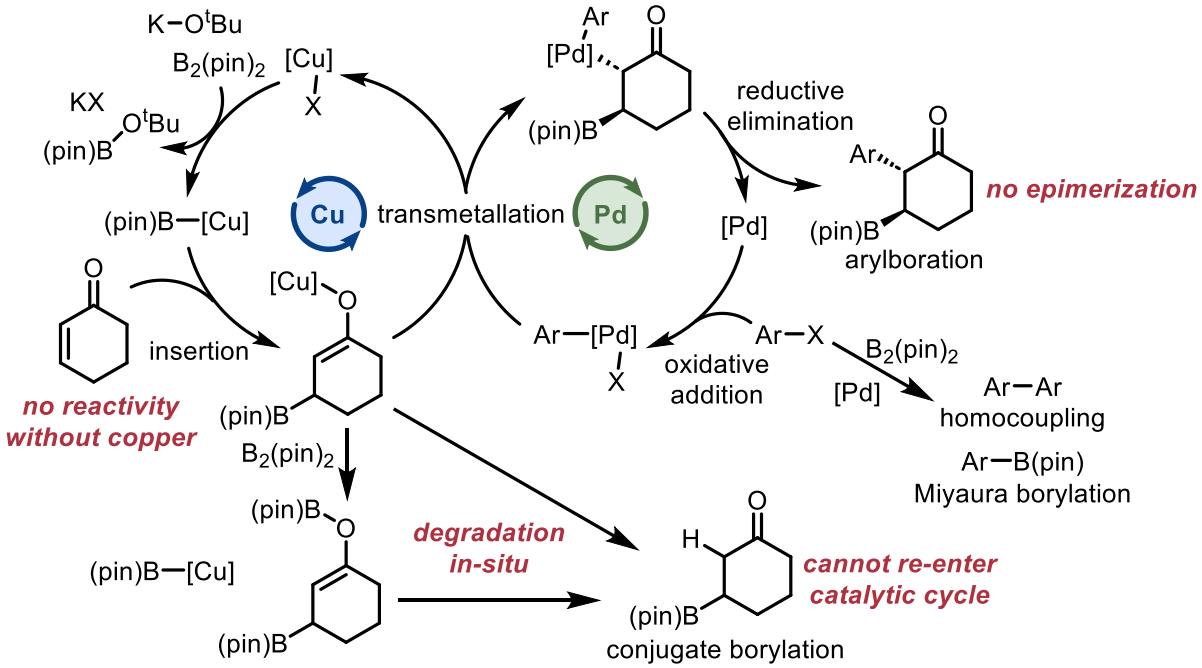

2.2.6: Enantioselective variant

Given the importance of chirality in nature and pharmaceuticals, the development of an asymmetric cyclic enone arylboration reaction would be desirable to allow access to enantiomerically enriched materials. Under the assumption that the initial migratory insertion of the Cu-B(pin) into the cyclic enone is the enantio-determining step (Scheme 32), asymmetry could be induced using a chiral NHC ligand on Cu. This assumption is warranted based on strong precedent in Cu-catalyzed asymmetric conjugate borylation of cyclic enones[33,34] and enantioselective Cu/Pd-catalyzed alkene arylboration reactions.[83,84,86] Given the often difficult and

step-intensive synthesis sequences required to assemble chiral ligands, care was taken to select an NHC ligand which had a high likelihood of providing non-zero yield and enantiomeric excess. In several literature reports[83,84,86] of Cu/Pd-catalyzed alkene arylboration reactions in which IMes or SIMes were the best achiral ligands, the chiral NHC-Cu complex **Chiral-Cu** (Scheme 45) proved to be the highest yielding and most enantioselective ligand. Thus, we decided to synthesize this chiral catalyst following known protocols,[82,136,137] and to test it in our arylboration conditions in hopes of discovering an enantioselective variant. To our delight, the reaction was high-yielding, providing a 52% yield of the arylboration product **3e**. Conversion of the alkyl boronate ester into the corresponding alcohol via oxidation (as outlined in Section 2.2.4) was then performed to make the analytical resolution of enantiomers simpler. The enantiomeric excess of the alcohol product was assessed by supercritical fluid chromatography (SFC) with a chiral column, and determined that the product **5** only has a 10% ee. While disappointing, this result confirms that it is possible to introduce asymmetry through using a chiral ligand on Cu, and lays the groundwork for future developments in asymmetric enone arylboration. One may speculate that the reason for such a low ee is that the highly electron-rich NHC-Cu-B(pin) complex is too reactive, undergoing rapid insertion into the electron-poor enone, preventing any meaningful levels of enantioselectivity from being achieved. In contrast, high selectivity is achieved in arylboration reactions on vinyl arenes reported in previous enantioselective arylboration systems with chiral NHC-Cu catalysts[83,84,86] since the insertion step is likely slower and thus more selective with these less activated alkenes. Although Cu-catalyzed enantioselective cyclic enone conjugate borylations are known, these reactions all use chiral bidentate phosphine ligands,[33–35,112,133,138,139] with no known examples of chiral NHC-Cu complexes being reported. Perhaps the lower reactivity of the phosphine-Cu-B(pin) complexes, due to their reduced electron-donation compared to NHCs, is required to achieve high enantioselectivity in this key elementary step. This would mean that our current enone arylboration conditions are not fully amenable to asymmetric synthesis, and another round of re-optimization would likely be required to achieve reasonable product yields using bidentate phosphine ligands instead of NHCs.

Scheme 45. Attempt at developing an asymmetric Cu/Pd-catalyzed cyclic enone arylboration.

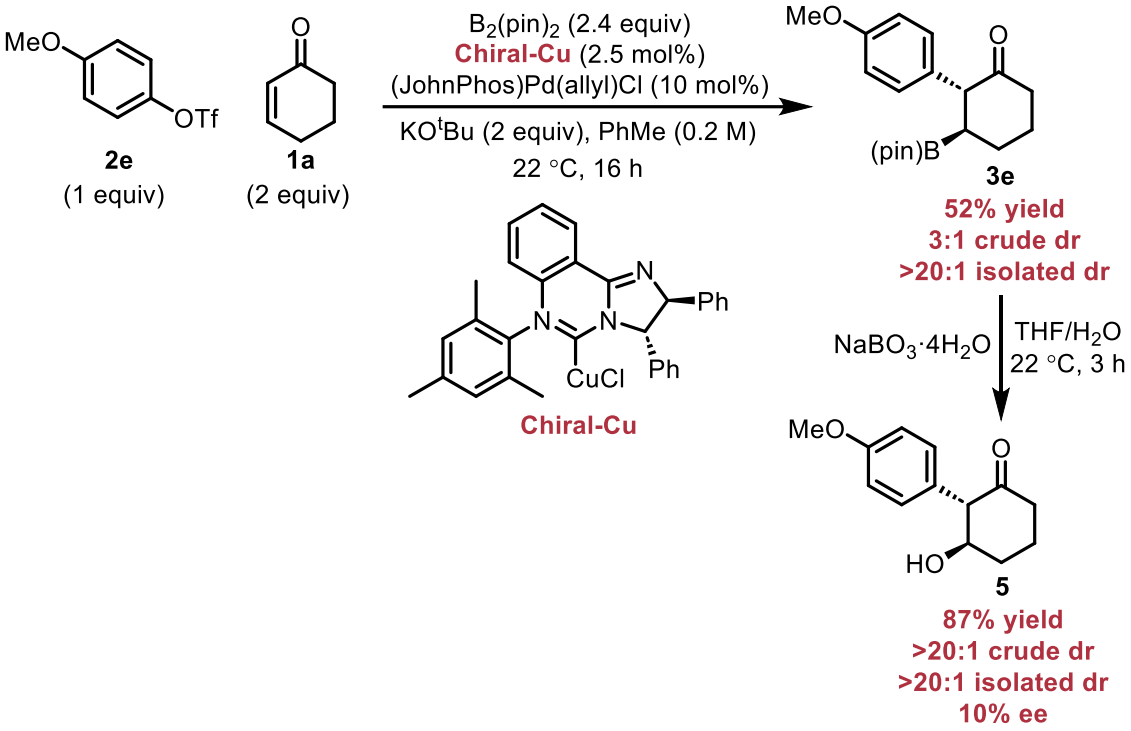

2.3: Conclusion and future directions

In summary, we have developed a mild, room-temperature, Cu/Pd-catalyzed method for the anti-selective arylboration of cyclic enones. Our initial mechanistic hypothesis, based on literature precedent from related transformations, aided us in the reaction discovery by providing key insight that balancing the Cu/Pd ratio would be crucial for achieving the desired arylboration over the unproductive conjugate borylation pathway. Extensive reaction optimization allowed us to arrive at the optimal conditions, employing NHC-Cu and JohnPhos-Pd catalysts. As predicted, low Cu loading and high Pd catalyst levels were necessary to ensure useful synthetic yields of arylboration and to out-compete conjugate borylation. JohnPhos also seems to impart beneficial properties on Pd which aid in trapping transient enolate intermediates, which is in line with previous findings in our group. Overall reaction yields are moderate, but this is acceptable given the previous three-step approach used to make similar molecules, and the amount of complexity gained in our one-step catalytic transformation. Scaling up to 1 mmol has no impact on yield, showing the practicality of our reaction. The scope includes a variety of aryl triflates with differing electronic and steric properties, in addition to some hetero-aryl bromides, alkenyl triflates, and an allyl carbonate. Diastereoselectivity is generally in the range of 5:1 to 10:1 (anti/syn), while ortho-substituted aryl triflate coupling partners give exclusively anti products (>20:1). This demonstrates that steric hindrance is crucial at the stereo-determining step. The reaction is sensitive to changes in ring size, with yields plummeting for cyclopentenone, but remaining moderate for cyclohexenone and cycloheptenone. Facial selectivity is observed in the arylboration reaction with cyclic enones that are substituted at the 4 or 5 position. The arylboration product was demonstrated to be a useful synthetic building block for accessing complex, multi-substituted cycloalkanes via subsequent derivatizations at both the B(pin) and ketone moieties. The B(pin) group was easily oxidized to the alcohol, and the ketone was leveraged for direct addition, deprotonation, and desaturation chemistry, enabling the installation of more functional groups on the other side of the ring. This approach allows rapid access to diverse carbocycles that would otherwise be challenging to synthesize. Plenty of opportunities remain unexplored in product functionalization, including B(pin) amination, deuteration, fluorination, and carbon–carbon bond formation reactions via transient ketone protection. Alternative difunctionalization methods for adding more groups to the ring after desaturation could also be explored further.

Additionally, our enone arylboration method could potentially be used as a key transformation in the total synthesis of pancratistatin (Scheme 46). While numerous total syntheses for pancratistatin have been reported,[96–104] most approaches require 15-25 steps and use chiral sugars as starting materials, limiting the possibilities for producing synthetic derivatives for evaluation in medicinal chemistry campaigns. The Sarlah group's approach to pancratistatin is the most concise and amenable to diversification, proceeding in 7 synthetic steps from benzene.[101] Though our proposed approach would likely not be an improvement over Sarlah's route in terms of step count, it could provide an alternative pathway with complementary options for derivatization (specifically at N5, C1, C2, and C3), in addition to demonstrating the utility of the arylboration reaction developed herein. The proposed synthesis could commence with a protected 4-hydroxy cyclohexenone substrate, which could be subjected to a facially selective Cu/Pd-catalyzed anti-arylboration using our protocol. This would form key stereocentres of the natural product, install the desired aromatic portion, and have the B(pin) moiety serve as a latent group which could later be transformed into the required amine. Next, Pt-catalyzed desaturation and diastereoselective ketone reduction with L-selectride (followed by alcohol protection) could be performed as outlined herein. To finish the synthesis, the B(pin) could be aminated, the remaining alcohols might be installed via epoxidation and hydrolysis (with substrate-controlled stereoselectivity provided by the existing substituents), and a cyclization and deprotection sequence could afford pancratistatin. The most problematic portion of the synthesis is expected to be the epoxidation and hydrolysis to install the final two alcohols,[100] so an alternative route involving nucleophilic epoxidation of the enone prior to ketone reduction could be considered. This would require amination of the B(pin) at an earlier stage in the synthesis to prevent undesired oxidation of the boronate ester during nucleophilic epoxidation. The proposed cyclization-deprotection sequence has ample precedent on a very similar substrate in a recent synthesis of pancratistatin,[104] supporting the feasibility of this route.

Scheme 46. Proposed total synthesis of pancratistatin with cyclic enone arylboration as a key step.

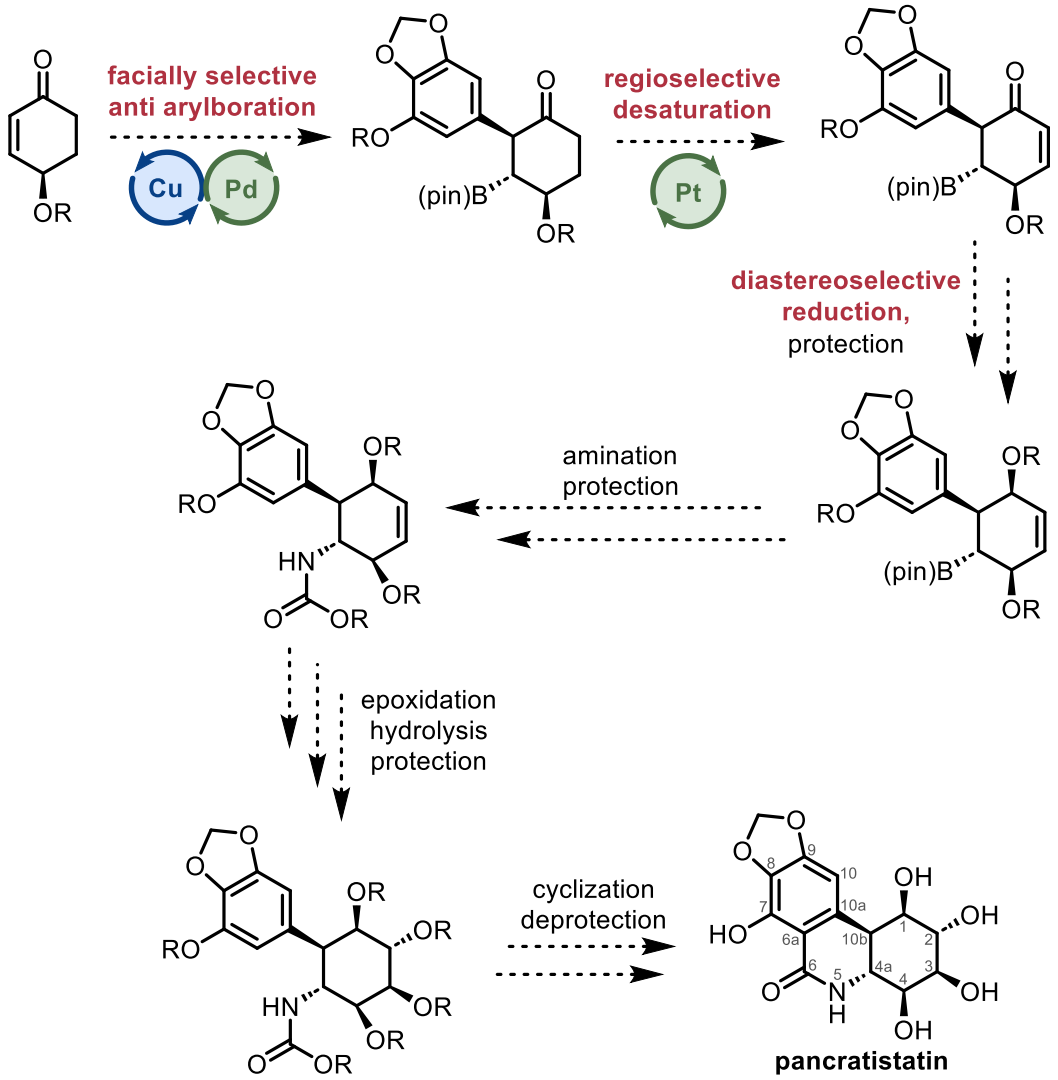

Reactions developed or demonstrated herein are denoted in red text.

Mechanistic experiments on our enone arylboration reaction indicate that there is no epimerization of the product under the reaction conditions, confirming that the observed selectivity towards the anti diastereomer is a result of the reaction mechanism. Though the conjugate borylation side product is believed to arise from protonolysis of enolate intermediates, the source of its generation could not be identified, and it is believed to form in situ rather than upon quenching. Attempts to provide an asymmetric arylboration variant through using a chiral NHC-Cu catalyst were unsuccessful, with only 10% ee obtained. While this is a non-zero level of enantio-induction and could be improved upon, we believe based on literature precedent in asymmetric enone conjugate borylation that chiral bidentate phosphine ligands would be more

suitable for an enantioselective arylboration. A possible future direction for this work would be to undertake another round of reaction optimization, geared towards bidentate phosphines and enantioselectivity.

We hope that this cyclic enone arylboration method not only becomes a useful tool in synthetic chemistry, but also that it inspires further developments in the catalytic difunctionalization of cyclic enones. Plenty of gaps remain in the types of functional group patterns that could be installed, and exploration of these avenues could provide great improvements in synthetic efficiency for accessing complex carbocycles without relying on cryogenic and stoichiometric cuprate chemistry. Some of these ideas are shown below in Scheme 47. Combining Cu-catalyzed conjugate borylation with Ir-catalyzed α-allylation could afford a method for direct catalytic allylboration of cyclic enones. Though we report one example of allylboration herein, a Cu/Ir system would likely provide higher yields and selectivity than our Cu/Pd catalysts for this application. Similarly, the merger of Rh-catalyzed β-arylation and trapping of the transient Rh enolate with Pd could provide an anti-selective 2,3-diarylation of cyclic enones. Overall, we hope that our Cu/Pd-catalyzed enone arylboration inspires future improvements and development in catalytic enone difunctionalization chemistry towards the goals of improving synthetic efficiency and sustainability.

Scheme 47. Ideas for future developments in catalytic cyclic enone difunctionalization.

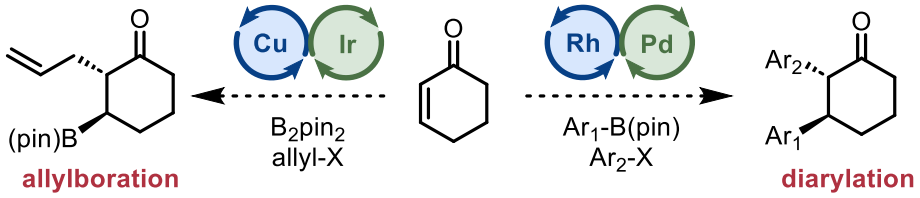

2.4: Experimental

2.4.1: General experimental details

Unless indicated otherwise, reactions were set up outside the glovebox under air atmosphere using oven-dried glassware (120 °C overnight, cooled in a desiccator). Flash column chromatography was either performed manually or with a Combi-Flash Rf automated chromatography system, in both cases with Silicycle F60 40-63 μm silica gel. Analysis by thin-layer chromatography were done using aluminum-backed EMD Millipore Silica Gel 60 F254 pre-coated plates, and eluted plates with visualized with both UV light (254 nm) and by $KMnO_4$ staining (heat gun).

2.4.2: Instrumentation

GC-MS data was obtained with an Agilent Technologies 7890B GC with a 30 m x 0.25 mm HP-5 column. GC-FID data was recorded on Agilent 7890A gas chromatography fitted with a HP-5 column and a flame ionization detector. Crude yields of products and side products (by either GC-MS or GC-FID) were determined through relative integrations compared to an internal standard (0.5 equiv naphthalene) via comparison to calibration curves constructed with pure materials. Crude diastereomeric ratios of products were determined by relative GC-FID integrations of peaks which show the same m/z by GC-MS. Accurate mass data (EI) was obtained from an Agilent 5977A GC/MSD using MassWorks 4.0 from CERNO Bioscience.[140] ^{1}H, ^{13}C, and ^{19}F NMR were recorded at 25 °C on a Bruker AVANCE 300 MHz, a Bruker AVANCEII 400 MHz, a Bruker AVANCEIII 500 MHz, or a Bruker AVANCEIII 600 MHz NMR spectrometer. Difficult stereochemical patterns were characterized further by 2D NMR experiments (COSY and NOESY) on a Bruker AVANCEII 400 MHz or a Bruker AVANCEIII 600 MHz NMR spectrometer. Spectra were internally referenced to residual solvent peaks (7.26 ppm for ^{1}H spectra and 77.16 ppm for the residual $CHCl_3$ in $CDCl_3$). Data for ^{1}H NMR are reported as follows: chemical shift (δ ppm), multiplicity (s = singlet, d = doublet, t = triplet, q = quartet, m = multiplet, dd = doublet of doublets, ddd = doublet of doublet of doublets, dddd = doublet of doublet of doublet of doublets), coupling constant (Hz), integration. In compounds containing a C-B bond, the carbon atom bound to the boron was not detected by ^{13}C NMR because of quadrupolar relaxation.

2.4.3: Materials

Unless otherwise noted, all commercially available reagents, starting materials, catalysts, and ligands were purchased from Sigma-Aldrich, TCI America, Fisher Scientific, Acros Organics, Alfa Aesar, Combi-Blocks, Aaron Chemicals, or Oakwood Chemicals, and were used as received without any purification. Molecular sieves (4 Å, 1/16-inch pellets) were obtained from BDH Chemicals, and were dried at 280 °C for 3 hours inside a vacuum oven and stored inside the glovebox. Ground molecular sieves were prepared by crushing pellets into powders using a mortar and pestle in the glovebox. Organic solvents were degassed using nitrogen and were then filtered through a Puresolv solvent purification system (SPS) to remove water. Aryl triflates that were not commercially available were synthesized following general literature procedures,[141,142] and were stored inside a nitrogen-filled glovebox in a freezer (-16 °C). IMesCuCl, SIMesCuCl, IPrCuCl, and SIPrCuCl were synthesized as reported in the literature,[143] and were stored in a nitrogen-filled glovebox. ICyCuCl and I^{t}BuCuCl were synthesized as reported in the literature,[88] and were stored in a nitrogen-filled glovebox. Pd-JohnPhos-G3 was synthesized as reported previously.[144] ($P^{Ph}N^{ArCF3}$)$_2$ was synthesized as reported.[114] (JohnPhos)Pd(allyl)Cl was synthesized as reported,[119] and was stored in a fridge (6 °C) under argon. New, fresh bottles of KO^{t}Bu were shipped into a nitrogen-filled glovebox without opening under air, and were stored in the glovebox. The reaction was not sensitive to changes in KO^{t}Bu supplier. Cyclohexenyl triflate,[145] cyclopentenyl triflate,[146] and N-Boc piperidone triflate[147] were synthesized according to the literature. 5-methyl-cyclohex-2-ene-1-one, cyclic enone substrate **1ag** was synthesized according to a literature protocol.[148] 1,4-benzoquinone (BQ) was purified by sublimation before use. Barium oxide (95% purity) was purchased from Combi-Blocks and was only opened in the glovebox and stored there. Chlorobenzene (PhCl) was degassed with an argon balloon for 5 min prior to use as a solvent. (COD)Pt(TFA)$_2$ was synthesized as reported previously.[131] 3-(4,4,5,5-tetramethyl-1,3,2-dioxaborolan-2-yl)cyclohexan-1-one, compound **4**, was synthesized as reported previously.[112] 2-phenyl-cyclohex-2-ene-1-one was synthesized as reported previously.[37] The chiral NHC-CuCl complex, **Chiral Cu**, was synthesized as reported previously.[82,136,137]

2.4.4: General procedures for reaction discovery and optimization

High-throughput screening for reaction discovery in Figure 2 was performed by methods reported by our group.[108] In brief, a 96-well plate in an aluminum block assembly (Analytical Sales

and Services, cat. no. 96973) was loaded with vials (8 × 40-mm, 1.2-mL vials; Chemglass Life Sciences, cat. no. CV2103-0840) and all vials were charged with micro-stir bars (Parylene-coated micro stir bars, VP Scientific, cat. no. VP 712-1) using a stir bar dispenser (VP Scientific, cat. no. VP-711A-1S/D). The plate was then shipped inside a nitrogen-filled glovebox. Phosphine ligands were then added to each vial (10 mol% for bidentate ligands for Pd, 20 mol% for monodentate ligands for Pd, 20% mol for bidentate ligands for both Pd and Cu, 40 mol% for monodentate ligands for both Pd and Cu). Next, either CuCl (5 mol%) or IMesCuCl (5 mol%) was added to each vial, followed by $Pd_2(dba)_3 \cdot CHCl_3$ (5 mol% of the dimer). The appropriate base (2 equiv, 0.05 mmol) was then added. Then, a solution of $B_2(pin)_2$ (2 equiv, 0.05 mmol, 0.1 mL from a 0.5 M solution in the appropriate solvent) was added to each vial via micropipette. Lastly, a combined solution of bromobenzene (2 equiv, 0.05 mmol) and 2-cyclohexene-1-one (1 equiv, 0.025 mmol) was added via micropipette (0.1 mL from a 0.5 M bromobenzene and 0.25 M enone solution in the appropriate solvent), bringing the reaction to a total volume of 0.2 mL (0.125 M in the limiting enone). The plate was sealed with a PFA sheet (Analytical Sales and Services, cat. no. 96967) and two rubber gaskets (Analytical Sales and Services, cat. no. 96965) that were secured on top of the aluminum block by screwing in the plate lid with 1.5" stainless steel screws. The sealed HTE plate was removed from the glovebox and placed in a heated tumble stirrer at 80 °C equipped with a mica deck insert (V&P Scientific, cat. no. VP 710C5-7A-CC, VP741D, VP710C5-7-2) and stirred for 16 hours. Upon completion, the plate was allowed to cool, then a solution of internal standard (naphthalene, 0.5 equiv, 0.0125 mmol, 0.1 mL from a 0.125 M solution in toluene) was added to each vial via micropipette. The plate was sealed once again and stirred at room temperature by the same method for 30 min to ensure mixing of internal standard and the reaction mixture. At this point, the plate was opened again, and a 30 μL aliquot was taken from each vial and eluted through 96-well filter plate (Pall Laboratory, cat. no. 8684) filled with silica gel (0.5 cm), and then subsequently eluted into a second 96-well plate with clean vials through elution with EtOAc by pushing with compressed air using CEREX 96 II Multi Channel SPE System to facilitate filtration. Reaction outcomes (crude yields) were then analyzed by GC-MS.

High-throughput screening of solvent and base in Figure 3 were performed in a manner similar to that described above, with the only differences being the order of reagent addition. For this screen, IMesCuCl (5 mol%) was first added, followed by the appropriate base (2 equiv). Next, $B_2(pin)_2$ (2 equiv, 0.1 mmol) was added as a solid, followed by 0.1 mL of the appropriate solvent

by micropipette. Next, a solution of 2-cyclohexen-1-one (1 equiv, 0.05 mmol, 0.1 mL from a 0.5 M solution in the appropriate solvent) was added via micropipette to each vial. Lastly, a pre-mixed solution (2 h of stirring all components together in an 8 mL catalysis vial inside the glovebox) of $[Pd(allyl)Cl]_2$ (5 mol% of the dimer), JohnPhos (20 mol%), and PhOTf (2 equiv, 0.1 mmol) was added to each vial (0.1 mL of a solution with [PhOTf] = 1 M, [JohnPhos] = 0.1 M, [Pd dimer] = 0.025 M in the appropriate solvent). The final reaction volume and concentration were thus 0.3 mL and 0.17 M, respectively. The plate was sealed and stirred at room temperature (without any heating, 22 °C), then analyzed by the method described above (0.5 equiv naphthalene internal standard, GC-MS for crude yield).

For the reaction in Scheme 30 and optimization studies in Tables 1-7 and Table 8 (entry 1), the following general procedure was followed. To an oven-dried 8 mL catalysis vial equipped with a stir bar was added the appropriate ligand (20 mol%) and Pd precatalyst (10 mol%). This was then taken into a nitrogen-filled glovebox, and a solution of PhBr or PhOTf (1-2 equiv, 0.1-0.2 mmol scale) in 0.2 mL toluene was added. This mixture was allowed to stir inside the glovebox at room temperature for 30 min. In a separate vial inside the glovebox were added the NHC-CuCl catalyst (5 mol%), the appropriate base (1.2-2.5 equiv), and a solution of $B_2(pin)_2$ (1.7-2.4 equiv) in 0.2 mL toluene. Next, a solution of 2-cyclohexene-1-one (1-2 equiv, 0.1-0.2 mmol scale) in 0.2 mL toluene was added, followed by the entire 0.2 mL solution of ligand/Pd/PhX from earlier. The vial walls were rinsed with 0.2 mL toluene, bringing the reaction volume to 0.8 mL (for 0.1 mmol reactions), and concentration to 0.125 M. For 0.2 mmol scale reactions, an extra 0.8 mL of toluene was added to equalize concentration. The vial was sealed with a screw cap, removed from the glovebox, and stirred for 16 h at the appropriate temperature (typically room temperature). Upon completion, internal standard was added (naphthalene, 0.5 equiv), and the reaction was diluted to a volume of around 7 mL through the addition of EtOAc. An aliquot (100 µL) was then taken and eluted through a cotton-stopped Pasteur pipette silica plug (2.5 cm height and 0.5 cm in diameter) with 2 mL EtOAc. Crude yields of **3a** and **4** were analyzed by either GC-MS or GC-FID analysis as indicated in each optimization table.

For optimization studies in Table 8 (entries 2-3) and Tables 9-13, the following general procedure was followed. To an oven-dried 8 mL catalysis vial equipped with a stir bar was added (JohnPhos)Pd(allyl)Cl (5-10 mol%). The vial was then taken into the glovebox, and to it were

added IMesCuCl (0-10 mol%), KO^{t}Bu (2 equiv), and $B_2(pin)_2$ (2.4 equiv). At this point, solid additives were added if applicable. Next, a solution of 2-cyclohexene-1-one (2 equiv) in 0.1-0.2 mL toluene was added, followed by PhOTf or PhBr (1 equiv, 0.1 or 0.2 mmol scale) as a solution in 0.1-0.2 mL toluene. Liquid additives, if applicable, were added at this point. The walls of the vial were then rinsed with the appropriate amount of toluene to deliver a final concentration of 0.1 to 0.5 M. The vial was sealed with a screw cap, removed from the glovebox, and stirred for 16 h at room temperature (22 °C). Upon completion, internal standard was added (naphthalene, 0.5 equiv), and the reaction was diluted to a volume of around 7 mL through the addition of EtOAc. An aliquot (100 µL) was then taken and eluted through a cotton-stopped Pasteur pipette silica plug (2.5 cm height and 0.5 cm in diameter) with 2 mL EtOAc. Crude yields of **3a** and **4** were analyzed by GC-FID analysis.

2.4.5: Troubleshooting arylboration reaction and purification

Changes to stirring rates between 300-800 RPM have no impact on yields. The reaction typically commences as a translucent yellow solution with white solids in suspension, then the solids dissolve and the reaction gradually changes colours through orange, red, and dark brown. In some cases, the reaction clumps up after turning dark brown, the stir bar gets stuck, and stirring ceases. However, this does not affect reaction yields, and stirring is only important in the initial phases of the reaction to ensure that the white solids dissolve fully.

Contamination of ^{1}H NMR spectra with grease (large signal for methylenes at 1.2 ppm, small signal at 0.8 ppm for methyl) was a common issue encountered in our purified arylboration products. Extensive effort was dedicated towards trying to determine the source of the grease and to eliminate it. The solvent purification system, column frits, column solvents, and squirt bottles used for benchtop solvents were found to contain the same grease which contaminates isolated arylboration products, but the amount of grease in NMR spectra could not be reduced even after extensively cleaning glassware or using different equipment. Efforts for removing grease from isolated materials through trituration, filtration, silica plugs, and columns proved unfruitful due to solubility of products in nonpolar solvents and co-elution of grease with the desired material. It is possible that our arylboration products may have a high affinity towards retaining grease. Grease could only be removed from our products by liquid-liquid extraction between pentane and

acetonitrile, but this would cause drastic reduction in yield since material was lost in the pentane layers. Oxidation of the crude arylboration products, prior to column chromatography, to the corresponding alcohol, followed by trituration with pentane, allowed for the removal of grease, but this was low yielding. The alcohol products were often contaminated with pinacol in these cases. Oxidation of the purified arylboration product, on the other hand, was simple and efficient. The integration of the major grease signal at 1.2 ppm is typically between 1 and 4 relative to the arylboration product (normalized to 1H for the benzylic proton), and the size of the grease peak within this range bears no impact on the measured yields. For several batches of product **3a**, isolated yield was consistently within 2% error, independent of the size of the grease peak between 1 and 4. This suggests that the actual mass of grease in the purified sample is negligible. Based on this observation, we report some of our scope examples (performed on 0.2 mmol scale) with leftover grease peaks, and believe that this grease bears no impact on the reported isolated yields. Grease affects some compounds more than others, so the level of contamination varies. Importantly, grease removal on larger scales (1 mmol scale reaction) was simple, as grease-free product could be precipitated out of solution after chromatographic purification.

2.4.6: Procedures and characterizations for substrate scope and scale-up

General Procedure A: Carboboration of Enones with Aryl Triflates

An oven-dried (120 °C) 8 mL screw-cap vial equipped with an oven-dried micro-stir bar was first cooled in a desiccator, then (JohnPhos)Pd(allyl)Cl (9.6 mg, 0.02 mmol, 10 mol%) was added under air. The vial was taken into a nitrogen-filled glovebox, then IMesCuCl (2.0 mg, 0.005 mmol, 2.5 mol%), KO^{t}Bu (44.9 mg, 0.4 mmol, 2 equiv), and $B_2(pin)_2$ (122 mg, 0.48 mmol, 2.4 equiv) were added in that order. A solution of aryl triflate (0.2 mmol, 1 equiv) in toluene (0.2 mL) was then added to the reaction, and the vial containing the aryl triflate was rinsed once with another 0.2 mL of toluene and added to the reaction to ensure a complete transfer. Immediately afterwards, a solution of enone (0.4 mmol, 2 equiv) in toluene (0.2 mL) was added to the reaction, and the vial containing the enone was rinsed once with 0.2 mL toluene before adding to the reaction again. Lastly, the side walls of the reaction vial were rinsed with 0.2 mL toluene, producing a final reaction concentration of 0.2 M relative to the limiting reagent (aryl triflate). At this point, the vial was sealed tightly with a screwcap, removed from the glovebox, and stirred at room temperature (22 °C) for 16 hours (any stir rate from 300 to 800 RPM). The initial reaction mixtures were

typically a yellow solution with a white solid, and overnight they formed opaque brown or black gels. Upon completion, internal standard was added (naphthalene, 12.8 mg, 0.1 mmol, 0.5 equiv), and the reaction was diluted to a volume of around 7 mL through the addition of EtOAc. An aliquot (100 μL) was then taken and eluted through a cotton-stopped Pasteur pipette silica plug (2.5 cm height and 0.5 cm in diameter) with 2 mL EtOAc. The eluted sample was analyzed by GC-MS and GC-FID to confirm product formation and determine the anti/syn diastereomeric ratio (FID integrations). The remainder of the diluted reaction mixture (6.9 mL) was eluted through a glass-fritted cylindrical-funnel silica plug (2.5 cm in both height and diameter) with approximately 80 mL EtOAc, and the flowthrough was concentrated through rotary evaporation to provide a crude brown oil. This crude product was then purified by column chromatography (wet loading in DCM; either using a manual flash column or the Combi Flash separation system), concentrated by rotary evaporation, and dried under high vacuum to yield pure anti products, typically as white solids. Diastereomeric ratios are reported based on FID integrations of crude material. Isolated yields are reported for the single anti (major) product, unless noted otherwise.

General Procedure B: Carboboration of Enones with Aryl Bromides

The protocol for carboboration using aryl bromides is identical to that of aryl triflates described in General Procedure A, except with different loadings of (JohnPhos)Pd(allyl)Cl (7.2 mg, 0.015 mmol, 7.5 mol%) and IMesCuCl (6.1 mg, 0.015 mmol, 7.5 mol%).

Compound **3a**

(2*RS*,3*RS*)-2-phenyl-3-(4,4,5,5-tetramethyl-1,3,2-dioxaborolan-2-yl)cyclohexan-1-one

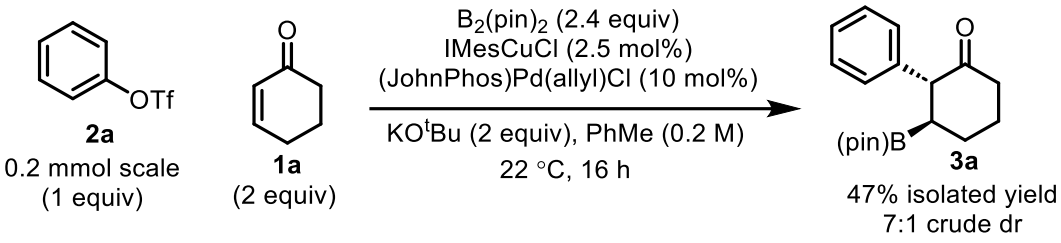

Compound **3a** was prepared through General Procedure A using phenyl triflate **2a** (45.2 mg, 0.2 mmol, 1 equiv) and 2-cyclohexene-1-one **1a** (38.5 mg, 0.4 mmol, 2 equiv). The product (7:1 crude dr) was purified by flash column chromatography (17 cm height, 2.5 cm diameter, 18 mL fractions, 100 mL 10%, 200 mL 15%, 200 mL 20% ether in toluene), and pure material was obtained in fractions 8 and 9 (TLC: Rf = 0.48 in 20% ether in toluene). Compound **3a** was obtained as a white solid (28.3 mg, 0.094 mmol, 47% yield). ^{1}H NMR (400 MHz, $CDCl_3$) δ 7.35 – 7.27 (m, 2H), 7.25 – 7.18 (m, 1H), 7.17 – 7.11 (m, 2H), 3.68 (d, J = 12.3 Hz, 1H), 2.60 – 2.45 (m, 2H), 2.32 – 2.20 (m, 1H), 2.03 – 1.79 (m, 4H), 0.97 (s, 6H), 0.95 (s, 6H); ^{13}C NMR (101 MHz, $CDCl_3$) δ 210.8, 138.4, 129.4, 128.2, 127.0, 83.4, 58.4, 42.6, 30.2, 27.5, 24.5, 24.4; Accurate Mass (EI) *m/z* calcd for $C_{18}H_{25}BO_3$ $[M]^+$ 300.1891, Found: 300.1821, Spectral Accuracy 98.8%.

Compound **3b**

(2*RS*,3*RS*)-2-([1,1'-biphenyl]-4-yl)-3-(4,4,5,5-tetramethyl-1,3,2-dioxaborolan-2-yl)cyclohexan-1-one

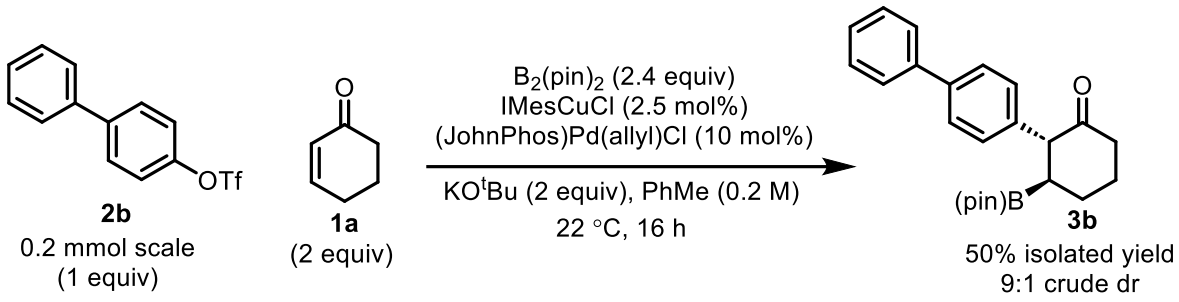

Compound **3b** was prepared through General Procedure A using 4-(phenyl) phenyl triflate **2b** (60.5 mg, 0.2 mmol, 1 equiv) and 2-cyclohexene-1-one **1a** (38.5 mg, 0.4 mmol, 2 equiv). The product (9:1 crude dr) was purified by flash column chromatography (17 cm height, 2.5 cm diameter, 18 mL fractions, 100 mL 5%, 200 mL 10%, 100 mL 15% ether in toluene), and pure material was obtained in fractions 11-14 (TLC: Rf = 0.45 in 25% EtOAc in hexane). Compound **3b** was obtained as a white solid (37.8 mg, 0.100 mmol, 50% yield). ^{1}H NMR (400 MHz, $CDCl_3$) δ 7.59 – 7.55 (m, 2H), 7.53 (d, J = 8.2 Hz, 2H), 7.47 – 7.37 (m, 2H), 7.35 – 7.30 (m, 1H), 7.21 (d, J = 8.2 Hz, 2H), 3.73 (d, J = 12.0 Hz, 1H), 2.61 – 2.47 (m, 2H), 2.33 – 2.20 (m, 1H), 2.02 – 1.81 (m, 4H), 0.98 (s, 6H), 0.96 (s, 6H); ^{13}C NMR (101 MHz, $CDCl_3$) δ 210.9, 141.4, 139.9, 137.6, 129.8, 128.8, 127.2, 127.1, 126.9, 83.5, 58.1, 42.6, 30.2, 27.5, 24.5; Accurate Mass (EI) *m/z* calcd for $C_{24}H_{29}BO_3$ $[M]^+$ 376.2204, Found: 376.2212, Spectral Accuracy 98.9%.

Compound **3c**

(2*RS*,3*RS*)-2-(4-(*tert*-butyl)phenyl)-3-(4,4,5,5-tetramethyl-1,3,2-dioxaborolan-2-yl)cyclohexan-1-one

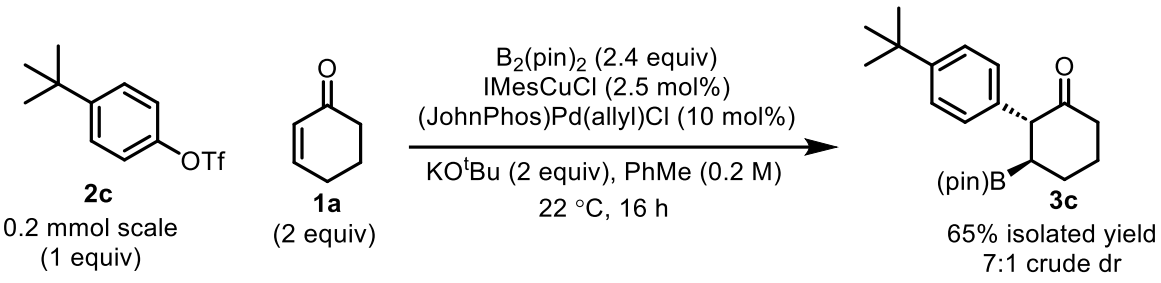

Compound **3c** was prepared through General Procedure A using 4-(*tert*-butyl)phenyl triflate **2c** (56.5 mg, 0.2 mmol, 1 equiv) and 2-cyclohexene-1-one **1a** (38.5 mg, 0.4 mmol, 2 equiv). The product (7:1 crude dr) was purified using the Combi Flash (24-gram column, 5 to 15% Et_2O in toluene gradient over 20 minutes, 35 mL/min flow rate, 18 mL fractions), and mostly pure product was obtained in fractions 16-22 (TLC: Rf = 0.40 in 20% EtOAc in hexane). A second purification by flash column chromatography (17 cm height and 1.5 cm diameter silica gel column, 7 mL fractions, gradient of 5, 10, 15, 20% EtOAc in hexanes, 50 mL of each eluent) was performed to obtain analytically pure material (fractions 17 to 19). Compound **3c** was obtained as a white solid (46.1 mg, 0.129 mmol, 65% yield). ^{1}H NMR (400 MHz, $CDCl_3$) δ 7.29 (d, J = 8.3 Hz, 2H), 7.04 (d, J = 8.3 Hz, 2H), 3.64 (d, J = 12.1 Hz, 1H), 2.58 – 2.43 (m, 2H), 2.28 – 2.15 (m, 1H), 1.97 – 1.73 (m, 4H), 1.26 (s, 9H), 0.96 (s, 6H), 0.90 (s, 6H); ^{13}C NMR (101 MHz, $CDCl_3$) δ 211.0, 149.6, 135.2, 129.0, 125.1, 83.4, 58.1, 42.6, 34.5, 31.5, 30.3, 27.5, 24.5, 24.3; Accurate Mass (EI) *m/z* calcd for $C_{22}H_{33}BO_3$ $[M]^+$ 356.2517, Found: 356.2540, Spectral Accuracy 98.0%.

Compound **3d**

(2*RS*,3*RS*)-3-(4,4,5,5-tetramethyl-1,3,2-dioxaborolan-2-yl)-2-(*p*-tolyl)cyclohexan-1-one

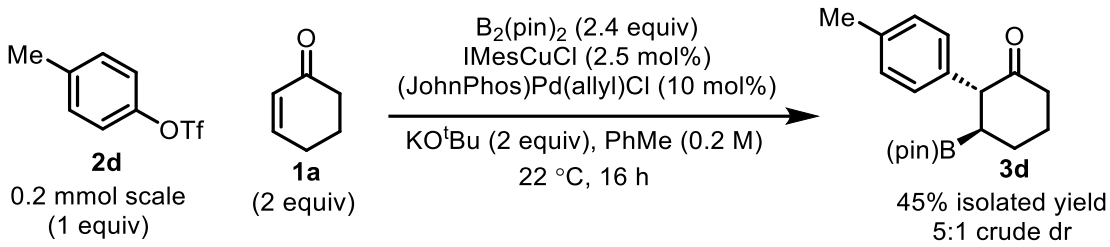

Compound **3d** was prepared through General Procedure A using 4-methylphenyl triflate **2d** (48.0 mg, 0.2 mmol, 1 equiv) and 2-cyclohexene-1-one **1a** (38.5 mg, 0.4 mmol, 2 equiv). The product (5:1 crude dr) was purified using the Combi Flash (24-gram column, 5 to 15% Et_2O in toluene gradient over 20 minutes, 35 mL/min flow rate, 18 mL fractions), and pure material was obtained in fractions 18 to 22 (TLC: Rf = 0.60 in 25% ether in toluene). Compound **3d** was obtained as a white solid (28.2 mg, 0.090 mmol, 45% yield). ^{1}H NMR (400 MHz, $CDCl_3$) δ 7.09 (d, *J* = 7.9 Hz, 2H), 7.00 (d, *J* = 7.9 Hz, 2H), 3.64 (d, *J* = 11.9 Hz, 1H), 2.56 – 2.43 (m, 2H), 2.29 (s, 3H), 2.27 – 2.18 (m, 1H), 1.97 – 1.75 (m, 4H), 0.98 (s, 6H), 0.96 (s, 6H); ^{13}C NMR (101 MHz, $CDCl_3$) δ 211.1, 136.4, 135.3, 129.2, 128.9, 83.4, 58.0, 42.6, 30.2, 27.5, 24.5, 24.5, 21.2; Accurate Mass (EI) *m/z* calcd for $C_{19}H_{27}BO_3$ $[M]^+$ 314.2048, Found: 314.2081, Spectral Accuracy 97.9%.

Compound **3e**

(2*RS*,3*RS*)-2-(4-methoxyphenyl)-3-(4,4,5,5-tetramethyl-1,3,2-dioxaborolan-2-yl)cyclohexan-1-one

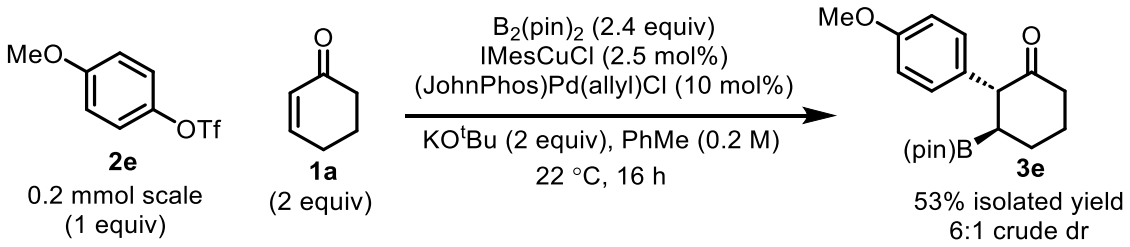

Compound **3e** was prepared through General Procedure A using 4-(methoxy)phenyl triflate **2e** (51.2 mg, 0.2 mmol, 1 equiv) and 2-cyclohexene-1-one **1a** (38.5 mg, 0.4 mmol, 2 equiv). The product (6:1 crude dr) was purified by Combi Flash (24-gram column, 10 to 30% EtOAc in hexanes gradient over 20 minutes, 35 mL/min flow rate, 18 mL fractions), and pure material was obtained in fractions 26-30 (TLC: Rf = 0.48 in 30% ether in toluene, Rf = 0.35 in 20% EtOAc in hexanes). Compound **3e** was obtained as a white solid (34.8 mg, 0.105 mmol, 53% yield). ^{1}H NMR (400 MHz, $CDCl_3$) δ 7.04 (d, J = 8.7 Hz, 2H), 6.83 (d, J = 8.7 Hz, 2H), 3.77 (s, 3H), 3.63 (d, J = 12.2 Hz, 1H), 2.57 – 2.42 (m, 2H), 2.31 – 2.18 (m, 1H), 1.98 – 1.71 (m, 4H), 0.98 (s, 6H), 0.97 (s, 6H); ^{13}C NMR (101 MHz, $CDCl_3$) δ 211.3, 158.6, 130.6, 130.4, 113.7, 83.5, 57.6, 55.4, 42.6, 30.3, 27.6, 24.6, 24.5; Accurate Mass (EI) *m/z* calcd for $C_{19}H_{27}BO_4$ $[M]^+$ 330.1997, Found: 330.1975, Spectral Accuracy 98.5%.

Compound **3e – large scale**

(2*RS*,3*RS*)-2-(4-methoxyphenyl)-3-(4,4,5,5-tetramethyl-1,3,2-dioxaborolan-2-yl)cyclohexan-1-one

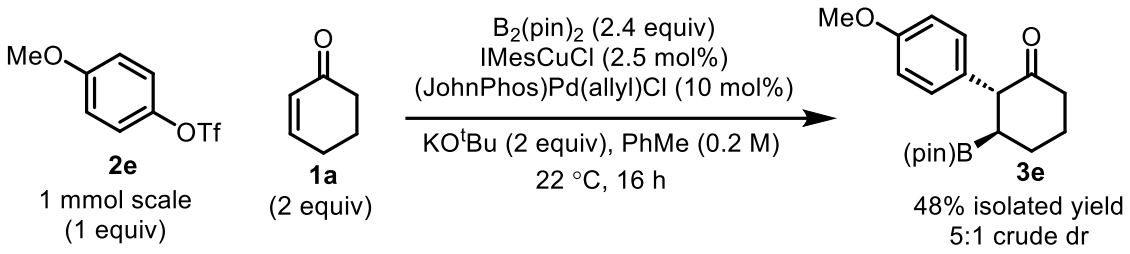

Compound **3e** was also prepared on a 1 mmol scale. An oven-dried (120 °C) 30 mL screw-cap vial with a stir bar was cooled in a desiccator. Then, (JohnPhos)Pd(allyl)Cl (48.1 mg, 0.1 mmol, 10 mol%) was added, followed by $B_2(pin)_2$ (609 mg, 2.4 mmol, 2.4 equiv). The vial was taken into a nitrogen-filled glovebox, then IMesCuCl (10.1 mg, 0.025 mmol, 2.5 mol%) and KO^{t}Bu (224 mg, 2 mmol, 2 equiv) were added. A solution of 4-(methoxy)phenyl triflate **2e** (256 mg, 1 mmol, 1 equiv) in toluene (1 mL) was added, and the vial was rinsed once with 1 mL of toluene and added. Immediately afterwards, a solution of 2-cyclohexene-1-one **1a** (192 mg, 2 mmol, 2 equiv) in toluene (1 mL) was added to the reaction, and the vial was rinsed once with 1 mL toluene before adding to the reaction. The walls of the vial were rinsed with 1 mL toluene, producing a final reaction concentration of 0.2 M relative to aryl triflate. The vial was sealed with a screwcap, removed from the glovebox, and stirred at room temperature (22 °C) for 16 hours at 800 rpm. The reaction was quenched with 50 mL of brine and extracted thrice into 50 mL EtOAc. The combined organic phases were washed twice with 50 mL brine, dried over $MgSO_4$, filtered, and concentrated. GC-FID analysis of the crude (before concentration) provided a 5:1 dr. This was purified by Combi Flash (60-gram column, 10 to 30% EtOAc in hexanes gradient over 35 minutes, 60 mL/min flow rate, 18 mL fractions), and product was obtained in fractions 53-66. After concentration, the resulting yellow oil was dissolved in minimal DCM and precipitated through addition of roughly 5 mL pentane, sonication (5 min), and letting rest overnight. Solvents were removed to leave the white solid, which was dried under high vacuum. Compound **3e** was obtained as a white solid (160 mg, 0.48 mmol, 48% yield) with characterization data matching the above. No grease was detected, and a higher purity NMR spectrum was obtained. ^{1}H NMR (400 MHz, $CDCl_3$) δ 7.08 – 7.00 (m, 2H), 6.88 – 6.79 (m, 2H), 3.78 (s, 3H), 3.63 (d, J = 12.2 Hz, 1H), 2.57 – 2.42 (m, 2H), 2.30 – 2.17 (m, 1H), 1.98 – 1.71 (m, 4H), 0.99 (s, 6H), 0.97 (s, 6H).

Compound **3f**

(2*RS*,3*RS*)-2-(4-chlorophenyl)-3-(4,4,5,5-tetramethyl-1,3,2-dioxaborolan-2-yl)cyclohexan-1-one

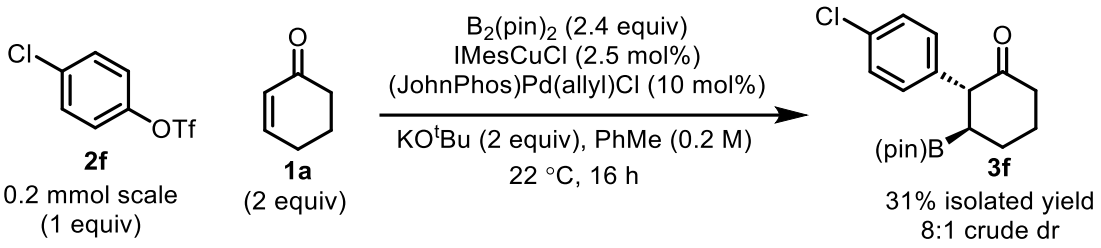

Compound **3f** was prepared through General Procedure A using 4-chloro phenyl triflate **2f** (52.1 mg, 0.2 mmol, 1 equiv) and 2-cyclohexene-1-one **1a** (38.5 mg, 0.4 mmol, 2 equiv). The product (8:1 crude dr) was purified by flash column chromatography (17 cm height, 1.5 cm diameter, 7 mL fractions, 50 mL 5%, 50 mL 10%, 50 mL 15%, 50 mL 20% ether in toluene), and pure material was obtained in fractions 11 through 14 (TLC: Rf = 0.56 in 30% ether in toluene). Compound **3f** was obtained as a white solid (20.7 mg, 0.062 mmol, 31% yield). ^{1}H NMR (400 MHz, $CDCl_3$) δ 7.26 (d, J = 8.4 Hz, 2H), 7.06 (d, J = 8.4 Hz, 2H), 3.66 (d, J = 12.3 Hz, 1H), 2.58 – 2.44 (m, 2H), 2.31 – 2.20 (m, 1H), 1.99 – 1.70 (m, 4H), 0.99 (s, 12H); ^{13}C NMR (101 MHz, $CDCl_3$) δ 210.4, 137.0, 132.8, 130.8, 128.3, 83.6, 57.8, 42.5, 30.2, 27.5, 24.6, 24.5; Accurate Mass (EI) *m/z* calcd for $C_{18}H_{24}BClO_3$ $[M]^+$ 334.1502, Found: 334.1493, Spectral Accuracy 98.5%.

Compound **3g**

(2*RS*,3*RS*)-2-(4-fluorophenyl)-3-(4,4,5,5-tetramethyl-1,3,2-dioxaborolan-2-yl)cyclohexan-1-one

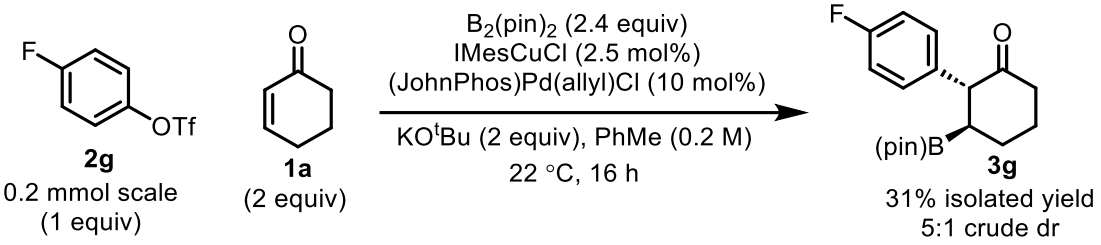

Compound **3g** was prepared through General Procedure A using 4-fluoro phenyl triflate **2g** (48.8 mg, 0.2 mmol, 1 equiv) and 2-cyclohexene-1-one **1a** (38.5 mg, 0.4 mmol, 2 equiv). The product (5:1 crude dr) was purified by flash column chromatography (17 cm height, 1.5 cm diameter, 7 mL fractions, 50 mL 5%, 100 mL 10%, 50 mL 15% ether in toluene), and pure material was obtained in fractions 13 through 17 (TLC: Rf = 0.50 in 20% ether in toluene). Compound **3g** was obtained as a white solid (20.0 mg, 0.063 mmol, 31% yield). ^{1}H NMR (600 MHz, $CDCl_3$) δ 7.08 (dd, J = 8.6, 5.5 Hz, 2H), 6.98 (dd, J = 8.6, 8.6 Hz, 2H), 3.67 (d, J = 12.7 Hz, 1H), 2.57 – 2.45 (m, 2H), 2.28 – 2.21 (m, 1H), 1.99 – 1.72 (m, 4H), 0.98 (s, 6H), 0.98 (s, 6H); ^{13}C NMR (151 MHz, $CDCl_3$) δ 210.7, 162.0 (d, J = 244.6 Hz), 134.3 (d, J = 3.2 Hz), 130.9 (d, J = 7.8 Hz), 115.0 (d, J = 21.2 Hz), 83.5, 57.6, 42.6, 30.2, 27.5, 24.5, 24.5; ^{19}F NMR (283 MHz, CDCl3) δ -116.3; Accurate Mass (EI) *m/z* calcd for $C_{18}H_{24}BO_3F$ $[M]^+$ 318.1797, Found: 318.1835, Spectral Accuracy 97.2%.

Compound **3h**

(2*RS*,3*RS*)-2-(4-nitrophenyl)-3-(4,4,5,5-tetramethyl-1,3,2-dioxaborolan-2-yl)cyclohexan-1-one

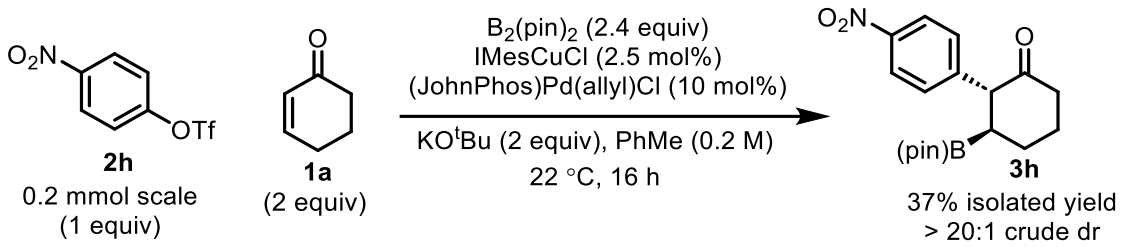

Compound **3h** was prepared through General Procedure A using 4-nitro phenyl triflate **2h** (54.2 mg, 0.2 mmol, 1 equiv) and 2-cyclohexene-1-one **1a** (38.5 mg, 0.4 mmol, 2 equiv). The product (>20:1 crude dr) was purified by flash column chromatography (17 cm height, 1.5 cm diameter, 7 mL fractions, 50 mL 10%, 50 mL 20%, 50 mL 30%, 50 mL 40% EtOAc in hexanes), and the product was obtained in fractions 16 through 20. This was purified again by flash column chromatography (17 cm height, 1.5 cm diameter, 7 mL fractions, 50 mL 10%, 100 mL 15%, 50 mL 20% ether in toluene), and pure material was obtained in fractions 11 through 13 (TLC: Rf = 0.63 in 40% ether in toluene, or 0.56 in 40% EtOAc in hexane). Compound **3h** was obtained as a yellow solid (25.2 mg, 0.073 mmol, 37% yield). ^{1}H NMR (400 MHz, $CDCl_3$) δ 8.17 (d, J = 8.8 Hz, 2H), 7.30 (d, J = 8.8 Hz, 2H), 3.81 (d, J = 12.2 Hz, 1H), 2.61 – 2.46 (m, 2H), 2.37 – 2.23 (m, 1H), 2.04 – 1.76 (m, 4H), 0.98 (s, 6H), 0.97 (s, 6H); ^{13}C NMR (101 MHz, $CDCl_3$) δ 209.6, 146.5, 130.5, 123.3, 83.8, 58.2, 42.5, 30.1, 27.4, 24.6, 24.4; Accurate Mass (EI) *m/z* calcd for $C_{18}H_{24}NO_5B$ $[M]^+$ 345.1742, Found: 345.1753, Spectral Accuracy 98.3%. The signal from one of the substituted aromatic carbons was too weak to be detected by ^{13}C NMR.

Compound **3i**

methyl 4-((1*RS*,6*RS*)-2-oxo-6-(4,4,5,5-tetramethyl-1,3,2-dioxaborolan-2-yl)cyclohexyl)benzoate

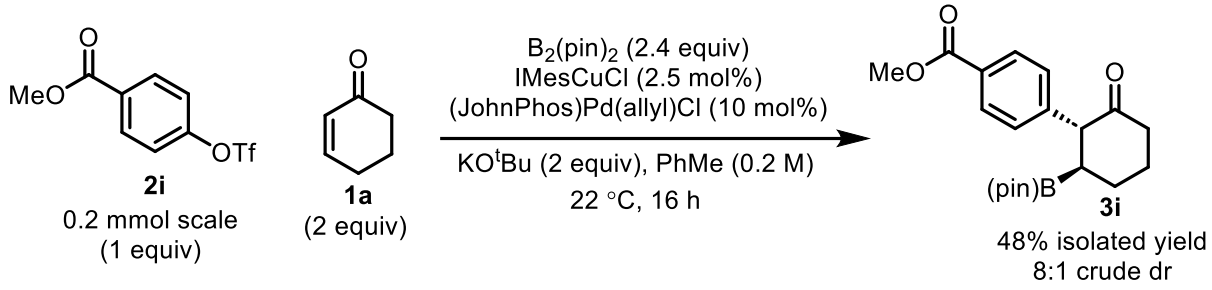

Compound **3i** was prepared through General Procedure A using 4-(methoxycarbonyl) phenyl triflate **2i** (56.8 mg, 0.2 mmol, 1 equiv) and 2-cyclohexene-1-one **1a** (38.5 mg, 0.4 mmol, 2 equiv). The product (8:1 crude dr) was purified by flash column chromatography (17 cm height, 2.5 cm diameter, 18 mL fractions, 100 mL 15%, 200 mL 20%, 200 mL 25% EtOAc in hexanes), and pure material was obtained in fractions 14 through 19 (TLC: Rf = 0.39 in 30% EtOAc in hexane). Compound **3i** was obtained as a white solid (34.2 mg, 0.095 mmol, 48% yield). ^{1}H NMR (400 MHz, $CDCl_3$) δ 7.97 (d, *J* = 8.2 Hz, 2H), 7.20 (d, *J* = 8.2 Hz, 2H), 3.89 (s, 3H), 3.75 (d, *J* = 12.3 Hz, 1H), 2.58 – 2.44 (m, 2H), 2.29 – 2.22 (m, 1H), 2.00 – 1.76 (m, 4H), 0.95 (s, 6H), 0.95 (s, 6H); ^{13}C NMR (101 MHz, $CDCl_3$) δ 210.1, 167.3, 144.0, 129.6, 129.5, 128.8, 83.6, 58.4, 52.1, 42.5, 30.1, 27.4, 24.5, 24.4; Accurate Mass (EI) *m/z* calcd for $C_{20}H_{27}BO_5$ $[M]^+$ 358.1946, Found: 358.1900, Spectral Accuracy 98.2%.

Compound **3j**

(2*RS*,3*RS*)-3-(4,4,5,5-tetramethyl-1,3,2-dioxaborolan-2-yl)-2-(3-(trifluoromethyl)phenyl)cyclohexan-1-one

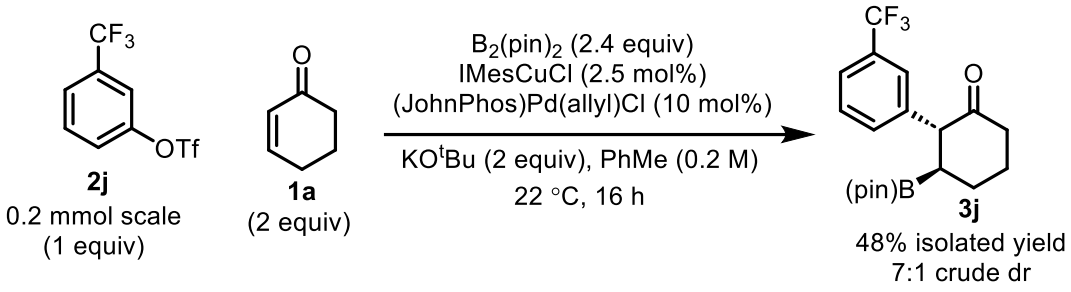

Compound **3j** was prepared through General Procedure A using 3-(trifluoromethyl)phenyl triflate **2j** (58.8 mg, 0.2 mmol, 1 equiv) and 2-cyclohexene-1-one **1a** (38.5 mg, 0.4 mmol, 2 equiv). The product (7:1 crude dr) was purified by flash column chromatography (17 cm height, 2.5 cm diameter, 18 mL fractions, 100 mL 5%, 200 mL 10%, 200 mL 15% ether in toluene), and pure material was obtained in fractions 10 to 13 (TLC: Rf = 0.56 in 30% ether in toluene). Compound **3j** was obtained as a white solid (35.4 mg, 0.096 mmol, 48% yield). ^{1}H NMR (600 MHz, $CDCl_3$) δ 7.48 (d, J = 7.7 Hz, 1H), 7.42 (dd, J = 7.7, 7.7 Hz, 1H), 7.38 (s, 1H), 7.32 (d, J = 7.7 Hz, 1H), 3.75 (d, J = 12.4 Hz, 1H), 2.59 – 2.47 (m, 2H), 2.30 – 2.23 (m, 1H), 2.01 – 1.76 (m, 4H), 0.94 (s, 6H), 0.93 (s, 6H); ^{13}C NMR (151 MHz, $CDCl_3$) δ 210.0, 139.5, 133.0, 130.4 (q, J = 31.8 Hz), 128.6, 126.5 (q, J = 3.8 Hz), 124.4 (q, J = 271.9 Hz), 123.8 (q, J = 4.0 Hz), 83.6, 58.2, 42.5, 30.2, 29.8, 27.5, 24.4; ^{19}F NMR (282 MHz, $CDCl_3$) δ -62.6; Accurate Mass (EI) *m/z* calcd for $C_{19}H_{24}BF_3O_3$ $[M]^+$ 368.1765, Found: 368.1798, Spectral Accuracy 98.2%.

Compound **3k**

(2*RS*,3*RS*)-2-(naphthalen-2-yl)-3-(4,4,5,5-tetramethyl-1,3,2-dioxaborolan-2-yl)cyclohexan-1-one

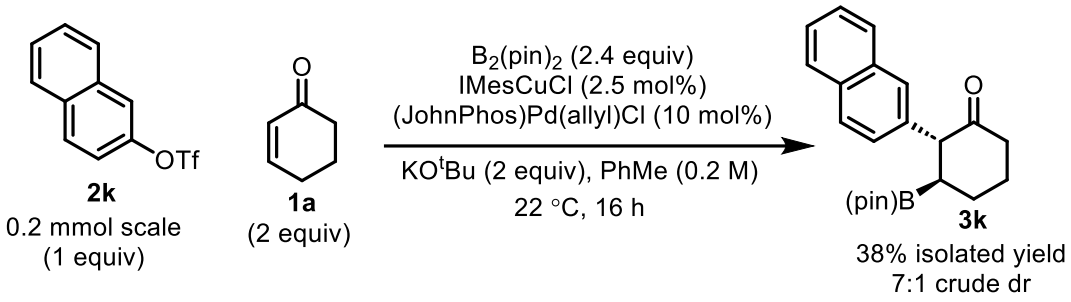

Compound **3k** was prepared through General Procedure A using 2-naphthyl triflate **2k** (55.2 mg, 0.2 mmol, 1 equiv) and 2-cyclohexene-1-one **1a** (38.5 mg, 0.4 mmol, 2 equiv). The product (7:1 crude dr) was purified using the Combi Flash (24-gram column, 5 to 15% Et_2O in toluene gradient over 30 minutes, 35 mL/min flow rate, 18 mL fractions), and pure material was obtained in fractions 37 to 45 (TLC: Rf = 0.39 in 20% ether in toluene). Compound **3k** was obtained as a white solid (26.3 mg, 0.075 mmol, 38% yield). ^{1}H NMR (400 MHz, $CDCl_3$) δ 7.83 – 7.74 (m, 3H), 7.61 – 7.56 (m, 1H), 7.45 – 7.38 (m, 2H), 7.29 – 7.26 (m, 1H), 3.87 (d, J = 11.9 Hz, 1H), 2.62 – 2.50 (m, 2H), 2.32 – 2.23 (m, 1H), 2.05 – 1.86 (m, 4H), 0.89 (s, 6H), 0.87 (s, 6H); ^{13}C NMR (101 MHz, $CDCl_3$) δ 210.9, 136.2, 133.4, 132.7, 128.0, 127.8, 127.7, 125.8, 125.5, 83.5, 58.4, 42.6, 30.1, 27.5, 24.5, 24.4; Accurate Mass (EI) *m/z* calcd for $C_{22}H_{27}BO_3$ $[M]^+$ 350.2048, Found: 350.2067, Spectral Accuracy 98.6%.

Compound **3l**

(*2RS*,3*RS*)-2-(2-methoxyphenyl)-3-(4,4,5,5-tetramethyl-1,3,2-dioxaborolan-2-yl)cyclohexan-1-one

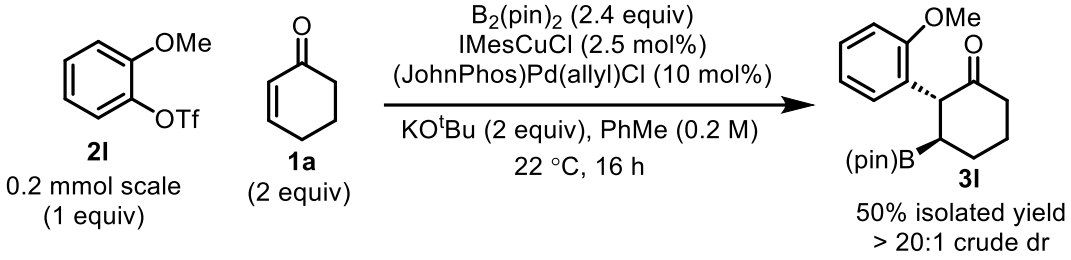

Compound **3l** was prepared through General Procedure A using 2-(methoxy)phenyl triflate **2l** (51.2 mg, 0.2 mmol, 1 equiv) and 2-cyclohexene-1-one **1a** (38.5 mg, 0.4 mmol, 2 equiv). The product (>20:1 crude dr) was purified using the Combi Flash (24-gram column, 10 to 30% EtOAc in hexanes gradient over 20 minutes, 35 mL/min flow rate, 18 mL fractions), and pure material was obtained in fractions 24 to 28 (TLC: Rf = 0.38 in 20% EtOAc in hexanes). Compound **3l** was obtained as a colourless oil (33.1 mg, 0.100 mmol, 50% yield). ^{1}H NMR (400 MHz, $CDCl_3$) δ 7.18 (ddd, J = 8.2, 7.5, 1.7 Hz, 1H), 7.08 (dd, J = 7.5, 1.7 Hz, 1H), 6.89 (ddd, J = 7.5, 7.5, 1.2 Hz, 1H), 6.82 (dd, J = 8.2, 1.2 Hz, 1H), 4.02 (d, J = 12.5 Hz, 1H), 3.76 (s, 3H), 2.57 – 2.43 (m, 2H), 2.26 – 2.16 (m, 1H), 1.99 – 1.79 (m, 4H), 0.99 (s, 6H), 0.96 (s, 6H); ^{13}C NMR (101 MHz, $CDCl_3$) δ 210.5, 157.3, 129.8, 128.0, 127.7, 120.4, 110.6, 83.3, 55.6, 51.9, 42.4, 29.7, 27.5, 24.5, 24.4; Accurate Mass (EI) *m/z* calcd for $C_{19}H_{27}BO_4$ $[M]^+$ 330.1997, Found: 330.2044, Spectral Accuracy 97.4%.

Compound **3m**

(2*RS*,3*RS*)-2-(naphthalen-1-yl)-3-(4,4,5,5-tetramethyl-1,3,2-dioxaborolan-2-yl)cyclohexan-1-one

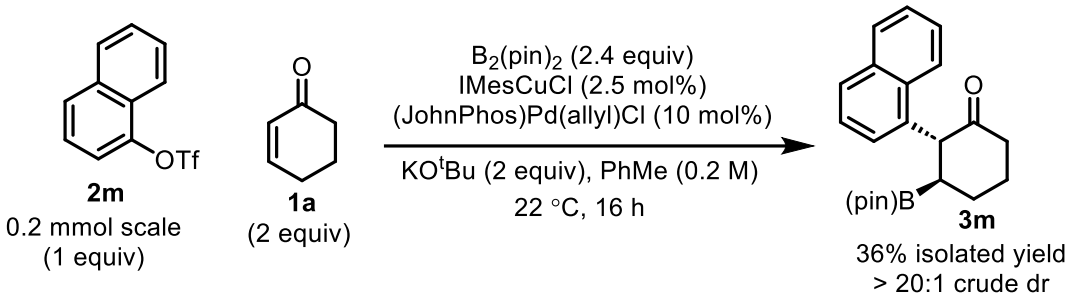

Compound **3m** was prepared through General Procedure A using 1-naphthyl triflate **2m** (55.2 mg, 0.2 mmol, 1 equiv) and 2-cyclohexene-1-one **1a** (38.5 mg, 0.4 mmol, 2 equiv). The product (>20:1 crude dr) was purified by flash column chromatography (17 cm height, 2.5 cm diameter, 18 mL fractions, 100 mL 5%, 200 mL 10%, 200 mL 15% ether in toluene), and pure material was obtained in fractions 11 to 14 (TLC: Rf = 0.61 in 30% ether in toluene). Compound **3m** was obtained as a white solid (25.3 mg, 0.072 mmol, 36% yield). ^{1}H NMR (600 MHz, $CDCl_3$) δ 7.85 – 7.79 (m, 2H), 7.73 (d, J = 8.2 Hz, 1H), 7.49 – 7.39 (m, 3H), 7.33 (dd, J = 7.2, 1.2 Hz, 1H), 4.51 (d, J = 12.6 Hz, 1H), 2.76 – 2.57 (m, 2H), 2.37 – 2.29 (m, 1H), 2.15 – 1.93 (m, 4H), 0.86 (s, 6H), 0.76 (s, 6H); ^{13}C NMR (151 MHz, $CDCl_3$) δ 210.6, 135.3, 133.9, 132.3, 128.9, 127.7, 126.4, 125.7, 125.3, 125.3, 123.9, 83.4, 42.9, 30.3, 29.8, 27.9, 24.3, 24.3; Accurate Mass (EI) *m/z* calcd for $C_{22}H_{27}BO_3$ $[M]^+$ 350.2048, Found: 350.2050, Spectral Accuracy 98.5%.

Compound **3n**

(2*RS*,3*RS*)-3-(4,4,5,5-tetramethyl-1,3,2-dioxaborolan-2-yl)-2-(*o*-tolyl)cyclohexan-1-one

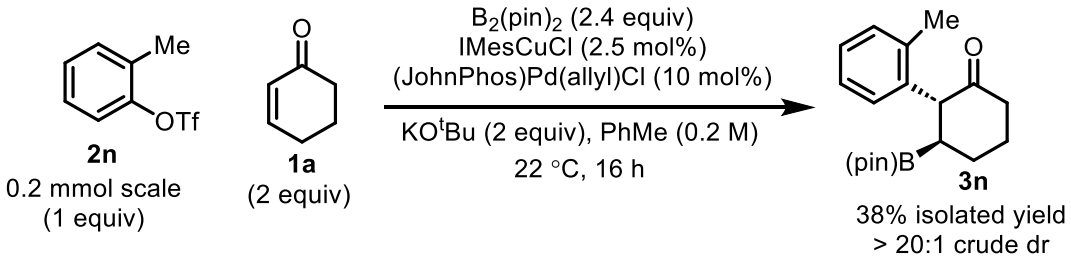

Compound **3n** was prepared through General Procedure A using 2-(methyl) phenyl triflate **2n** (48.0 mg, 0.2 mmol, 1 equiv) and 2-cyclohexene-1-one **1a** (38.5 mg, 0.4 mmol, 2 equiv). The product (>20:1 crude dr) was purified by flash column chromatography (17 cm height, 2.5 cm diameter, 18 mL fractions, 100 mL 5%, 100 mL 10%, 200 mL 15% ether in toluene), and mostly pure material was obtained in fractions 11 through 14 (TLC: Rf = 0.38 in 20% EtOAc in hexane). A second purification was performed through flash column chromatography (17 cm height, 1.5 cm diameter, 7 mL fractions, 50 mL 5%, 50 mL 10%, 50 mL 15%, 50 mL 20% EtOAc in hexane), giving pure product in fractions 17 and 18. Compound **3n** was obtained as a white solid (23.9 mg, 0.076 mmol, 38% yield). ^{1}H NMR (400 MHz, $CDCl_3$) δ 7.19 – 7.12 (m, 1H), 7.12 – 7.06 (m, 3H), 3.90 (d, J = 11.9 Hz, 1H), 2.59 – 2.47 (m, 2H), 2.29 – 2.25 (m, 1H), 2.24 (s, 3H), 2.02 – 1.81 (m, 4H), 0.95 (s, 6H), 0.93 (s, 6H); ^{13}C NMR (101 MHz, $CDCl_3$) δ 210.8, 137.2, 136.6, 130.1, 128.6, 126.9, 125.9, 83.4, 54.2, 42.8, 30.2, 27.7, 24.4, 20.1; Accurate Mass (EI) *m/z* calcd for $C_{19}H_{27}BO_3$ $[M]^+$ 314.2048, Found: 314.1980, Spectral Accuracy 97.6%.

Compound **3o**

(2*SR*,3*RS*)-2-allyl-3-(4,4,5,5-tetramethyl-1,3,2-dioxaborolan-2-yl)cyclohexan-1-one

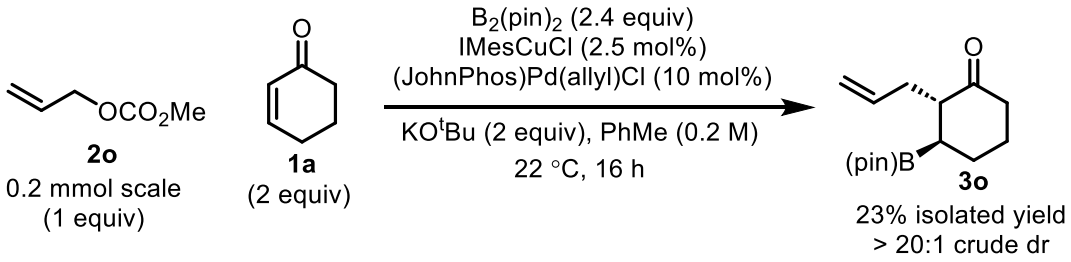

Compound **3o** was prepared through General Procedure A using allyl methyl carbonate **2o** (23.2 mg, 0.2 mmol, 1 equiv) and 2-cyclohexene-1-one **1a** (38.5 mg, 0.4 mmol, 2 equiv). The product (>20:1 crude dr) was purified by flash column chromatography (17 cm height, 1.5 cm diameter, 7 mL fractions, 50 mL 5%, 50 mL 10%, 50 mL 15%, 50 mL 20% ether in toluene), and pure material was obtained in fractions 9 through 12 (TLC: Rf = 0.50 in 25% EtOAc in hexane). Compound **3o** was obtained as a colourless oil (12.2 mg, 0.046 mmol, 23% yield). ^{1}H NMR (400 MHz, $CDCl_3$) δ 5.82 (dddd, J = 17.1, 10.1, 7.0, 7.0 Hz, 1H), 5.01 (dd, J = 17.1, 1.5 Hz, 1H), 4.96 (dd, J = 10.1, 1.5 Hz, 1H), 2.51 (ddd, J = 11.6, 7.6, 3.8 Hz, 1H), 2.44 – 2.27 (m, 4H), 2.21 – 2.13 (m, 1H), 2.13 – 2.05 (m, 1H), 1.87 – 1.78 (m, 1H), 1.75 – 1.63 (m, 2H), 1.26 (s, 6H), 1.25 (s, 6H); ^{13}C NMR (101 MHz, $CDCl_3$) δ 213.1, 137.0, 116.3, 83.6, 50.7, 42.4, 34.1, 29.7, 27.1, 25.0, 24.7; Accurate Mass (EI) *m/z* calcd for $C_{15}H_{25}BO_3$ $[M]^+$ 264.1891, Found: 264.1886, Spectral Accuracy 98.3%.

Compound **3p**

(1*RS*,6*RS*)-6-(4,4,5,5-tetramethyl-1,3,2-dioxaborolan-2-yl)-[1,1'-bi(cyclohexan)]-1'-en-2-one

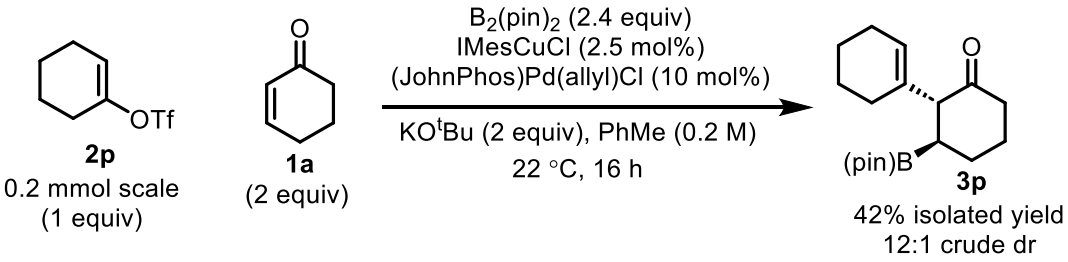

Compound **3p** was prepared through General Procedure A using 1-cyclohexenyl triflate **2p** (46.0 mg, 0.2 mmol, 1 equiv) and 2-cyclohexene-1-one **1a** (38.5 mg, 0.4 mmol, 2 equiv). The product (12:1 crude dr) was purified by flash column chromatography (17 cm height, 1.5 cm diameter, 7 mL fractions, 50 mL 5%, 50 mL 10%, 50 mL 15%, 50 mL 20% ether in toluene), and pure material was obtained in fractions 10 through 14 (TLC: Rf = 0.57 in 20% EtOAc in hexane). Compound **3p** was obtained as a colourless oil (27.8 mg, 0.084 mmol, 42% yield). ^{1}H NMR (400 MHz, $CDCl_3$) δ 5.46 – 5.36 (m, 1H), 2.94 (d, J = 12.6 Hz, 1H), 2.44 – 2.23 (m, 2H), 2.16 – 2.06 (m, 1H), 2.04 – 1.97 (m, 2H), 1.96 – 1.88 (m, 2H), 1.86 – 1.80 (m, 1H), 1.75 – 1.67 (m, 2H), 1.65 – 1.58 (m, 3H), 1.57 – 1.50 (m, 2H), 1.21 (s, 6H), 1.19 (s, 6H); ^{13}C NMR (101 MHz, $CDCl_3$) δ 211.7, 136.4, 124.5, 83.4, 59.6, 42.6, 29.7, 27.5, 27.1, 25.3, 24.9, 24.7, 22.9, 22.6; Accurate Mass (EI) *m/z* calcd for $C_{18}H_{29}BO_3$ $[M]^+$ 304.2204, Found: 304.2194, Spectral Accuracy 99.2%.

Compound **3q**

(2*RS*,3*RS*)-2-(cyclopent-1-en-1-yl)-3-(4,4,5,5-tetramethyl-1,3,2-dioxaborolan-2-yl)cyclohexan-1-one

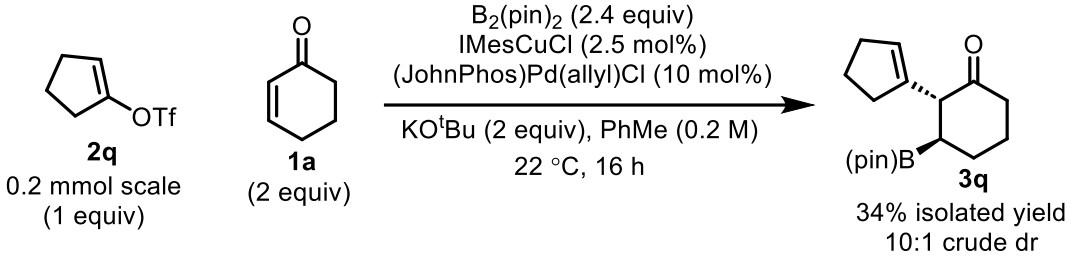

Compound **3q** was prepared through General Procedure A using 1-cyclopentenyl triflate **2q** (43.2 mg, 0.2 mmol, 1 equiv) and 2-cyclohexene-1-one **1a** (38.5 mg, 0.4 mmol, 2 equiv). The product (10:1 crude dr) was purified by flash column chromatography (17 cm height, 1.5 cm diameter, 7 mL fractions, 50 mL 5%, 50 mL 10%, 50 mL 15%, 50 mL 20% ether in toluene), and pure material was obtained in fractions 13 through 16 (TLC: Rf = 0.53 in 25% EtOAc in hexane). Compound **3q** was obtained as a colourless oil (19.9 mg, 0.069 mmol, 34% yield). ^{1}H NMR (400 MHz, $CDCl_3$) δ 5.47 – 5.40 (m, 1H), 3.24 (d, J = 12.1 Hz, 1H), 2.44 – 2.22 (m, 7H), 2.17 – 2.05 (m, 1H), 1.90 – 1.81 (m, 3H), 1.79 – 1.68 (m, 1H), 1.65 – 1.57 (m, 1H), 1.20 (s, 6H), 1.18 (s, 6H); ^{13}C NMR (101 MHz, $CDCl_3$) δ 211.4, 142.8, 127.1, 83.4, 53.7, 42.4, 33.9, 32.3, 29.7, 26.8, 24.8, 24.7, 23.5; Accurate Mass (EI) *m/z* calcd for $C_{17}H_{27}BO_3$ $[M]^+$ 290.2048, Found: 290.2046, Spectral Accuracy 98.4%.

Compound **3r**

(2*RS*,3*RS*)-2-(4-methoxyphenyl)-3-(4,4,5,5-tetramethyl-1,3,2-dioxaborolan-2-yl)cyclohexan-1-one

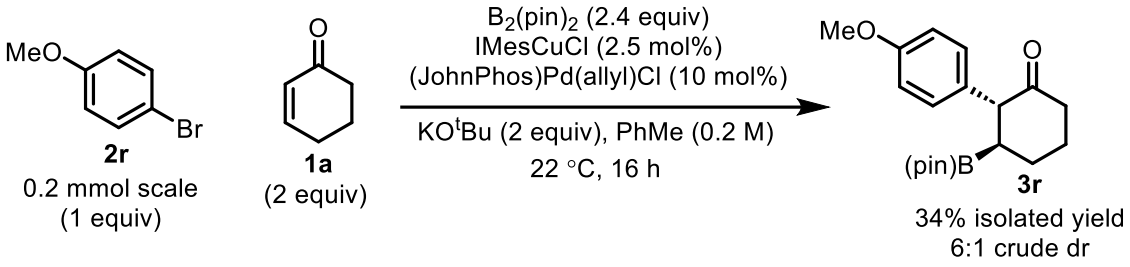

Compound **3r**, which is the same as Compound **3e**, was also prepared here through General Procedure A (2.5 mol% Cu catalyst, 10 mol% Pd catalyst) using 4-bromoanisole **2r** (37.5 mg, 0.2 mmol, 1 equiv) and 2-cyclohexene-1-one **1a** (38.5 mg, 0.4 mmol, 2 equiv). The product (6:1 crude dr) was purified by flash column chromatography, and was obtained as a white solid (22.5 mg, 0.068 mmol, 34% yield). Characterization matches that for **3e**.

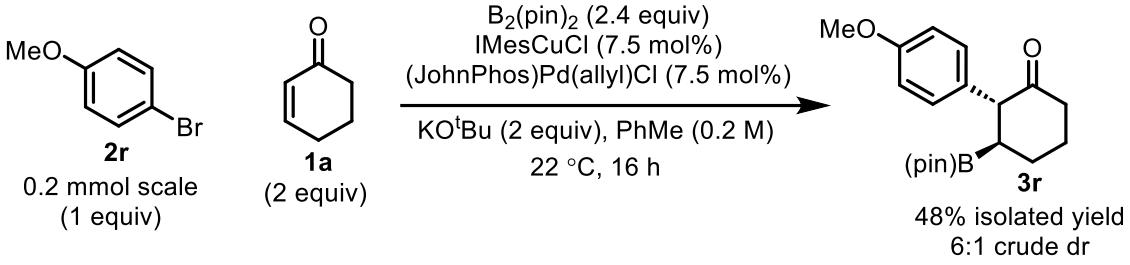

Compound **3r**, which is the same as Compound **3e**, was also prepared here through General Procedure B (7.5 mol% Cu catalyst, 7.5 mol% Pd catalyst) using 4-bromoanisole **2r** (37.5 mg, 0.2 mmol, 1 equiv) and 2-cyclohexene-1-one **1a** (38.5 mg, 0.4 mmol, 2 equiv). The product (6:1 crude dr) was purified by flash column chromatography, and was obtained as a white solid (31.7 mg, 0.096 mmol, 48% yield). Characterization matches that for **3e**.

Compound **3s**

(2*RS*,3*RS*)-3-(4,4,5,5-tetramethyl-1,3,2-dioxaborolan-2-yl)-2-(4-vinylphenyl)cyclohexan-1-one

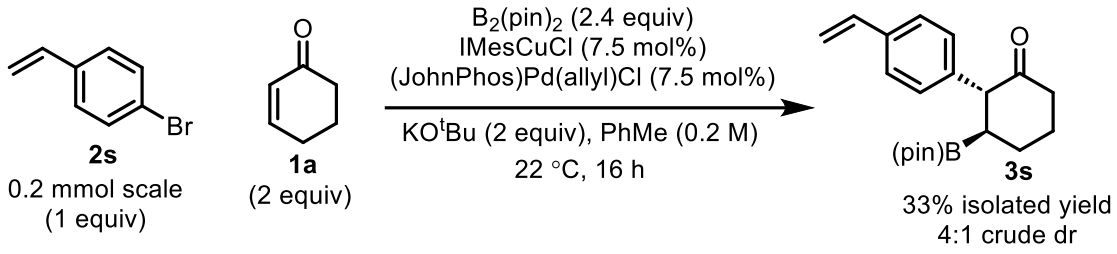

Compound **3s** was prepared through General Procedure B using 4-bromo styrene **2s** (36.6 mg, 0.2 mmol, 1 equiv) and 2-cyclohexene-1-one **1a** (38.5 mg, 0.4 mmol, 2 equiv). The product (4:1 crude dr) was purified by flash column chromatography (17 cm height, 1.5 cm diameter, 7 mL fractions, 50 mL 5%, 50 mL 10%, 50 mL 15%, 50 mL 20% ether in toluene), and product was obtained in fractions 11 through 14 (TLC: Rf = 0.58 in 30% ether in toluene). A second purification was performed through flash column chromatography (17 cm height, 1.5 cm diameter, 7 mL fractions, 50 mL 10%, 50 mL 15%, 50 mL 20%, 50 mL 25% EtOAc in hexane), giving pure product in fractions 14 through 16 (TLC: Rf = 0.55 in 30% EtOAc in hexane). Compound **3s** was obtained as a white solid (21.7 mg, 0.067 mmol, 33% yield). ^{1}H NMR (400 MHz, $CDCl_3$) δ 7.33 (d, J = 8.2 Hz, 2H), 7.08 (d, J = 8.2 Hz, 2H), 6.68 (dd, J = 17.6, 10.9 Hz, 1H), 5.69 (dd, J = 17.6, 1.0 Hz, 1H), 5.18 (dd, J = 10.9, 1.0 Hz, 1H), 3.67 (d, J = 12.1 Hz, 1H), 2.58 – 2.43 (m, 2H), 2.29 – 2.19 (m, 1H), 1.99 – 1.75 (m, 4H), 0.98 (s, 6H), 0.97 (s, 6H); ^{13}C NMR (101 MHz, $CDCl_3$) δ 210.8, 138.2, 137.0, 136.4, 129.6, 126.1, 113.3, 83.5, 58.1, 42.6, 30.2, 27.5, 24.5, 24.5; Accurate Mass (EI) *m/z* calcd for $C_{20}H_{27}BO_3$ $[M]^+$ 326.2048, Found: 326.2024, Spectral Accuracy 98.8%.

Compound **3t**

(2*RS*,3*RS*)-2-(6-methoxypyridin-3-yl)-3-(4,4,5,5-tetramethyl-1,3,2-dioxaborolan-2-yl)cyclohexan-1-one

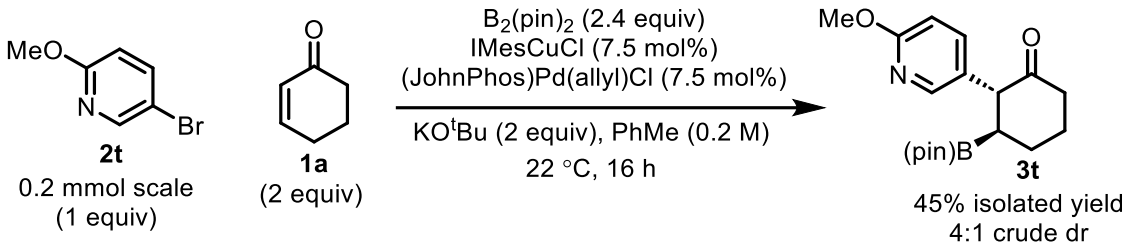

Compound **3t** was prepared through General Procedure B using 5-bromo-2-methoxypyridine **2t** (40.5 mg, 0.2 mmol, 1 equiv) and 2-cyclohexene-1-one **1a** (38.5 mg, 0.4 mmol, 2 equiv). The product (4:1 crude dr) was purified by flash column chromatography (17 cm height, 1.5 cm diameter, 7 mL fractions, 50 mL 10%, 50 mL 15%, 50 mL 20%, 50 mL 30% EtOAc in hexane), and impure product was obtained (TLC: Rf = 0.53 in 25% EtOAc in hexane). A second purification was performed through flash column chromatography (17 cm height, 1.5 cm diameter, 7 mL fractions, 50 mL 5%, 50 mL 10%, 50 mL 15%, 50 mL 20% ether in toluene), giving pure product (TLC: Rf = 0.45 in 20% ether in toluene). Compound **3t** was obtained as a white solid (29.8 mg, 0.090 mmol, 45% yield). ^{1}H NMR (600 MHz, $CDCl_3$) δ 7.90 (d, J = 2.5 Hz, 1H), 7.38 (dd, J = 8.5, 2.5 Hz, 1H), 6.71 (d, J = 8.5 Hz, 1H), 3.90 (s, 3H), 3.64 (d, J = 13.0 Hz, 1H), 2.57 – 2.45 (m, 2H), 2.29 – 2.22 (m, 1H), 1.98 – 1.82 (m, 3H), 1.74 – 1.67 (m, 1H), 1.01 (s, 6H), 1.00 (s, 6H); ^{13}C NMR (151 MHz, $CDCl_3$) δ 210.5, 163.4, 147.3, 139.7, 126.9, 110.4, 83.6, 54.9, 53.5, 42.5, 30.3, 27.5, 24.6, 24.5; Accurate Mass (EI) *m/z* calcd for $C_{18}H_{26}BNO_4$ $[M]^+$ 331.1949, Found: 331.1961. Spectral Accuracy 97.2%.

Compound **3u**

(2*RS*,3*RS*)-2-(benzofuran-7-yl)-3-(4,4,5,5-tetramethyl-1,3,2-dioxaborolan-2-yl)cyclohexan-1-one

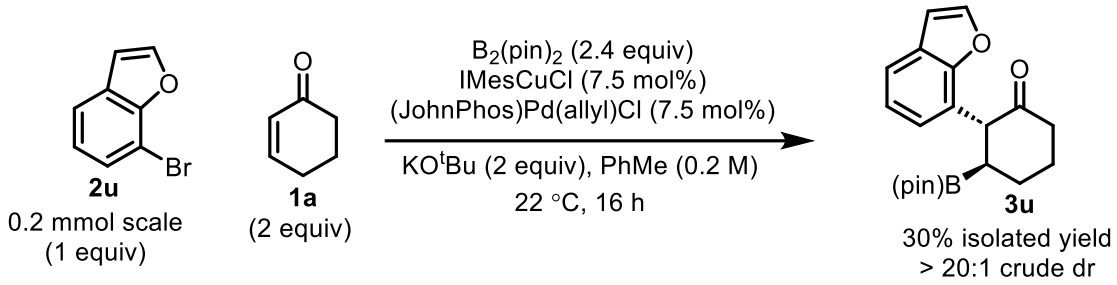

Compound **3u** was prepared through General Procedure B using 7-bromobenzofuran **2u** (39.5 mg, 0.2 mmol, 1 equiv) and 2-cyclohexene-1-one **1a** (38.5 mg, 0.4 mmol, 2 equiv). The product (>20:1 crude dr) was purified by flash column chromatography (17 cm height, 1.5 cm diameter, 7 mL fractions, 50 mL 10%, 50 mL 15%, 50 mL 20%, 50 mL 30% EtOAc in hexane), and impure product was obtained (TLC: Rf = 0.50 in 30% EtOAc in hexane). A second purification was performed through flash column chromatography (17 cm height, 1.5 cm diameter, 7 mL fractions, 50 mL 5%, 50 mL 10%, 50 mL 15%, 50 mL 20% ether in toluene), giving pure product (TLC: Rf = 0.45 in 20% ether in toluene). Compound **3u** was obtained as a yellow oil (20.4 mg, 0.060 mmol, 30% yield). ^{1}H NMR (500 MHz, $CDCl_3$) δ 7.57 (d, J = 2.2 Hz, 1H), 7.46 (dd, J = 7.6, 1.2 Hz, 1H), 7.18 (dd, J = 7.6, 7.6 Hz, 1H), 7.08 (dd, J = 7.6, 1.2 Hz, 1H), 6.72 (d, J = 2.2 Hz, 1H), 4.22 (d, J = 13.1 Hz, 1H), 2.63 – 2.52 (m, 2H), 2.33 – 2.24 (m, 1H), 2.13 – 2.05 (m, 1H), 2.03 – 1.87 (m, 3H), 0.87 (s, 6H), 0.82 (s, 6H); ^{13}C NMR (126 MHz, $CDCl_3$) δ 209.5, 153.6, 144.5, 127.2, 124.7, 122.8, 120.0, 106.8, 83.3, 52.8, 42.5, 29.9, 27.5, 24.3, 24.2; Accurate Mass (EI) *m/z* calcd for $C_{20}H_{25}BO_4$ $[M]^+$ 340.1840, Found: 340.1817, Spectral Accuracy 98.2%.

Compound **3v**

(2*RS*,3*RS*)-2-(1-methyl-1H-indol-5-yl)-3-(4,4,5,5-tetramethyl-1,3,2-dioxaborolan-2-yl)cyclohexan-1-one

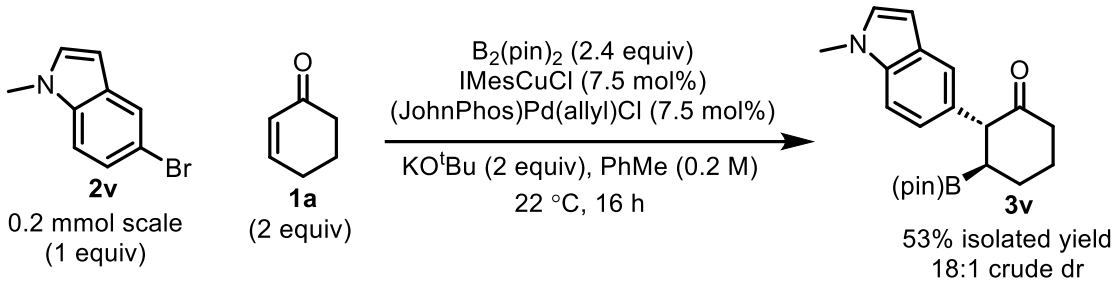

Compound **3v** was prepared through General Procedure B using 5-bromo-1-methylindole **2v** (42 mg, 0.2 mmol, 1 equiv) and 2-cyclohexene-1-one **1a** (38.5 mg, 0.4 mmol, 2 equiv). The product (18:1 crude dr) was purified by flash column chromatography (17 cm height, 1.5 cm diameter, 7 mL fractions, 50 mL 10%, 50 mL 15%, 50 mL 20%, 100 mL 30% EtOAc in hexane), and impure product was obtained (TLC: Rf = 0.45 in 30% EtOAc in hexane). A second purification was performed through flash column chromatography (17 cm height, 1.5 cm diameter, 7 mL fractions, 50 mL 5%, 50 mL 10%, 50 mL 15%, 100 mL 20% ether in toluene), giving pure product (TLC: Rf = 0.40 in 20% ether in toluene). Compound **3v** was obtained as a red solid (37.5 mg, 0.106 mmol, 53% yield). ^{1}H NMR (400 MHz, $CDCl_3$) δ 7.37 – 7.34 (m, 1H), 7.24 (d, J = 8.5 Hz, 1H), 7.02 – 6.95 (m, 2H), 6.42 – 6.36 (m, 1H), 3.79 (d, J = 11.9 Hz, 1H), 3.75 (s, 3H), 2.59 – 2.44 (m, 2H), 2.29 – 2.20 (m, 1H), 2.00 – 1.82 (m, 4H), 0.93 (s, 6H), 0.90 (s, 6H); ^{13}C NMR (101 MHz, $CDCl_3$) δ 211.8, 136.1, 129.2, 128.7, 128.6, 123.1, 121.4, 108.9, 101.0, 83.3, 58.4, 42.6, 33.0, 30.2, 27.6, 24.6, 24.4; Accurate Mass (EI) *m/z* calcd for $C_{21}H_{28}BNO_3$ $[M]^+$ 353.2157, Found: 353.2187, Spectral Accuracy 99.4%.

Compound **3w**

(2*RS*,3*RS*)-2-(4-(dimethylamino)phenyl)-3-(4,4,5,5-tetramethyl-1,3,2-dioxaborolan-2-yl)cyclohexan-1-one

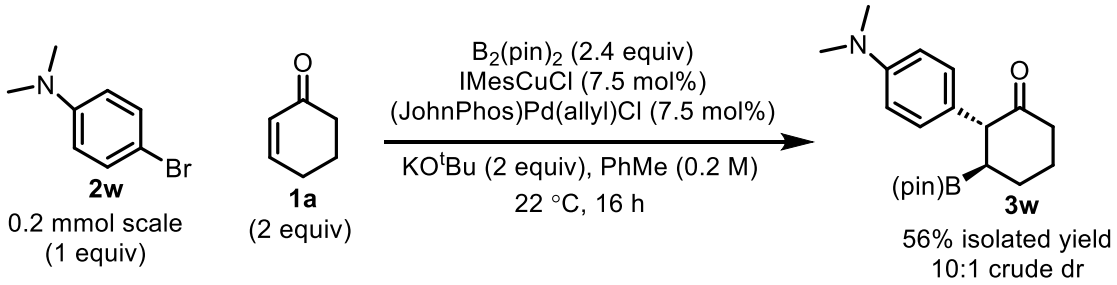

Compound **3w** was prepared through General Procedure B using 4-bromo-N,N-dimethylaniline **2w** (40 mg, 0.2 mmol, 1 equiv) and 2-cyclohexene-1-one **1a** (38.5 mg, 0.4 mmol, 2 equiv). The product (10:1 crude dr) was purified by flash column chromatography (17 cm height, 1.5 cm diameter, 7 mL fractions, 50 mL 10%, 50 mL 15%, 50 mL 20%, 100 mL 30% EtOAc in hexane), and impure product was obtained (TLC: Rf = 0.40 in 25% EtOAc in hexane). A second purification was performed through flash column chromatography (17 cm height, 1.5 cm diameter, 7 mL fractions, 50 mL 5%, 50 mL 10%, 50 mL 15%, 100 mL 20% ether in toluene), giving pure product (TLC: Rf = 0.35 in 20% ether in toluene). Compound **3w** was obtained as a white solid (38.5 mg, 0.112 mmol, 56% yield). ^{1}H NMR (400 MHz, $CDCl_3$) δ 7.10 – 6.96 (m, 2H), 6.92 – 6.50 (m, 2H), 3.60 (d, J = 11.8 Hz, 1H), 2.92 (s, 6H), 2.56 – 2.41 (m, 2H), 2.27 – 2.14 (m, 1H), 1.97 – 1.72 (m, 4H), 0.99 (s, 6H), 0.97 (s, 6H); ^{13}C NMR (126 MHz, $CDCl_3$) δ 211.6, 136.5, 129.9, 129.2, 112.4, 83.4, 57.4, 42.6, 30.2, 27.5, 24.6, 24.5; Accurate Mass (EI) *m/z* calcd for $C_{20}H_{30}BNO_3$ $[M]^+$ 343.2313, Found: 343.2317, Spectral Accuracy 97.8%.

Compound **3ab**

(2*RS*,3*RS*)-2-phenyl-3-(4,4,5,5-tetramethyl-1,3,2-dioxaborolan-2-yl)cycloheptan-1-one

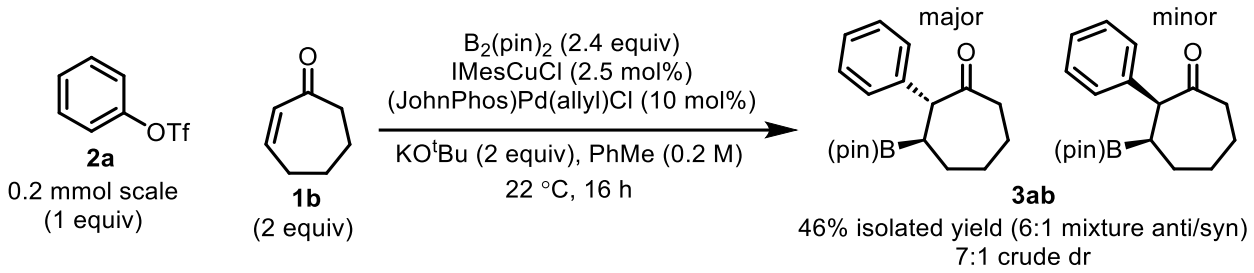

Compound **3ab** was prepared through General Procedure A using phenyl triflate **2a** (45.2 mg, 0.2 mmol, 1 equiv) and 2-cycloheptene-1-one **1b** (44.1 mg, 0.4 mmol, 2 equiv). The product (7:1 crude dr) was purified by flash column chromatography (17 cm height, 1.5 cm diameter, 7 mL fractions, 50 mL 5%, 50 mL 10%, 50 mL 15%, 50 mL 20% ether in toluene), and material was obtained in fractions 10 through 13 (TLC: Rf = 0.39 in 20% EtOAc in hexane). A second purification was performed by flash column chromatography (17 cm height, 1.5 cm diameter, 7 mL fractions, 50 mL 10%, 50 mL 15%, 50 mL 20%, 50 mL 25% EtOAc in hexane), and the product was obtained in fractions 9 through 12, but was contaminated with the syn diastereomer. The two diastereomers were inseparable, and the final isolated Compound **3ab** is reported as a 6:1 ratio of anti to syn diastereomers (by ^{1}H NMR integration ratios of the benzylic proton). Compound **3ab** was obtained as a colourless oil (29.2 mg, 0.093 mmol, 46% yield, 6:1 isolated dr). Major (anti) diastereomer: ^{1}H NMR (600 MHz, $CDCl_3$) δ 7.30 – 7.26 (m, 4H), 7.20 – 7.17 (m, 1H), 3.78 (d, J = 11.9 Hz, 1H), 2.74 (ddd, J = 12.4, 12.2, 3.6 Hz, 1H), 2.49 – 2.42 (m, 1H), 2.04 – 1.94 (m, 3H), 1.77 – 1.68 s(m, 1H), 1.65 – 1.56 (m, 1H), 1.52 – 1.38 (m, 2H), 0.99 (s, 6H), 0.96 (s, 6H); ^{13}C NMR (151 MHz, $CDCl_3$) δ 213.4, 139.8, 128.7, 128.4, 127.1, 83.3, 60.2, 42.3, 30.9, 30.3, 25.5, 24.5, 24.4. Peaks detected from the minor (syn) diastereomer: ^{1}H NMR (600 MHz, $CDCl_3$) δ 3.86 (d, J = 4.0 Hz, 0.17 H, benzylic proton), 1.13 (s, 1.15 H, two B(pin) methyl groups), 1.12 (s, 1.14 H, two B(pin) methyl groups); ^{13}C NMR (151 MHz, $CDCl_3$) δ 129.4, 128.2, 126.7, 83.8, 60.5, 43.7, 31.0, 30.9, 25.1, 25.0, 24.8; Accurate Mass (EI) *m/z* calcd for $C_{19}H_{27}BO_3$ $[M]^+$ 314.2048, Found: 314.2046, Spectral Accuracy 98.1%.

Compound **3ac**

(2*RS*,3*RS*)-2-phenyl-3-(4,4,5,5-tetramethyl-1,3,2-dioxaborolan-2-yl)cyclopentan-1-one

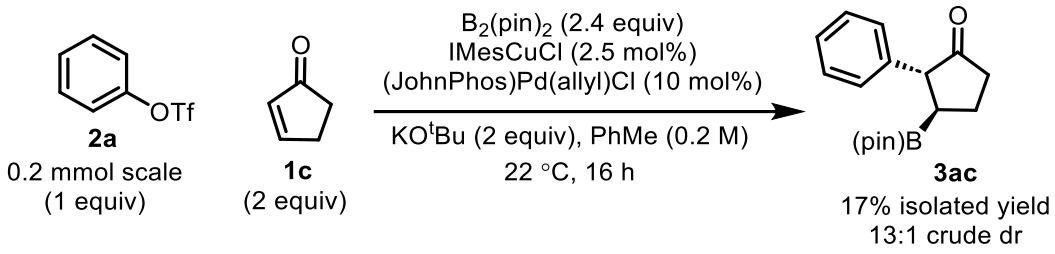

Compound **3ac** was prepared through General Procedure A using phenyl triflate **2a** (45.2 mg, 0.2 mmol, 1 equiv) and 2-cyclopentene-1-one **1c** (32.8 mg, 0.4 mmol, 2 equiv). The product (13:1 crude dr) was purified using the Combi Flash (24-gram column, 5 to 25% Et_2O in toluene gradient over 20 minutes, 35 mL/min flow rate, 18 mL fractions), and pure material was obtained in fractions 27 through 31 (TLC: Rf = 0.48 in 20% Et_2O in toluene). Compound **3ac** was obtained as a colourless oil (9.8 mg, 0.034 mmol, 17% yield). ^{1}H NMR (400 MHz, $CDCl_3$) δ 7.33 – 7.27 (m, 2H), 7.24 – 7.19 (m, 1H), 7.17 – 7.14 (m, 2H), 3.38 (d, J = 12.0 Hz, 1H), 2.56 – 2.46 (m, 1H), 2.38 – 2.27 (m, 1H), 2.26 – 2.14 (m, 1H), 1.96 – 1.77 (m, 2H), 1.19 (s, 6H), 1.18 (s, 6H); ^{13}C NMR (101 MHz, $CDCl_3$) δ 218.9, 138.7, 128.6, 128.5, 126.9, 83.7, 58.1, 39.3, 24.9, 24.7, 23.2; Accurate Mass (EI) *m/z* calcd for $C_{17}H_{23}BO_3$ $[M]^+$ 286.1735, Found: 286.1703, Spectral Accuracy 98.0%.

Compound **3ad**

(2*RS*,3*SR*)-4,4-dimethyl-2-phenyl-3-(4,4,5,5-tetramethyl-1,3,2-dioxaborolan-2-yl)cyclohexan-1-one

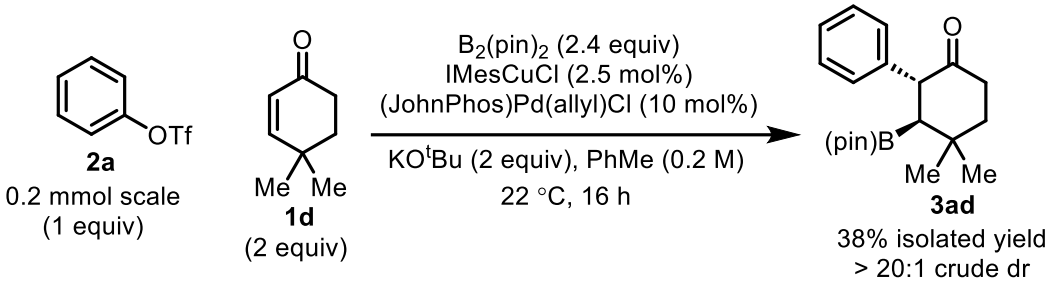

Compound **3ad** was prepared through General Procedure A using phenyl triflate **2a** (45.2 mg, 0.2 mmol, 1 equiv) and 4,4-dimethyl-2-cyclohexene-1-one **1d** (49.7 mg, 0.4 mmol, 2 equiv). The product (>20:1 crude dr) was purified using the Combi Flash (24-gram column, 5% to 25% Et_2O in toluene gradient over 20 minutes, 35 mL/min flow rate, 18 mL fractions), and pure material was obtained in fractions 17 through 19 (TLC: Rf = 0.74 in 40% EtOAc in hexane). Compound **3ad** was obtained as a white solid (25.2 mg, 0.077 mmol, 38% yield). ^{1}H NMR (400 MHz, $CDCl_3$) δ 7.35 – 7.24 (m, 2H), 7.22 – 7.16 (m, 1H), 7.14 – 7.09 (m, 2H), 3.78 (d, J = 13.6 Hz, 1H), 2.74 – 2.60 (m, 1H), 2.44 – 2.35 (m, 1H), 1.96 – 1.84 (m, 2H), 1.82 (d, J = 13.6 Hz, 1H), 1.36 (s, 3H), 1.09 (s, 3H), 0.91 (s, 6H), 0.89 (s, 6H); ^{13}C NMR (101 MHz, $CDCl_3$) δ 211.6, 138.6, 129.9, 128.2, 127.0, 83.4, 54.4, 44.3, 38.8, 32.9, 31.5, 24.7, 24.4, 22.7; Accurate Mass (EI) *m/z* calcd for $C_{20}H_{29}BO_3$ $[M]^+$ 328.2204, Found: 328.2168, Spectral Accuracy 99.4%.

Compound **3ae**

(2*RS*,3*RS*,4*SR*)-4-methyl-2-phenyl-3-(4,4,5,5-tetramethyl-1,3,2-dioxaborolan-2-yl)cyclohexan-1-one

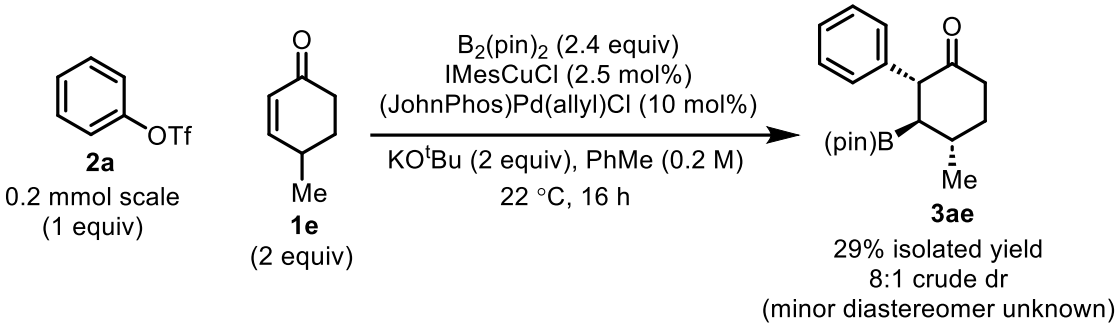

Compound **3ae** was prepared through General Procedure A using phenyl triflate **2a** (45.2 mg, 0.2 mmol, 1 equiv) and 4-methyl-2-cyclohexene-1-one **1e** (44.1 mg, 0.4 mmol, 2 equiv). The product (8:1 crude dr; the stereochemistry of the minor diastereomer is unknown) was purified by flash column chromatography (17 cm height, 1.5 cm diameter, 7 mL fractions, 50 mL 5%, 50 mL 10%, 50 mL 15%, 50 mL 20% ether in toluene), and pure material was obtained in fractions 11 through 14 (TLC: Rf = 0.31 in 20% EtOAc in hexane). Compound **3ae** was obtained as a white solid (18.0 mg, 0.057 mmol, 29% yield). ^{1}H NMR (600 MHz, $CDCl_3$) δ 7.30 – 7.26 (m, 2H), 7.22 – 7.18 (m, 1H), 7.13 – 7.10 (m, 2H), 3.71 (d, J = 13.2 Hz, 1H), 2.59 (dddd, J = 13.7, 13.7, 5.9, 1.1 Hz, 1H), 2.48 (ddd, J = 13.7, 4.4, 2.5 Hz, 1H), 2.26 – 2.14 (m, 2H), 1.71 – 1.61 (m, 1H), 1.58 (dd, J = 13.2, 11.2 Hz, 1H), 1.03 (d, J = 6.5 Hz, 3H), 0.98 (s, 6H), 0.89 (s, 6H); ^{13}C NMR (151 MHz, $CDCl_3$) δ 211.0, 138.1, 129.7, 128.2, 127.1, 83.5, 57.7, 41.9, 38.8, 34.1, 24.7, 24.5, 21.2; Accurate Mass (EI) *m/z* calcd for $C_{19}H_{27}BO_3$ $[M]^+$ 314.2048, Found: 314.2010, Spectral Accuracy 99.3%. The stereochemistry is confirmed by coupling constants and NOESY correlation.

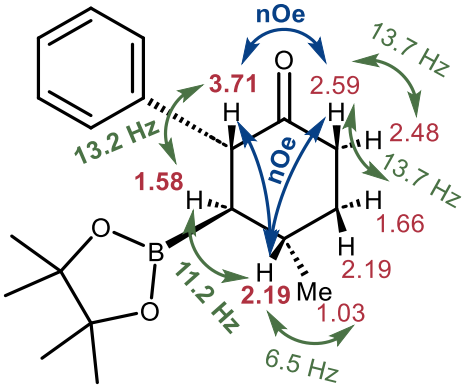

Compound **3af**

(2*RS*,3*SR*,4*SR*)-4-methyl-2,4-diphenyl-3-(4,4,5,5-tetramethyl-1,3,2-dioxaborolan-2-yl)cyclohexan-1-one

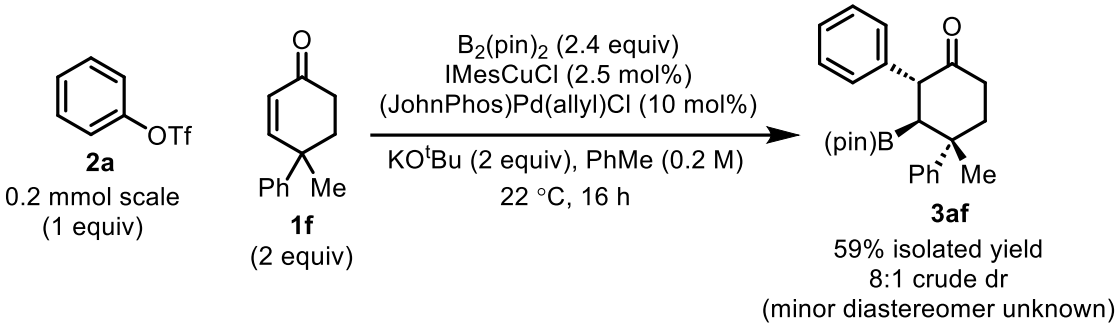

Compound **3af** was prepared through General Procedure A using phenyl triflate **2a** (45.2 mg, 0.2 mmol, 1 equiv) and 4-methyl-4-phenyl-2-cyclohexene-1-one **1f** (74.5 mg, 0.4 mmol, 2 equiv). The product (8:1 crude dr; the stereochemistry of the minor diastereomer is unknown) was purified by flash column chromatography (17 cm height, 1.5 cm diameter, 7 mL fractions, 50 mL 5%, 50 mL 10%, 50 mL 15%, 50 mL 20% ether in toluene), and product was obtained in fractions 7 through 10 (TLC: Rf = 0.63 in 30% ether in toluene). A second purification was performed by flash column chromatography (17 cm height, 1.5 cm diameter, 7 mL fractions, 100 mL 5%, 50 mL 10% ether in toluene), and pure material was obtained in fractions 11 through 14. Compound **3af** was obtained as a white solid (46.3 mg, 0.119 mmol, 59% yield). ^{1}H NMR (400 MHz, $CDCl_3$) δ 7.56 – 7.52 (m, 2H), 7.36 – 7.26 (m, 4H), 7.23 – 7.15 (m, 4H), 3.97 (d, *J* = 13.7 Hz, 1H), 2.92 – 2.79 (m, 1H), 2.63 – 2.43 (m, 3H), 2.05 – 1.94 (m, 1H), 1.91 (s, 3H), 0.69 (s, 6H), 0.58 (s, 6H); ^{13}C NMR (101 MHz, $CDCl_3$) δ 210.7, 147.8, 137.9, 129.9, 128.4, 128.3, 127.2, 126.5, 126.0, 83.1, 55.0, 44.0, 39.9, 39.4, 24.7, 24.3, 19.6; Accurate Mass (EI) *m/z* calcd for $C_{25}H_{31}BO_3$ $[M]^+$ 390.2361, Found: 390.2353, Spectral Accuracy 97.2%. The stereochemistry was confirmed by NOESY correlations.

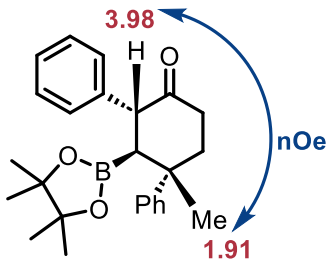

Compound **3ag**

(2*RS*,3*RS*,5*RS*)-5-methyl-2-phenyl-3-(4,4,5,5-tetramethyl-1,3,2-dioxaborolan-2-yl)cyclohexan-1-one

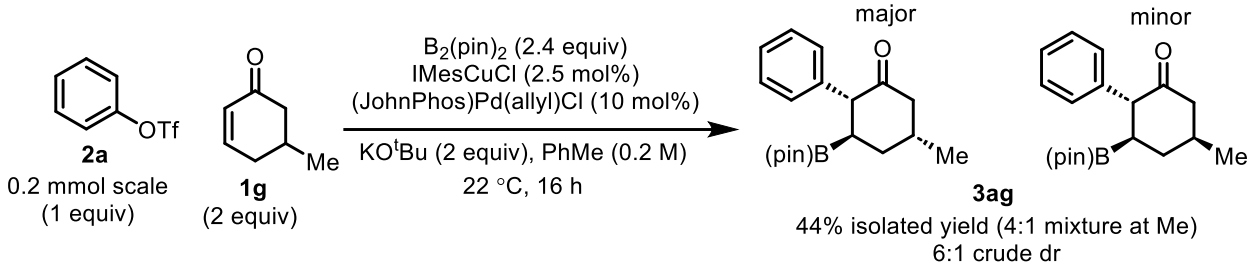

Compound **3ag** was prepared through General Procedure A using phenyl triflate **2a** (45.2 mg, 0.2 mmol, 1 equiv) and 5-methyl-2-cyclohexene-1-one **1g** (44.1 mg, 0.4 mmol, 2 equiv). The product (6:1 crude dr) was purified by flash column chromatography (17 cm height, 1.5 cm diameter, 7 mL fractions, 50 mL 5%, 50 mL 10%, 50 mL 15%, 50 mL 20% ether in toluene), and product was obtained in fractions 6 through 10 (TLF: Rf = 0.64 in 30% ether in toluene). Compound **3ag** (27.7 mg, 0.088 mmol, 44% yield) was isolated as a white solid, but in an inseparable 4:1 mixture of diastereomers (benzylic proton relative integrations) which differ at the methyl-bearing stereocentre. Both compounds present an anti relationship between the phenyl and B(pin) moieties based on the axial coupling constants of the major and minor ^{1}H NMR signals of the benzylic protons. ^{1}H NMR (400 MHz, $CDCl_3$) δ 7.31 – 7.26 (m, 2H), 7.23 – 7.18 (m, 1H), 7.16 – 7.08 (m, 2H), 3.68 (d, J = 11.2 Hz, H), 3.60 (d, J = 13.1 Hz, 0.78 H; major), 2.71 – 2.62 (m, 0.18 H; minor), 2.59 – 2.48 (m, 1H), 2.33 – 2.16 (m, 1H), 2.16 – 2.02 (m, 2H), 1.74 – 1.66 (m, 1H), 1.07 (d, J = 7.0 Hz, 3H), 1.01 (s, 5H; major), 0.99 (s, 5H; major), 0.96 (s, 1H; minor), 0.95 (s, 1H; minor); ^{13}C NMR (101 MHz, $CDCl_3$) δ 210.9, 138.5, 129.5 (minor), 129.2, 128.2, 128.2 (minor), 126.9, 83.5, 83.5 (minor), 57.7, 48.5, 33.6, 32.7, 24.5, 24.5, 24.4 (minor), 19.2. Accurate Mass (EI) *m/z* calcd for $C_{19}H_{27}BO_3$ $[M]^+$ 314.2048, Found: 314.2106, Spectral Accuracy 99.2%. The stereochemistry of the major diastereomer was confirmed by NOESY and COSY analysis.

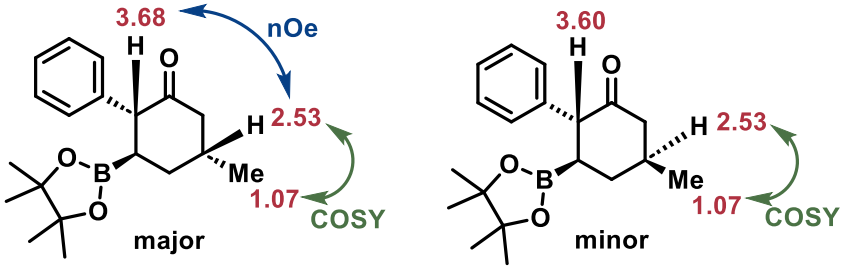

2.4.7: Product functionalization procedures

Compound **5**

(2*SR*,3*RS*)-3-hydroxy-2-(4-methoxyphenyl)cyclohexan-1-one

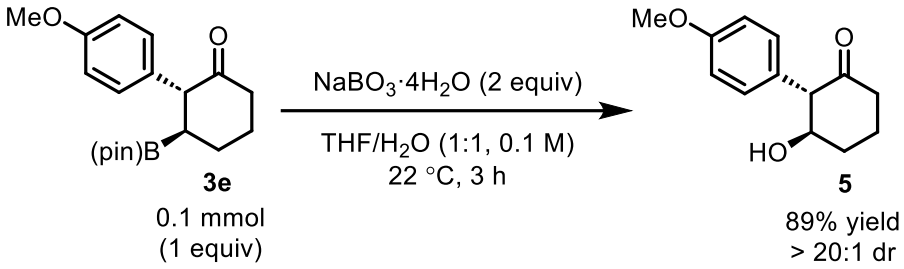

Compound **5** was prepared via oxidation of Compound **3e**. To an 8 mL screw-cap vial, under air and at room temperature (22 °C), equipped with a micro-stir bar was added Compound **3e** (33.0 mg, 0.1 mmol, 1 equiv). This was then dissolved in THF (0.5 mL), then water (0.5 mL) was added, bringing the reaction to a total volume of 1.0 mL (0.1 M concentration). Stirring was commenced, then $NaBO_3 \cdot 4H_2O$ (30.8 mg, 0.2 mmol, 2 equiv) was added in one portion. The reaction was sealed with a screw-cap, and was allowed to stir under air at room temperature for 3 hours. Upon completion, the reaction was diluted with 6 mL EtOAc and transferred to a separatory funnel. An additional 10 mL of water and 10 mL of EtOAc were added, and the layers were separated. The aqueous phase was extracted twice more with 10 mL EtOAc, then the combined organic phases were washed twice with 10 mL brine. At this point, a small (100 μL) aliquot was taken for GC-MS and GC-FID analysis, showing the desired product as one exclusive diastereomer. The combined organics were dried over $MgSO_4$, filtered, and concentrated by rotary evaporation. The crude material was then filtered through a short silica plug (2 cm in height, 2 cm in diameter) and eluted with EtOAc prior to concentration through rotary evaporation. This material was finally purified by flash column chromatography (15 cm height and 1.5 cm diameter silica gel column, 7 mL fractions, elution with 200 mL of 55% EtOAc in hexanes) providing pure material in fractions 9 through 15 (TLC: Rf = 0.27 in 50% EtOAc in hexanes). After rotary evaporation and drying under high vacuum, Compound **5** was obtained as a white solid (19.7 mg, 0.089 mmol, 89% yield). ^{1}H NMR (600 MHz, $CDCl_3$) δ 7.09 (d, J = 8.6 Hz, 2H), 6.93 (d, J = 8.6 Hz, 2H), 3.98 – 3.91 (m, 1H), 3.81 (s, 3H), 3.51 (d, J = 10.3 Hz, 1H), 2.54 – 2.48 (m, 1H), 2.47 – 2.39 (m, 1H), 2.37 – 2.29 (m, 1H), 2.17 – 2.08 (m, 1H), 1.91 – 1.80 (m, 1H), 1.75 – 1.64 (m, 2H);

^{13}C NMR (151 MHz, $CDCl_3$) δ 207.6, 159.3, 130.9, 126.5, 114.5, 75.0, 66.4, 55.4, 41.1, 33.1, 21.0; Accurate Mass (EI) *m/z* calcd for $C_{13}H_{16}O_3$ $[M]^+$ 220.1094, Found: 220.1013, Spectral Accuracy 98.6%.

Compound **6**

(1*RS*,2*RS*,3*RS*)-2-(4-methoxyphenyl)-3-(4,4,5,5-tetramethyl-1,3,2-dioxaborolan-2-yl)cyclohexan-1-ol

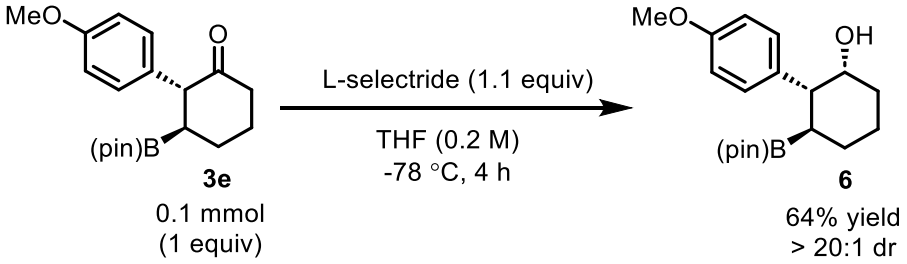

Compound **6** was prepared via reduction of Compound **3e** through a protocol adapted from related literature on the diastereoselective reduction of β-boryl cyclobutanones.[33] To an oven-dried 8 mL screw-cap vial, under air and at room temperature (22 ℃), equipped with a micro-stir bar was added Compound **3e** (33.0 mg, 0.1 mmol, 1 equiv). The vial was sealed with a screw-cap bearing a pierceable septum, and was flushed with an argon balloon. Then, THF (0.5 mL, 0.2 M concentration) was added, stirring was commenced to dissolve the substrate, and the solution was cooled in an acetone-dry ice bath (-78 ℃). At this point, L-selectride (0.11 mL, 0.11 mmol, 1.1 equiv) was added dropwise. The reaction was allowed to stir at -78 ℃ for 4 hours, at which point the reaction was allowed to warm to room temperature. Next, the reaction was diluted with 6 mL ether and quenched with 1 mL saturated aqueous NH_4Cl. The resulting mixture was transferred to a separatory funnel, and another 10 mL saturated aqueous NH_4Cl solution was added. The layers were separated, and the aqueous was extracted twice more with 10 mL ether. The combined organics were washed once with 10 mL brine, then dried over $MgSO_4$, and filtered. Prior to rotary evaporation, a small (100 μL) aliquot was taken for GC-MS and GC-FID analysis, showing the desired product as one exclusive diastereomer. The solvent was evaporated through rotary evaporation, and the crude product was purified through flash column chromatography (17 cm height and 1.5 cm diameter silica gel column, 7 mL fractions, elution with 50 mL 20%, 50 mL 25%, 50 mL 30%, 50 mL 35% EtOAc in hexanes) providing pure material in fractions 13 to 16 (TLC: Rf = 0.54 in 45% EtOAc in hexanes, Rf = 0.36 in 25% EtOAc in hexanes). After rotary evaporation and drying under high-vacuum, Compound **6** was obtained as a white solid (21.3 mg, 0.064 mmol, 64% yield). ^{1}H NMR (400 MHz, $CDCl_3$) δ 7.16 (d, J = 8.6 Hz, 2H), 6.84 (d, J = 8.6 Hz, 2H), 3.88 – 3.82 (m, 1H), 3.78 (s, 3H), 2.79 (dd, J = 12.7, 2.3 Hz, 1H), 2.02 – 1.91 (m, 1H),

1.87 – 1.73 (m, 2H), 1.73 – 1.57 (m, 2H), 1.57 – 1.47 (m, 1H), 1.45 – 1.32 (m, 2H), 0.98 (s, 6H), 0.92 (s, 6H); ^{13}C NMR (101 MHz, $CDCl_3$) δ 158.4, 136.1, 129.4, 113.9, 82.9, 70.2, 55.4, 48.8, 32.9, 27.8, 24.5, 24.3, 20.0; Accurate Mass (EI) *m/z* calcd for $C_{19}H_{29}BO_4$ $[M]^+$ 332.2153, Found 332.2169, Spectral Accuracy 98.4%. The stereochemical assignment is supported both by coupling constants and NOESY correlations.

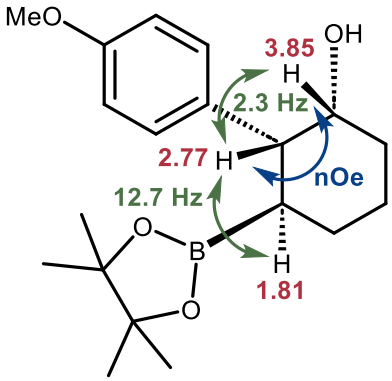

Compound **7**

(1*RS*,2*RS*,3*RS*)-1-(4-fluorophenyl)-2-(4-methoxyphenyl)-3-(4,4,5,5-tetramethyl-1,3,2-dioxaborolan-2-yl)cyclohexan-1-ol

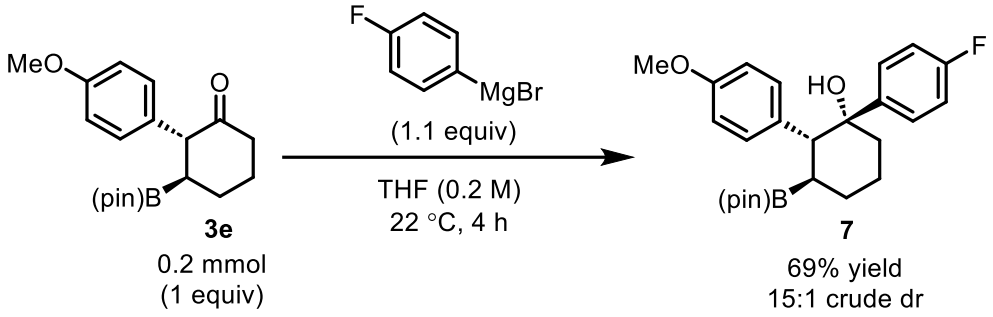

Compound **7** was prepared through addition of 4-fluorophenylmagnesium bromide to Compound **3e** through a protocol adapted from related literature.[33] To an oven-dried 8 mL screw-cap vial, under air and at room temperature (22 °C), equipped with a micro-stir bar was added Compound **3e** (66.0 mg, 0.2 mmol, 1 equiv). This was then taken into a nitrogen-filled glovebox and dissolved in 1 mL THF (0.2 M). Then, a solution of 4-fluorophenylmagnesium bromide (0.22 mL, 1 M in THF, 0.22 mmol, 1.1 equiv) was added dropwise. The vial was sealed with a screw-cap, removed from the glovebox, and stirred for 4 h at room temperature. Upon completion, the reaction was quenched with 1 mL saturated aqueous NH_4Cl solution, then diluted with another 10 mL saturated aqueous NH_4Cl solution while transferring to a separatory funnel. This was extracted thrice into 10 mL EtOAc, and the combined organics were washed once with 10 mL brine, dried over $MgSO_4$, and filtered. At this point, a small aliquot (100 µL) was taken for GC-MS and GC-FID analysis, showing the desired product formed as a 15:1 mixture of diastereomers. After rotary evaporation, the resulting crude was purified by flash column chromatography (17 cm height and 1.5 cm diameter silica gel column, 7 mL fractions, elution with 50 mL 10%, 50 mL 15%, 50 mL 20%, 50 mL 25% EtOAc in hexanes) providing pure material (only the major diastereomer was isolated) in fractions 13 to 18 (Rf = 0.56 in 30% EtOAc/hexane). After rotary evaporation and drying under high-vacuum, Compound **7** was obtained as a white solid (59.2 mg, 0.139 mmol, 69% yield). ^{1}H NMR (600 MHz, $CDCl_3$) δ 7.17 (dd, *J* = 8.8, 5.5 Hz, 2H), 6.84 (dd, *J* = 8.8, 8.8 Hz, 2H), 6.77 (d, *J* = 8.5 Hz, 2H), 6.57 (d, *J* = 8.5 Hz, 2H), 3.67 (s, 3H), 3.01 (d, *J* = 12.5 Hz, 1H), 2.09 – 2.01 (m, 1H), 1.97 – 1.78 (m, 5H), 1.76 – 1.69 (m, 1H), 1.58 – 1.47 (m, 1H), 0.91 (s, 6H), 0.87 (s, 6H); ^{13}C NMR (151 MHz, $CDCl_3$) δ 161.4 (d, J = 244.1 Hz), 158.1, 144.0 (d, J = 3.0 Hz),

133.1, 130.5, 126.6 (d, J = 7.8 Hz), 114.4 (d, J = 20.9 Hz), 113.0, 82.9, 75.0, 55.2, 53.1, 40.2, 27.8, 24.4, 24.3, 22.7; ^{19}F NMR (283 MHz, $CDCl_3$) δ -117.7; Accurate Mass (EI) *m/z* calcd for $C_{25}H_{32}BFO_4$ $[M]^+$ 426.2372, Found 426.2285, Spectral Accuracy 97.0%. The stereochemical assignment is supported by NOESY correlations.

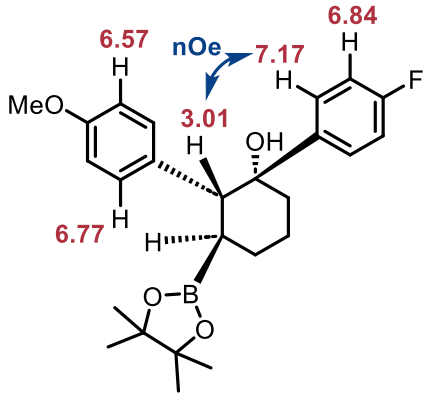

Compound **8**

(((1*RS*,6*RS*)-4'-methoxy-6-(4,4,5,5-tetramethyl-1,3,2-dioxaborolan-2-yl)-1,4,5,6-tetrahydro-[1,1'-biphenyl]-2-yl)oxy)trimethylsilane

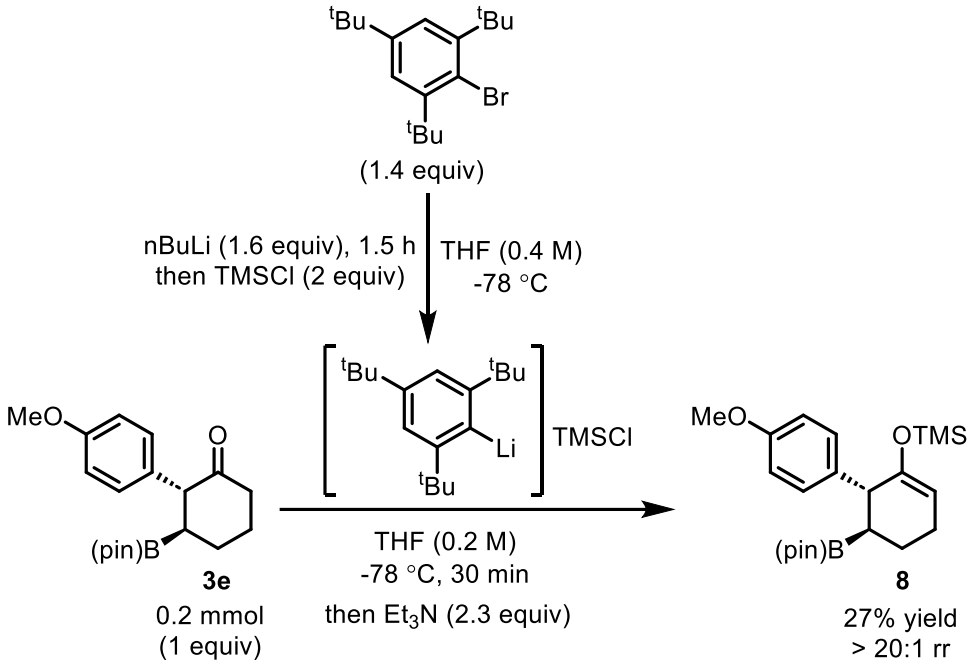

Compound **8** was prepared through deprotonation and trapping of Compound **3e** through a protocol adapted from related literature on methyl benzyl ketone.[126–128] To an oven-dried catalysis vial equipped with a micro-stir bar was added 2,4,6-tri-*tert*-butyl-phenylbromide (91.1 mg, 0.28 mmol, 1.4 equiv). The vial was sealed with a septum-pierceable screw-cap, and was sparged with argon via balloon. Dry THF (0.7 mL, 0.4 M in aryl bromide) was added, and stirring was commenced. Once fully dissolved, the solution was cooled to -78 ℃ (dry ice and acetone bath), then n-BuLi (0.126 mL of 2.5 M in hexanes solution, 0.32 mmol, 1.6 equiv) was added. The reaction was stirred for 1.5 h at -78 ℃, then a solution of TMSCl (43.5 mg, 0.4 mmol, 2 equiv) in THF (0.2 mL, 2 M in TMSCl) was added. Immediately afterwards, a solution of the ketone, Compound **3e** (66.0 mg, 0.2 mmol, 1 equiv) in THF (0.2 mL, 1 M in ketone) was added dropwise. After this addition, the reaction was allowed to stir -78 ℃ for 30 min, at which point a solution of Et_3N (46.5 mg, 0.46 mmol, 2.3 equiv) in THF (0.23 mL, 2 M in amine) was added, and the reaction was allowed to warm to room temperature. The reaction was quenched with 1 mL saturated aqueous $NaHCO_3$, then diluted with 10 mL ether and another 10 mL of saturated aqueous $NaHCO_3$ while transferring to a separatory funnel. The layers were separated, and the aqueous was re-

extracted twice with another 10 mL ether. The combined organics were washed twice with 10 mL water, twice with 10 mL 0.1 N (0.033 M) citric acid solution, and once with 10 mL brine prior to drying over $MgSO_4$, filtration, and concentration by rotary evaporation. The crude product was purified through flash column chromatography (17 cm height and 1.5 cm diameter silica gel column, 7 mL fractions, elution with 100 mL of 5% EtOAc in hexane with 0.2% Et_3N additive) providing pure material in fractions 10 and 11 (Rf = 0.43 in 5% EtOAc in hexane). Compound **8** was isolated as one exclusive regioisomer (22.1 mg, 0.055 mmol, 27% yield) as a colourless oil. ^{1}H NMR (300 MHz, $CDCl_3$) δ 7.15 (d, *J* = 8.6 Hz, 2H), 6.79 (d, *J* = 8.6 Hz, 2H), 5.01 (dd, *J* = 4.0, 2.3 Hz, 1H), 3.78 (s, 3H), 3.44 (d, *J* = 6.3 Hz, 1H), 2.20 – 2.08 (m, 2H), 1.69 – 1.59 (m, 1H), 1.57 – 1.46 (m, 1H), 1.40 – 1.34 (m, 1H), 1.18 (s, 6H), 1.17 (s, 6H), 0.04 (s, 9H); ^{13}C NMR (75 MHz, $CDCl_3$) δ 157.8, 151.7, 137.0, 129.5, 113.3, 106.1, 83.2, 55.3, 46.2, 25.0, 24.6, 24.4, 21.5, 0.5; Accurate Mass (EI) *m/z* calcd for $C_{22}H_{35}BO_4Si$ $[M]^+$ 402.2392, Found 402.2346, Spectral Accuracy 98.9%. Compound **8** was found to degrade rapidly in $CDCl_3$, so NMR characterization was performed swiftly.

Compound **9**

(*1RS*,6*RS*)-4'-methoxy-6-(4,4,5,5-tetramethyl-1,3,2-dioxaborolan-2-yl)-5,6-dihydro-[1,1'-biphenyl]-2(1H)-one

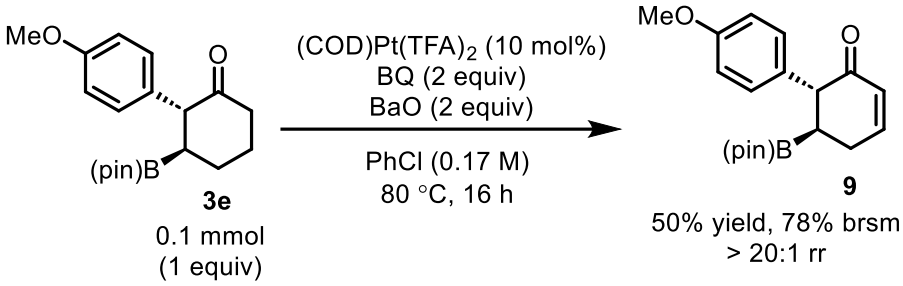

Compound **9** was prepared through a platinum-catalyzed desaturation[131] of Compound **3e**. To an oven-dried 8 mL screw-cap vial, under air and at room temperature (22 °C), equipped with a micro-stir bar was added Compound **3e** (33.0 mg, 0.1 mmol, 1 equiv), then 1,4-benzoquinone (21.6 mg, 0.2 mmol, 2 equiv; purified by sublimation before use), and $(COD)Pt(TFA)_2$ (5.3 mg, 0.01 mmol, 10 mol%). The vial was then taken into a nitrogen-filled glovebox. Next, BaO (30.7 mg, 0.2 mmol, 2 equiv) was added, follow by chlorobenzene (0.6 mL, 0.17 M, de-gassed by argon balloon for 5 min before use). The vial was sealed shut, removed from the glovebox, and heated to 80 °C overnight (16 h). Upon completion, the reaction was concentrated by rotary evaporation. The crude product was then purified by flash column chromatography (17 cm height and 1.5 cm diameter silica gel column, 7 mL fractions, elution with 100 mL 20%, 50 mL 25%, 50 mL 30% EtOAc/hexane), providing pure material in fractions 12 to 16 (Rf = 0.41 in 30% EtOAc/hexane). After rotary evaporation and drying under high-vacuum, Compound **9** was obtained as a white solid (16.4 mg, 0.050 mmol, 50% yield). The remaining mass balance was predominantly starting Compound **3e**, and 11.9 mg (0.0360 mmol) was re-isolated (in fractions 9-11), meaning that Compound **9** yield based on recovered starting material was 78%. ^{1}H NMR (400 MHz, $CDCl_3$) δ 7.07 (d, J = 8.6 Hz, 2H), 7.01 (ddd, J = 10.0, 5.1, 2.9 Hz, 1H), 6.84 (d, J = 8.6 Hz, 2H), 6.11 (ddd, J = 10.0, 2.6, 1.4 Hz, 1H), 3.77 (s, 3H), 3.63 (d, J = 12.2 Hz, 1H), 2.61 – 2.49 (m, 1H), 2.48 – 2.38 (m, 1H), 2.14 – 2.02 (m, 1H), 1.03 (s, 6H), 1.00 (s, 6H); ^{13}C NMR (101 MHz, $CDCl_3$) δ 200.1, 158.6, 150.1, 131.5, 130.0, 129.9, 113.9, 83.7, 55.4, 53.8, 27.5, 24.6, 24.6; Accurate Mass (EI) *m/z* calcd for $C_{19}H_{25}BO_4$ $[M]^+$ 328.1840, Found: 328.1790, Spectral Accuracy 99.3%.

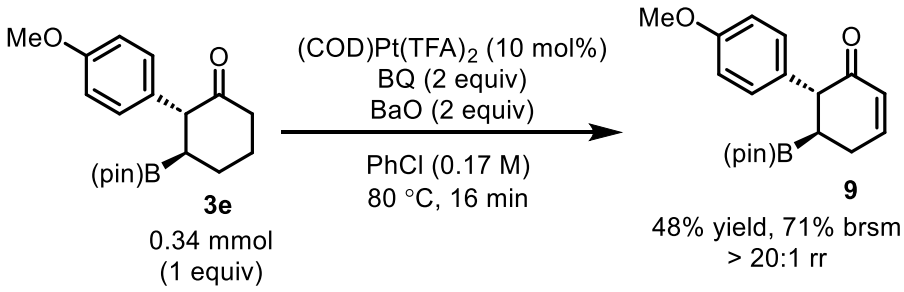

Compound **9** was also synthesized on a slightly larger scale following the above protocol, using Compound **3e** (112 mg, 0.34 mmol, 1.0 equiv), 1,4-benzoquinone (73.5 mg, 0.68 mmol, 2.0 equiv), BaO (104 mg, 0.68 mmol, 2.0 equiv), and $(COD)Pt(TFA)_2$ (18.0 mg, 0.034 mmol, 0.1 equiv) in 2.0 mL of chlorobenzene. The crude product was then purified by flash column chromatography (17 cm height and 2.5 cm diameter silica gel column, 18 mL fractions, elution with 100 mL 15%, 200 mL 20%, 100 mL 25%, 100 mL 30% EtOAc/hexane), providing pure product in fractions 15 through 18. After rotary evaporation and drying under high-vacuum, Compound **9** was obtained as a white solid (53.2 mg, 0.162 mmol, 48% yield). The remaining mass balance was predominantly starting Compound **3e**, and 36.8 mg (0.111 mmol) was re-isolated (in fractions 12 through 14), meaning that Compound **9** yield based on recovered starting material was 71%. Characterization matches that reported above.

Compound **10**

(2*RS*,3*RS*,5*RS*)-2-(4-methoxyphenyl)-3-(4,4,5,5-tetramethyl-1,3,2-dioxaborolan-2-yl)-5-vinylcyclohexan-1-one

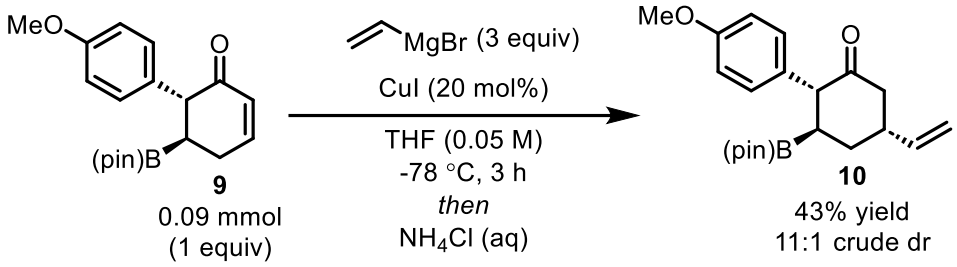

Compound **10** was prepared through a reported copper-catalyzed Grignard conjugate addition[35] to Compound **9**. To an oven-dried 8 mL screw-cap vial, under air and at room temperature (22 ºC), equipped with a micro-stir bar was added CuI (3.4 mg, 0.018 mmol, 20 mol%). The vial was then taken into a nitrogen-filled glovebox. Next, THF (0.9 mL) was added, the vial was sealed with a screw-cap equipped with a pierceable septum, and the vial was removed from the glovebox. The vial was then immediately equipped with a balloon filled with argon, and was subsequently cooled to -78 ºC in a dry ice and acetone bath, and stirring was commenced. At this point, a solution of vinyl magnesium bromide (0.27 mL of a 1 M solution in THF, 0.27 mmol, 3 equiv) was added dropwise. After the addition, the reaction was stirred at -78 ºC under argon for 40 min. At this point, a solution of Compound **9** (29.7 mg, 0.090 mmol, 1 equiv) in THF (0.9 mL) was added dropwise, then the reaction was allowed to stir at -78 °C under argon for 3 h. Finally, the reaction was removed from the cooling bath, and 3 mL of saturated aqueous NH_4Cl was added. The mixture was then transferred to a separatory funnel and diluted with 10 mL of water and 10 mL of EtOAc. The phases were separated, and the aqueous layer was re-extracted twice with another 10 mL EtOAc. The combined organics were washed twice with 10 mL brine, dried over $MgSO_4$, filtered, and concentrated by rotary evaporation. At this point, a small aliquot was taken for GC-MS and GC-FID analysis, and the crude product was determined to have 11:1 dr by GC-FID (at the centre of reactivity). The crude product was then purified by flash column chromatography (17 cm height and 1.5 cm diameter silica gel column, 7 mL fractions, elution with 50 mL 0% 50 mL 10%, 50 mL 20%, 50 mL 30% EtOAc/hexane), providing pure material in fractions 17 through 20 (Rf = 0.57 in 40% EtOAc/hexane). After rotary evaporation and drying under high-vacuum, Compound **10** was obtained as a white solid (13.8 mg, 0.039 mmol, 43%

yield). ^{1}H NMR (500 MHz, $CDCl_3$) δ 7.02 (d, J = 8.7 Hz, 2H), 6.82 (d, J = 8.7 Hz, 2H), 5.86 (ddd, J = 17.4, 10.7, 5.3 Hz, 1H), 5.23 – 5.01 (m, 2H), 3.77 (s, 3H), 3.59 (d, J = 11.8 Hz, 1H), 3.12 – 3.00 (m, 1H), 2.69 – 2.54 (m, 2H), 2.13 (ddd, J = 13.4, 12.0, 4.5 Hz, 1H), 2.00 (ddd, J = 12.0, 11.8, 3.4 Hz, 1H), 1.86 (dddd, J = 13.4, 3.6, 3.4, 1.6 Hz, 1H), 1.02 (s, 6H), 1.00 (s, 6H); ^{13}C NMR (126 MHz, $CDCl_3$) δ 210.4, 158.6, 140.3, 130.7, 130.2, 116.1, 113.7, 83.5, 57.1, 55.4, 45.0, 41.3, 31.4, 24.6, 24.6; Accurate Mass (EI) *m/z* calcd for $C_{21}H_{29}BO_4$ $[M]^+$ 356.2153, Found: 356.2229, Spectral Accuracy 98.9%. The stereochemistry of the product was confirmed through coupling constants, COSY, and NOESY analysis.

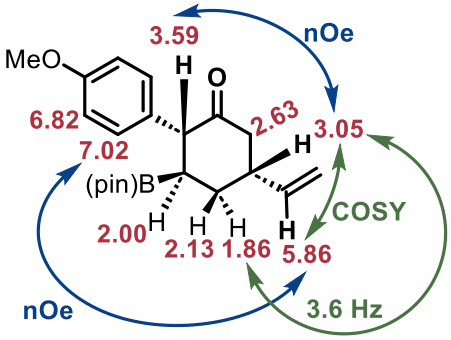

2.4.8: Mechanistic experiment procedures

Testing for competence of conjugate borylation side product **4**

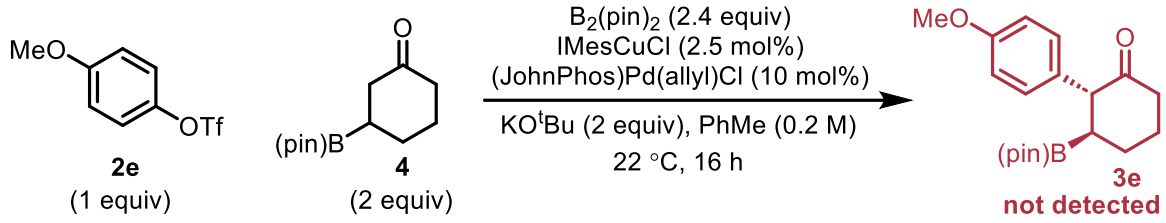

To an oven-dried 8 mL catalysis vial equipped with a micro-stir bar was added (JohnPhos)Pd(allyl)Cl (9.6 mg, 0.02 mmol, 10 mol%). This was transferred to a nitrogen-filled glovebox, then IMesCuCl (2.0 mg, 0.005 mmol, 2.5 mol%), KO^{t}Bu (44.9 mg, 0.4 mmol, 2 equiv), and $B_2(pin)_2$ (122 mg, 0.48 mmol, 2.4 equiv) were added in that order. A solution of 4-methoxy phenyl triflate **2e** (51.2 mg, 0.2 mmol, 1 equiv) in toluene (0.2 mL) was then added to the reaction, and the vial containing the aryl triflate was rinsed once with another 0.2 mL of toluene and added to the reaction to ensure a complete transfer. Immediately afterwards, a solution of 3-(4,4,5,5-tetramethyl-1,3,2-dioxaborolan-2-yl)cyclohexan-1-one **4** (89.6 mg, 0.4 mmol, 2 equiv) in toluene (0.2 mL) was added to the reaction, and the vial containing **4** was rinsed once with 0.2 mL toluene before adding to the reaction again. Lastly, the side walls of the reaction vial were rinsed with 0.2 mL toluene, producing a final reaction concentration of 0.2 M relative to the limiting reagent (aryl triflate). At this point, the vial was sealed tightly with a screwcap, removed from the glovebox, and stirred at room temperature (22 °C) for 16 hours. Upon completion, internal standard was added (naphthalene, 12.8 mg, 0.1 mmol, 0.5 equiv), and the reaction was diluted to a volume of around 7 mL through the addition of EtOAc. An aliquot (100 µL) was then taken and eluted through a cotton-stopped Pasteur pipette silica plug (2.5 cm height and 0.5 cm in diameter) with 2 mL EtOAc. The eluted sample was analyzed by GC-MS and GC-FID. Analysis by GC-MS and GC-FID show no traces of the arylboration product **3e**. Only starting materials and degradation products were detected.

Attempt to trap inactive enolates with D_2O

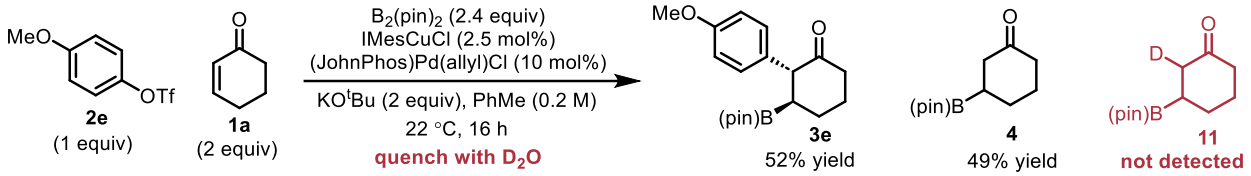

An oven-dried 8 mL screw-cap vial equipped with an oven-dried micro-stir bar was first cooled in a desiccator, then (JohnPhos)Pd(allyl)Cl (9.6 mg, 0.02 mmol, 10 mol%) was added under air. The vial was taken into a nitrogen-filled glovebox, then IMesCuCl (2.0 mg, 0.005 mmol, 2.5 mol%), KO^{t}Bu (44.9 mg, 0.4 mmol, 2 equiv), and $B_2(pin)_2$ (122 mg, 0.48 mmol, 2.4 equiv) were added in that order. A solution of 4-methoxy phenyl triflate **2e** (51.2 mg, 0.2 mmol, 1 equiv) in toluene (0.4 mL) was then added to the reaction. Immediately afterwards, a solution of 2-cyclohexene-1-one **1a** (38.5 mg, 0.4 mmol, 2 equiv) in toluene (0.4 mL) was added. Lastly, the side walls of the reaction vial were rinsed with 0.2 mL toluene, producing a final reaction concentration of 0.2 M relative to the limiting reagent (aryl triflate). At this point, the vial was sealed tightly with a screwcap, removed from the glovebox, and stirred at room temperature (22 °C) for 16 hours. At this point, the vial was taken back into a nitrogen-filled glovebox, and D_2O (100 µL, 111 mg, 5.5 mmol, 28 equiv) was added. The reaction was again sealed with a screw cap, removed from the glovebox, and allowed to stir at room temperature for 1 hour. Upon completion, internal standard was added (naphthalene, 12.8 mg, 0.1 mmol, 0.5 equiv), and the reaction was diluted to a volume of around 7 mL through the addition of EtOAc. An aliquot (100 µL) was then taken and eluted through a cotton-stopped Pasteur pipette silica plug (2.5 cm height and 0.5 cm in diameter) with 2 mL EtOAc. The eluted sample was analyzed by GC-MS and GC-FID. No traces of deuterated conjugate borylation product were detected by GC-MS; all conjugate borylation product detected had the regular protic m/z ratio. The arylboration product **3e** was formed as usual in an estimated GC-FID yield of 52%, along with the protic conjugate borylation product **4** in an estimated GC-FID yield of 49%.

Attempt to trap inactive enolates with benzaldehyde

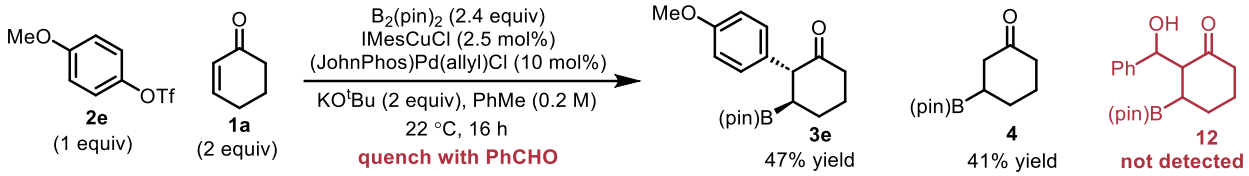

An oven-dried 8 mL screw-cap vial equipped with an oven-dried micro-stir bar was first cooled in a desiccator, then (JohnPhos)Pd(allyl)Cl (9.6 mg, 0.02 mmol, 10 mol%) was added under air. The vial was taken into a nitrogen-filled glovebox, then IMesCuCl (2.0 mg, 0.005 mmol, 2.5 mol%), KO^{t}Bu (44.9 mg, 0.4 mmol, 2 equiv), and $B_2(pin)_2$ (122 mg, 0.48 mmol, 2.4 equiv) were added in that order. A solution of 4-methoxy phenyl triflate **2e** (51.2 mg, 0.2 mmol, 1 equiv) in toluene (0.4 mL) was then added to the reaction. Immediately afterwards, a solution of 2-cyclohexene-1-one **1a** (38.5 mg, 0.4 mmol, 2 equiv) in toluene (0.4 mL) was added. Lastly, the side walls of the reaction vial were rinsed with 0.2 mL toluene, producing a final reaction concentration of 0.2 M relative to the limiting reagent (aryl triflate). At this point, the vial was sealed tightly with a screwcap, removed from the glovebox, and stirred at room temperature (22 °C) for 16 hours. At this point, the vial was taken back into a nitrogen-filled glovebox, and benzaldehyde (100 µL, 104 mg, 0.98 mmol, 4.9 equiv) was added as a solution in DMF (1.0 mL). The reaction was again sealed with a screw cap, removed from the glovebox, and allowed to stir at room temperature for 1 hour. Upon completion, internal standard was added (naphthalene, 12.8 mg, 0.1 mmol, 0.5 equiv), and the reaction was diluted to a volume of around 7 mL through the addition of EtOAc. An aliquot (100 µL) was then taken and eluted through a cotton-stopped Pasteur pipette silica plug (2.5 cm height and 0.5 cm in diameter) with 2 mL EtOAc. The eluted sample was analyzed by GC-MS and GC-FID. No traces of aldol addition product **12** were detected. Only arylboration product **3e** (47% estimated yield by GC-FID) and conjugate borylation side product **4** (41% estimated yield by GC-FID) were detected.

Synthesis of Compound **13**

(2*SR*,3*RS*)-2-phenyl-3-(4,4,5,5-tetramethyl-1,3,2-dioxaborolan-2-yl)cyclohexan-1-one

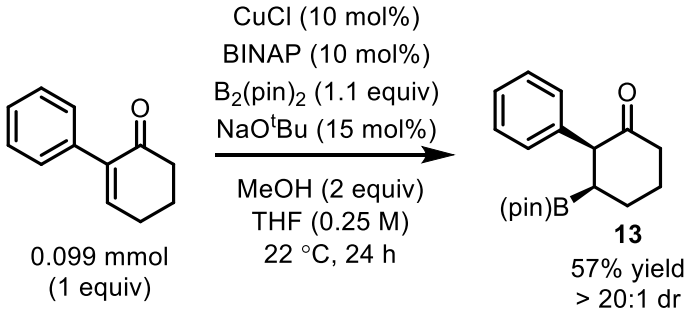

Compound **13** was prepared through conjugate borylation of 2-phenyl-cyclohex-2-ene-1-one through modification of a reported procedure.[112] To an oven-dried 8 mL catalysis vial equipped with a micro stir bar under air was added CuCl (1.3 mg, 0.0099 mmol, 10 mol%). The vial was then transferred to a nitrogen-filled glovebox, then NaO^tBu (1.4 mg, 0.015 mmol, 15 mol%) was added, followed by racemic BINAP (6.1 mg, 0.0099 mmol, 10 mol%). THF (0.2 mL) was then added, and the mixture was allowed to stir vigorously for 30 min. At this point, a solution of $B_2(pin)_2$ (27.6 mg, 0.11 mmol, 1.1 equiv) in THF (0.2 mL) was added, and the resulting mixture was vigorously stirred for another 10 min. Lastly, a solution of 2-phenyl-cyclohex-2-ene-1-one (17.0 mg, 0.099 mmol, 1 equiv) in THF (0.2 mL) was added, followed by MeOH (8 µL, 6.3 mg, 0.20 mmol, 2 equiv). The reaction was sealed with a screw-cap, removed from the glovebox, and allowed to stir for 24 hours at room temperature. Upon completion, the reaction was diluted with ether and filtered through a small celite plug. The resulting crude (>20:1 crude dr of syn:anti by GC-FID) was concentrated by rotary evaporation, then purified through flash column chromatography (17 cm height, 1.5 cm diameter, 7 mL fractions, 50 mL 5%, 50 mL 10%, 50 mL 15%, 50 mL 20% EtOAc in hexane), and material was obtained in fractions 12 and 13 (TLC: Rf = 0.46 in 20% EtOAc in hexane). A second purification was performed by flash column chromatography (17 cm height, 1.5 cm diameter, 7 mL fractions, 50 mL 5%, 50 mL 10%, 50 mL 15%, 50 mL 20% ether in toluene), providing pure product in fractions 9 through 11. After drying under vacuum, Compound **13** was obtained as a colourless oil (17.0 mg, 0.057 mmol, 57% yield) as one pure diastereomer by GC-FID and NMR analysis. ^1H NMR (400 MHz, $CDCl_3$) δ 7.33 – 7.24 (m, 2H), 7.24 – 7.17 (m, 2H), 7.15 – 7.09 (m, 1H), 3.72 (d, J = 5.7 Hz, 1H), 2.46 – 2.35 (m, 1H), 2.30 – 2.18 (m, 1H), 2.08 – 1.97 (m, 2H), 1.96 – 1.90 (m, 1H), 1.89 – 1.75 (m, 2H), 1.09 (s,

6H), 1.02 (s, 6H); ^{13}C NMR (101 MHz, $CDCl_3$) δ 210.7, 138.6, 129.0, 128.4, 126.8, 83.7, 57.2, 40.3, 27.4, 25.3, 24.9, 24.8; Accurate Mass (EI) *m/z* calcd for $C_{18}H_{25}BO_3$ $[M]^+$ 300.1891, Found: 300.1856, Spectral Accuracy 98.7%.

Epimerization experiment with syn product **13**

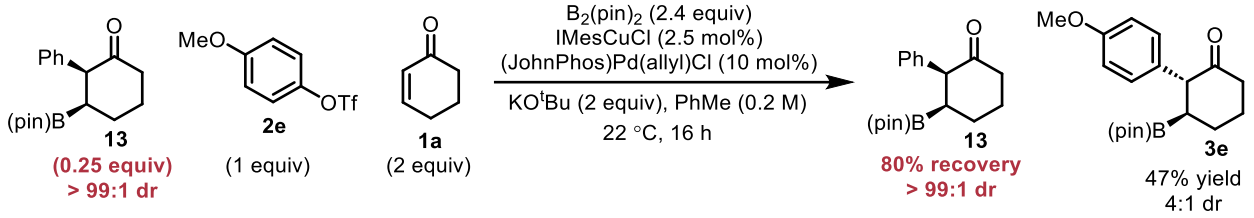

An oven-dried (120 °C) 8 mL screw-cap vial equipped with an oven-dried micro-stir bar was first cooled in a desiccator, then (JohnPhos)Pd(allyl)Cl (9.6 mg, 0.02 mmol, 10 mol%) was added under air. The vial was taken into a nitrogen-filled glovebox, then IMesCuCl (2.0 mg, 0.005 mmol, 2.5 mol%), KO^{t}Bu (44.9 mg, 0.4 mmol, 2 equiv), and $B_2(pin)_2$ (122 mg, 0.48 mmol, 2.4 equiv) were added in that order. A solution of 4-methoxy phenyl triflate **2e** (51.2 mg, 0.2 mmol, 1 equiv) in toluene (0.4 mL) was then added to the reaction. Immediately afterwards, a solution of 2-cyclohexene-1-one **1a** (38.5 mg, 0.4 mmol, 2 equiv) in toluene (0.2 mL) was added to the reaction. Lastly, a solution of compound **13** (15.0 mg, 0.050 mmol, 0.25 equiv, >99:1 dr syn/anti by ^{1}H NMR and GC-FID) in toluene (0.4 mL) was added. The vial was sealed with a screw cap, removed from the glovebox, and stirred for 16 hours at room temperature. Upon completion, internal standard was added (naphthalene, 12.8 mg, 0.1 mmol, 0.5 equiv), and the reaction was diluted to a volume of around 7 mL through the addition of EtOAc. An aliquot (100 µL) was then taken and eluted through a cotton-stopped Pasteur pipette silica plug (2.5 cm height and 0.5 cm in diameter) with 2 mL EtOAc. The eluted sample was analyzed by GC-MS and GC-FID, demonstrating that compound **13** remains as one pure diastereomer (>99:1 dr syn/anti by GC-FID) and in an estimated 80% recovery by GC-FID. Furthermore, compound **3e** forms in 4:1 crude dr (anti/syn) in 47% crude estimated yield by GC-FID. The remainder of the diluted reaction mixture was eluted through a glass-fritted cylindrical-funnel silica plug (2.5 cm in both height and diameter) with approximately 80 mL EtOAc. This crude product was then purified by column chromatography (17 cm height, 1.5 cm diameter, 7 mL fractions, 50 mL 5%, 50 mL 10%, 50 mL 15%, 50 mL 20%, 50 mL 25% EtOAc in hexane). Pure compound **13** (10.3 mg, 69% recovery, >99:1 dr by ^{1}H NMR) was obtained in fractions 15 and 16, while pure compound **3e** (33.9 mg, 0.103 mmol, 51% yield) was isolated from fractions 22 through 26. Spectral details (^{1}H NMR) match the characterizations obtained for compounds **3e** and **13** above.

2.4.9: Enantioselective reaction procedures

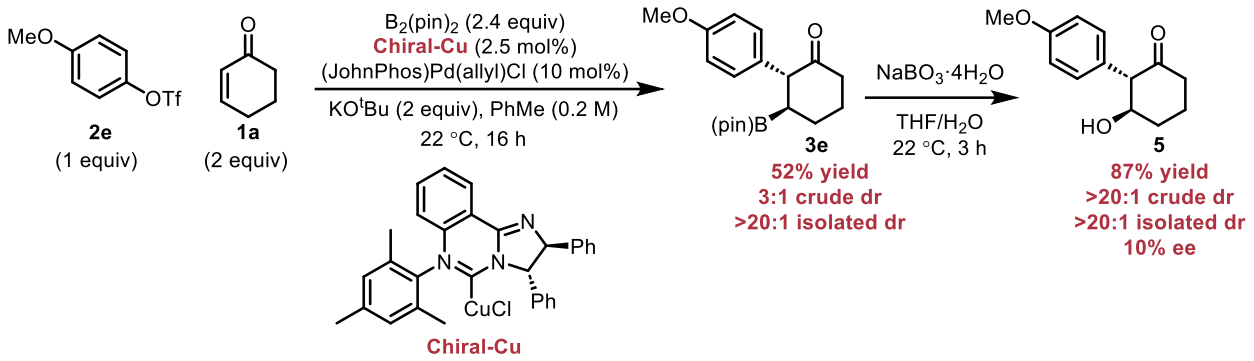

Chiral-Cu was synthesized according to literature protocols,[82,136,137] and was used as the catalyst in the arylboration reaction shown above. Compound **3e**, in this case, was prepared through General Procedure A using 4-(methoxy)phenyl triflate **2e** (51.2 mg, 0.2 mmol, 1 equiv) and 2-cyclohexene-1-one **1a** (38.5 mg, 0.4 mmol, 2 equiv), but with **Chiral-Cu** (2.7 mg, 0.005 mmol, 2.5 mol%) as the copper catalyst instead of IMesCuCl. The product (3:1 crude dr) was purified by Combi Flash (24-gram column, 10 to 30% EtOAc in hexanes gradient over 20 minutes, 35 mL/min flow rate, 18 mL fractions), and pure material was obtained in fractions 24-26 (TLC: Rf = 0.48 in 30% ether in toluene, Rf = 0.35 in 20% EtOAc in hexanes). Compound **3e** (pure anti diastereomer in >20:1 isolated dr) was obtained as a white solid (34.3 mg, 0.104 mmol, 52% yield). The ^{1}H NMR of this preparation of Compound **3e** prepared here matches those obtained from the racemic reaction with IMesCuCl as the catalyst. The B(pin) group in Compound **3e** was then oxidized to the alcohol **5** to enable the determination of enantiomeric excess. To an 8 mL screw-cap vial, under air and at room temperature (22 °C), equipped with a micro-stir bar was added Compound **3e** (34.3 mg, 0.104 mmol, 1 equiv). This was then dissolved in THF (0.5 mL), then water (0.5 mL) was added. Stirring was commenced, then $NaBO_3 \cdot 4H_2O$ (32.0 mg, 0.208 mmol, 2 equiv) was added in one portion. The reaction was sealed with a screw-cap, and was allowed to stir under air at room temperature for 3 hours. Upon completion, the reaction was diluted with 6 mL EtOAc and transferred to a separatory funnel. An additional 10 mL of water and 10 mL of EtOAc were added, and the layers were separated. The aqueous phase was extracted twice more with 10 mL EtOAc, then the combined organic phases were washed once with 10 mL brine. At this point, a small (100 µL) aliquot was taken for GC-MS and GC-FID analysis, showing the desired product as one exclusive diastereomer (>20:1). The combined organics were dried over

$MgSO_4$, filtered, and concentrated by rotary evaporation. This material was finally purified by flash column chromatography (15 cm height and 1.5 cm diameter silica gel column, 7 mL fractions, elution with 200 mL of 55% EtOAc in hexanes) providing pure material in fractions 12 through 14 (TLC: Rf = 0.27 in 50% EtOAc in hexanes). After rotary evaporation and drying under high vacuum, Compound **5** was obtained as a white solid (19.8 mg, 0.090 mmol, 87% yield). Characterization by ^{1}H NMR matches that from the racemic oxidation of Compound **3e** to Compound **5**. Enantiomeric excess was determined by SFC (Agilent Infinity SFC system [1260 Infinity SFC module, 1260 SFC binary pump, 1290 thermal column compartments, 1260 diode array detector, 1260 degasser]) equipped with a chiral column (Daicel ChiralPak IB column, 4.6 mm x 250 mm). Method settings were 3.5% MeOH in CO_2 at a flowrate of 2.0 mL/min, back pressure regulator at 200 bar and 60 ºC, column temperature at 15 ºC, injection volume of 10 µL, detection at 210 nm. Compound **5** was determined to have an ee of 10% (er of 55:45).

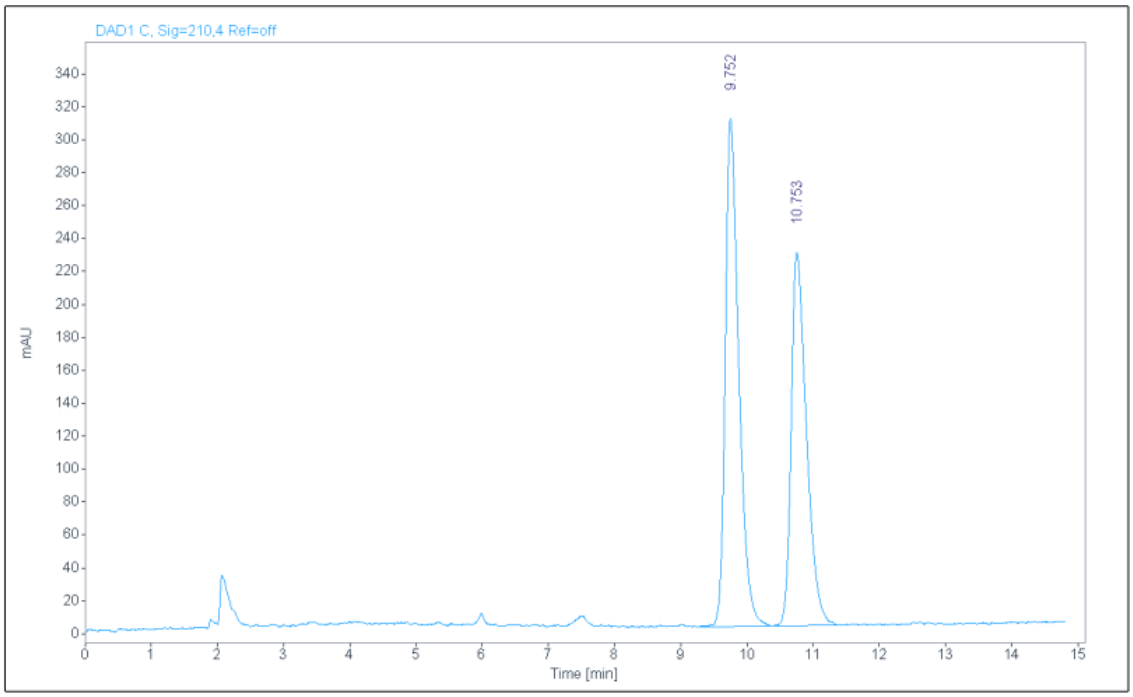

Signal: DAD1 C, Sig=210,4 Ref=off

RT [min]	Compound Name	Area	Height	Area%	RespFactor	Amount (ng/ul)
9.752		4356.739	308.475	54.6		0.000
10.753		3629.400	226.478	45.4		0.000

2.4.10: NMR spectra for novel compounds

Compound **3a** ($CDCl_3$, 400 MHz, ^1H NMR)

(2*RS*,3*RS*)-2-phenyl-3-(4,4,5,5-tetramethyl-1,3,2-dioxaborolan-2-yl)cyclohexan-1-one

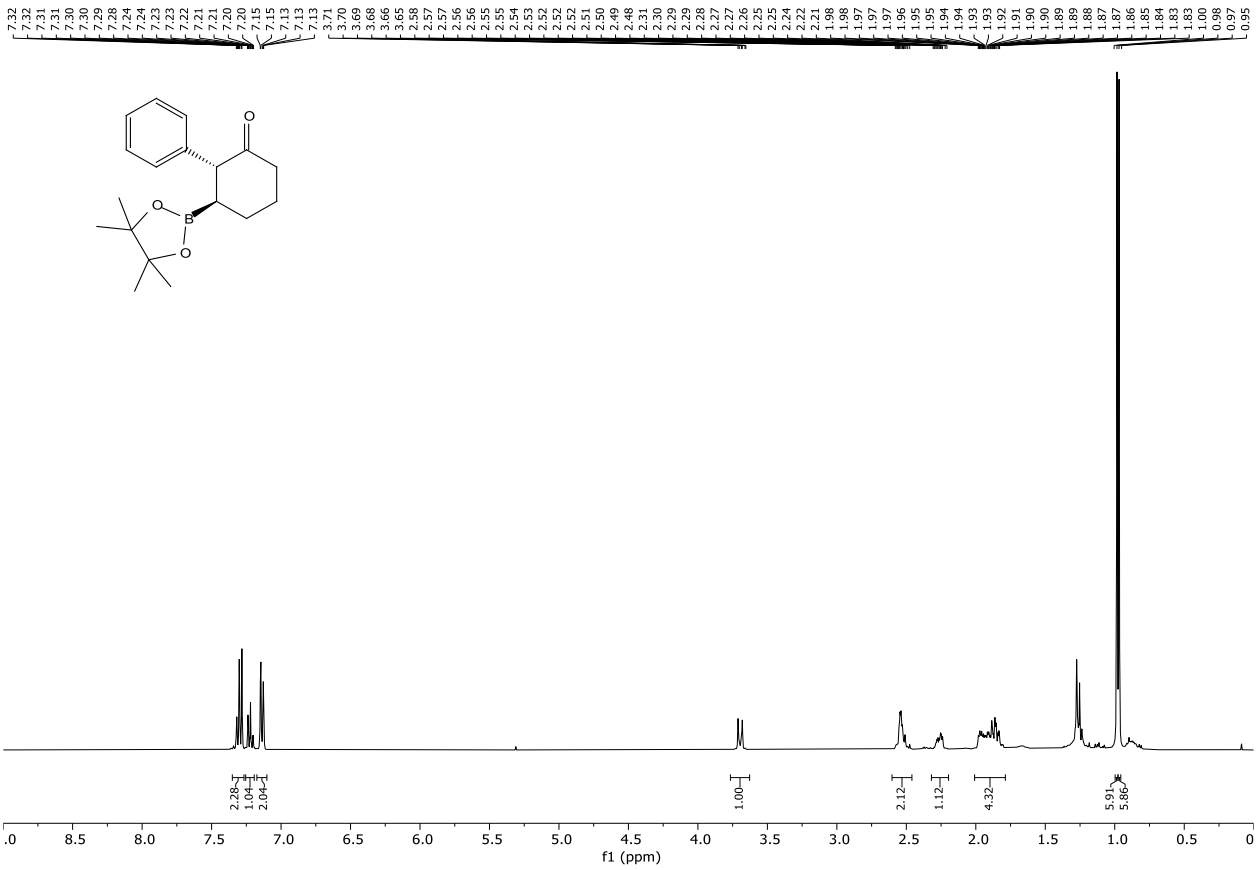

Compound **3a** ($CDCl_3$, 101 MHz, ^{13}C NMR)

(2*RS*,3*RS*)-2-phenyl-3-(4,4,5,5-tetramethyl-1,3,2-dioxaborolan-2-yl)cyclohexan-1-one

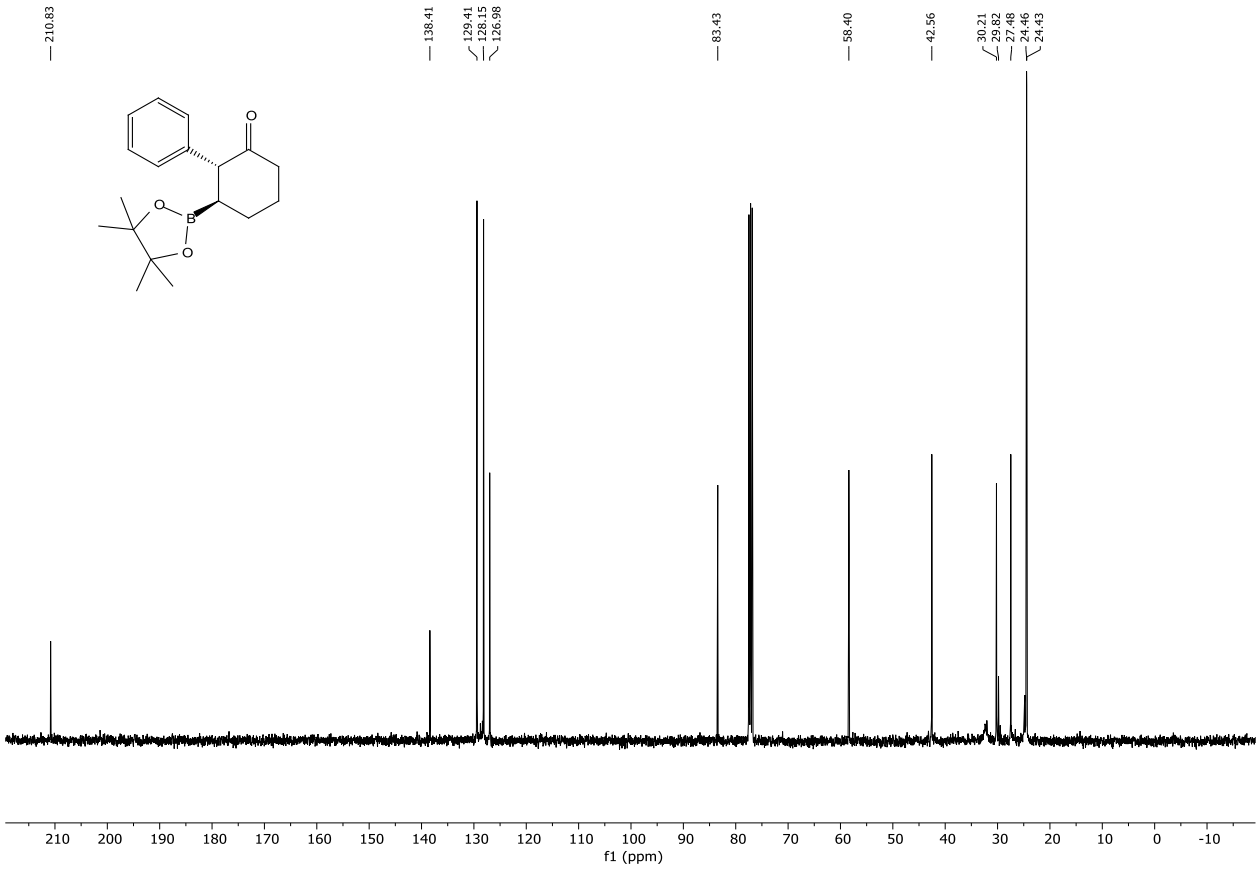

Compound **3b** ($CDCl_3$, 400 MHz, ^1H NMR)

(2*RS*,3*RS*)-2-([1,1'-biphenyl]-4-yl)-3-(4,4,5,5-tetramethyl-1,3,2-dioxaborolan-2-yl)cyclohexan-1-one

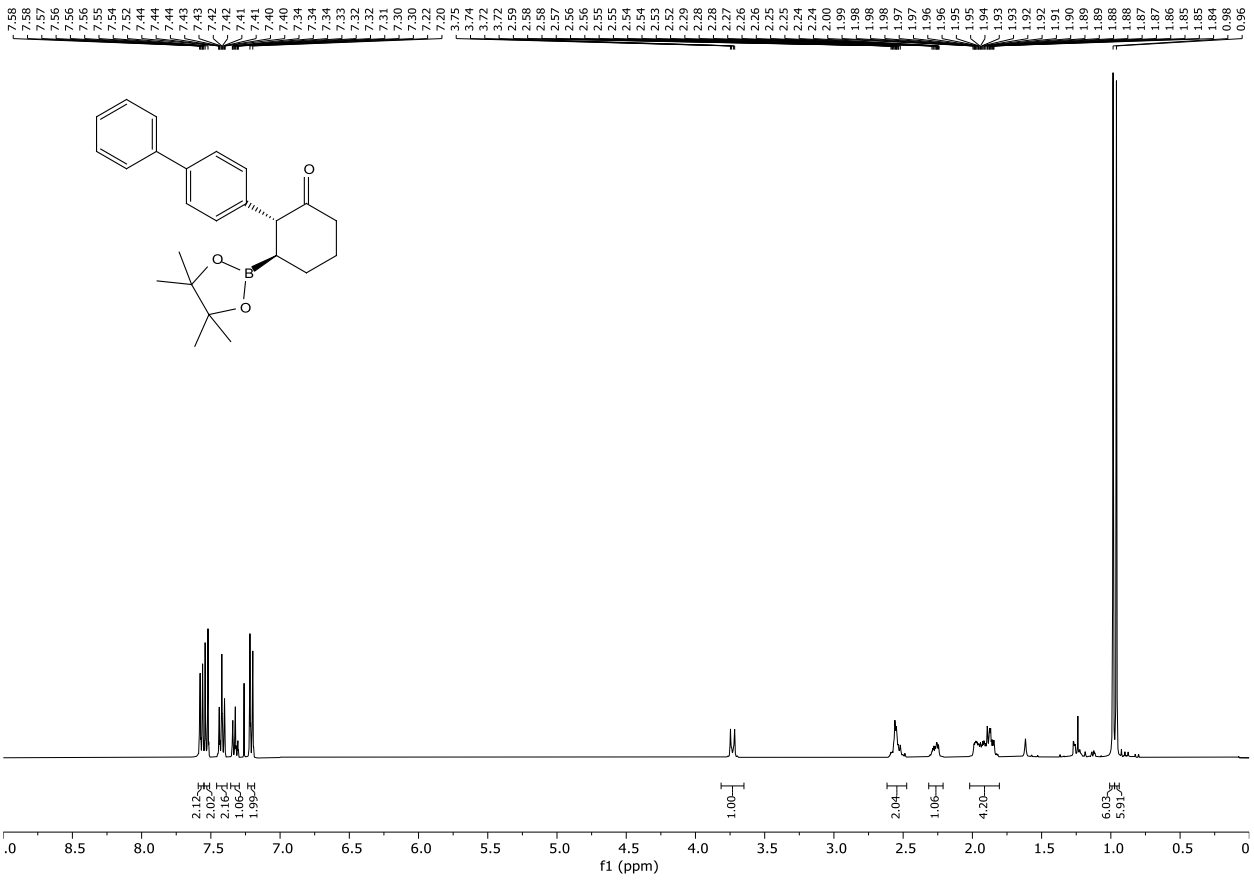

Compound **3b** ($CDCl_3$, 101 MHz, ^{13}C NMR)

(2*RS*,3*RS*)-2-([1,1'-biphenyl]-4-yl)-3-(4,4,5,5-tetramethyl-1,3,2-dioxaborolan-2-yl)cyclohexan-1-one

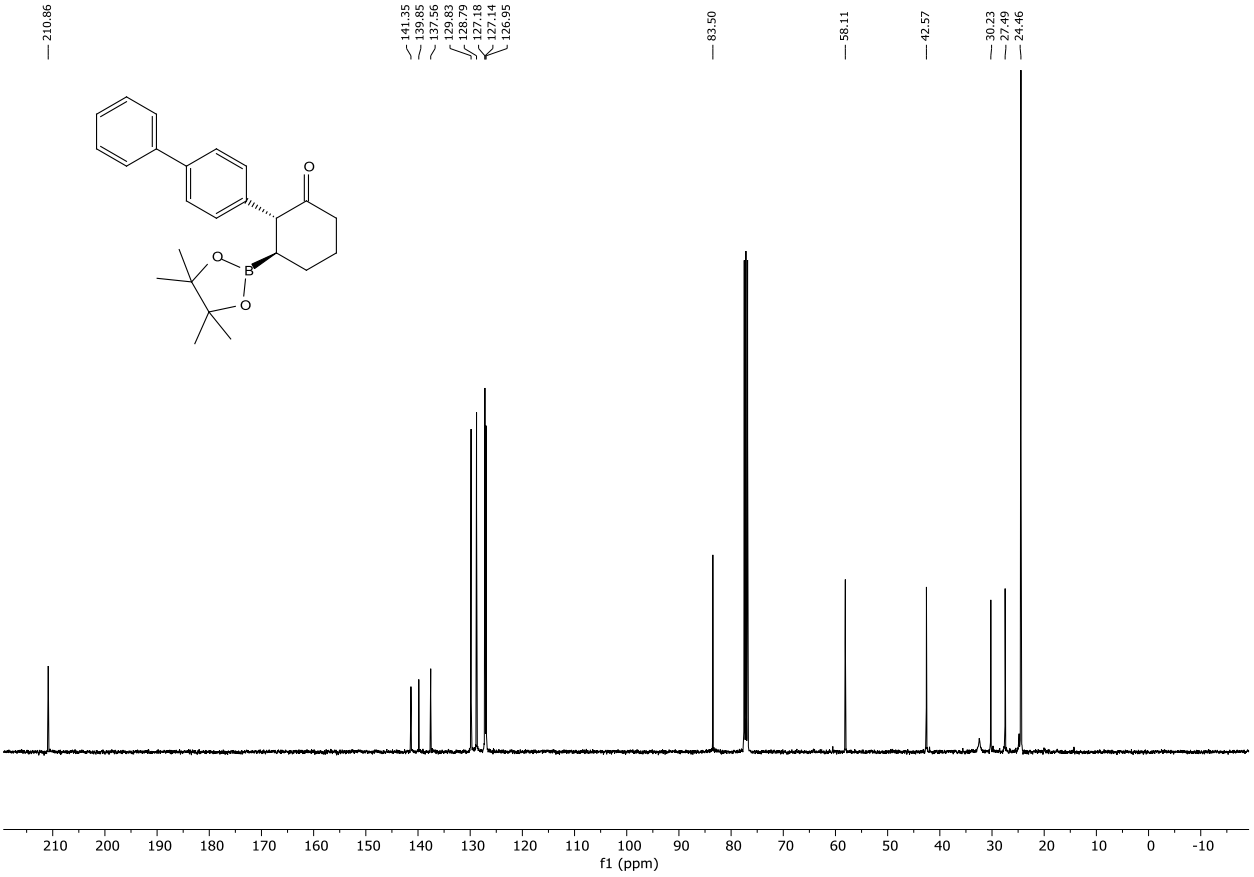

Compound **3c** ($CDCl_3$, 400 MHz, ^1H NMR)

(2*RS*,3*RS*)-2-(4-(*tert*-butyl)phenyl)-3-(4,4,5,5-tetramethyl-1,3,2-dioxaborolan-2-yl)cyclohexan-1-one

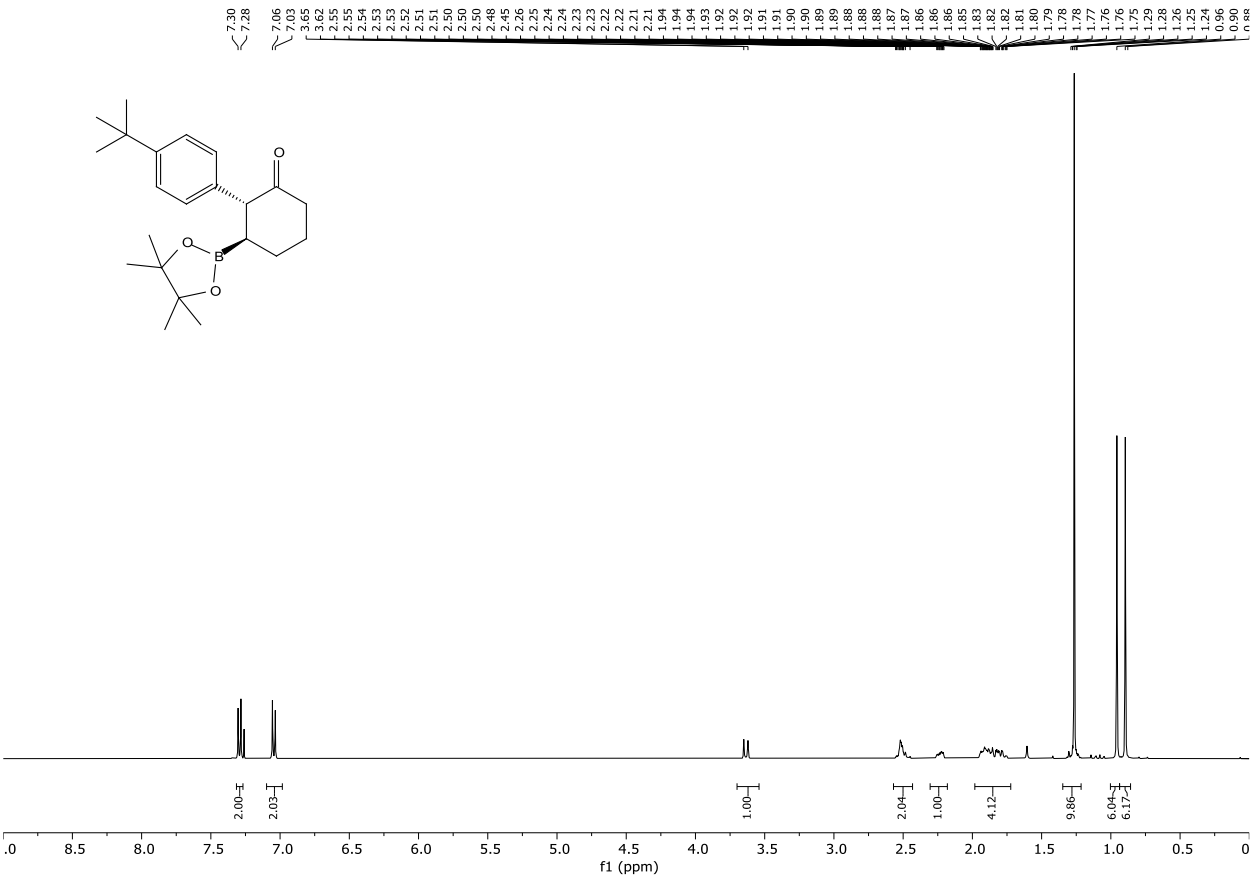

Compound **3c** ($CDCl_3$, 101 MHz, ^{13}C NMR)

(2*RS*,3*RS*)-2-(4-(*tert*-butyl)phenyl)-3-(4,4,5,5-tetramethyl-1,3,2-dioxaborolan-2-yl)cyclohexan-1-one

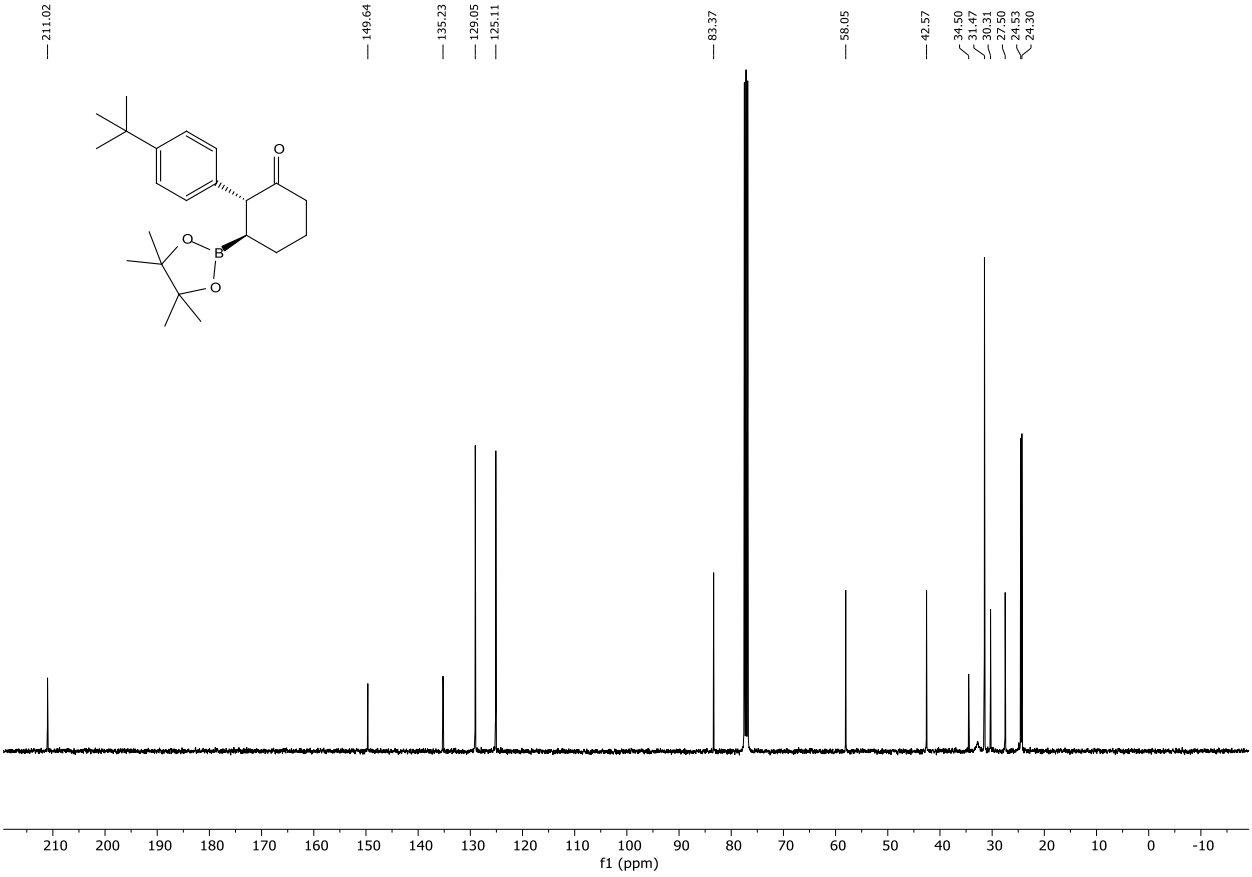

Compound **3d** ($CDCl_3$, 400 MHz, ^1H NMR)

(2*RS*,3*RS*)-3-(4,4,5,5-tetramethyl-1,3,2-dioxaborolan-2-yl)-2-(*p*-tolyl)cyclohexan-1-one

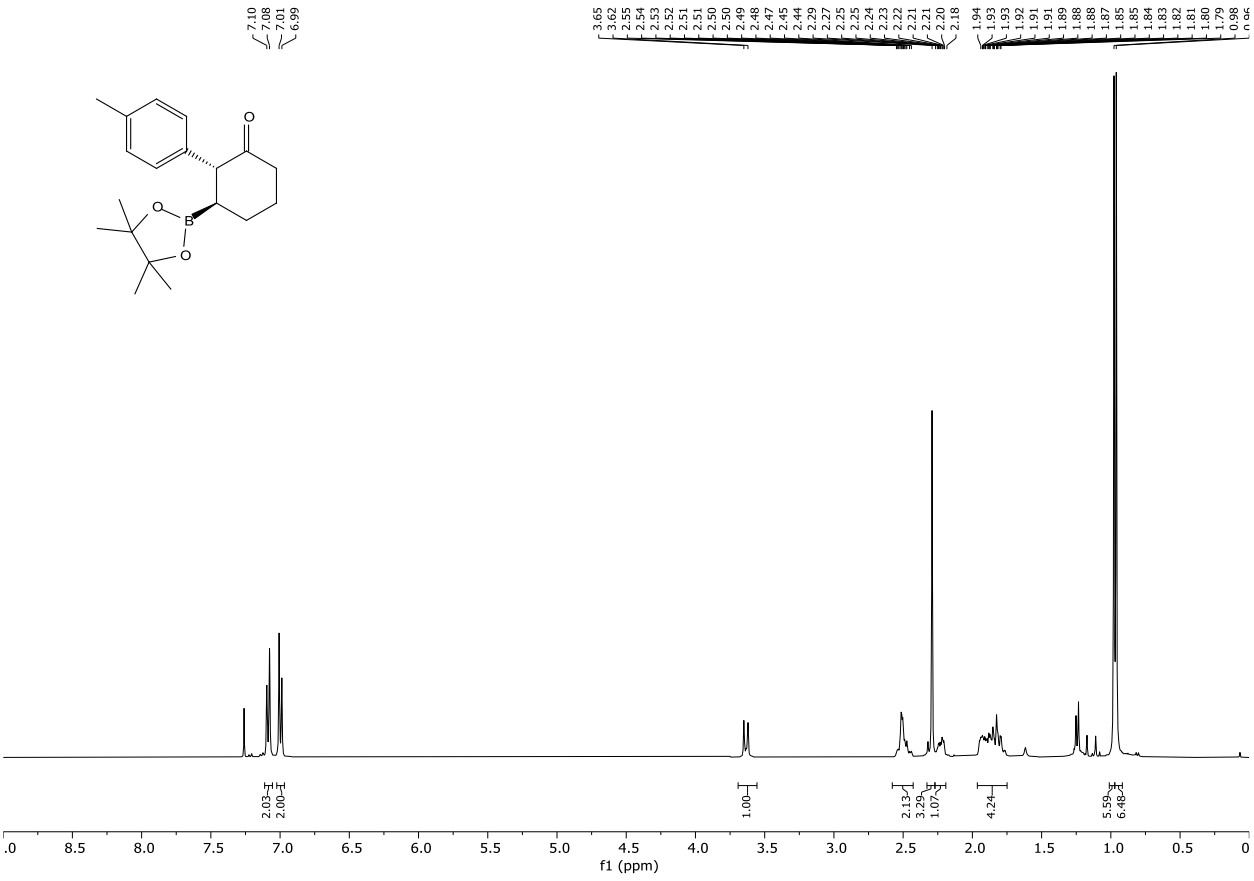

Compound **3d** ($CDCl_3$, 101 MHz, ^{13}C NMR)

(2*RS*,3*RS*)-3-(4,4,5,5-tetramethyl-1,3,2-dioxaborolan-2-yl)-2-(*p*-tolyl)cyclohexan-1-one

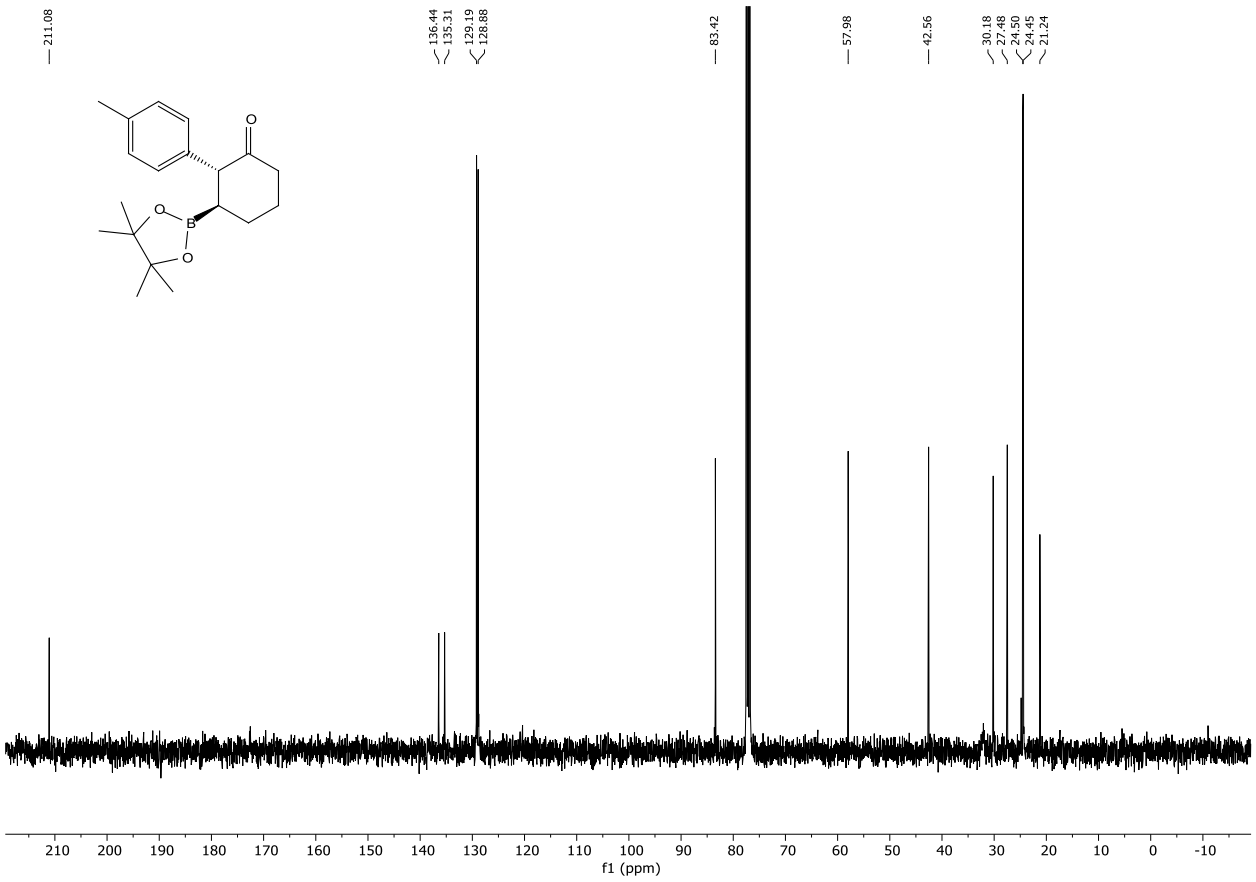

Compound **3e** [0.2 mmol scale] ($CDCl_3$, 400 MHz, ^1H NMR)

(2*RS*,3*RS*)-2-(4-methoxyphenyl)-3-(4,4,5,5-tetramethyl-1,3,2-dioxaborolan-2-yl)cyclohexan-1-one

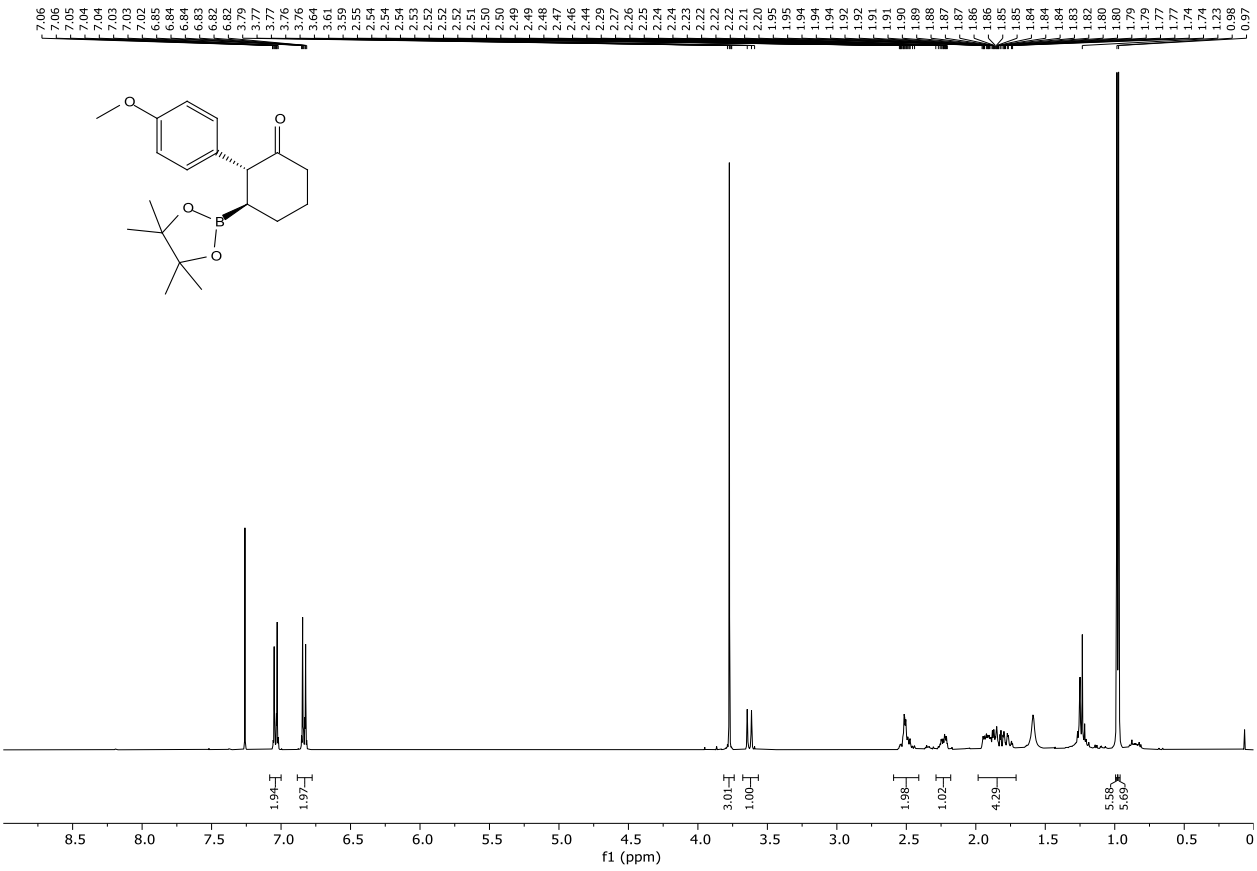

Compound **3e** [0.2 mmol scale] ($CDCl_3$, 101 MHz, ^{13}C NMR)

(2*RS*,3*RS*)-2-(4-methoxyphenyl)-3-(4,4,5,5-tetramethyl-1,3,2-dioxaborolan-2-yl)cyclohexan-1-one

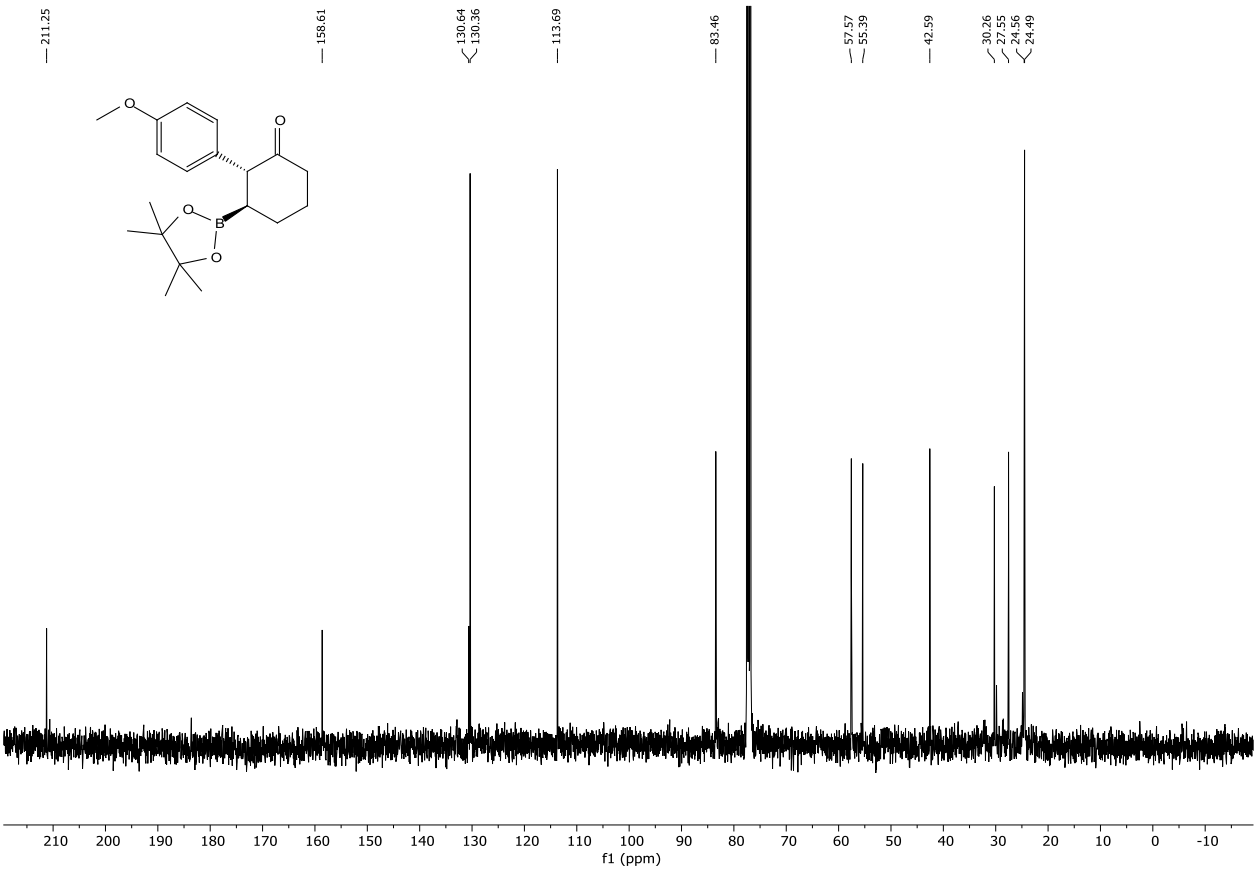

Compound **3e** [1 mmol scale] ($CDCl_3$, 400 MHz, ^1H NMR)

(2*RS*,3*RS*)-2-(4-methoxyphenyl)-3-(4,4,5,5-tetramethyl-1,3,2-dioxaborolan-2-yl)cyclohexan-1-one

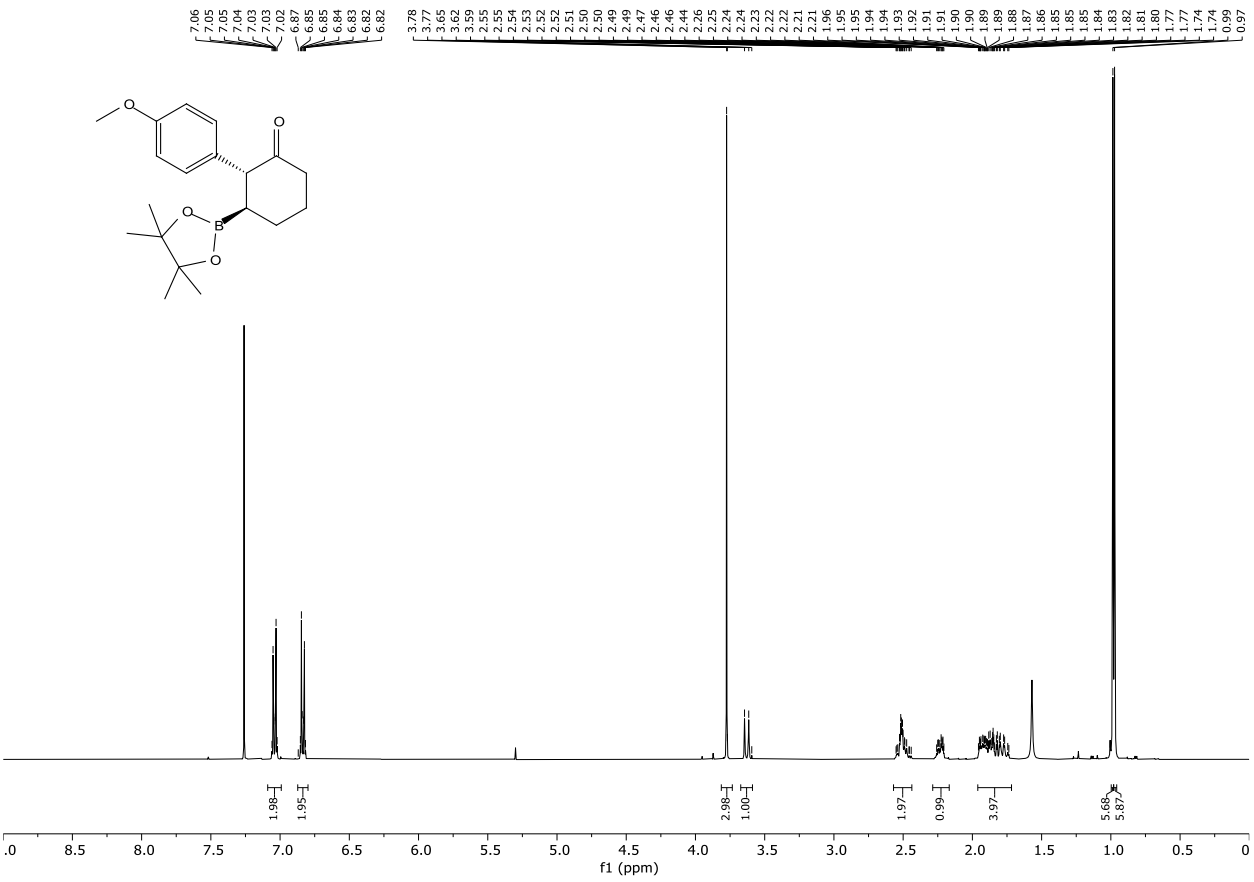

Compound **3f** ($CDCl_3$, 400 MHz, ^1H NMR)

(2*RS*,3*RS*)-2-(4-chlorophenyl)-3-(4,4,5,5-tetramethyl-1,3,2-dioxaborolan-2-yl)cyclohexan-1-one

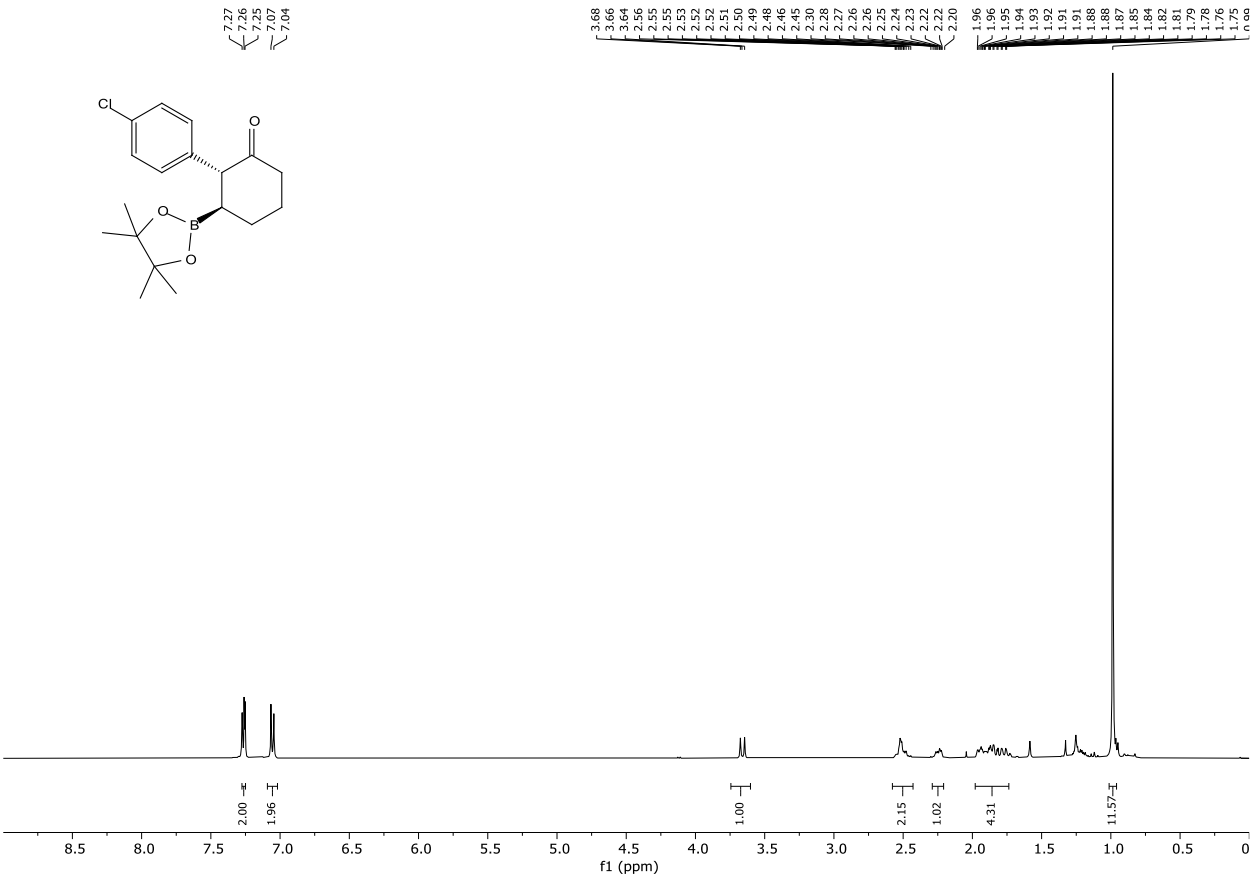

Compound **3f** ($CDCl_3$, 101 MHz, ^{13}C NMR)

(2*RS*,3*RS*)-2-(4-chlorophenyl)-3-(4,4,5,5-tetramethyl-1,3,2-dioxaborolan-2-yl)cyclohexan-1-one

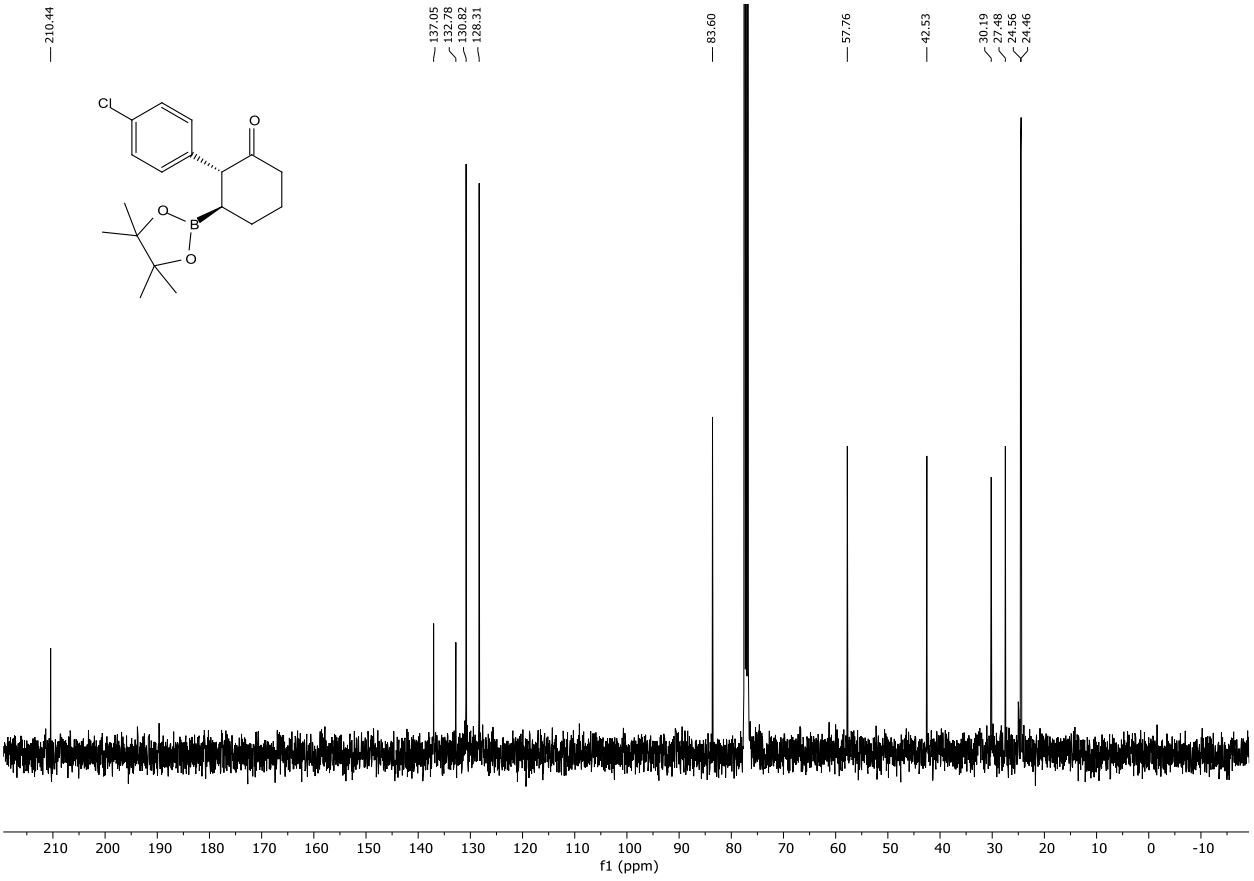

Compound **3g** ($CDCl_3$, 600 MHz, ^1H NMR)

(2*RS*,3*RS*)-2-(4-fluorophenyl)-3-(4,4,5,5-tetramethyl-1,3,2-dioxaborolan-2-yl)cyclohexan-1-one

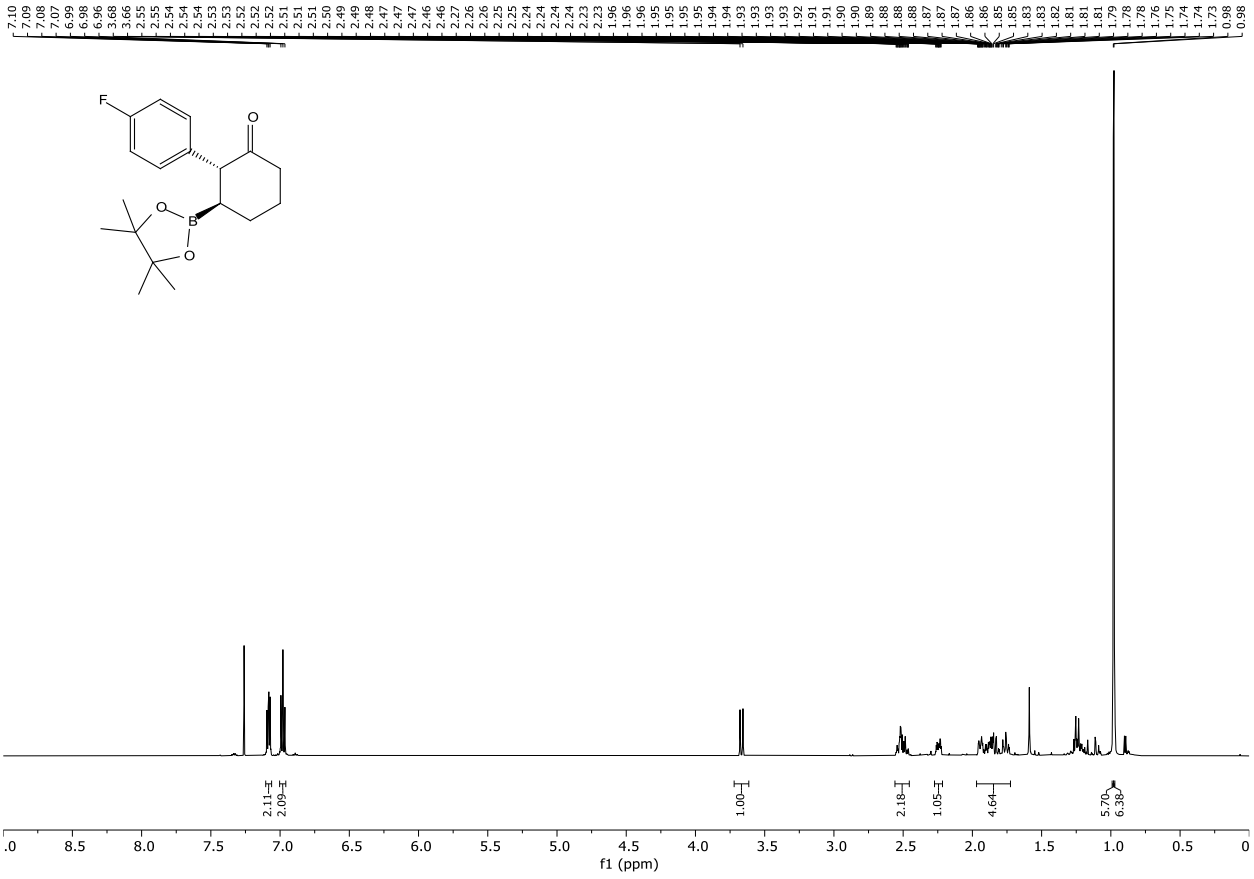

Compound **3g** ($CDCl_3$, 151 MHz, ^{13}C NMR)

(2*RS*,3*RS*)-2-(4-fluorophenyl)-3-(4,4,5,5-tetramethyl-1,3,2-dioxaborolan-2-yl)cyclohexan-1-one

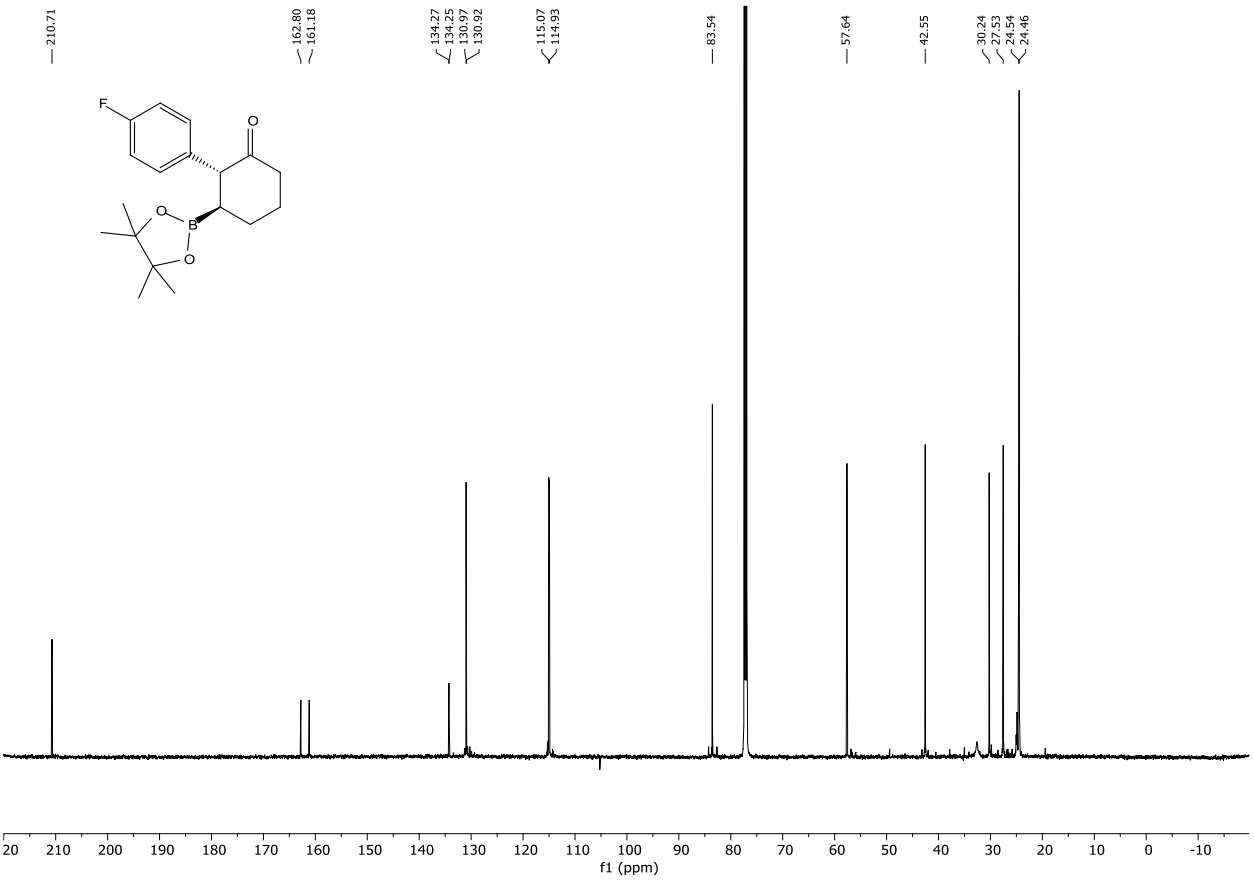

Compound **3g** ($CDCl_3$, 283 MHz, ^{19}F NMR)

(2*RS*,3*RS*)-2-(4-fluorophenyl)-3-(4,4,5,5-tetramethyl-1,3,2-dioxaborolan-2-yl)cyclohexan-1-one

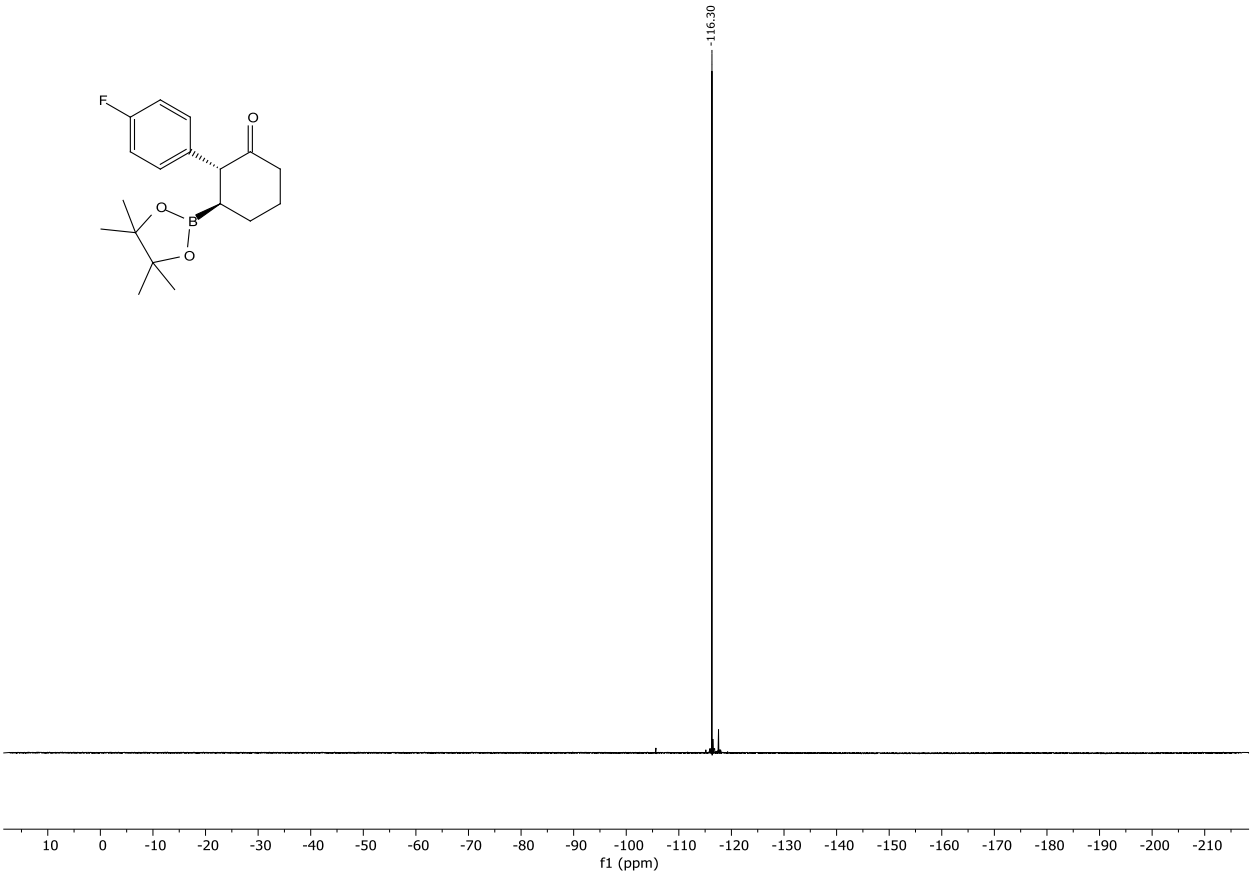

Compound **3h** ($CDCl_3$, 400 MHz, ^1H NMR)

(2*RS*,3*RS*)-2-(4-nitrophenyl)-3-(4,4,5,5-tetramethyl-1,3,2-dioxaborolan-2-yl)cyclohexan-1-one

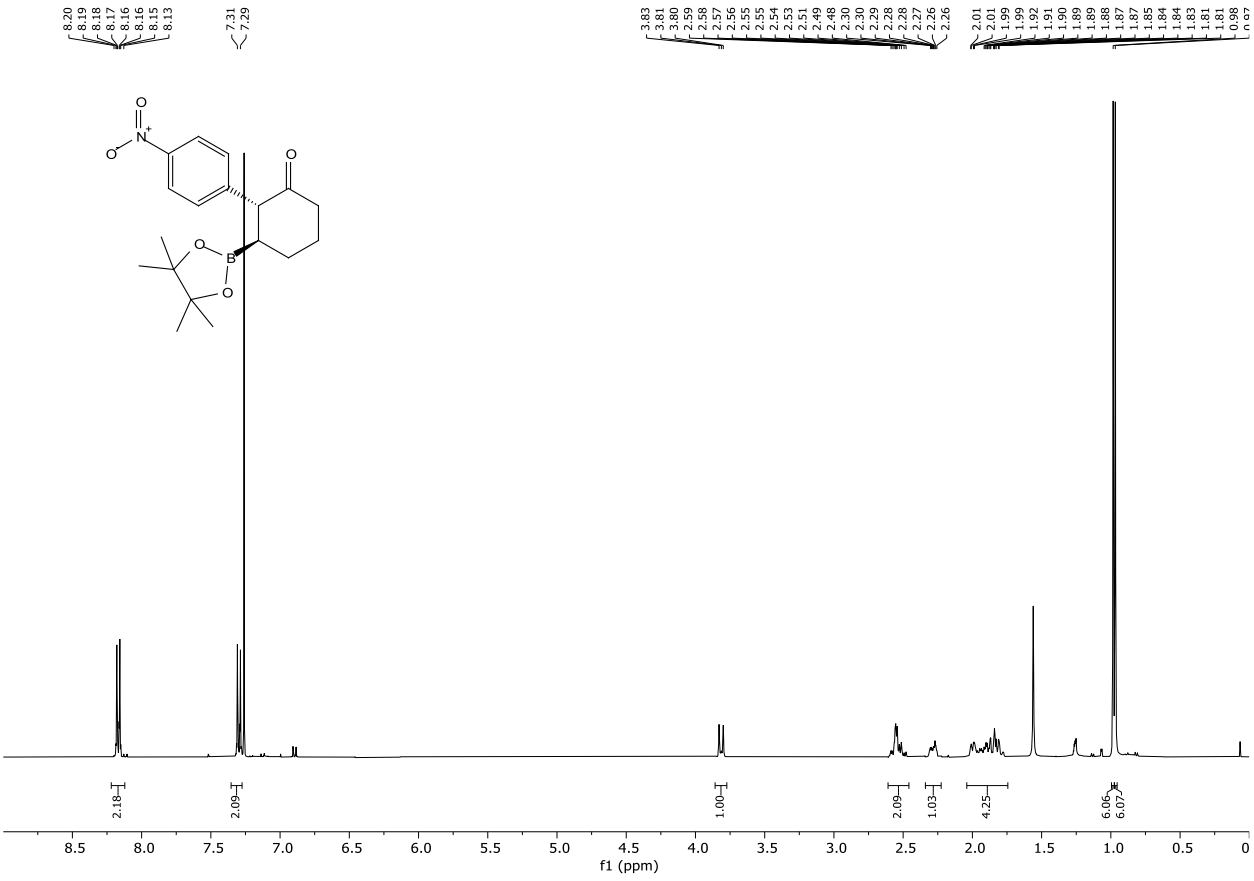

Compound **3h** ($CDCl_3$, 101 MHz, ^{13}C NMR)

(2*RS*,3*RS*)-2-(4-nitrophenyl)-3-(4,4,5,5-tetramethyl-1,3,2-dioxaborolan-2-yl)cyclohexan-1-one

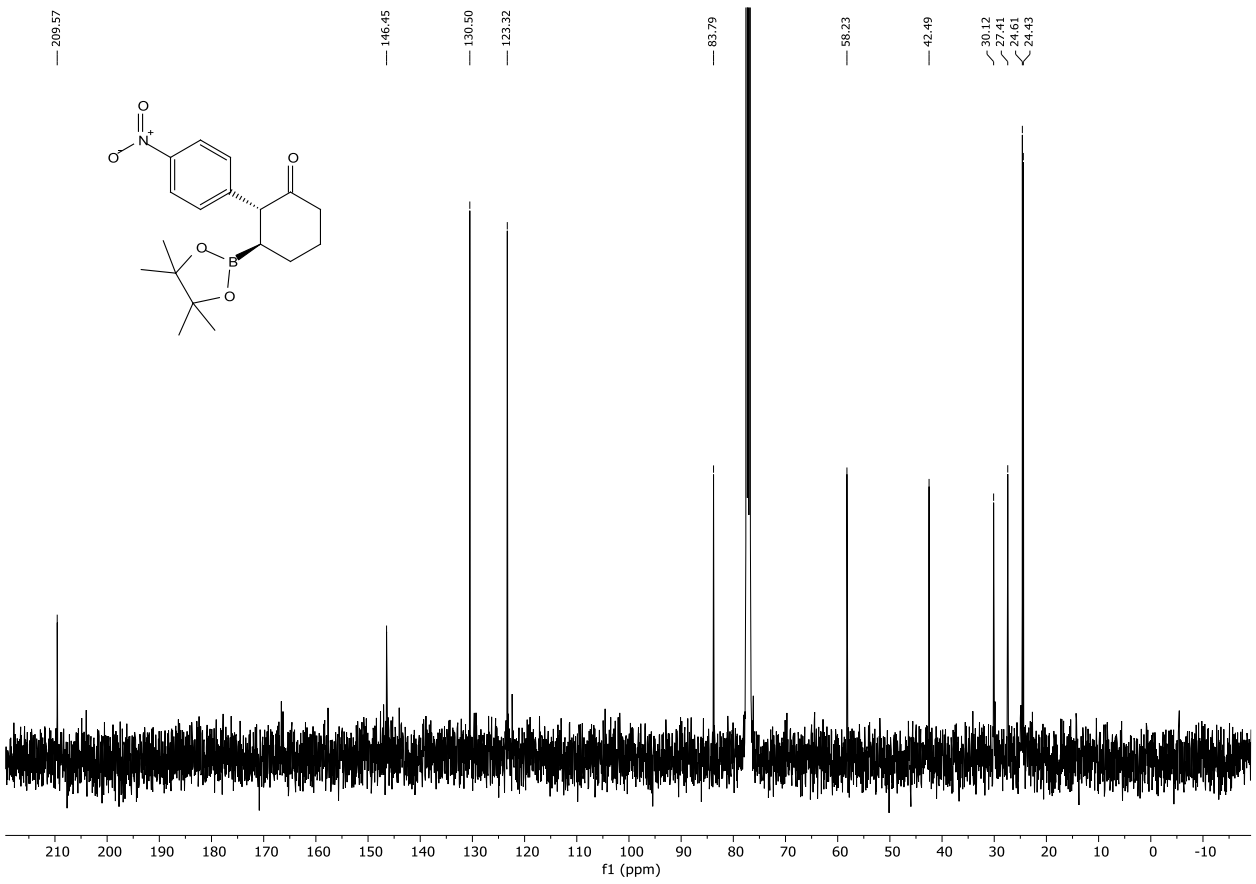

Compound **3i** ($CDCl_3$, 400 MHz, ^1H NMR)

methyl 4-((1*RS*,6*RS*)-2-oxo-6-(4,4,5,5-tetramethyl-1,3,2-dioxaborolan-2-yl)cyclohexyl)benzoate

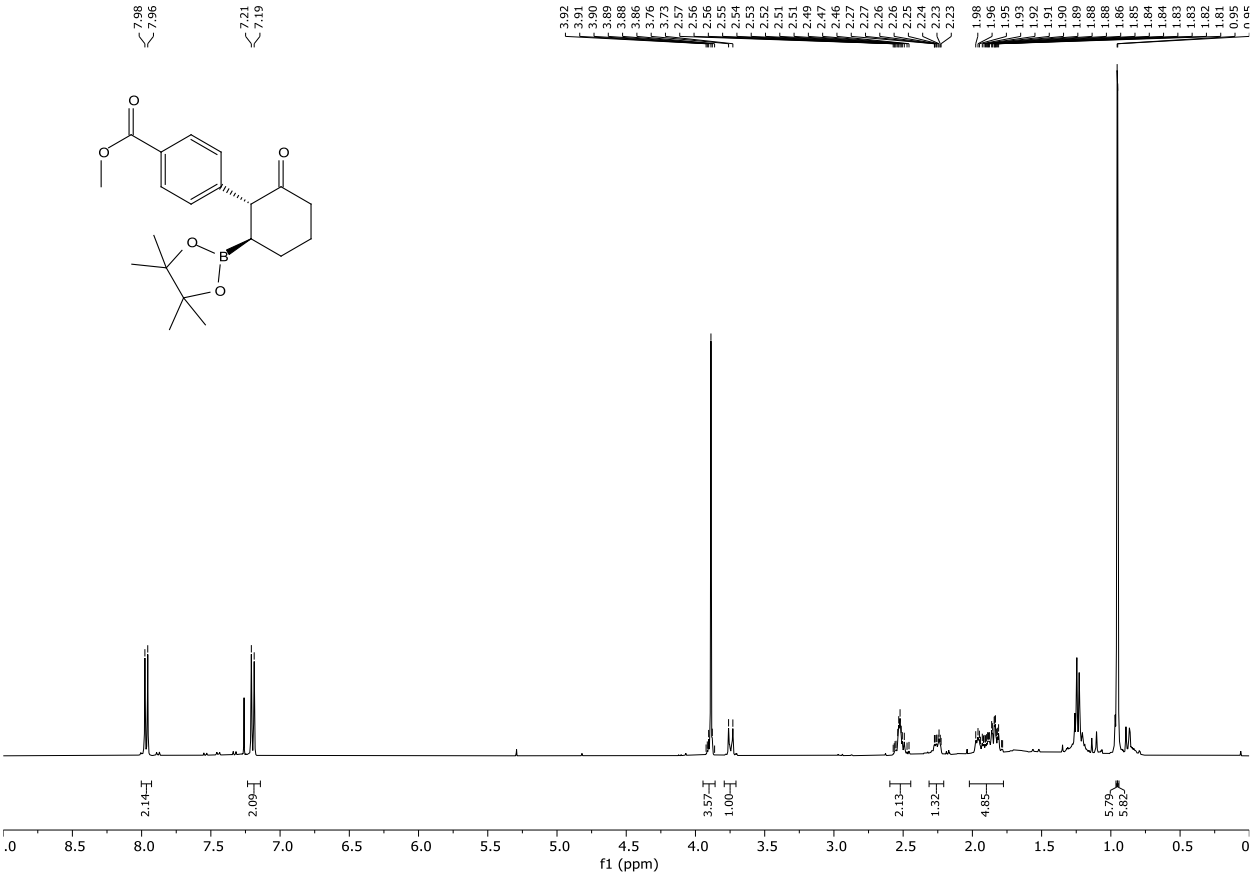

Compound **3i** ($CDCl_3$, 101 MHz, ^{13}C NMR)

methyl 4-((1*RS*,6*RS*)-2-oxo-6-(4,4,5,5-tetramethyl-1,3,2-dioxaborolan-2-yl)cyclohexyl)benzoate

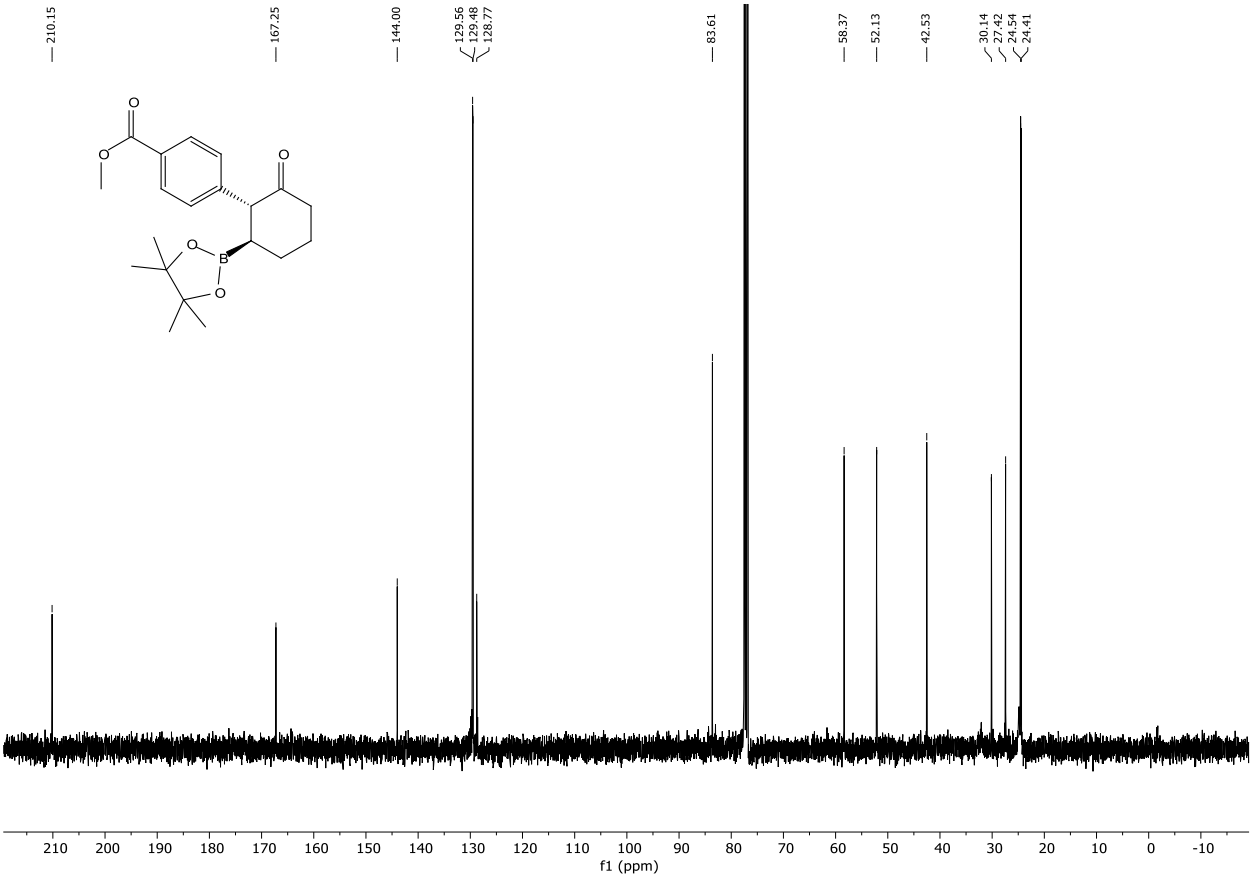

Compound **3j** ($CDCl_3$, 600 MHz, ^1H NMR)

(2*RS*,3*RS*)-3-(4,4,5,5-tetramethyl-1,3,2-dioxaborolan-2-yl)-2-(3-(trifluoromethyl)phenyl)cyclohexan-1-one

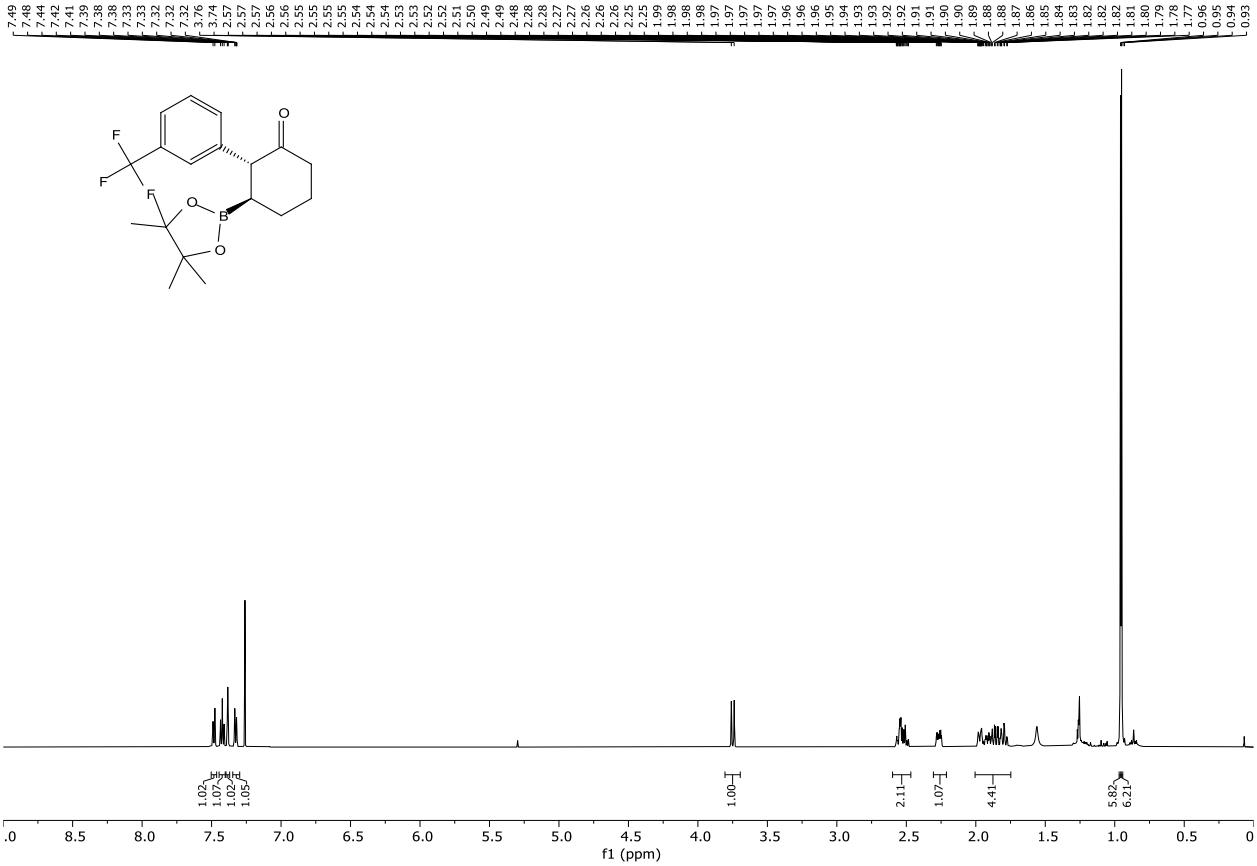

Compound **3j** ($CDCl_3$, 151 MHz, ^{13}C NMR)

(2*RS*,3*RS*)-3-(4,4,5,5-tetramethyl-1,3,2-dioxaborolan-2-yl)-2-(3-(trifluoromethyl)phenyl)cyclohexan-1-one

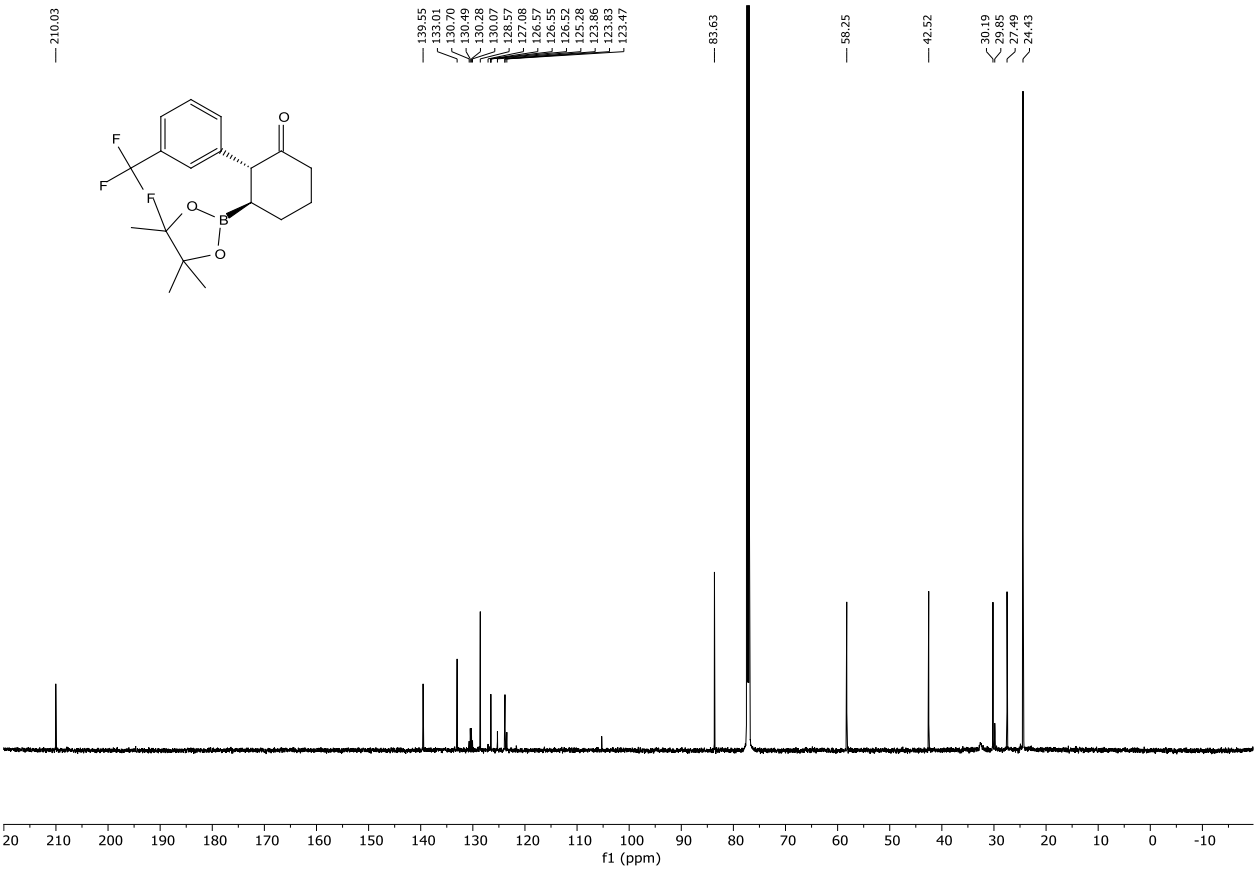

Compound **3j** ($CDCl_3$, 282 MHz, ^{19}F NMR)

(2*RS*,3*RS*)-3-(4,4,5,5-tetramethyl-1,3,2-dioxaborolan-2-yl)-2-(3-(trifluoromethyl)phenyl)cyclohexan-1-one

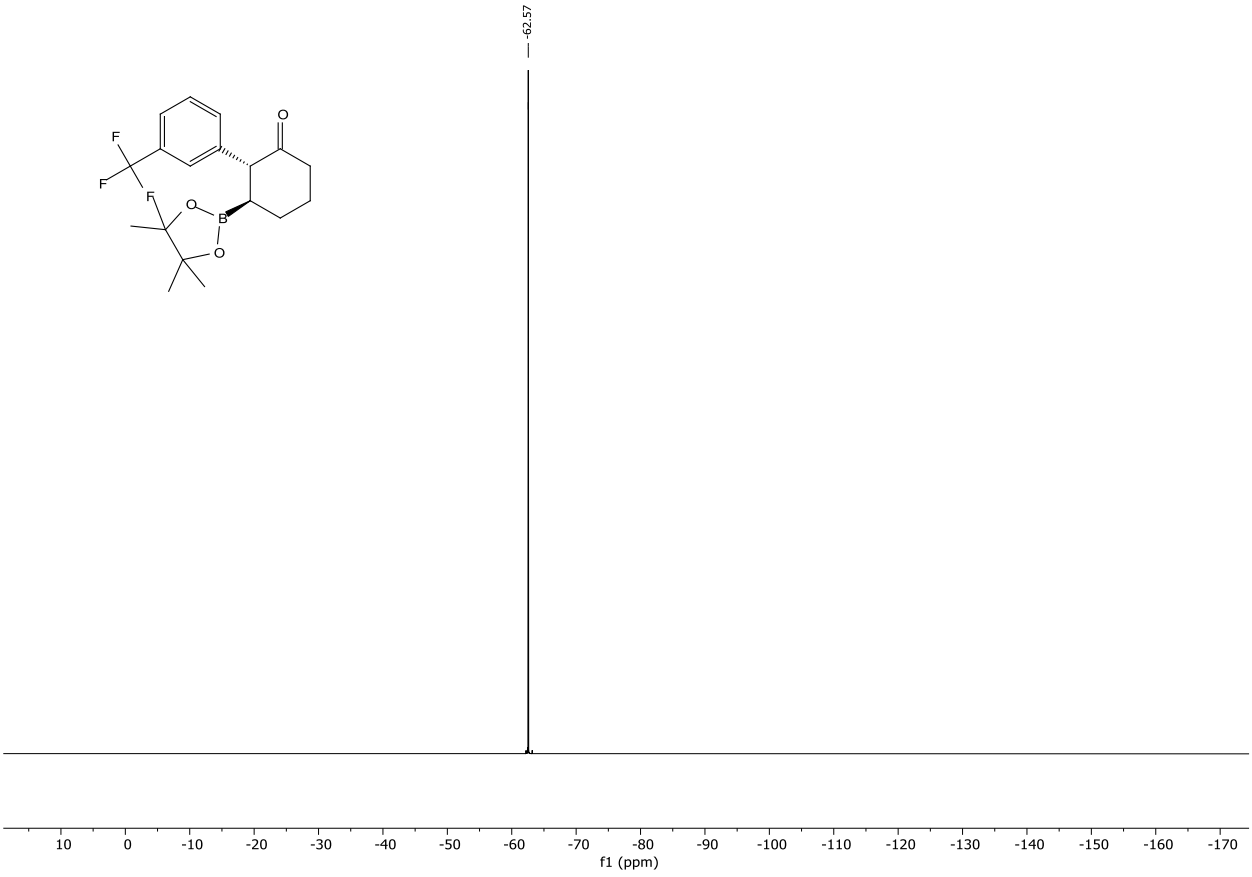

Compound **3k** ($CDCl_3$, 400 MHz, ^1H NMR)

(2*RS*,3*RS*)-2-(naphthalen-2-yl)-3-(4,4,5,5-tetramethyl-1,3,2-dioxaborolan-2-yl)cyclohexan-1-one

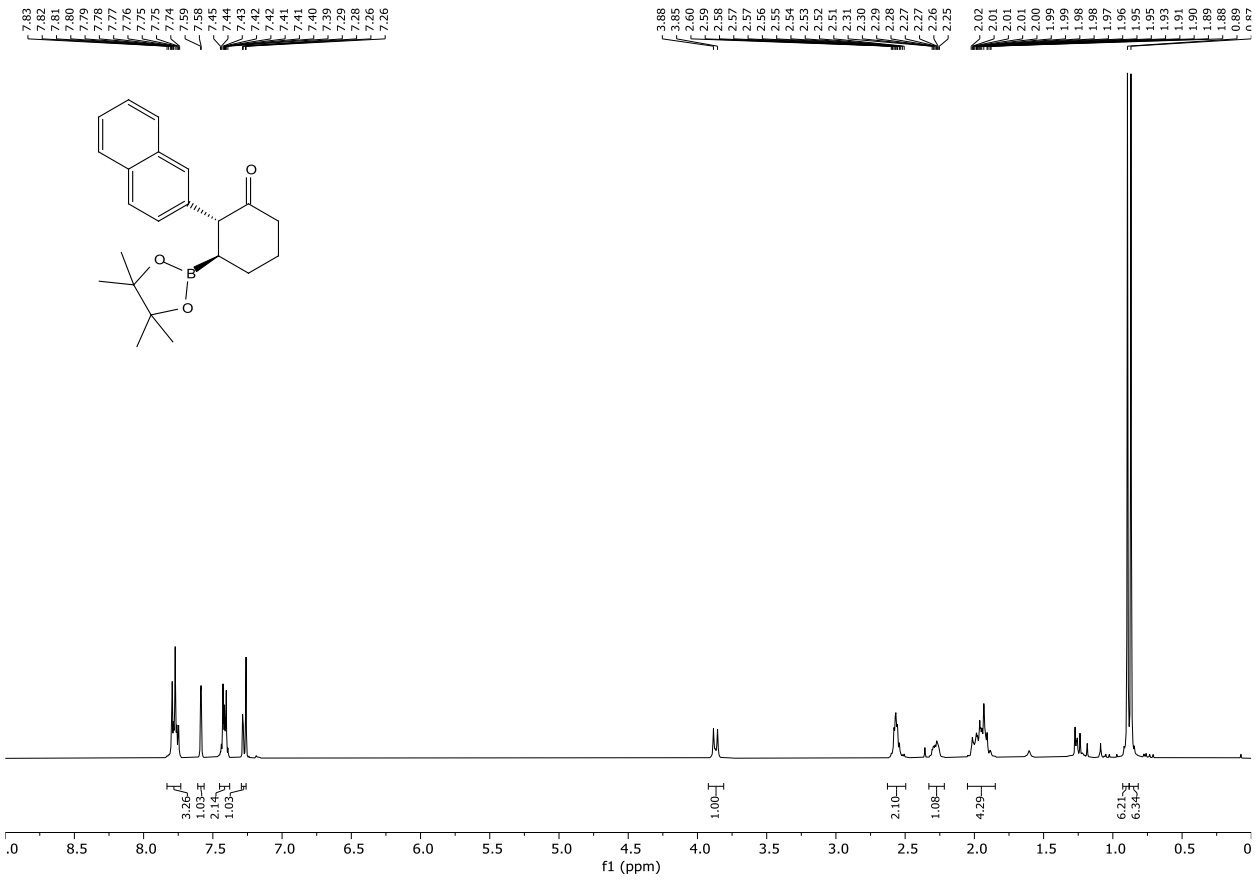

Compound **3k** ($CDCl_3$, 101 MHz, ^{13}C NMR)

(2*RS*,3*RS*)-2-(naphthalen-2-yl)-3-(4,4,5,5-tetramethyl-1,3,2-dioxaborolan-2-yl)cyclohexan-1-one

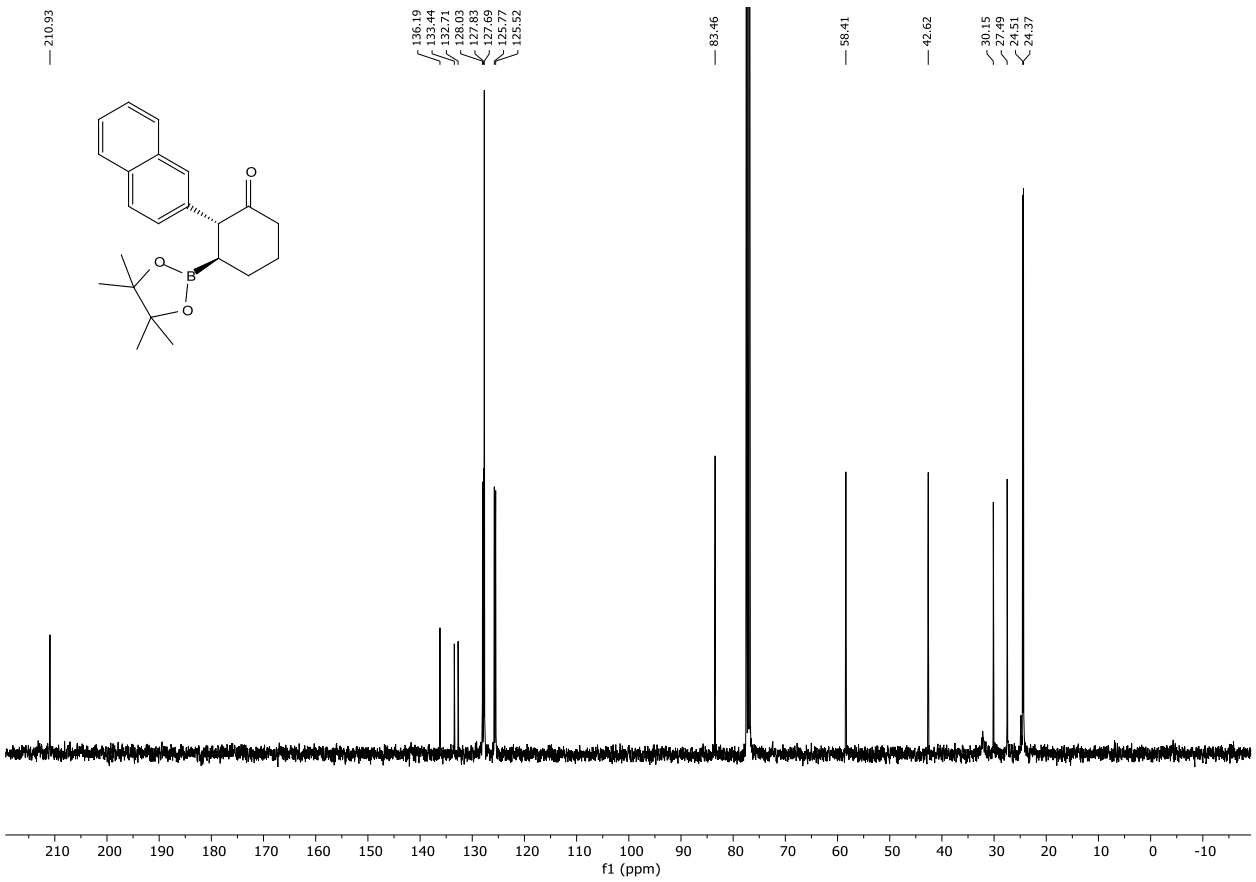

Compound **3l** ($CDCl_3$, 400 MHz, ^1H NMR)

(*2RS*,3*RS*)-2-(2-methoxyphenyl)-3-(4,4,5,5-tetramethyl-1,3,2-dioxaborolan-2-yl)cyclohexan-1-one

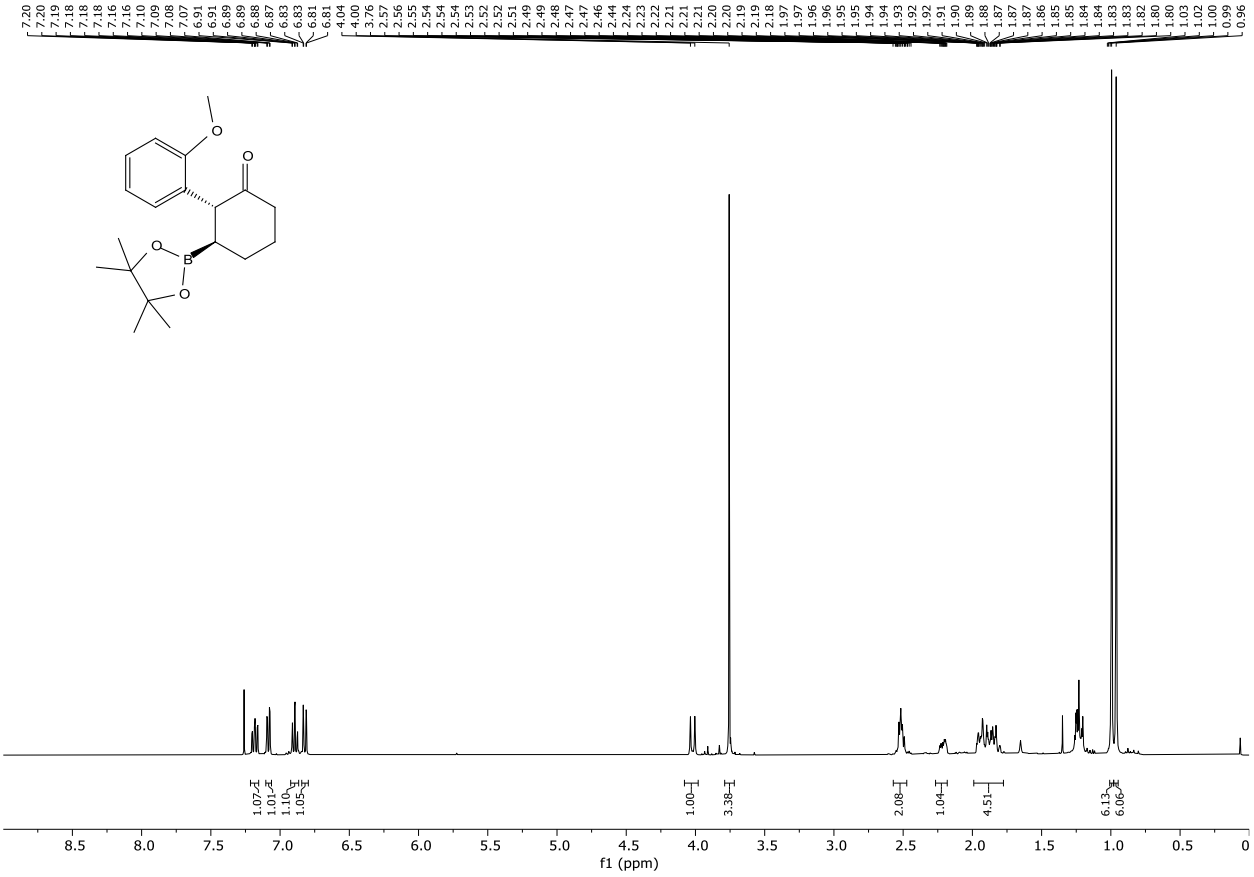

Compound **3l** ($CDCl_3$, 101 MHz, ^{13}C NMR)

(*2RS*,3*RS*)-2-(2-methoxyphenyl)-3-(4,4,5,5-tetramethyl-1,3,2-dioxaborolan-2-yl)cyclohexan-1-one

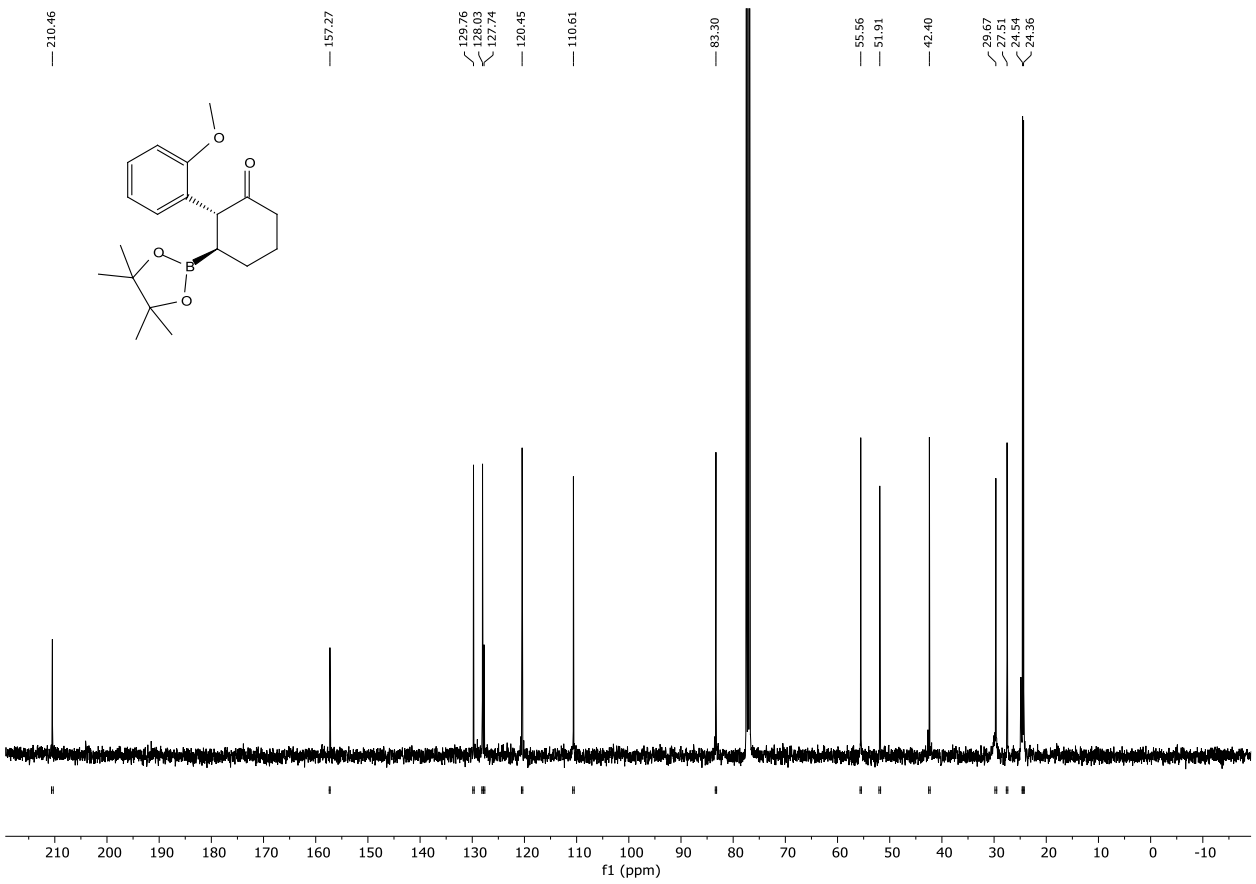

Compound **3m** ($CDCl_3$, 600 MHz, ^1H NMR)

(2*RS*,3*RS*)-2-(naphthalen-1-yl)-3-(4,4,5,5-tetramethyl-1,3,2-dioxaborolan-2-yl)cyclohexan-1-one

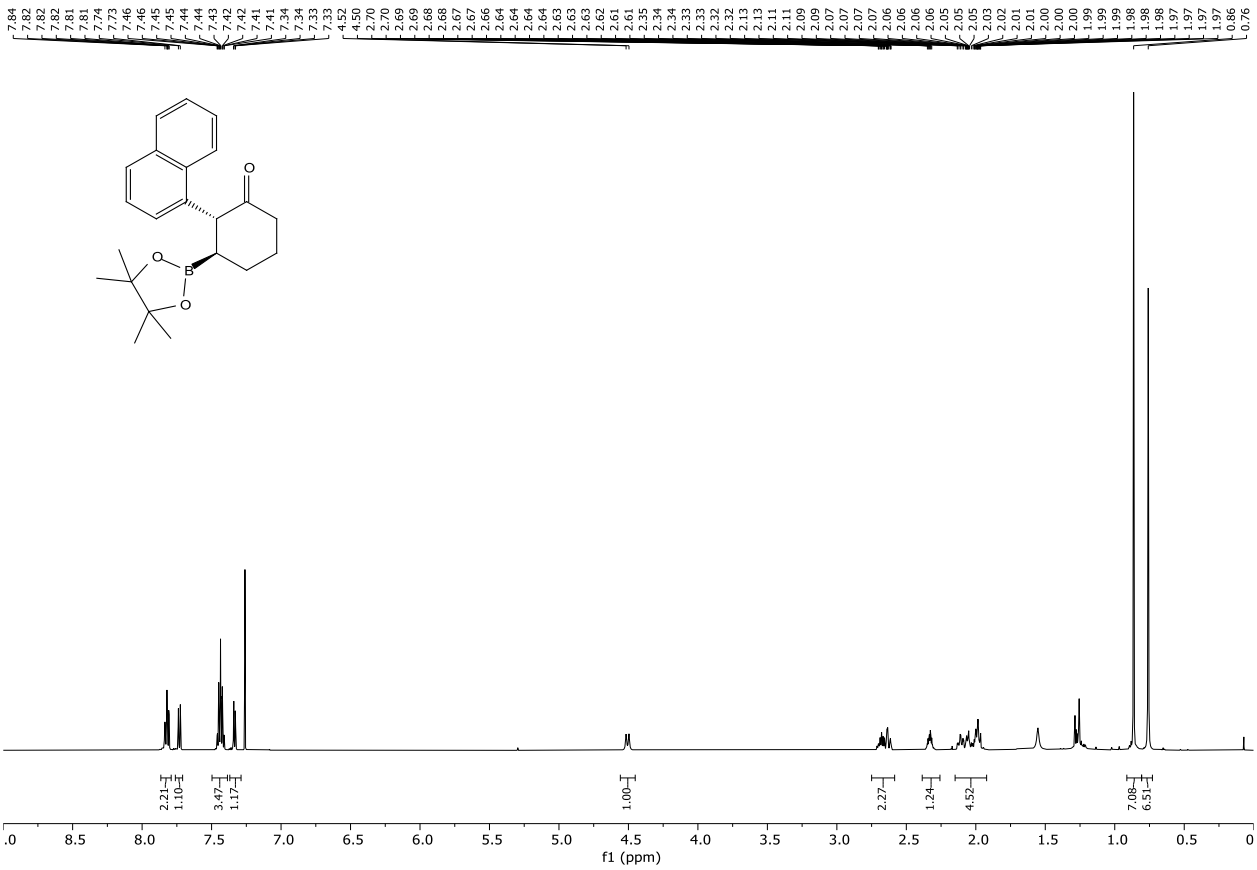

Compound **3m** ($CDCl_3$, 151 MHz, ^{13}C NMR)

(2*RS*,3*RS*)-2-(naphthalen-1-yl)-3-(4,4,5,5-tetramethyl-1,3,2-dioxaborolan-2-yl)cyclohexan-1-one

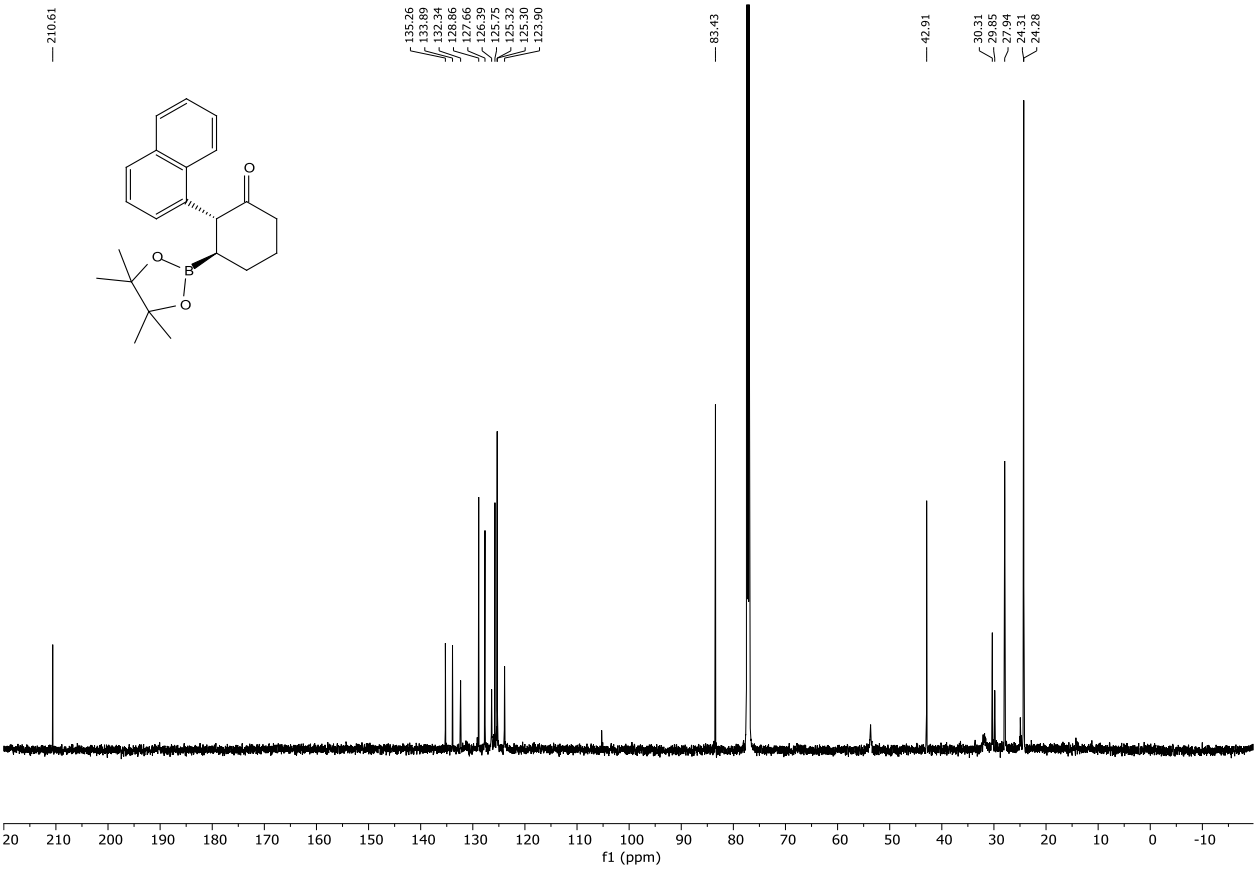

Compound **3n** ($CDCl_3$, 400 MHz, ^1H NMR)

(2*RS*,3*RS*)-3-(4,4,5,5-tetramethyl-1,3,2-dioxaborolan-2-yl)-2-(*o*-tolyl)cyclohexan-1-one

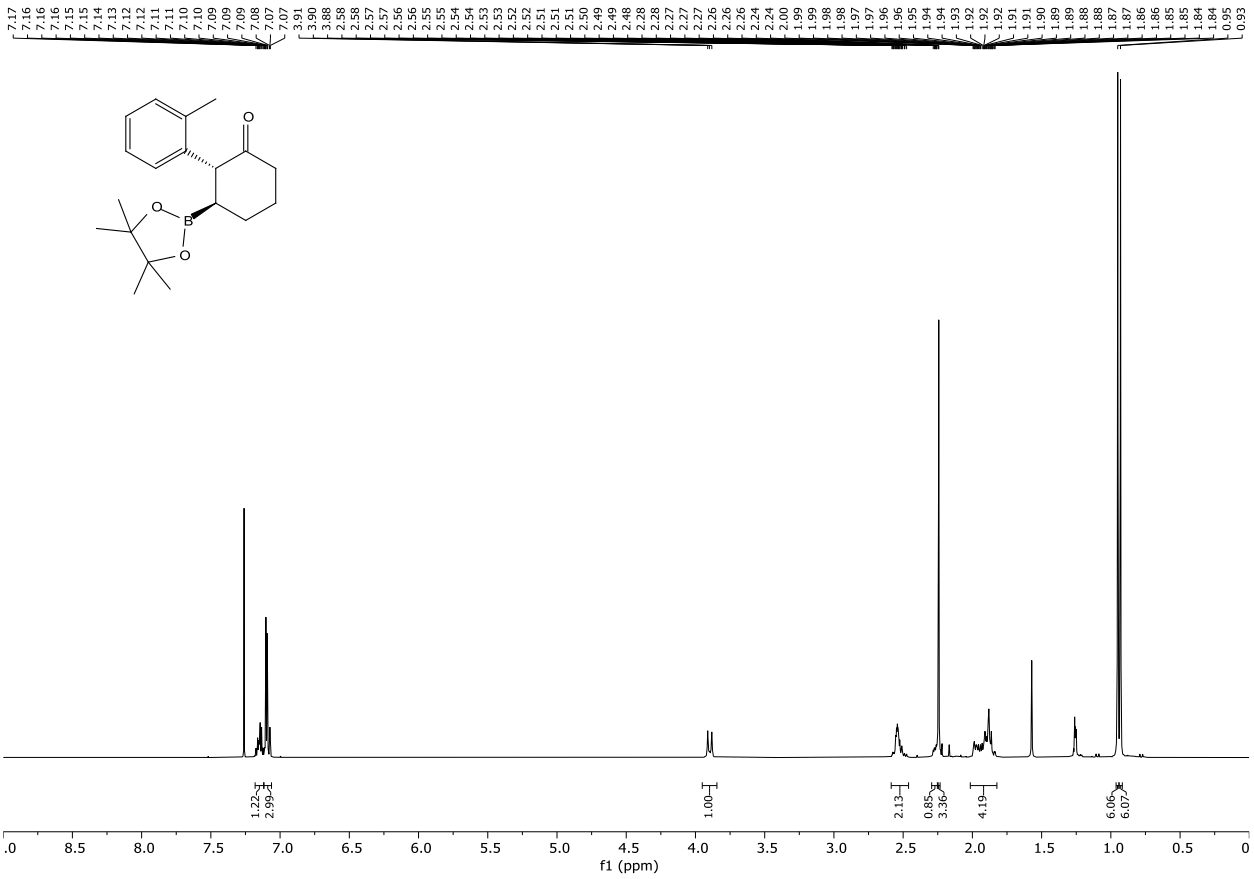

Compound **3n** ($CDCl_3$, 101 MHz, ^{13}C NMR)

(2*RS*,3*RS*)-3-(4,4,5,5-tetramethyl-1,3,2-dioxaborolan-2-yl)-2-(*o*-tolyl)cyclohexan-1-one

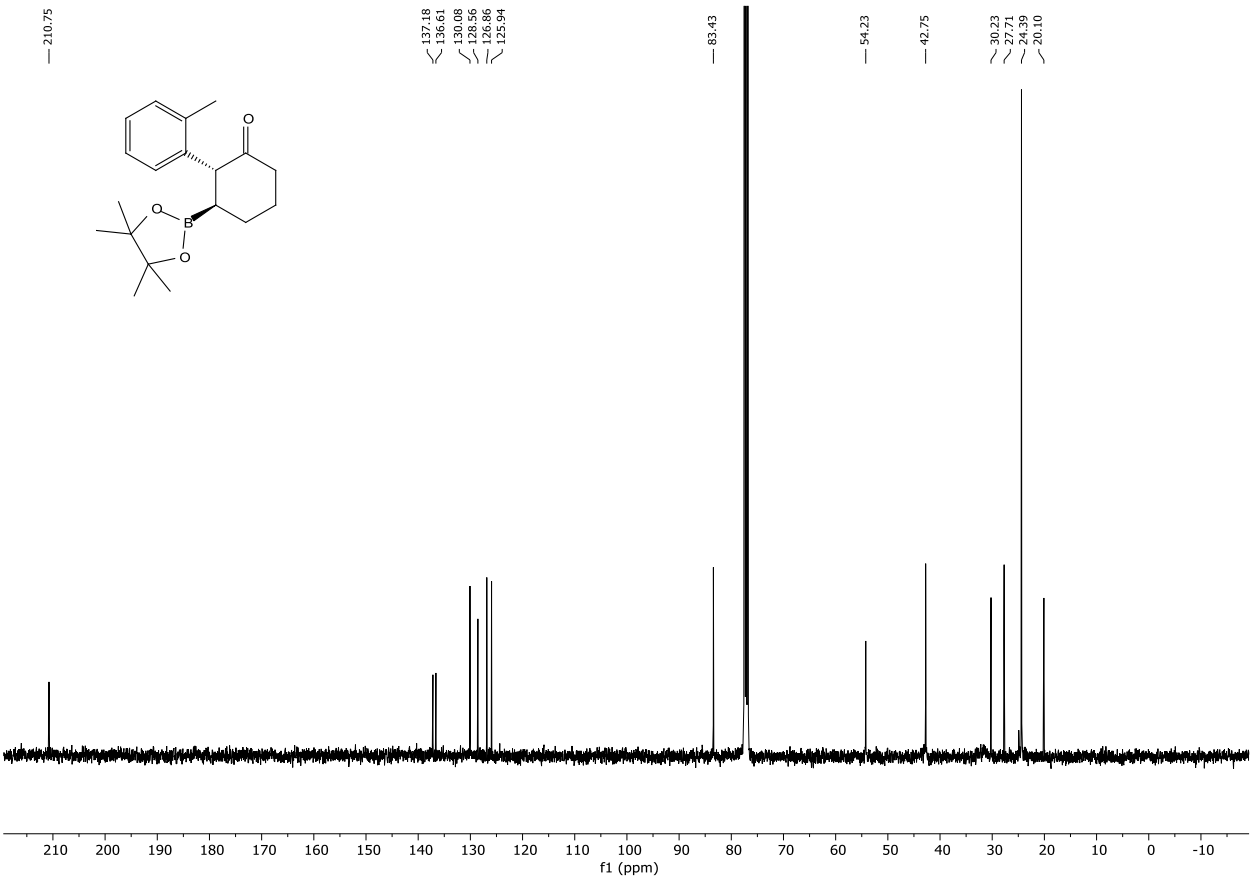

Compound **3o** ($CDCl_3$, 400 MHz, ^1H NMR)

(2*SR*,3*RS*)-2-allyl-3-(4,4,5,5-tetramethyl-1,3,2-dioxaborolan-2-yl)cyclohexan-1-one

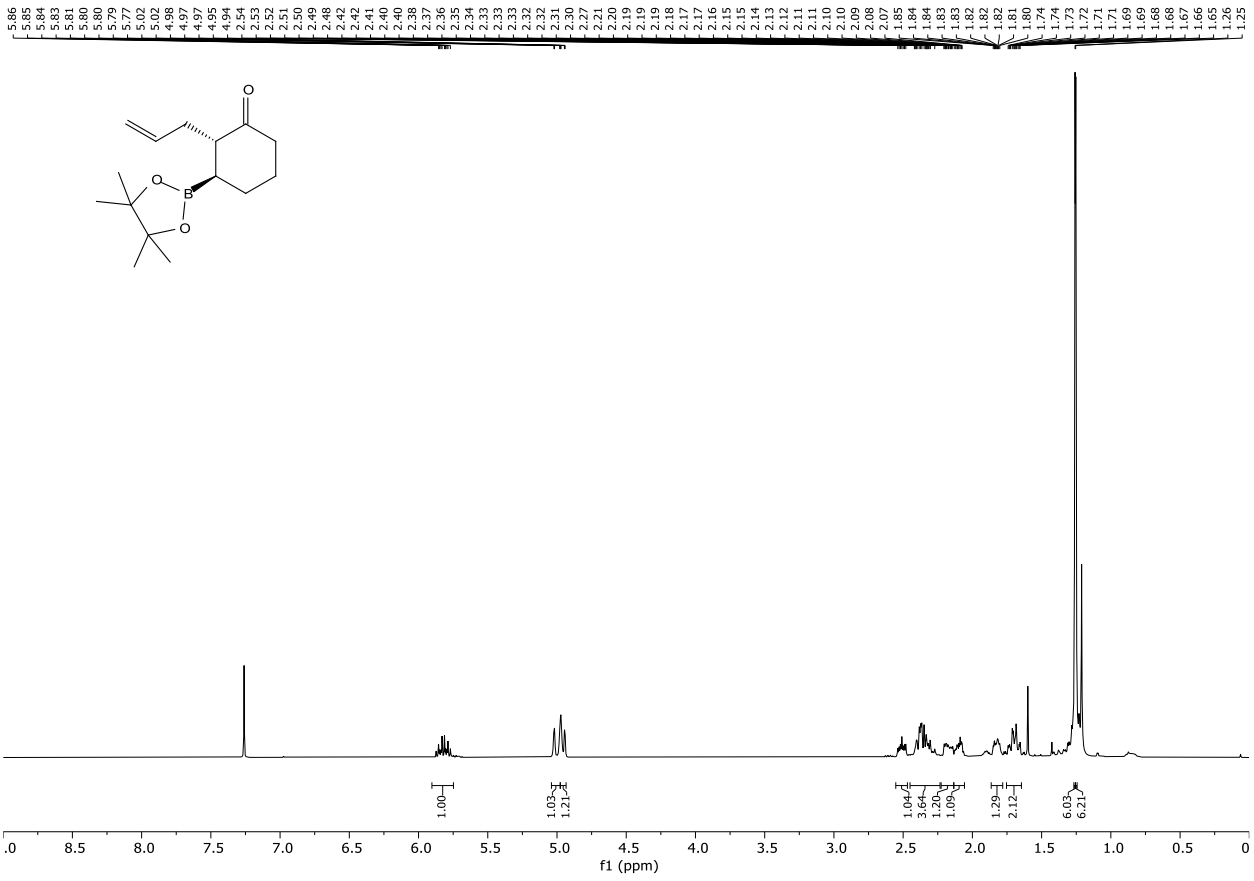

Compound **3o** ($CDCl_3$, 101 MHz, ^{13}C NMR)

(2*SR*,3*RS*)-2-allyl-3-(4,4,5,5-tetramethyl-1,3,2-dioxaborolan-2-yl)cyclohexan-1-one

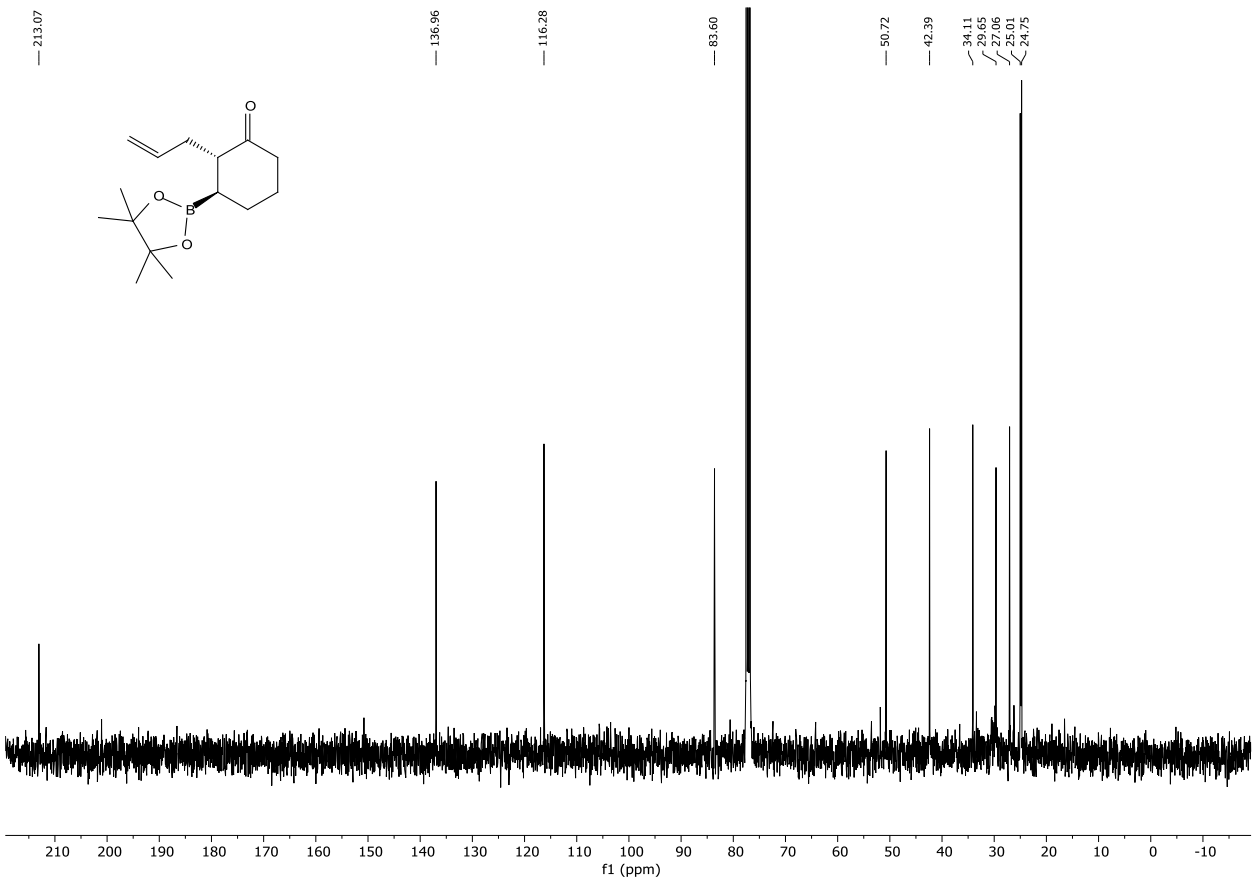

Compound **3p** ($CDCl_3$, 400 MHz, ^1H NMR)

(1*RS*,6*RS*)-6-(4,4,5,5-tetramethyl-1,3,2-dioxaborolan-2-yl)-[1,1'-bi(cyclohexan)]-1'-en-2-one

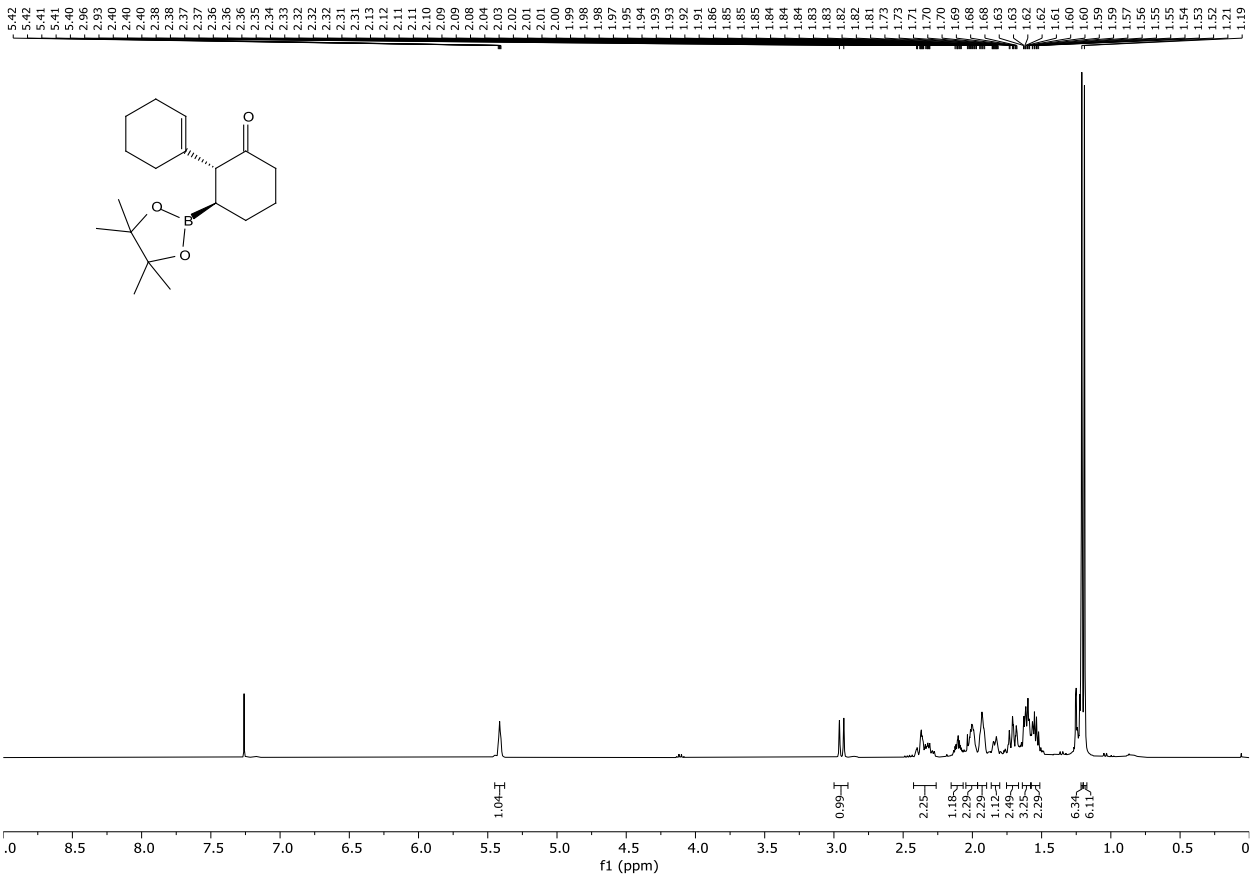

Compound **3p** ($CDCl_3$, 101 MHz, ^{13}C NMR)

(1*RS*,6*RS*)-6-(4,4,5,5-tetramethyl-1,3,2-dioxaborolan-2-yl)-[1,1'-bi(cyclohexan)]-1'-en-2-one

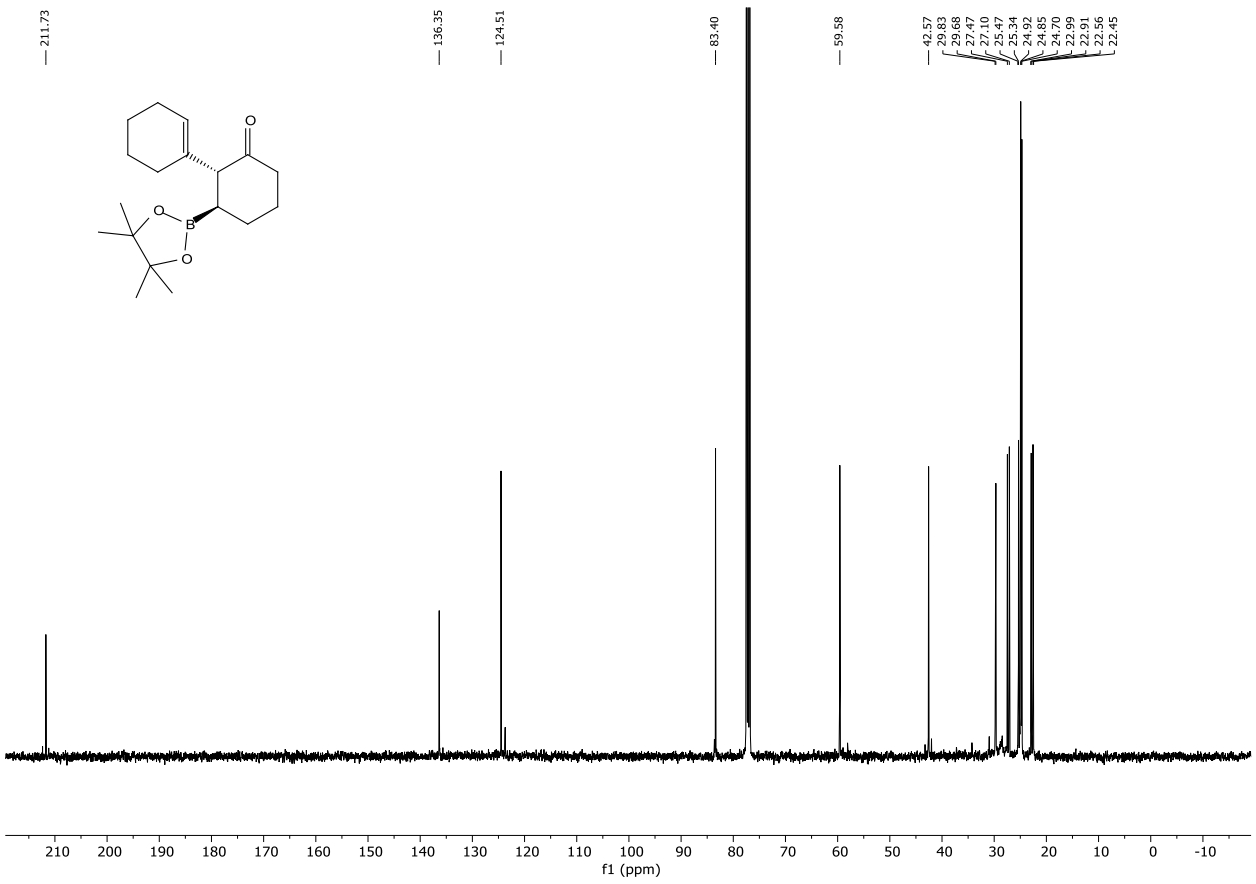

Compound **3q** ($CDCl_3$, 400 MHz, ^1H NMR)

(2*RS*,3*RS*)-2-(cyclopent-1-en-1-yl)-3-(4,4,5,5-tetramethyl-1,3,2-dioxaborolan-2-yl)cyclohexan-1-one

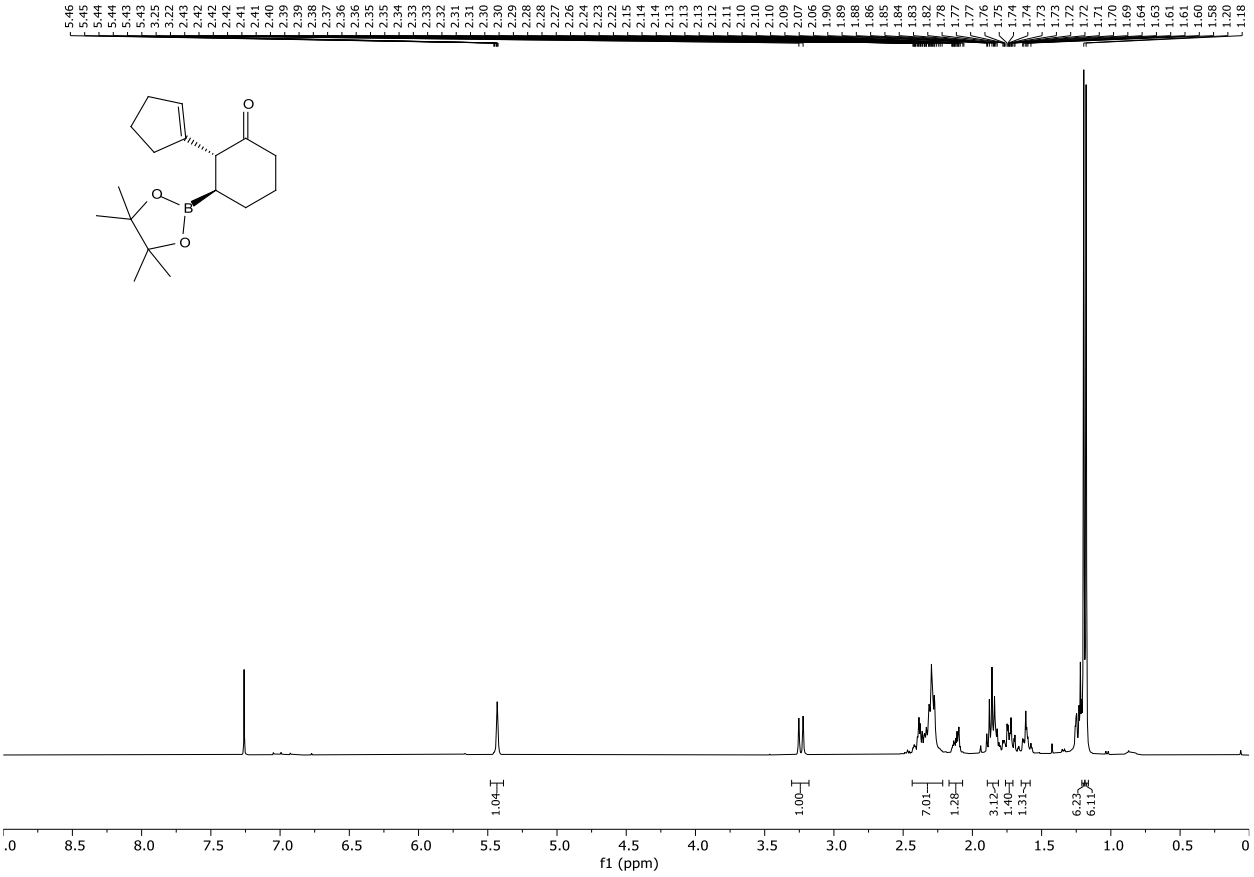

Compound **3q** ($CDCl_3$, 101 MHz, ^{13}C NMR)

(2*RS*,3*RS*)-2-(cyclopent-1-en-1-yl)-3-(4,4,5,5-tetramethyl-1,3,2-dioxaborolan-2-yl)cyclohexan-1-one

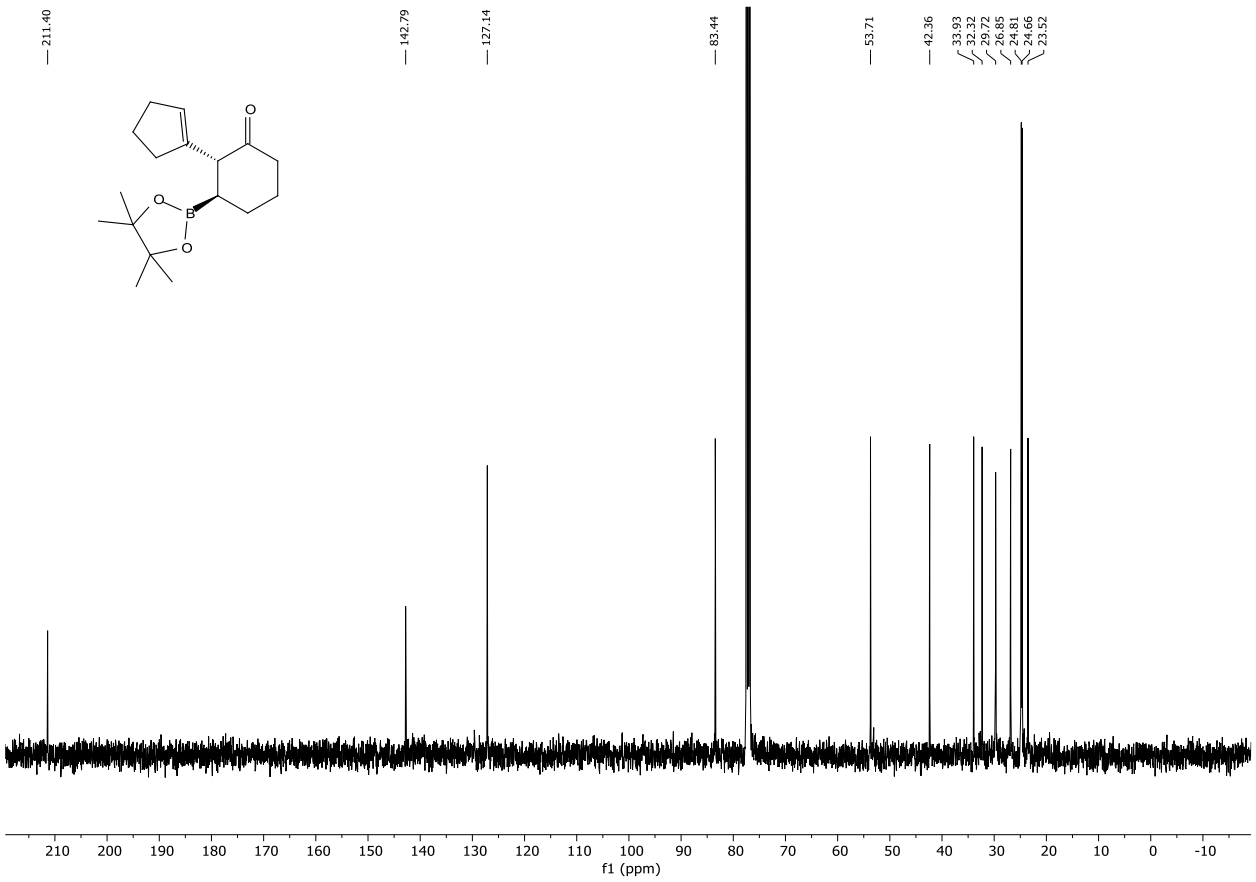

Compound **3s** ($CDCl_3$, 400 MHz, ^1H NMR)

(2*RS*,3*RS*)-3-(4,4,5,5-tetramethyl-1,3,2-dioxaborolan-2-yl)-2-(4-vinylphenyl)cyclohexan-1-one

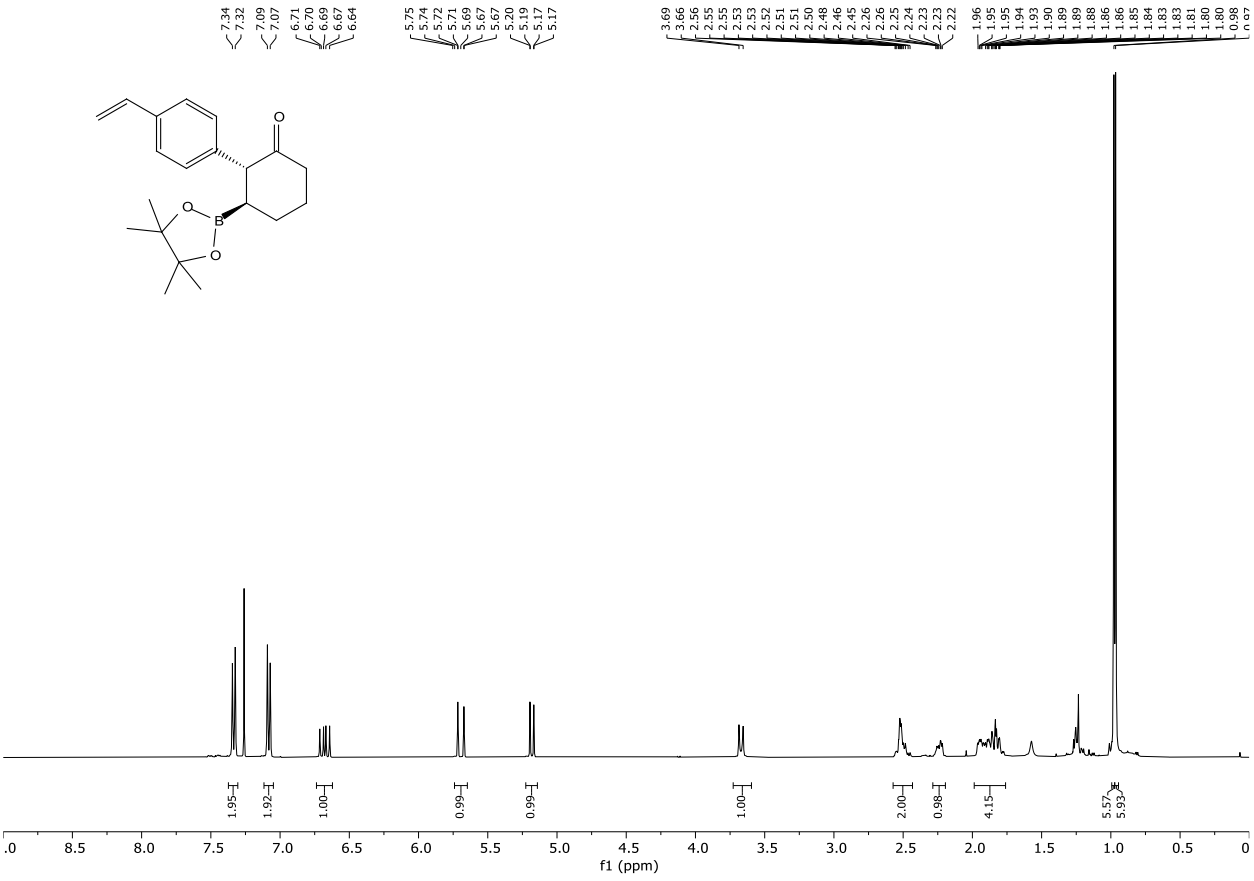

Compound **3s** ($CDCl_3$, 101 MHz, ^{13}C NMR)

(2*RS*,3*RS*)-3-(4,4,5,5-tetramethyl-1,3,2-dioxaborolan-2-yl)-2-(4-vinylphenyl)cyclohexan-1-one

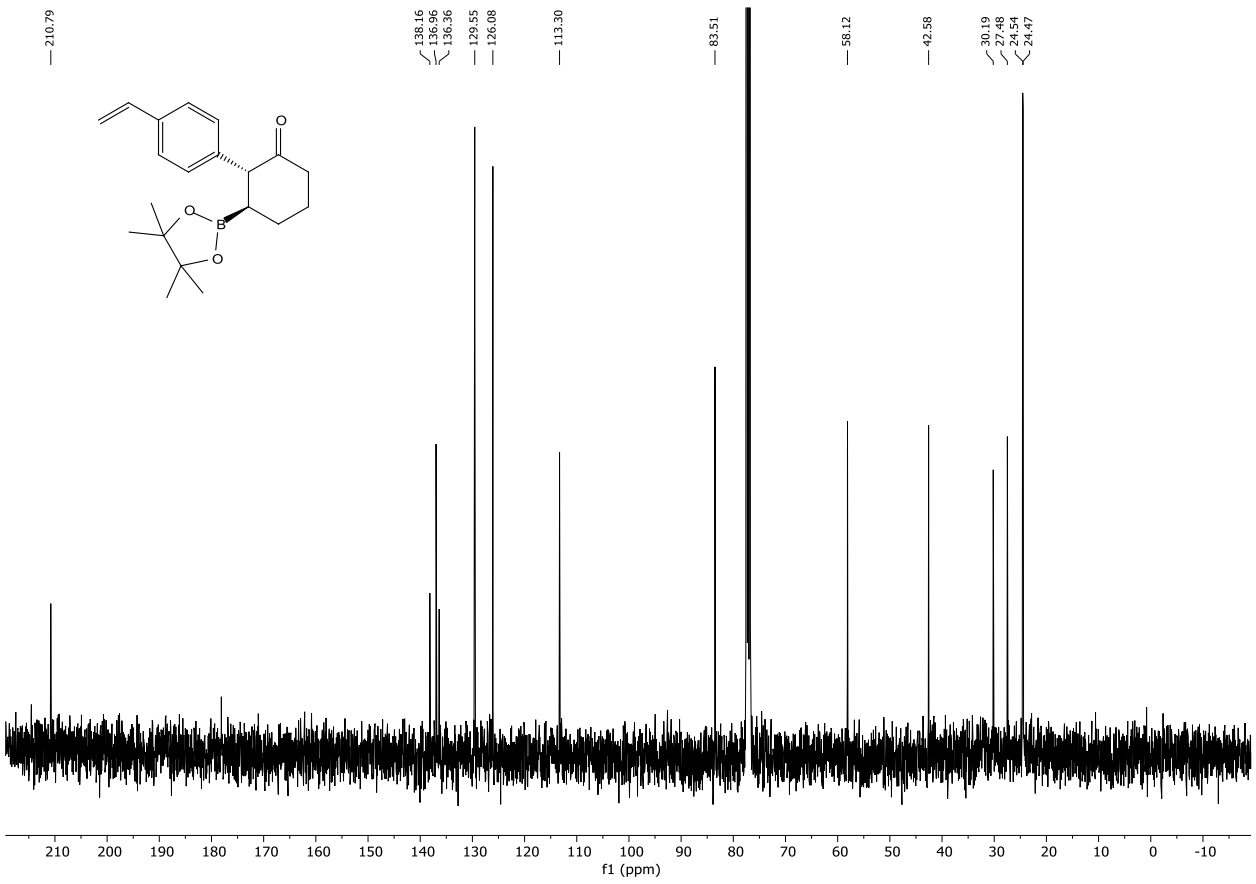

Compound **3t** ($CDCl_3$, 600 MHz, ^1H NMR)

(2*RS*,3*RS*)-2-(6-methoxypyridin-3-yl)-3-(4,4,5,5-tetramethyl-1,3,2-dioxaborolan-2-yl)cyclohexan-1-one

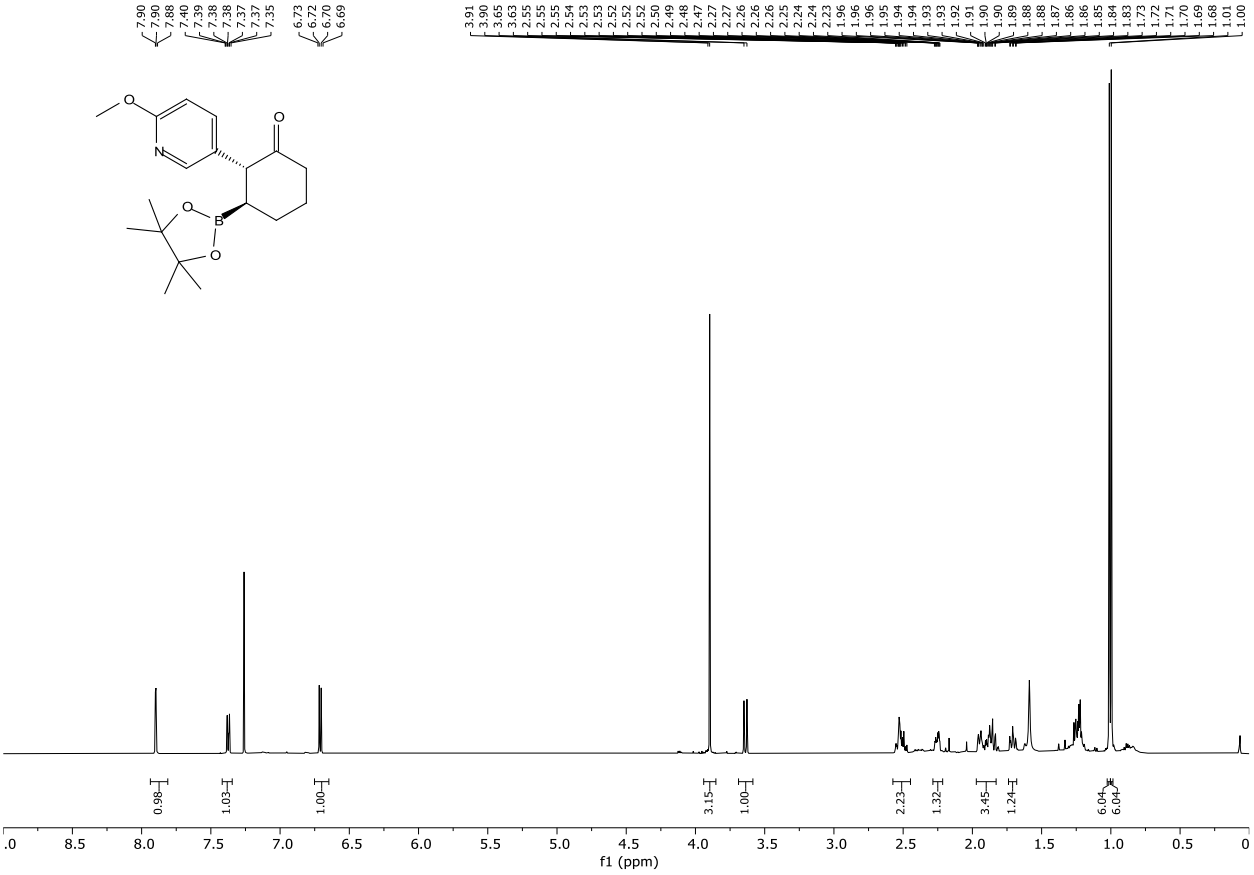

Compound **3t** ($CDCl_3$, 151 MHz, ^{13}C NMR)

(2*RS*,3*RS*)-2-(6-methoxypyridin-3-yl)-3-(4,4,5,5-tetramethyl-1,3,2-dioxaborolan-2-yl)cyclohexan-1-one

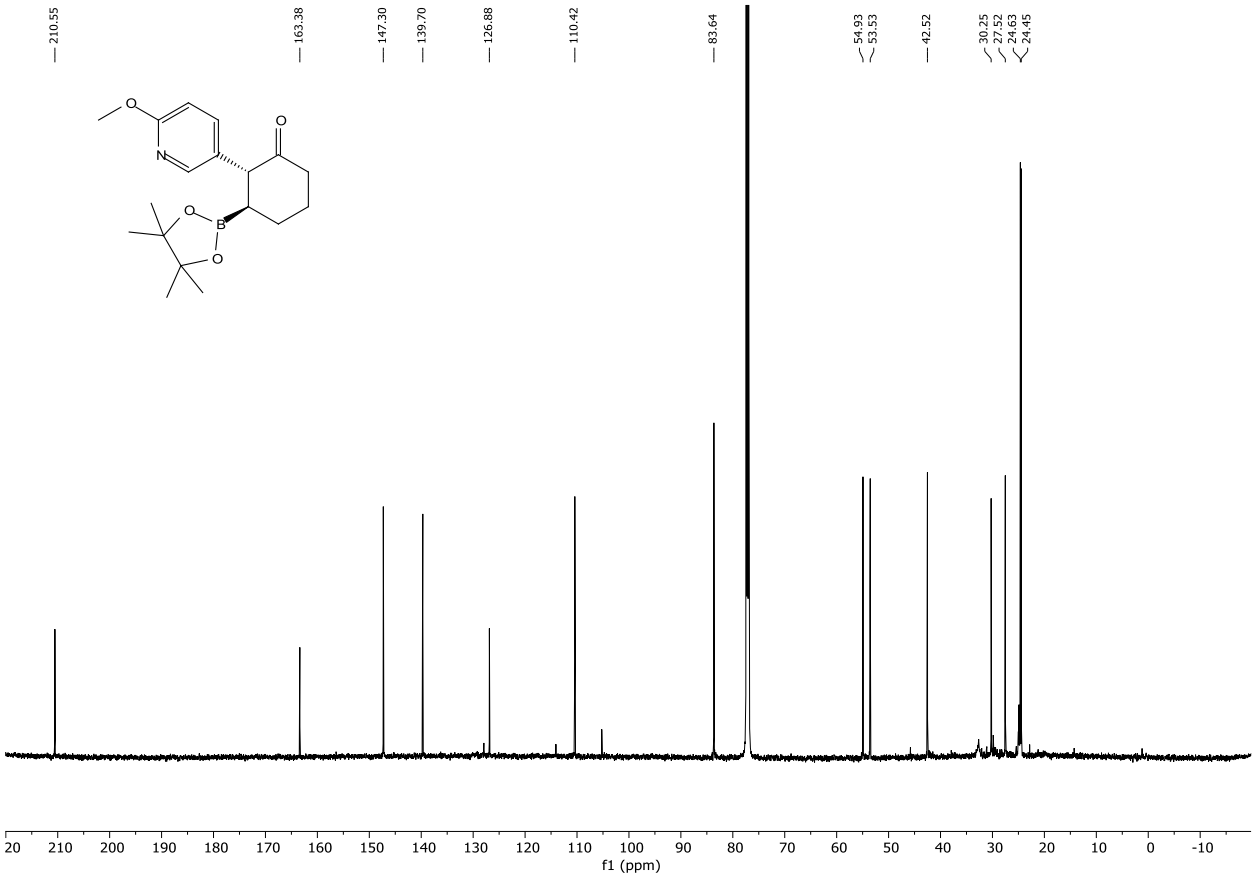

Compound **3u** ($CDCl_3$, 500 MHz, ^1H NMR)

(2*RS*,3*RS*)-2-(benzofuran-7-yl)-3-(4,4,5,5-tetramethyl-1,3,2-dioxaborolan-2-yl)cyclohexan-1-one

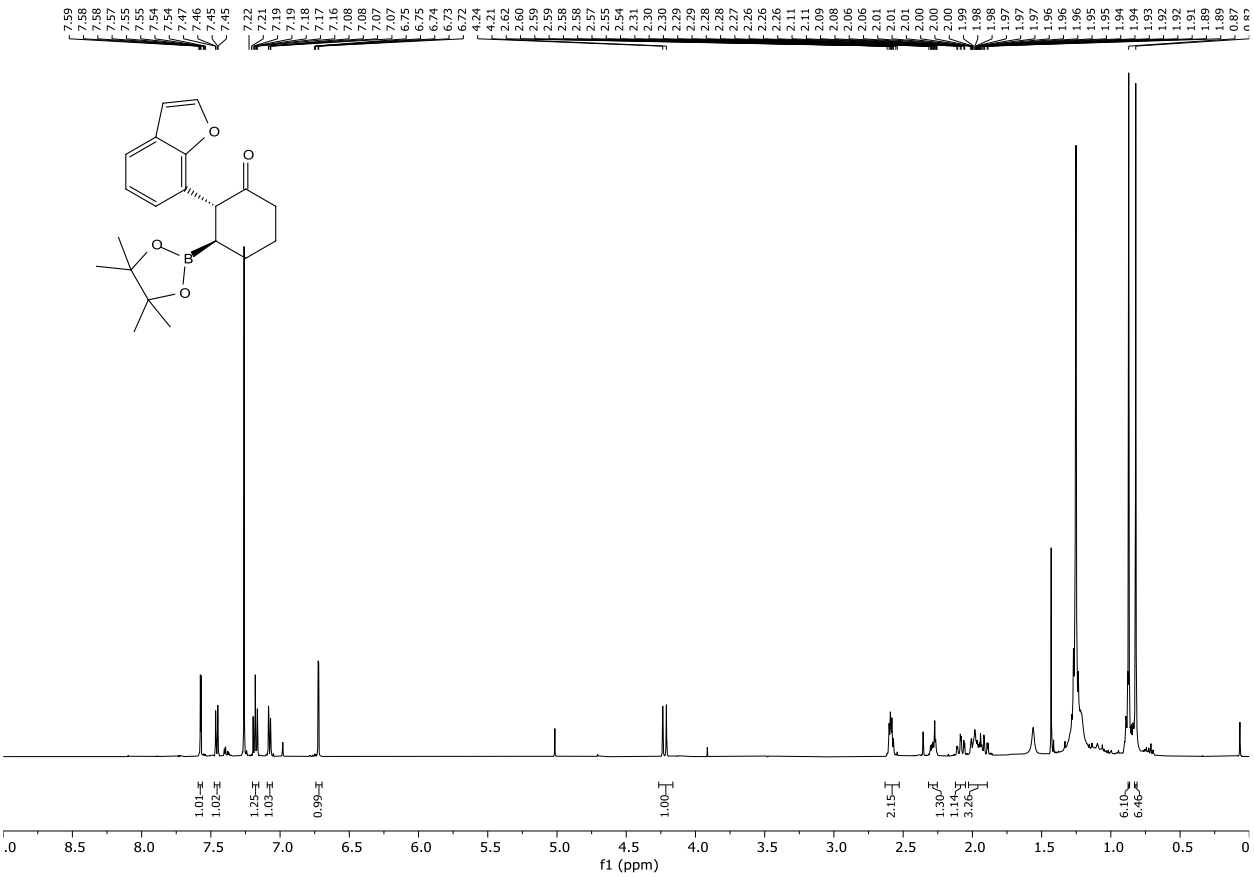

Compound **3u** ($CDCl_3$, 126 MHz, ^{13}C NMR)

(2*RS*,3*RS*)-2-(benzofuran-7-yl)-3-(4,4,5,5-tetramethyl-1,3,2-dioxaborolan-2-yl)cyclohexan-1-one

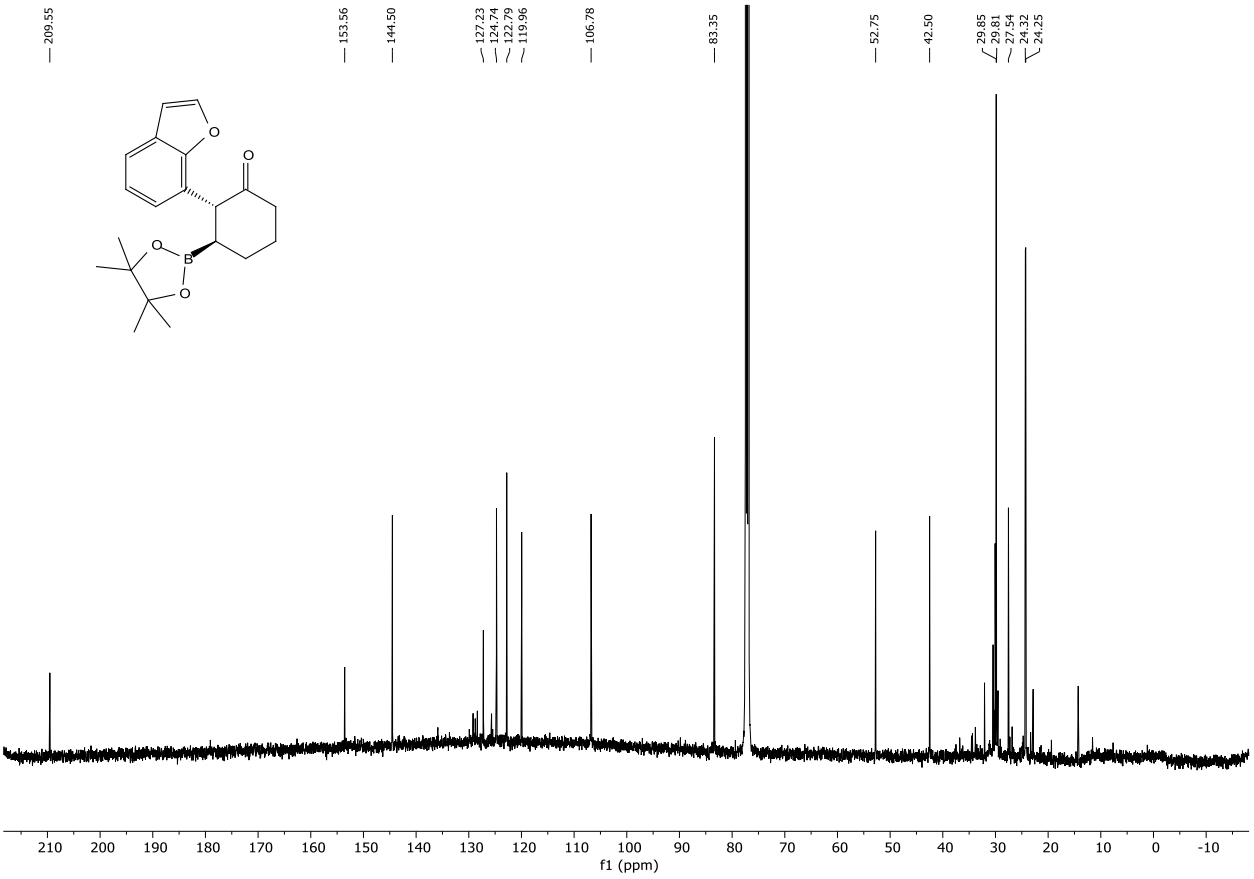

Compound **3v** ($CDCl_3$, 400 MHz, ^1H NMR)

(2*RS*,3*RS*)-2-(1-methyl-1H-indol-5-yl)-3-(4,4,5,5-tetramethyl-1,3,2-dioxaborolan-2-yl)cyclohexan-1-one

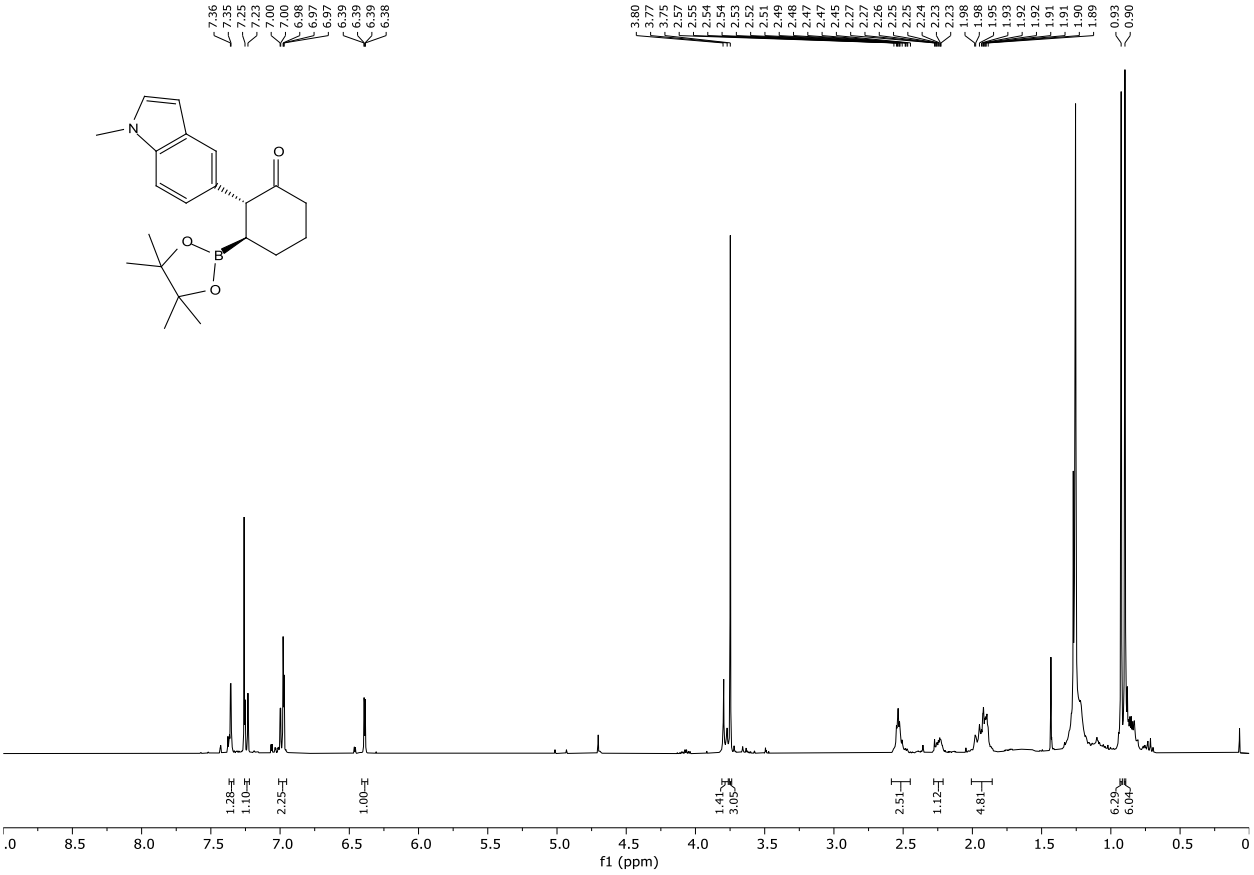

Compound **3v** ($CDCl_3$, 101 MHz, ^{13}C NMR)

(2*RS*,3*RS*)-2-(1-methyl-1H-indol-5-yl)-3-(4,4,5,5-tetramethyl-1,3,2-dioxaborolan-2-yl)cyclohexan-1-one

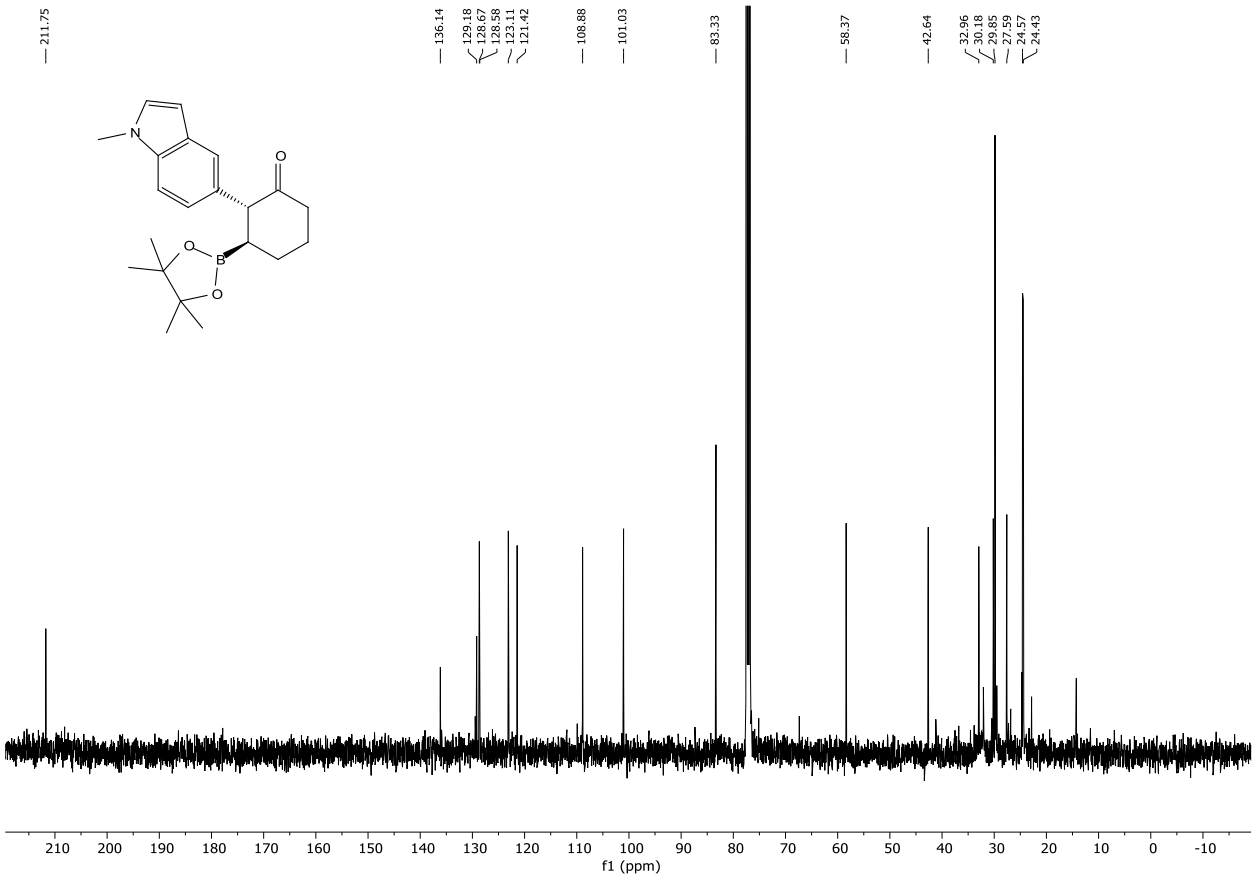

Compound **3w (**$CDCl_3$, 400 MHz, ^1H NMR)

(2*RS*,3*RS*)-2-(4-(dimethylamino)phenyl)-3-(4,4,5,5-tetramethyl-1,3,2-dioxaborolan-2-yl)cyclohexan-1-one

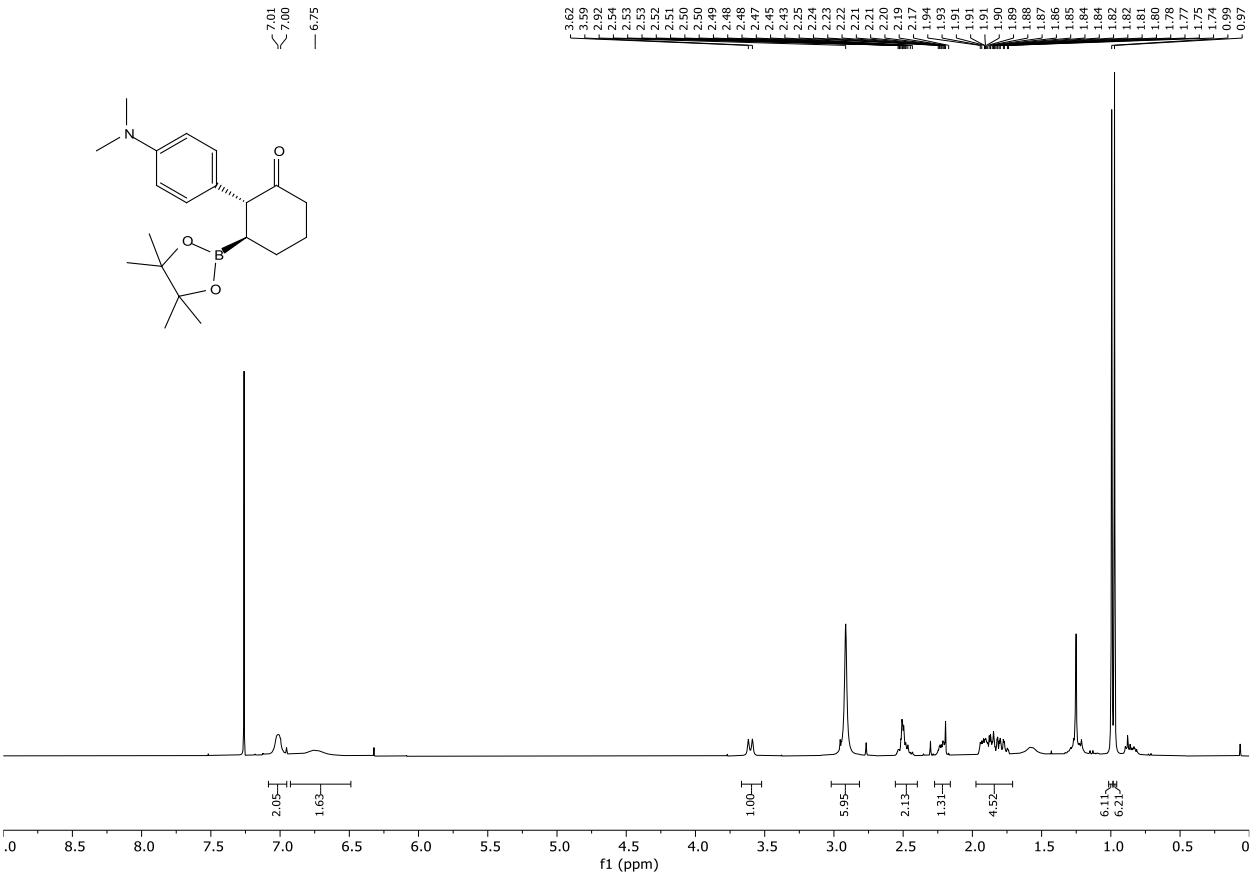

Compound **3w** ($CDCl_3$, 126 MHz, ^{13}C NMR)

(2*RS*,3*RS*)-2-(4-(dimethylamino)phenyl)-3-(4,4,5,5-tetramethyl-1,3,2-dioxaborolan-2-yl)cyclohexan-1-one

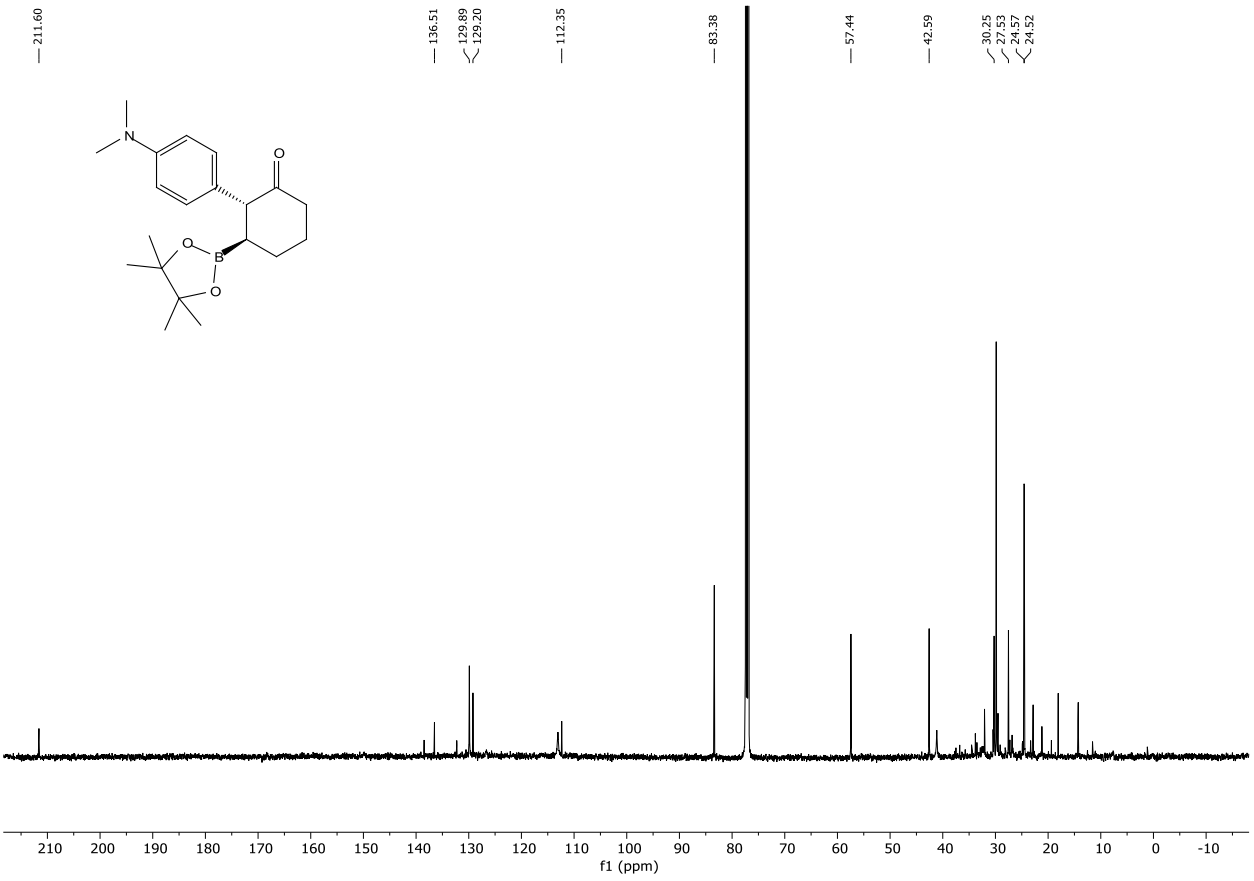

Compound **3ab** ($CDCl_3$, 600 MHz, ^1H NMR)

(2*RS*,3*RS*)-2-phenyl-3-(4,4,5,5-tetramethyl-1,3,2-dioxaborolan-2-yl)cycloheptan-1-one

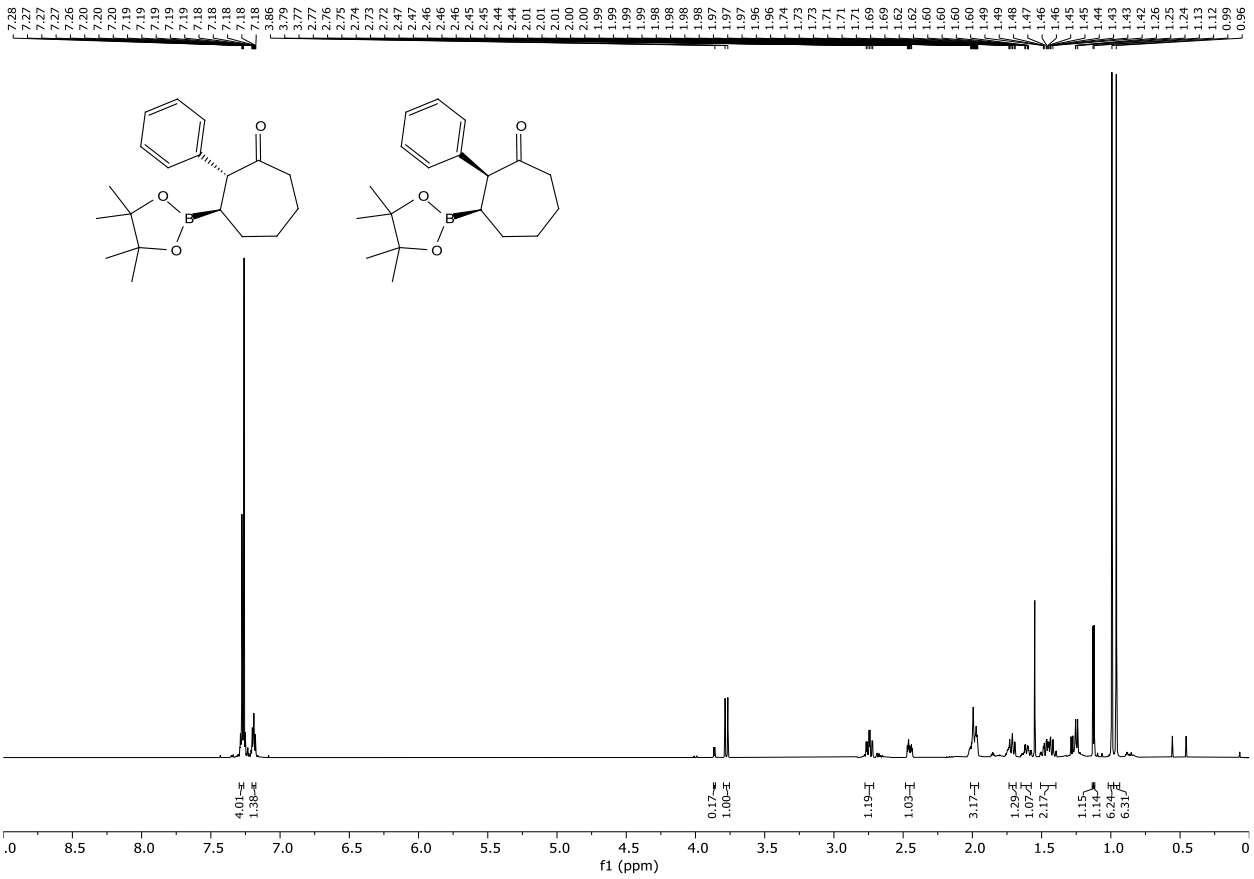

Compound **3ab** ($CDCl_3$, 151 MHz, ^{13}C NMR)

(2*RS*,3*RS*)-2-phenyl-3-(4,4,5,5-tetramethyl-1,3,2-dioxaborolan-2-yl)cycloheptan-1-one

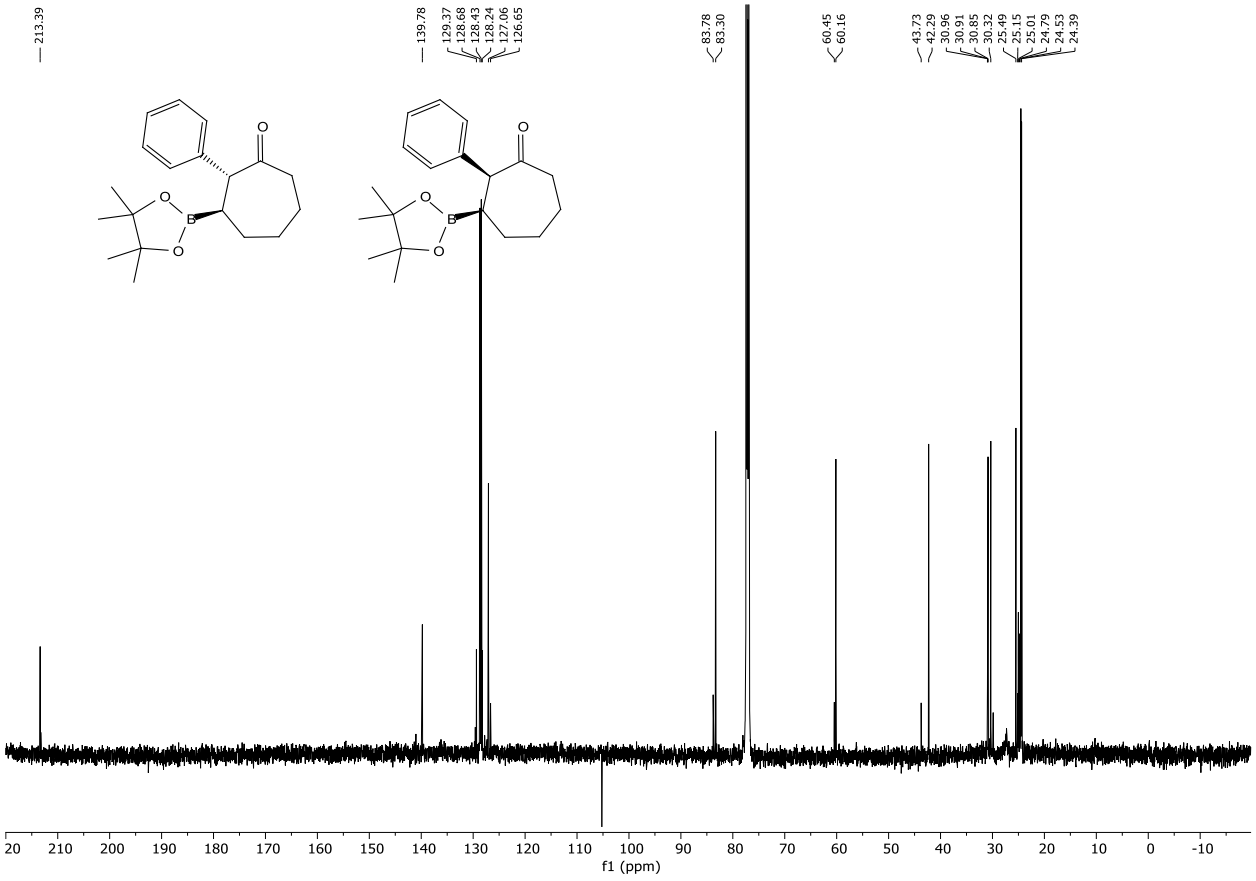

Compound **3ac** ($CDCl_3$, 400 MHz, ^1H NMR)

(2*RS*,3*RS*)-2-phenyl-3-(4,4,5,5-tetramethyl-1,3,2-dioxaborolan-2-yl)cyclopentan-1-one

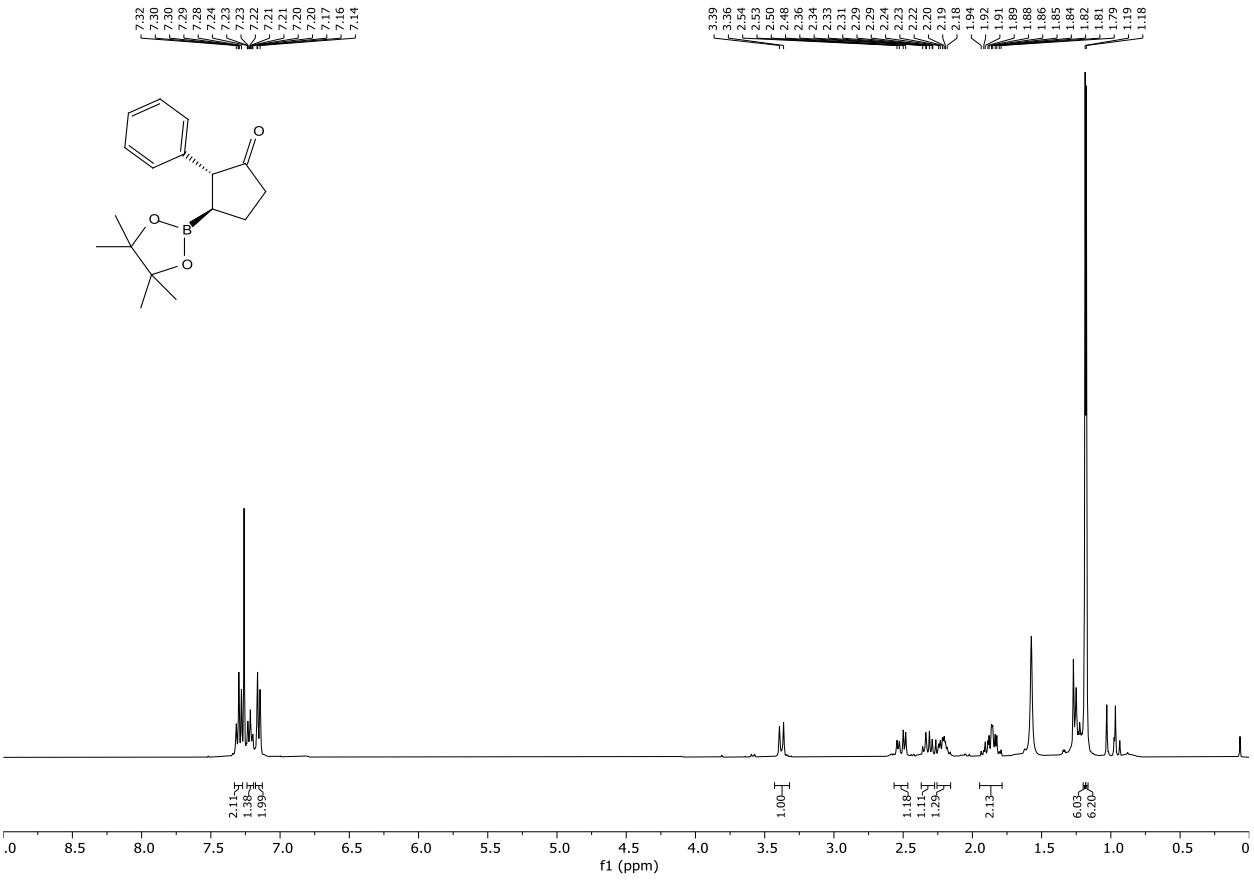

Compound **3ac** ($CDCl_3$, 101 MHz, ^{13}C NMR)

(2*RS*,3*RS*)-2-phenyl-3-(4,4,5,5-tetramethyl-1,3,2-dioxaborolan-2-yl)cyclopentan-1-one

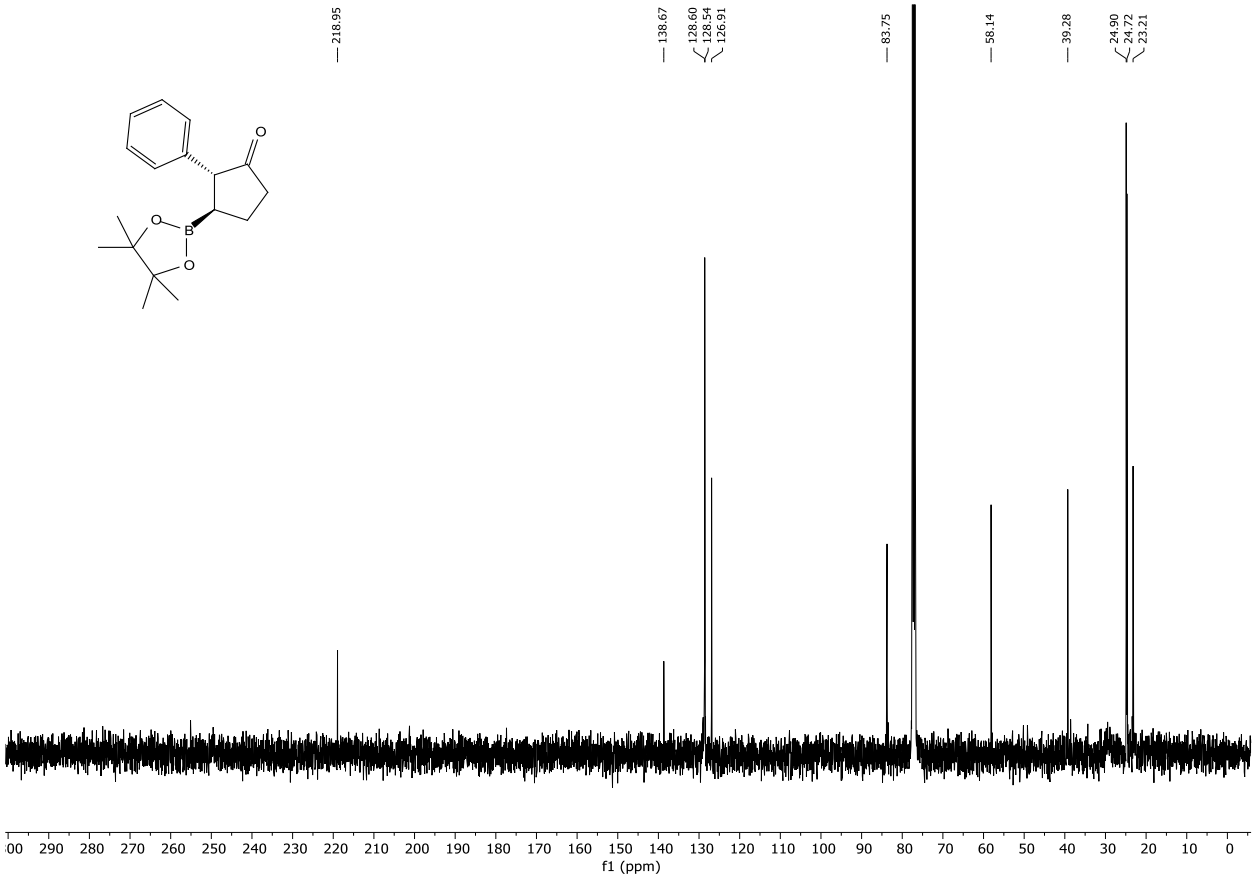

Compound **3ad** ($CDCl_3$, 400 MHz, ^1H NMR)

(2*RS*,3*SR*)-4,4-dimethyl-2-phenyl-3-(4,4,5,5-tetramethyl-1,3,2-dioxaborolan-2-yl)cyclohexan-1-one

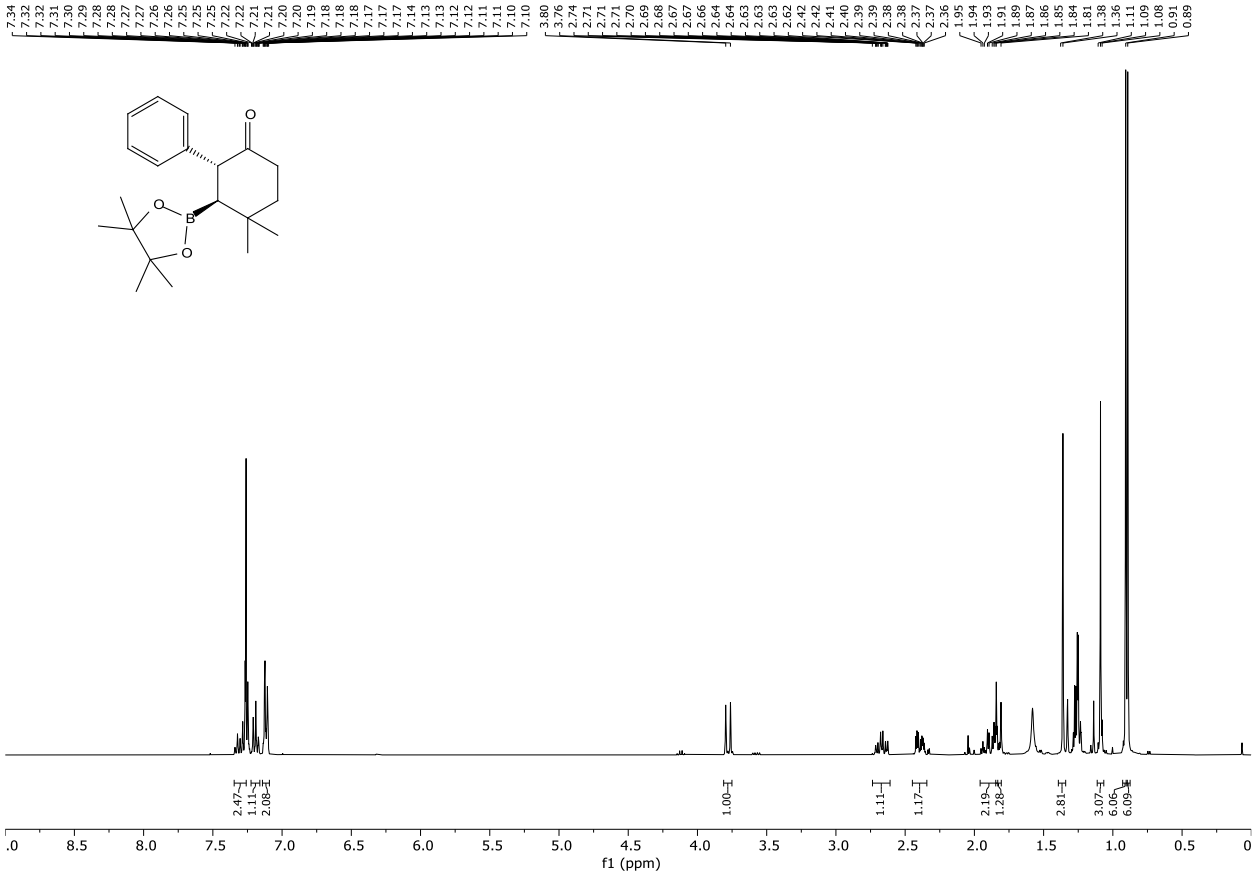

Compound **3ad** ($CDCl_3$, 101 MHz, ^{13}C NMR)

(2*RS*,3*SR*)-4,4-dimethyl-2-phenyl-3-(4,4,5,5-tetramethyl-1,3,2-dioxaborolan-2-yl)cyclohexan-1-one

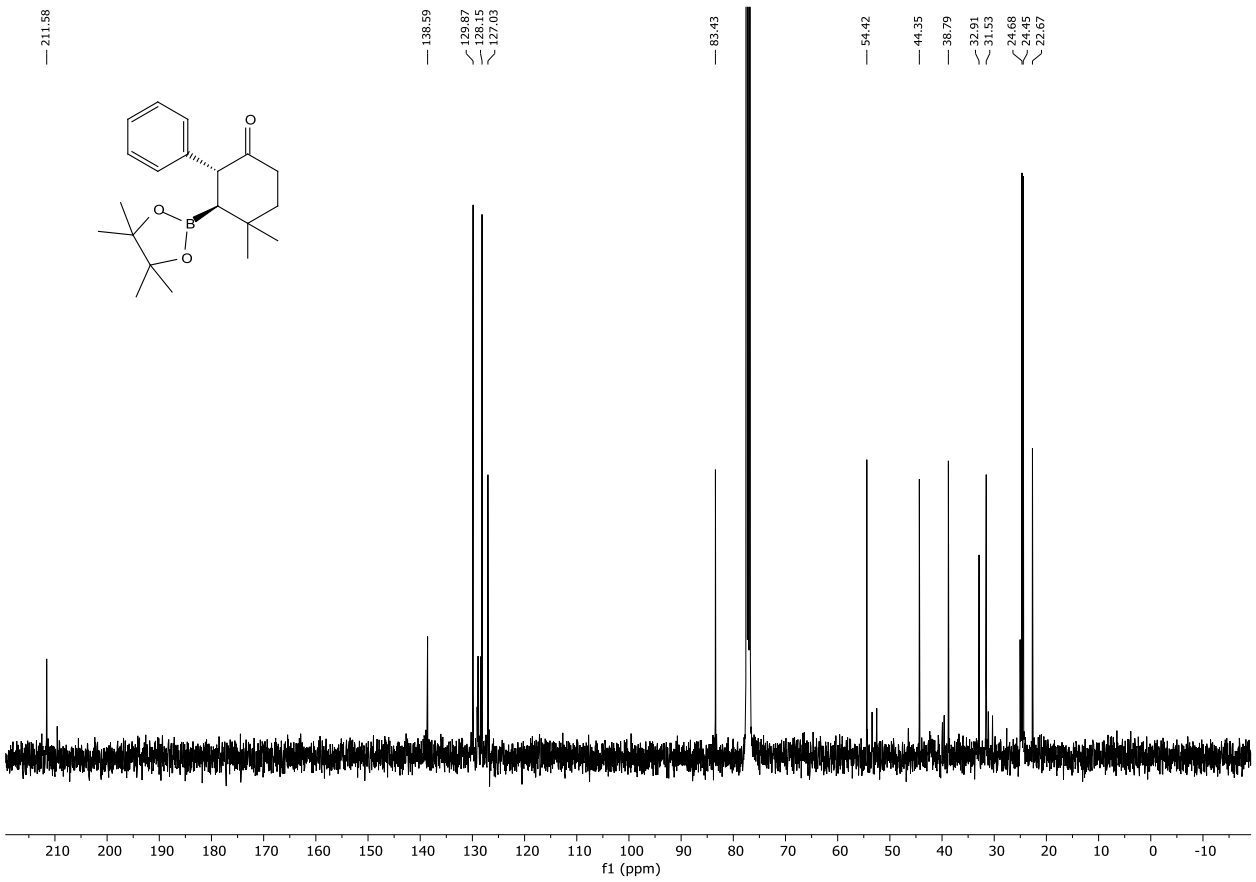

Compound **3ae** ($CDCl_3$, 600 MHz, ^1H NMR)

(2*RS*,3*RS*,4*SR*)-4-methyl-2-phenyl-3-(4,4,5,5-tetramethyl-1,3,2-dioxaborolan-2-yl)cyclohexan-1-one

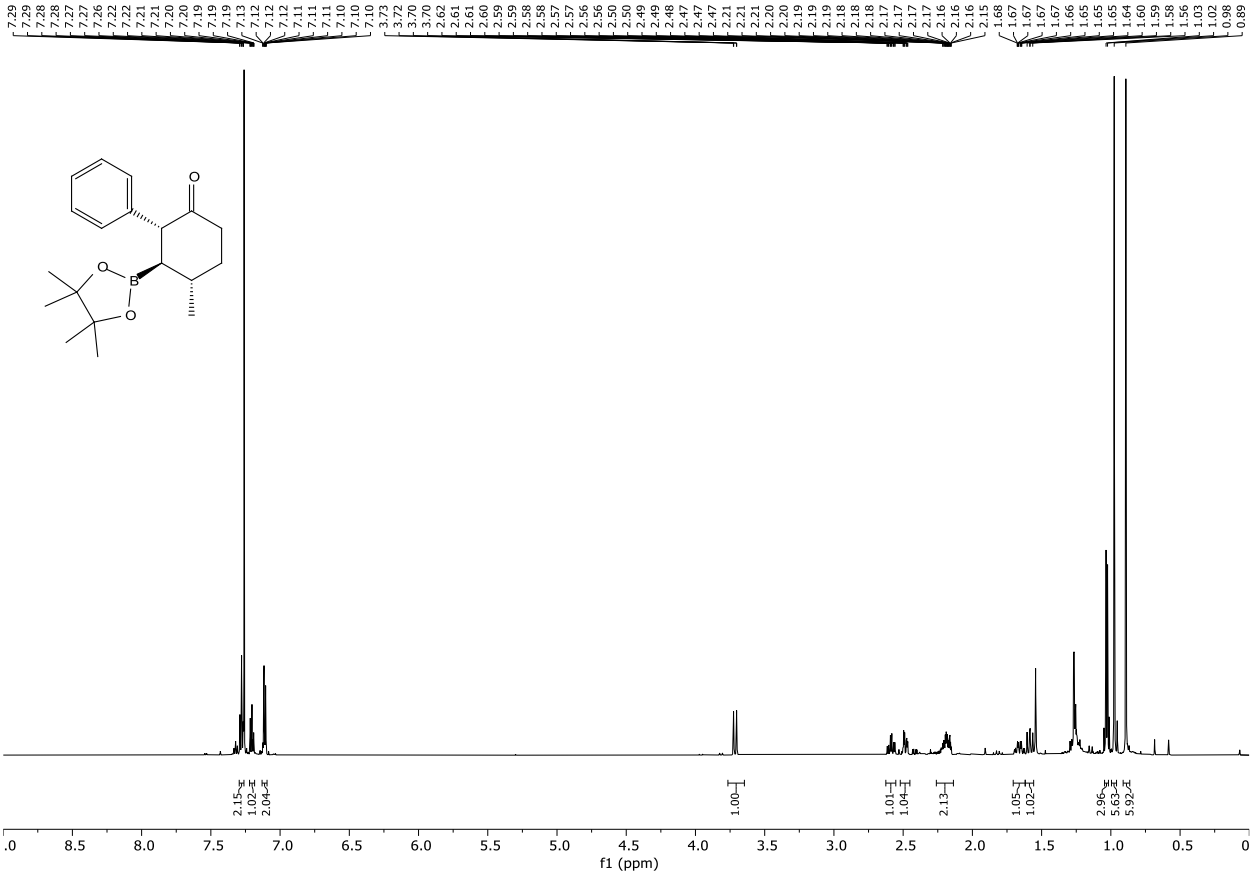

Compound **3ae** ($CDCl_3$, 151 MHz, ^{13}C NMR)

(2*RS*,3*RS*,4*SR*)-4-methyl-2-phenyl-3-(4,4,5,5-tetramethyl-1,3,2-dioxaborolan-2-yl)cyclohexan-1-one

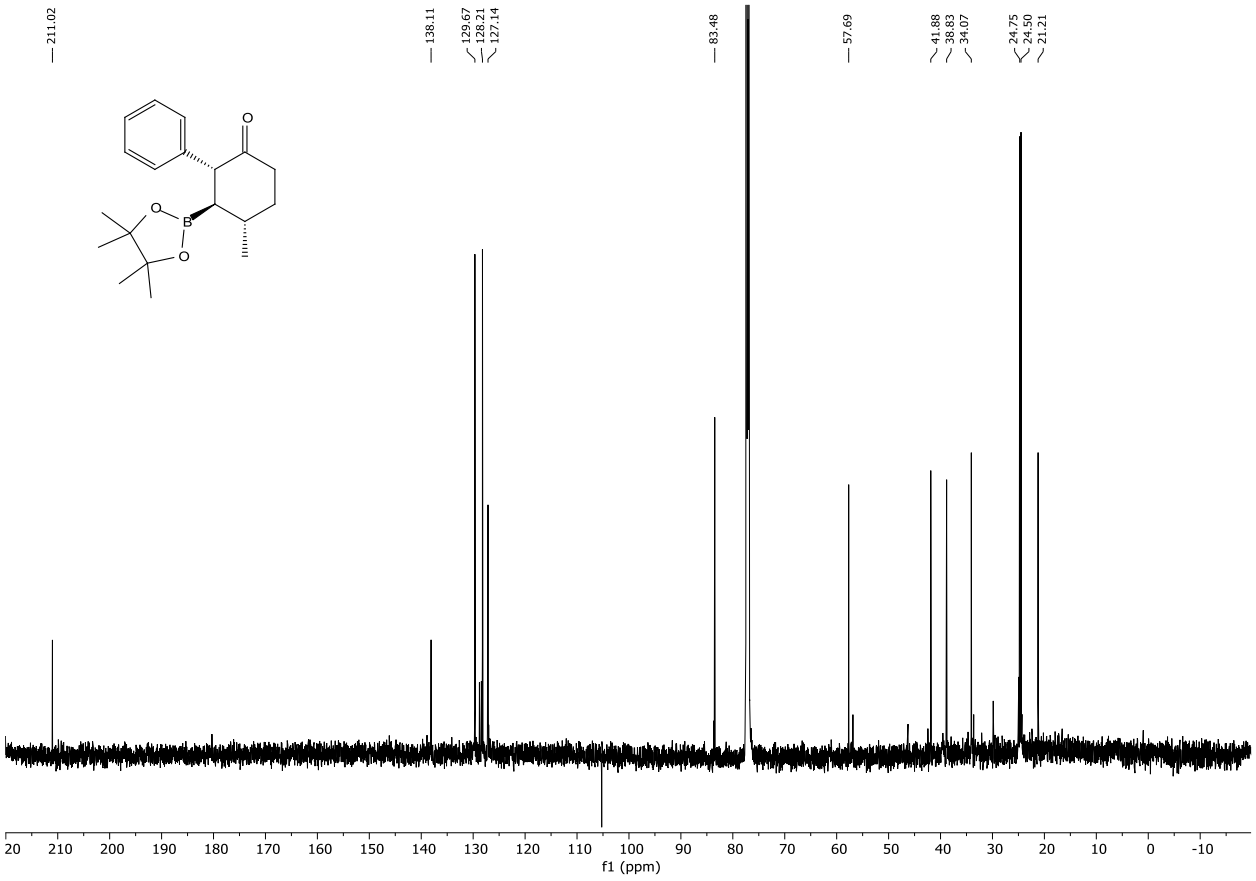

Compound **3af** ($CDCl_3$, 400 MHz, ^1H NMR)

(2*RS*,3*SR*,4*SR*)-4-methyl-2,4-diphenyl-3-(4,4,5,5-tetramethyl-1,3,2-dioxaborolan-2-yl)cyclohexan-1-one

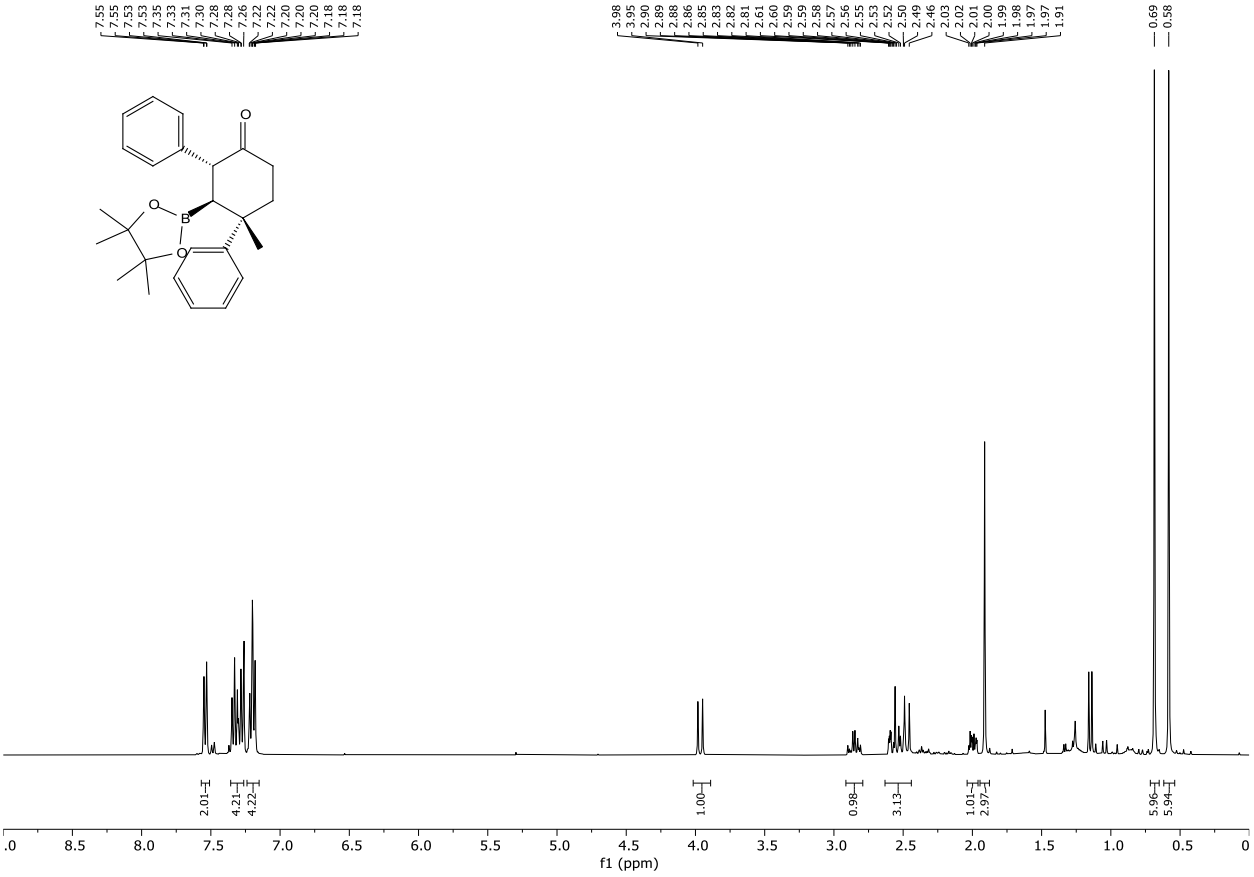

Compound **3af** ($CDCl_3$, 101 MHz, ^{13}C NMR)

(2*RS*,3*SR*,4*SR*)-4-methyl-2,4-diphenyl-3-(4,4,5,5-tetramethyl-1,3,2-dioxaborolan-2-yl)cyclohexan-1-one

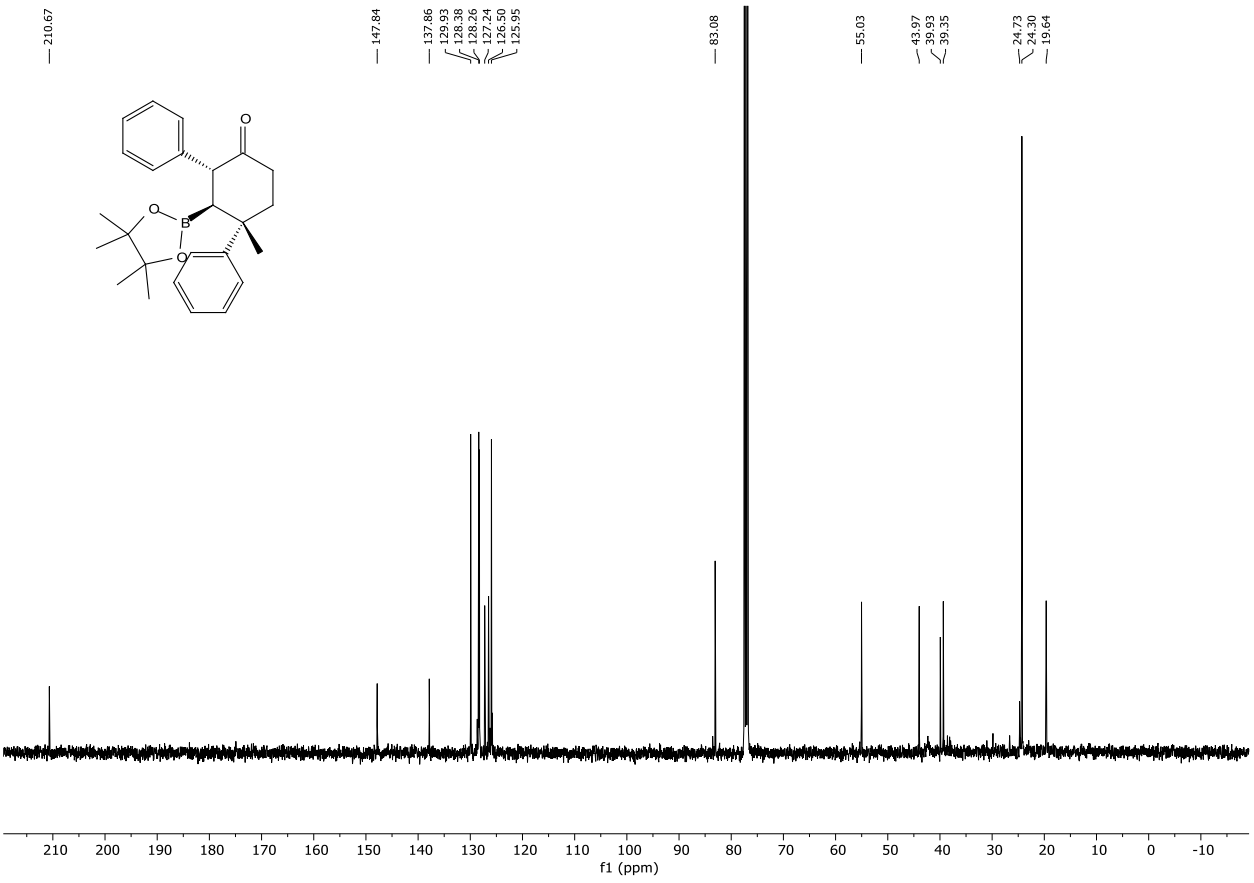

Compound **3ag** ($CDCl_3$, 400 MHz, ^1H NMR)

(2*RS*,3*RS*,5*RS*)-5-methyl-2-phenyl-3-(4,4,5,5-tetramethyl-1,3,2-dioxaborolan-2-yl)cyclohexan-1-one

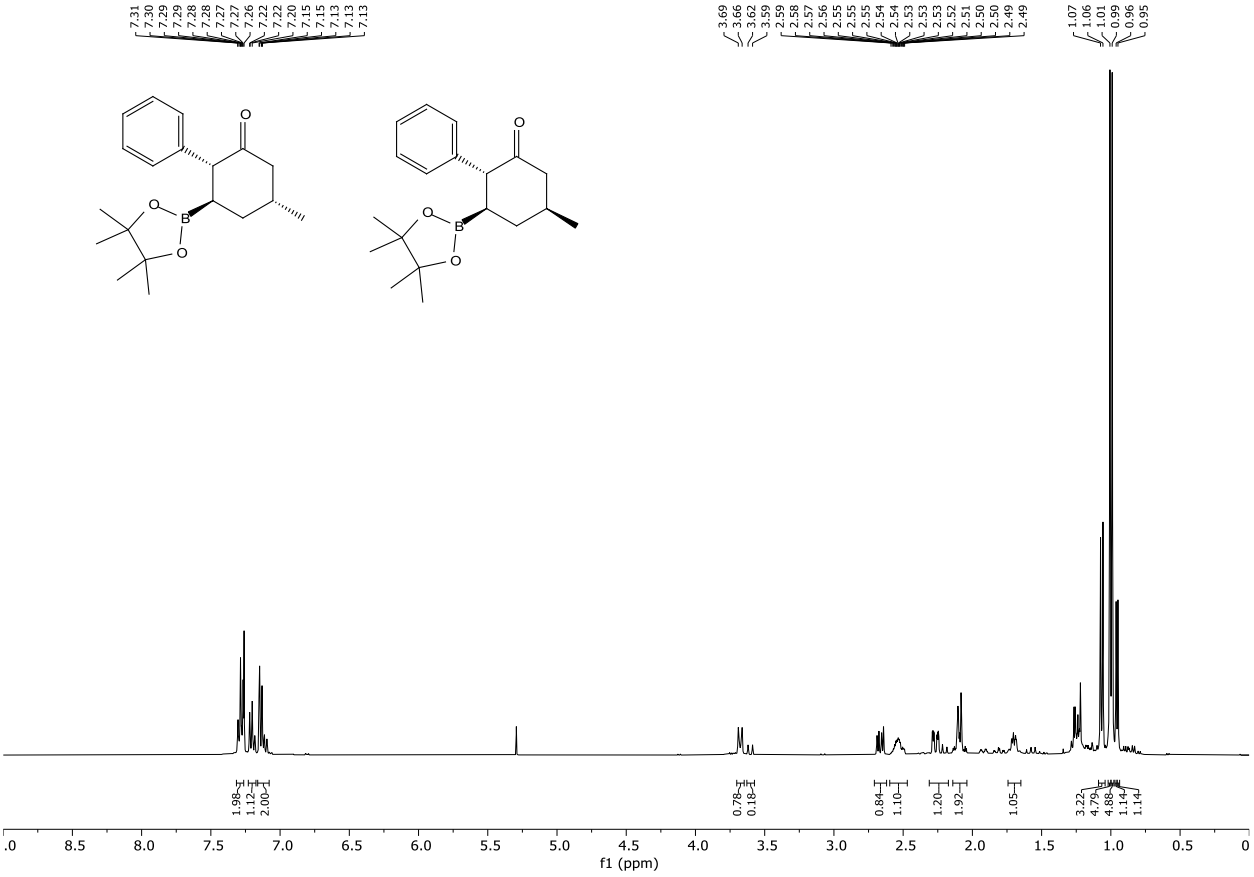

Compound **3ag** ($CDCl_3$, 101 MHz, ^{13}C NMR)

(2*RS*,3*RS*,5*RS*)-5-methyl-2-phenyl-3-(4,4,5,5-tetramethyl-1,3,2-dioxaborolan-2-yl)cyclohexan-1-one

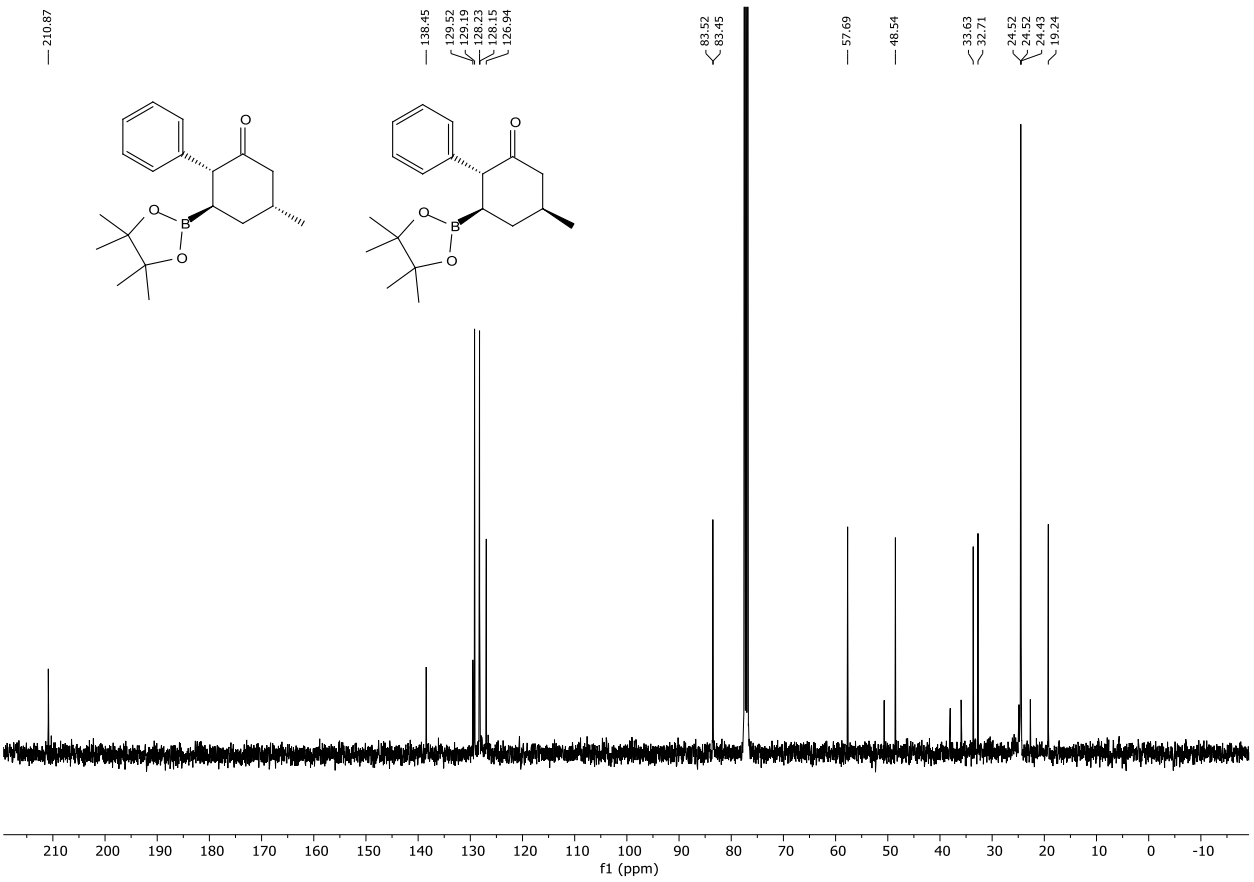

Compound **5** ($CDCl_3$, 600 MHz, ^1H NMR)

(2*SR*,3*RS*)-3-hydroxy-2-(4-methoxyphenyl)cyclohexan-1-one

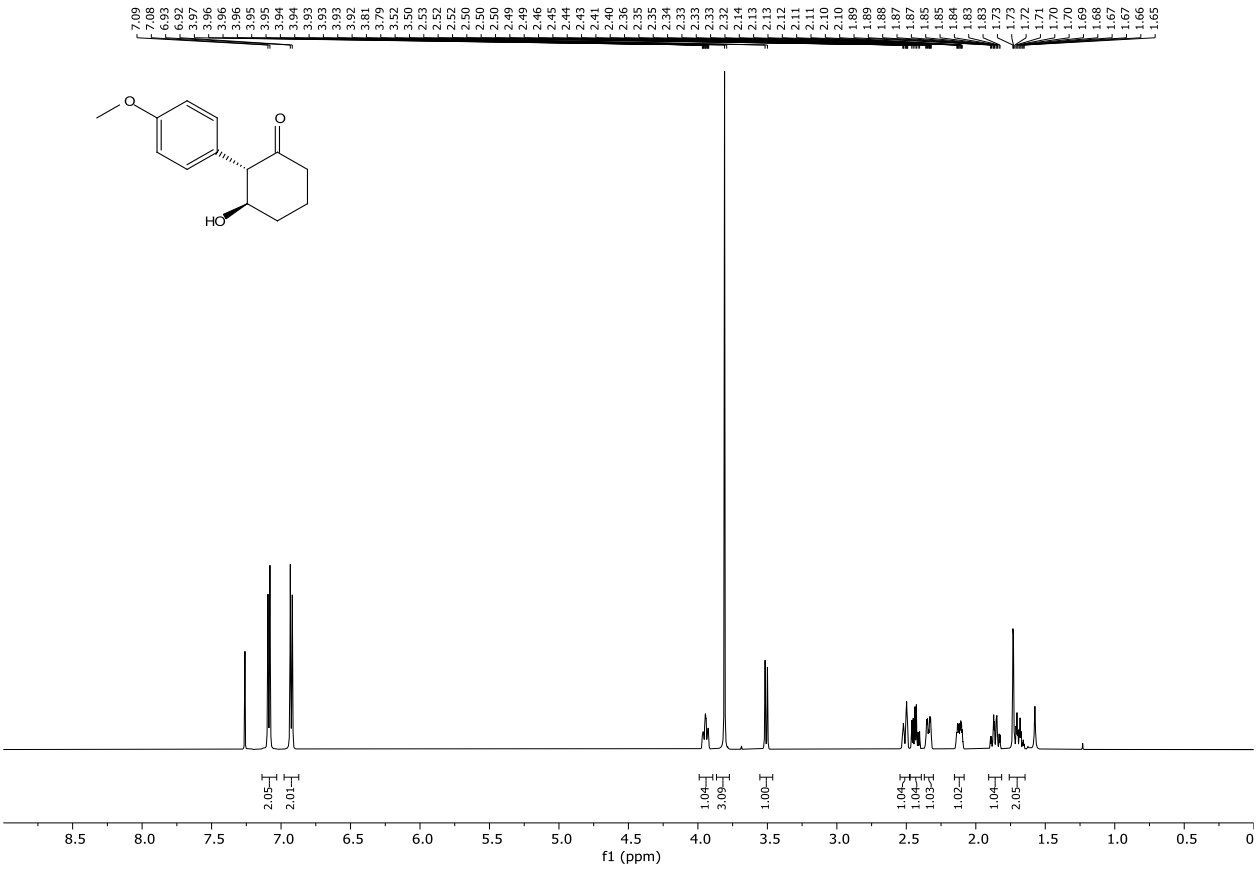

Compound **5** ($CDCl_3$, 151 MHz, ^{13}C NMR)

(2*SR*,3*RS*)-3-hydroxy-2-(4-methoxyphenyl)cyclohexan-1-one

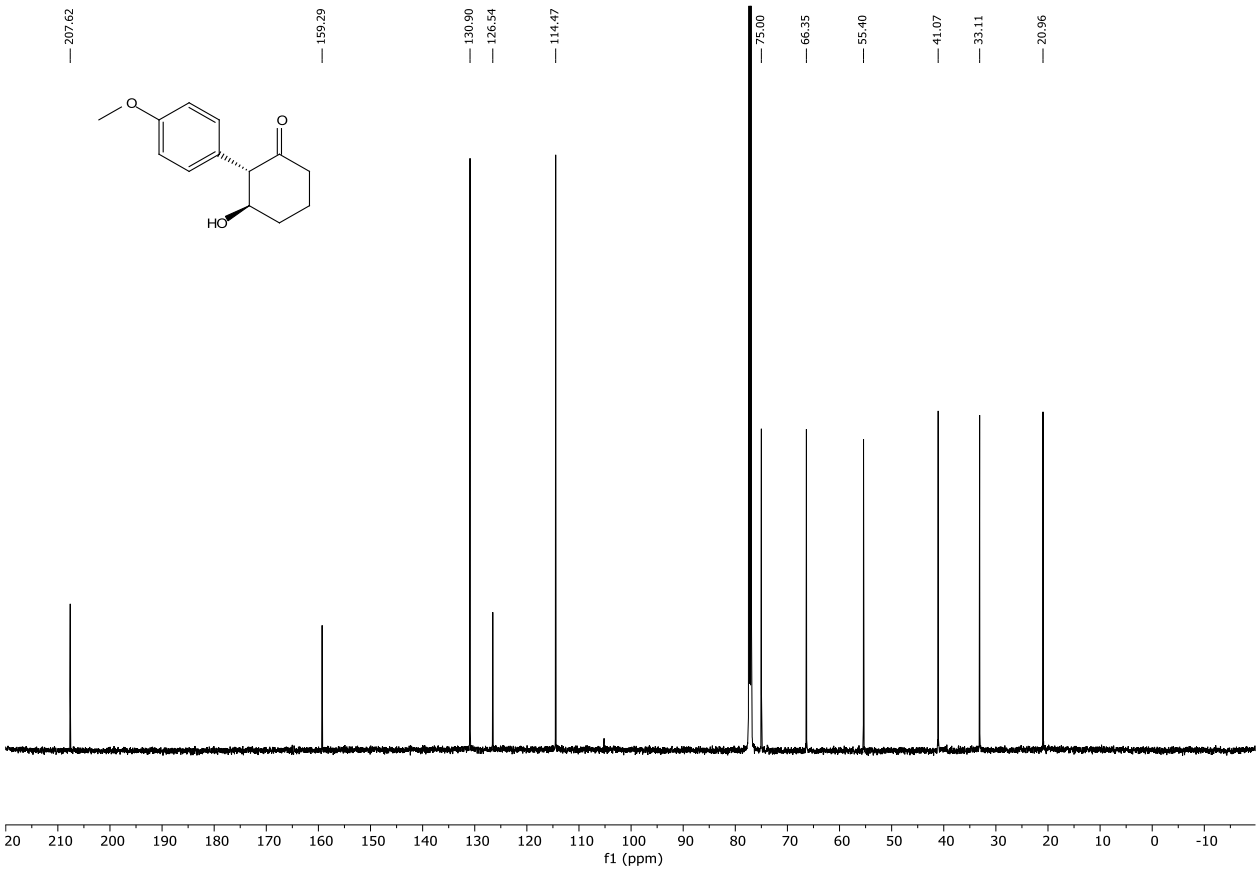

Compound **6** ($CDCl_3$, 400 MHz, ^1H NMR)

(1*RS*,2*RS*,3*RS*)-2-(4-methoxyphenyl)-3-(4,4,5,5-tetramethyl-1,3,2-dioxaborolan-2-yl)cyclohexan-1-ol

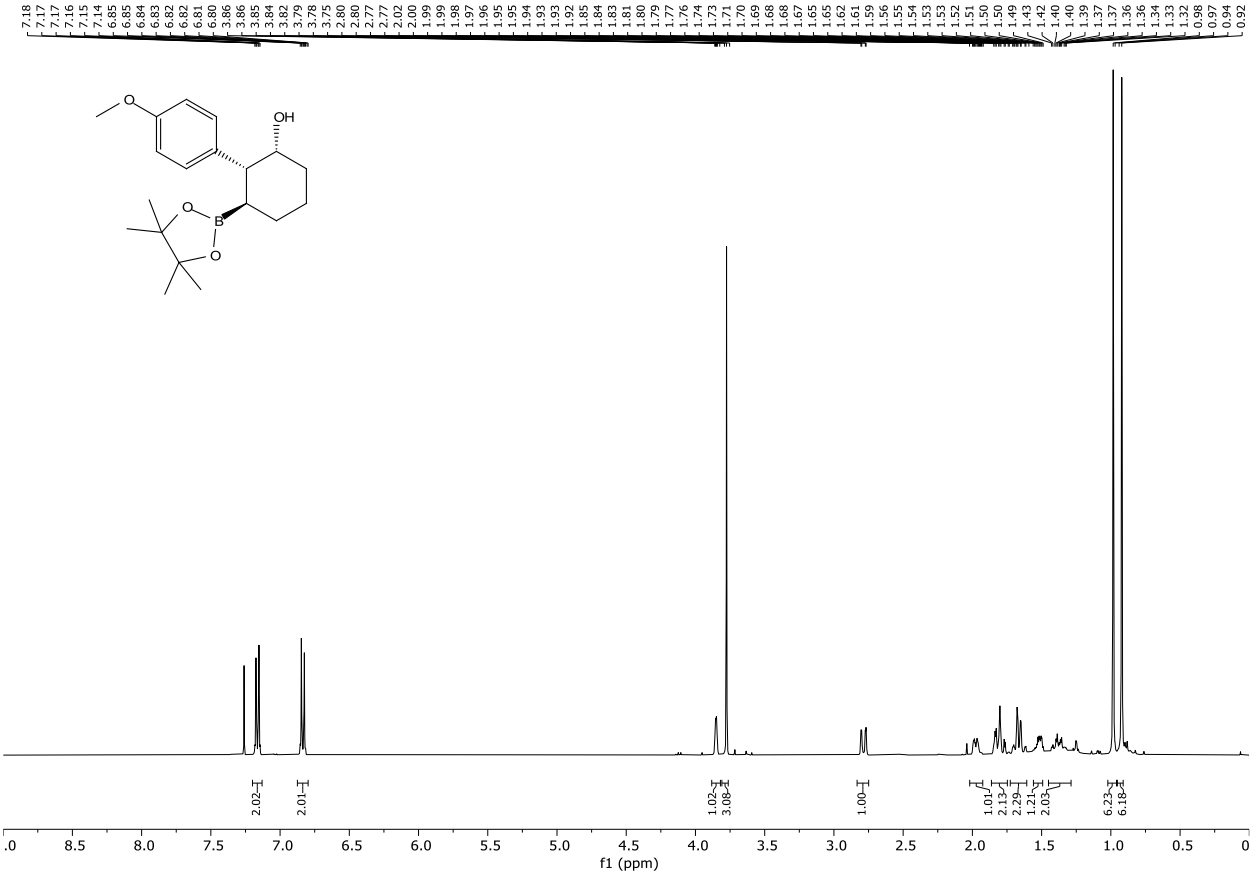

Compound **6** ($CDCl_3$, 101 MHz, ^{13}C NMR)

(1*RS*,2*RS*,3*RS*)-2-(4-methoxyphenyl)-3-(4,4,5,5-tetramethyl-1,3,2-dioxaborolan-2-yl)cyclohexan-1-ol

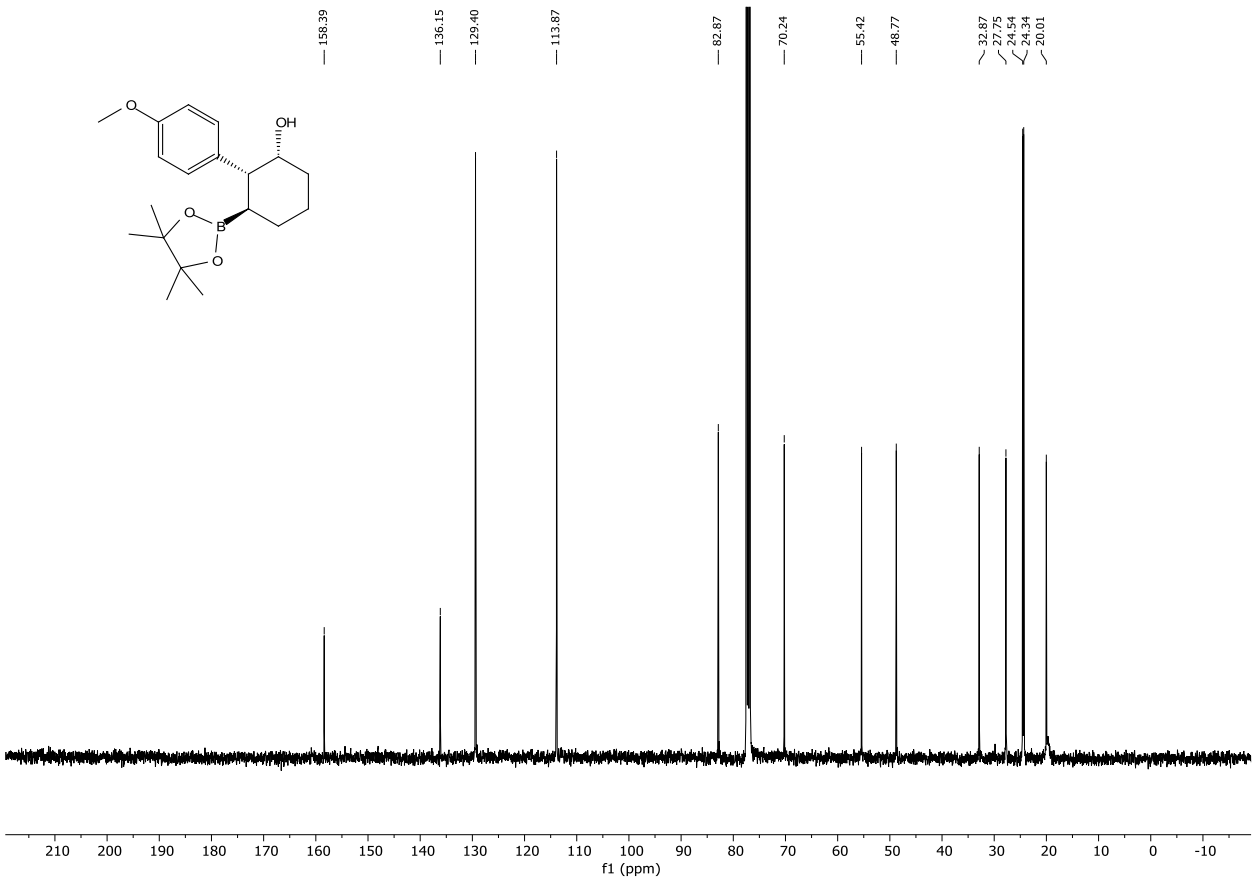

Compound **7** ($CDCl_3$, 600 MHz, ^1H NMR)

(1*RS*,2*RS*,3*RS*)-1-(4-fluorophenyl)-2-(4-methoxyphenyl)-3-(4,4,5,5-tetramethyl-1,3,2-dioxaborolan-2-yl)cyclohexan-1-ol

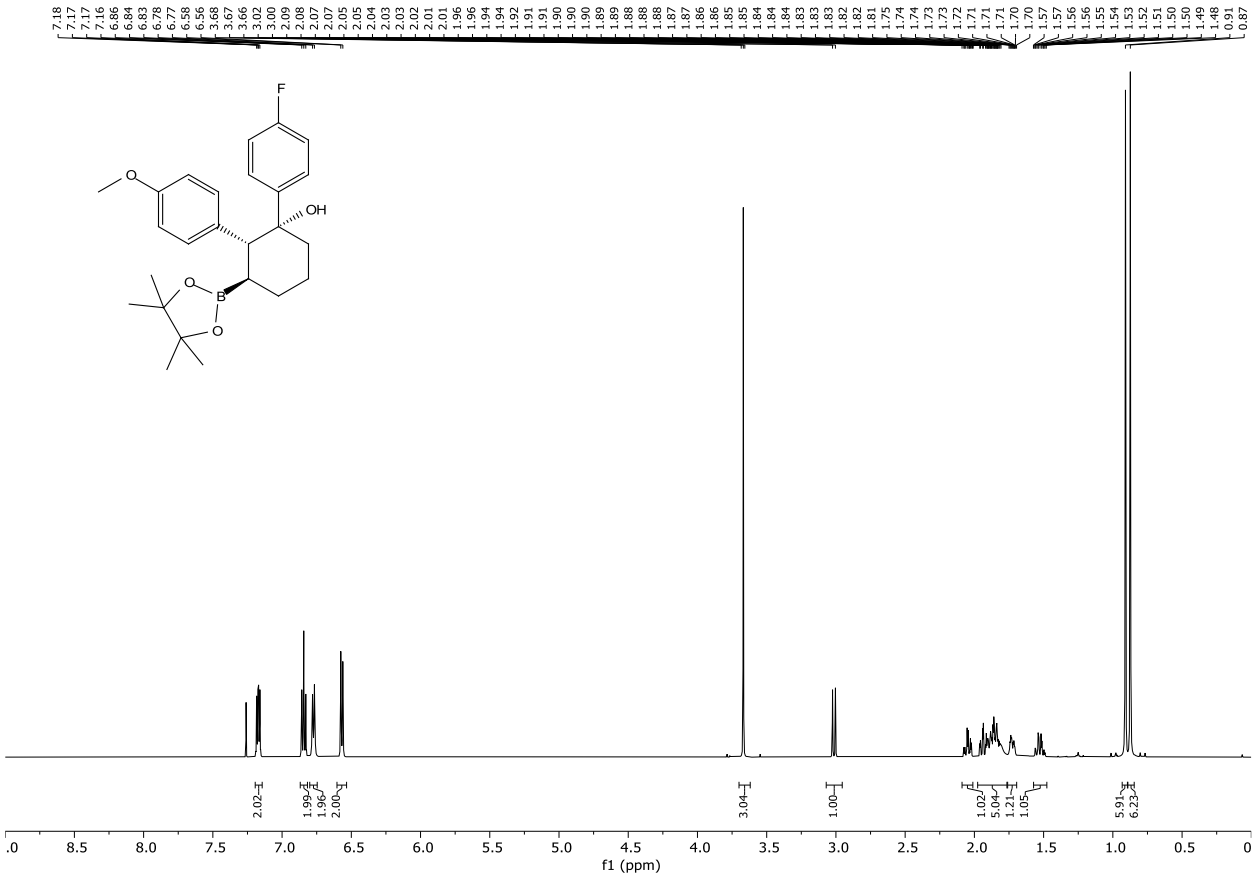

Compound **7** ($CDCl_3$, 151 MHz, ^{13}C NMR)

(1*RS*,2*RS*,3*RS*)-1-(4-fluorophenyl)-2-(4-methoxyphenyl)-3-(4,4,5,5-tetramethyl-1,3,2-dioxaborolan-2-yl)cyclohexan-1-ol

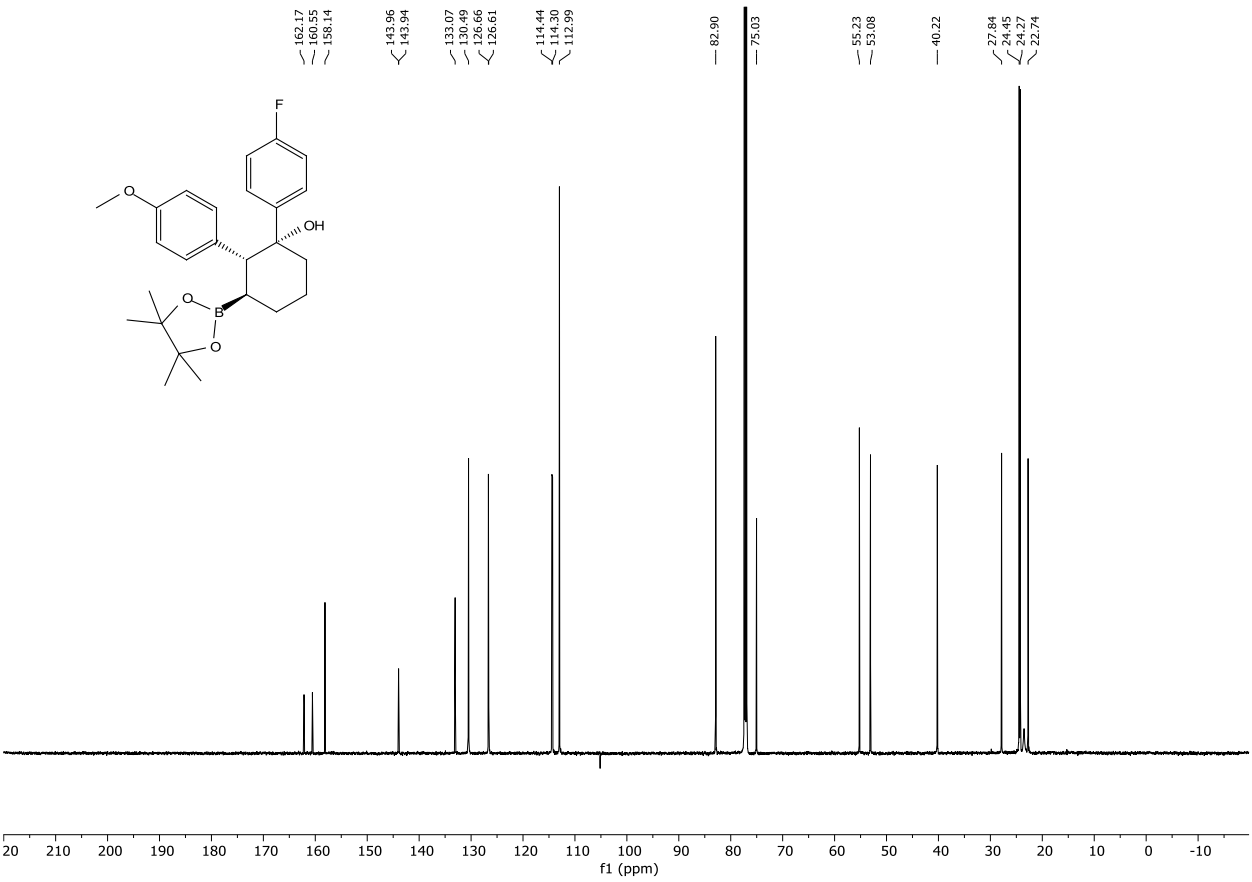

Compound **7** ($CDCl_3$, 283 MHz, ^{19}F NMR)

(1*RS*,2*RS*,3*RS*)-1-(4-fluorophenyl)-2-(4-methoxyphenyl)-3-(4,4,5,5-tetramethyl-1,3,2-dioxaborolan-2-yl)cyclohexan-1-ol

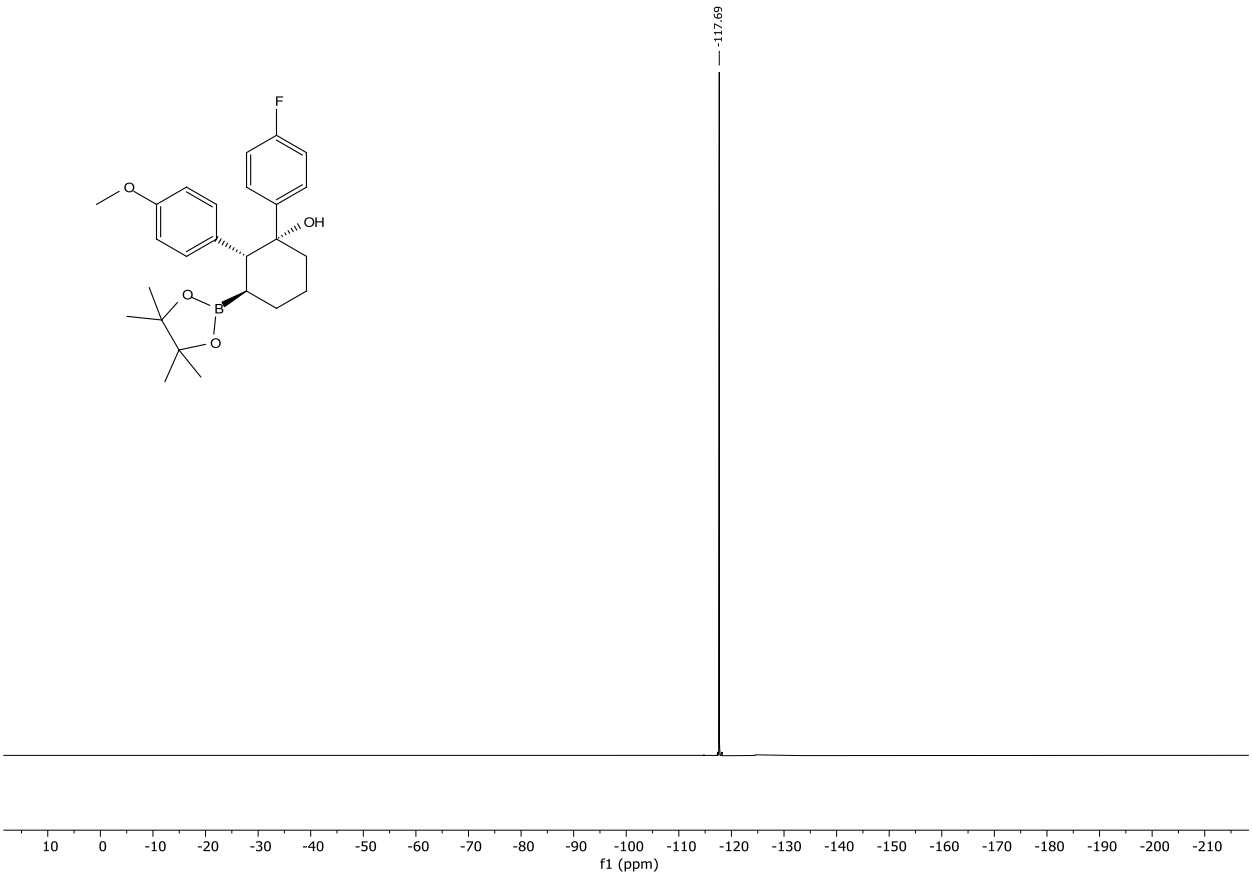

Compound **8** ($CDCl_3$, 300 MHz, ^1H NMR)

(((1*RS*,6*RS*)-4'-methoxy-6-(4,4,5,5-tetramethyl-1,3,2-dioxaborolan-2-yl)-1,4,5,6-tetrahydro-[1,1'-biphenyl]-2-yl)oxy)trimethylsilane

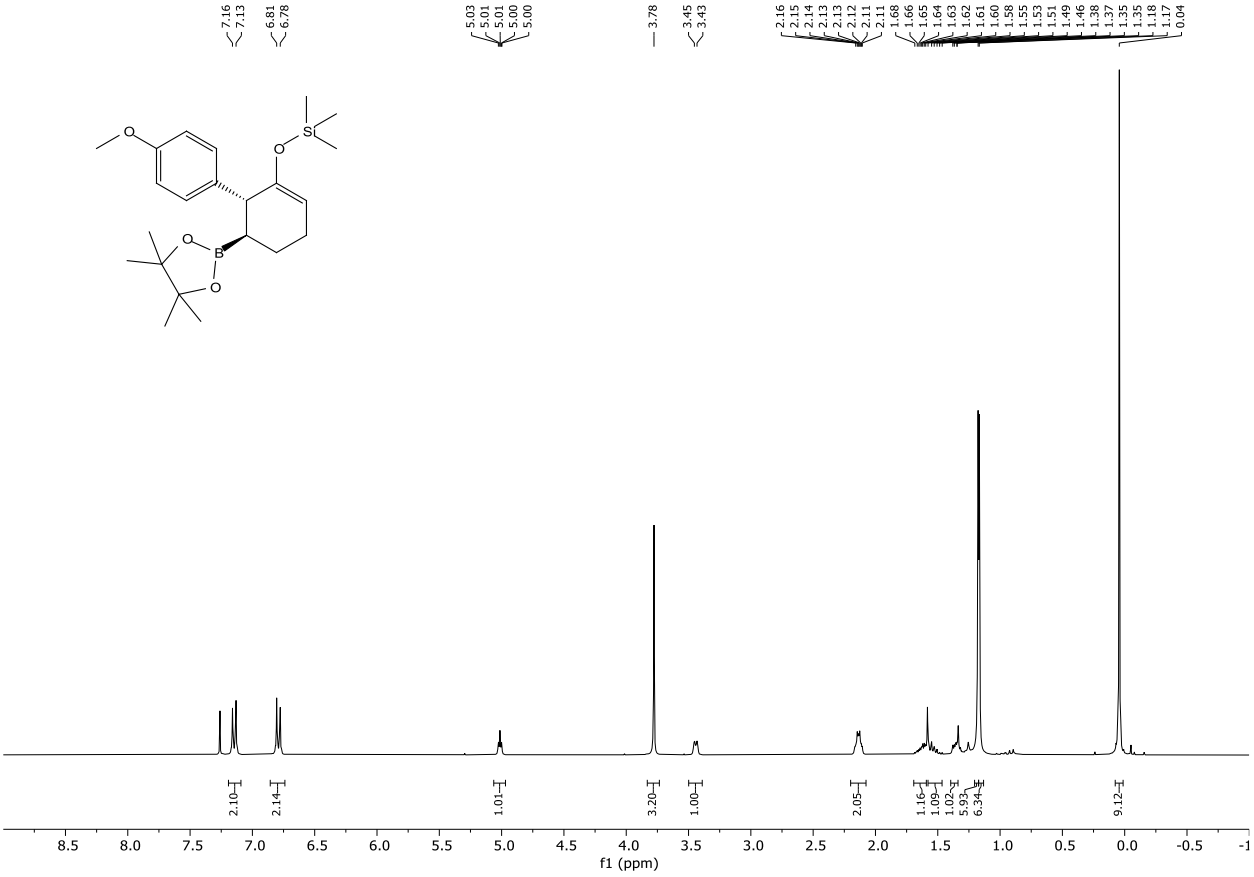

Compound **8** ($CDCl_3$, 75 MHz, ^{13}C NMR)

(((1*RS*,6*RS*)-4'-methoxy-6-(4,4,5,5-tetramethyl-1,3,2-dioxaborolan-2-yl)-1,4,5,6-tetrahydro-[1,1'-biphenyl]-2-yl)oxy)trimethylsilane

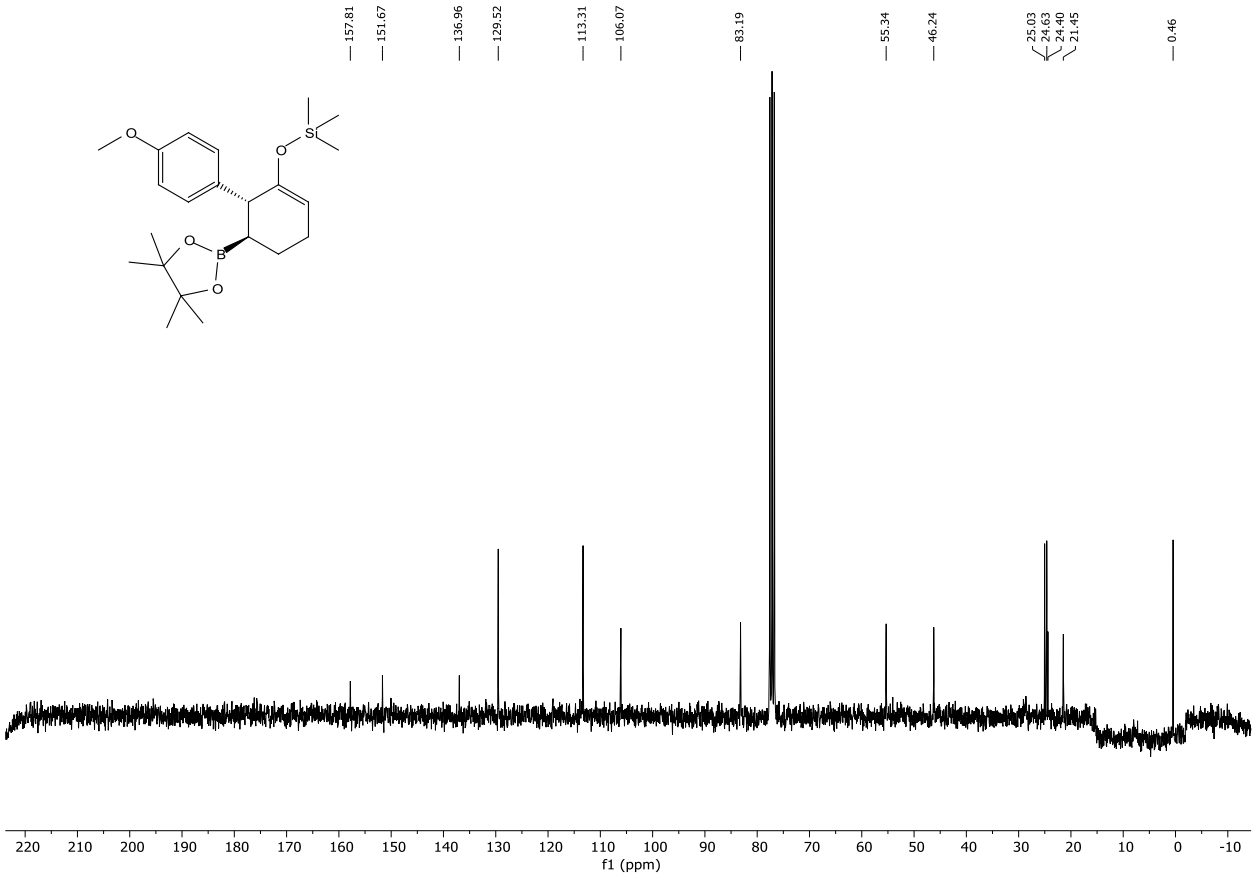

Compound **9** ($CDCl_3$, 400 MHz, ^1H NMR)

(*1RS*,6*RS*)-4'-methoxy-6-(4,4,5,5-tetramethyl-1,3,2-dioxaborolan-2-yl)-5,6-dihydro-[1,1'-biphenyl]-2(1H)-one

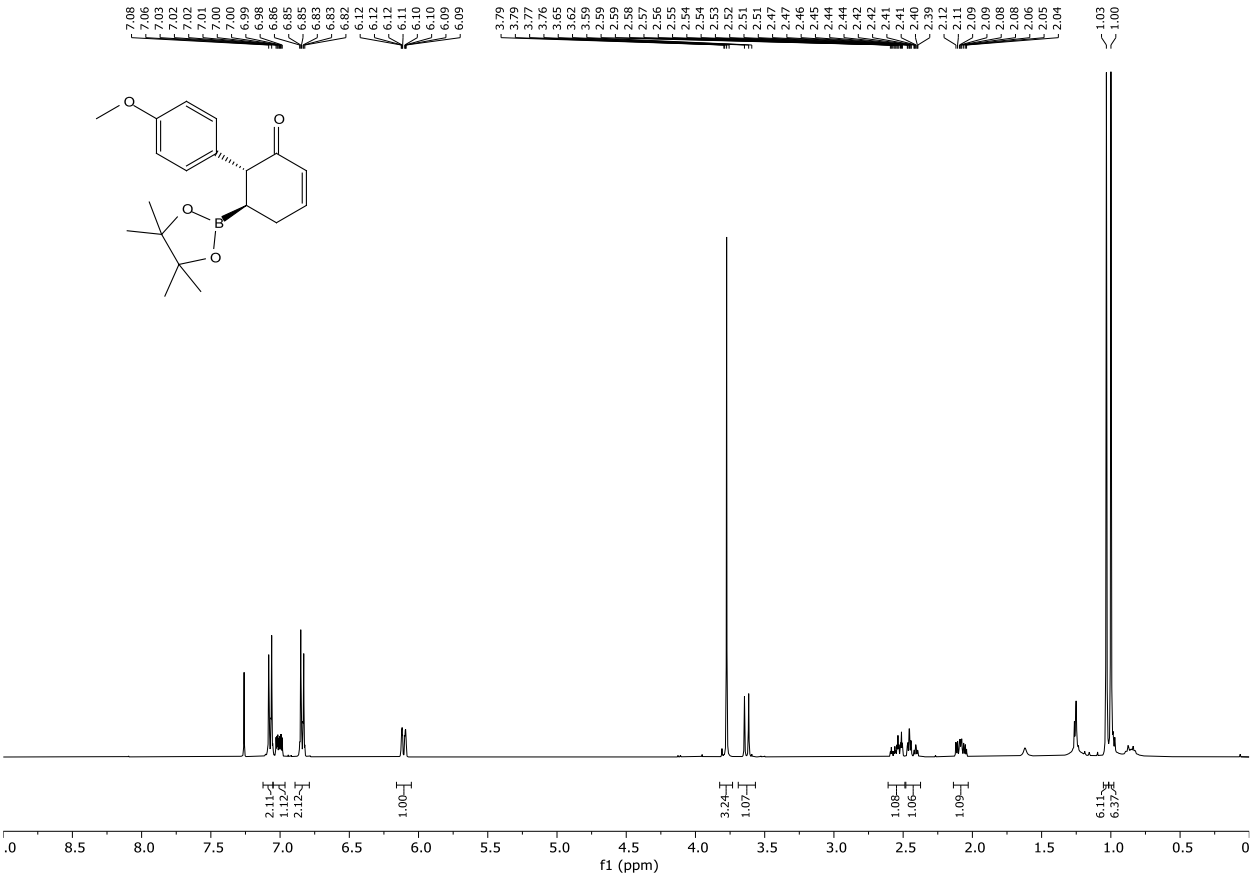

Compound **9** ($CDCl_3$, 101 MHz, ^{13}C NMR)

(*1RS*,6*RS*)-4'-methoxy-6-(4,4,5,5-tetramethyl-1,3,2-dioxaborolan-2-yl)-5,6-dihydro-[1,1'-biphenyl]-2(1H)-one

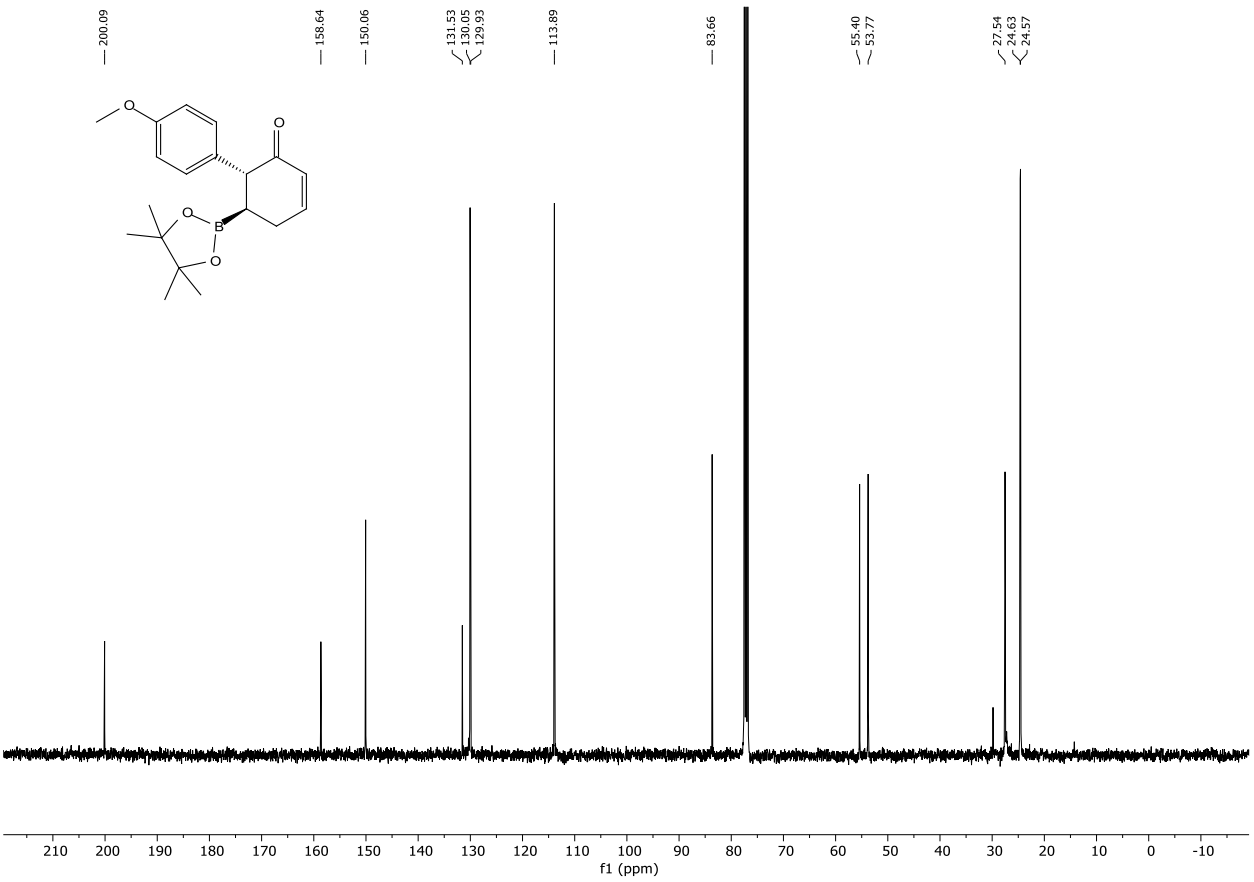

Compound **10** ($CDCl_3$, 500 MHz, ^1H NMR)

(2*RS*,3*RS*,5*RS*)-2-(4-methoxyphenyl)-3-(4,4,5,5-tetramethyl-1,3,2-dioxaborolan-2-yl)-5-vinylcyclohexan-1-one

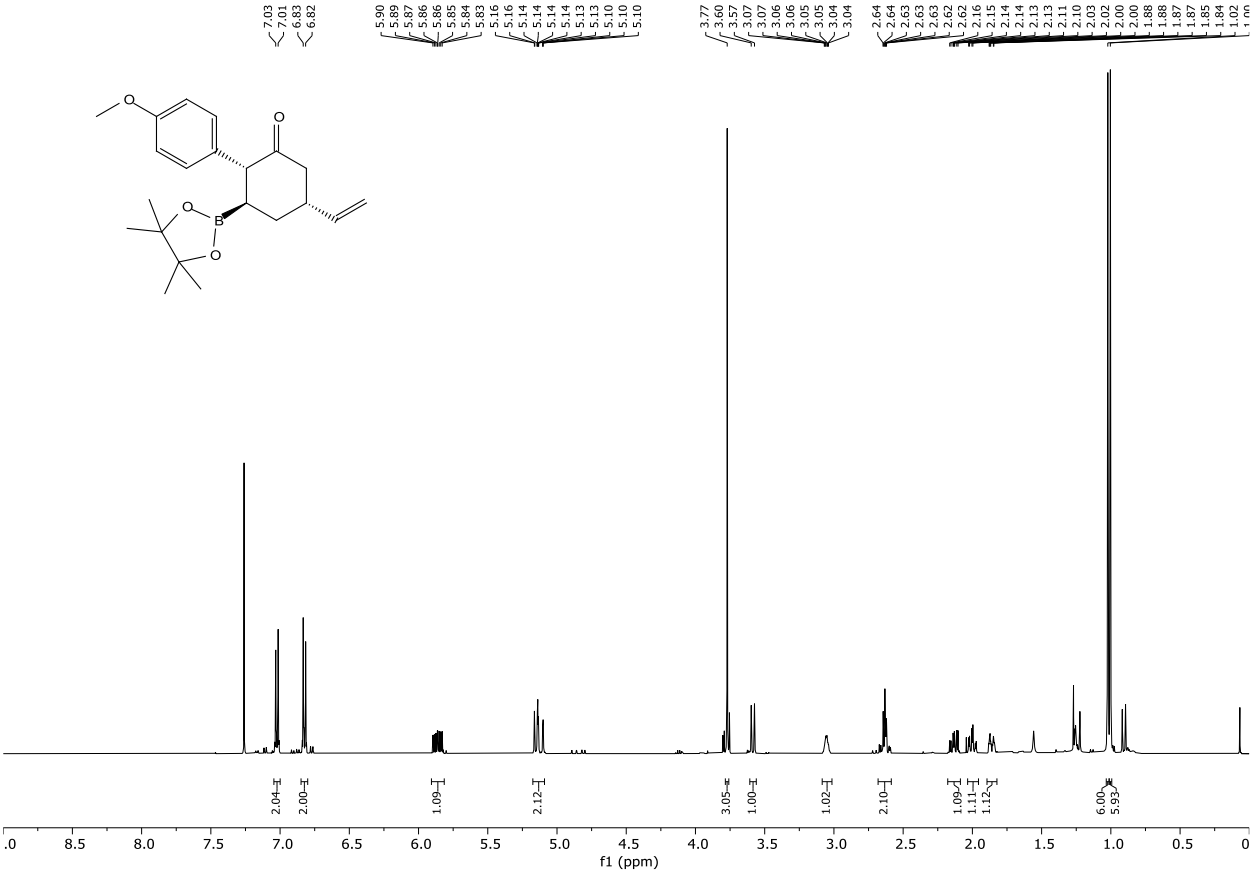

Compound **10** ($CDCl_3$, 126 MHz, ^{13}C NMR)

(2*RS*,3*RS*,5*RS*)-2-(4-methoxyphenyl)-3-(4,4,5,5-tetramethyl-1,3,2-dioxaborolan-2-yl)-5-vinylcyclohexan-1-one

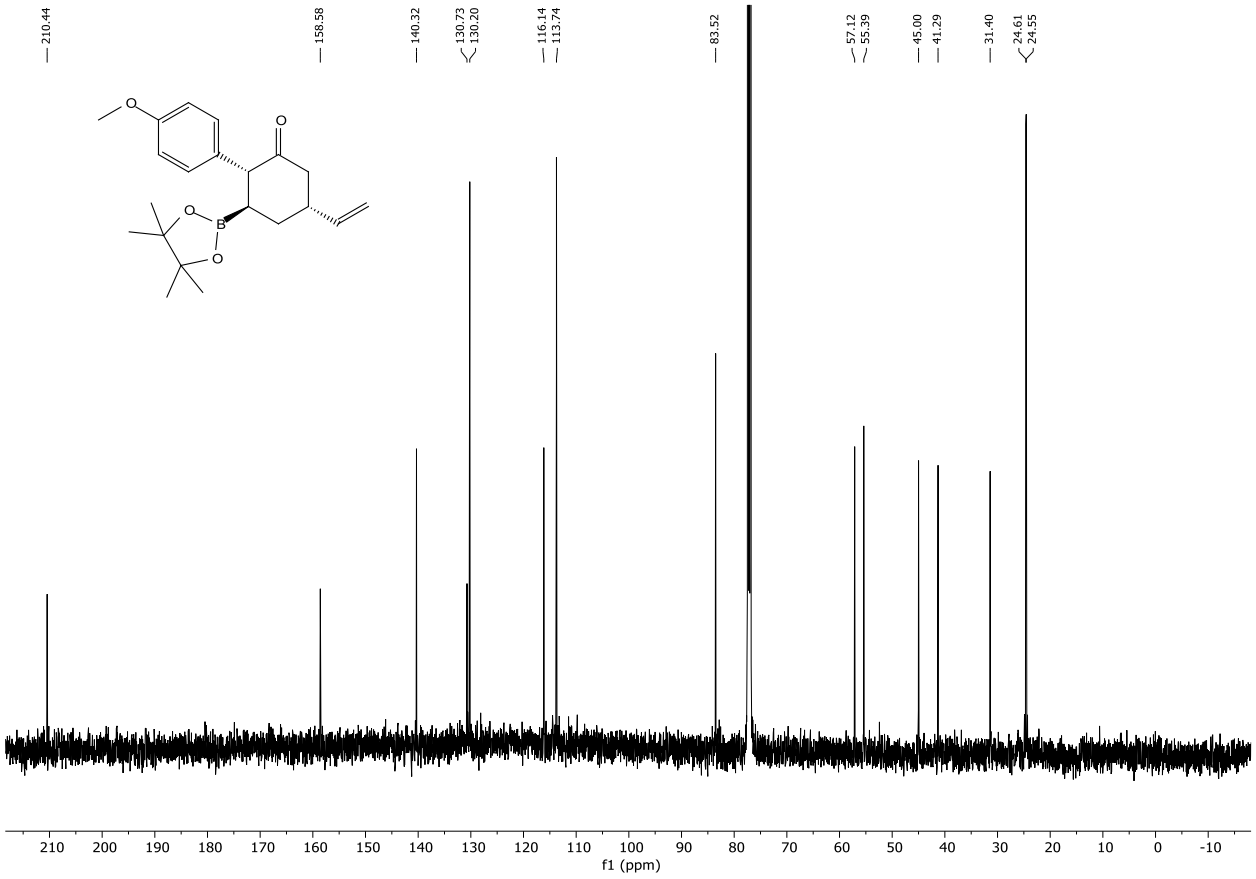

Compound **13** ($CDCl_3$, 400 MHz, ^1H NMR)

(2*SR*,3*RS*)-2-phenyl-3-(4,4,5,5-tetramethyl-1,3,2-dioxaborolan-2-yl)cyclohexan-1-one

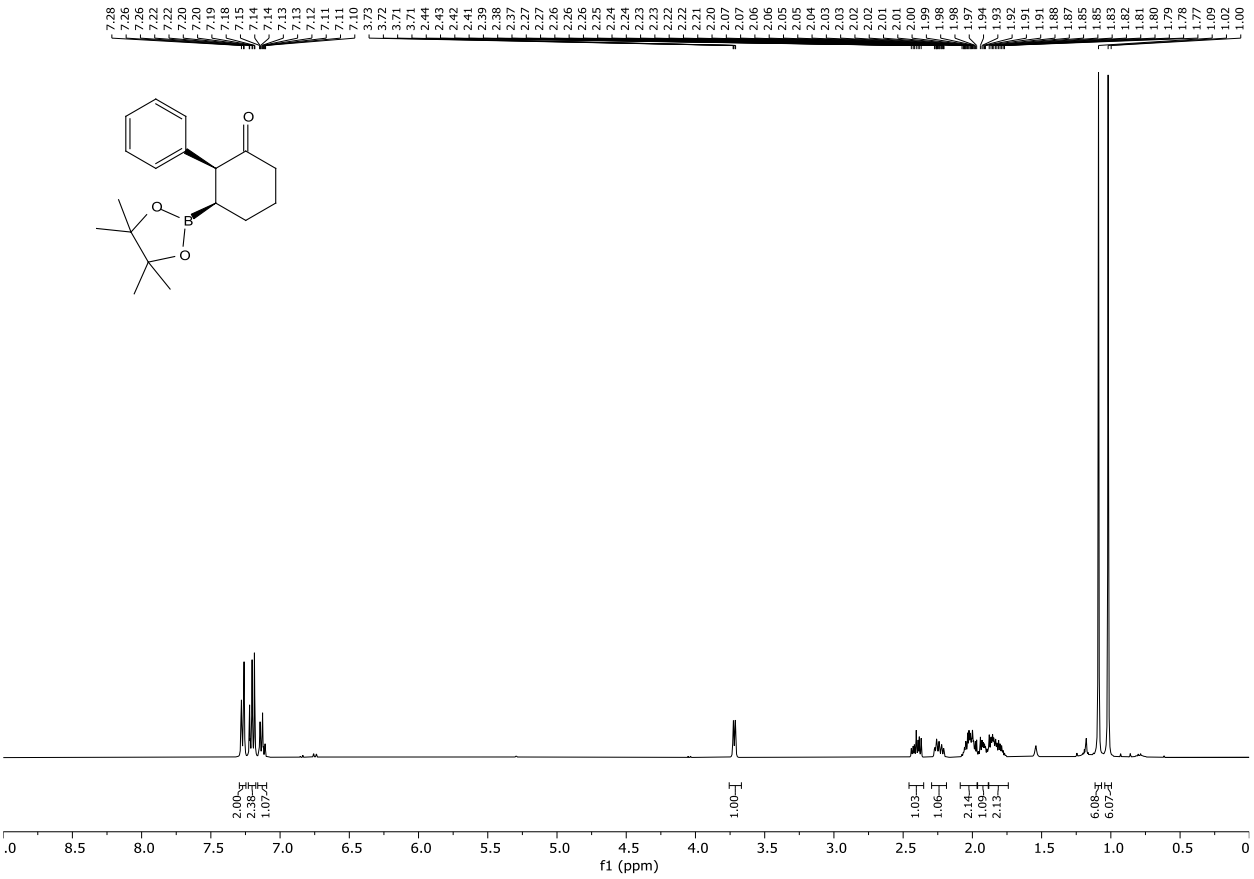

Compound **13** ($CDCl_3$, 101 MHz, ^{13}C NMR)

(2*SR*,3*RS*)-2-phenyl-3-(4,4,5,5-tetramethyl-1,3,2-dioxaborolan-2-yl)cyclohexan-1-one

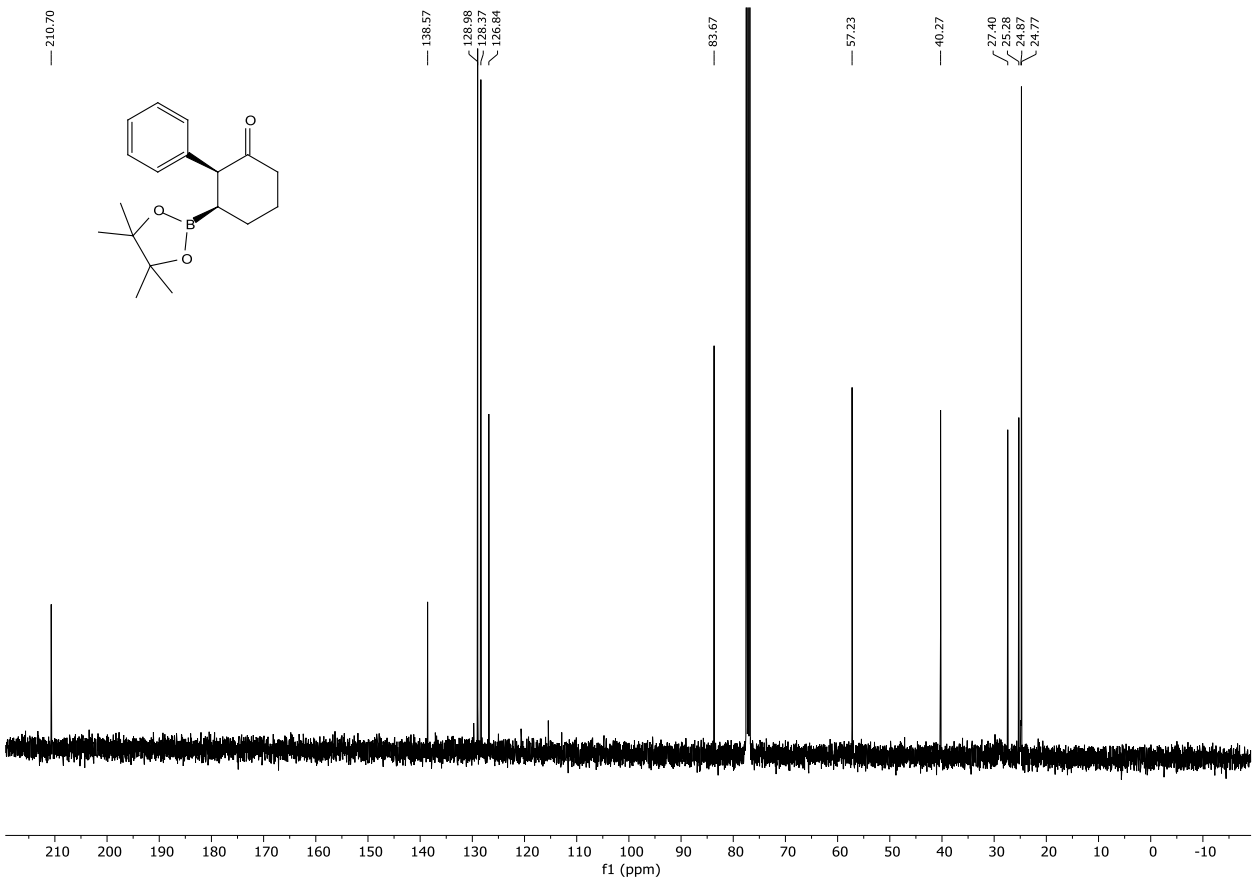

References

(1) EnamineStore. *Cyclohex-2-en-1-one. EN300-29848*. Accessed Jan 3, 2025.

(2) Leger, P. R.; Kuroda, Y.; Chang, S.; Jurczyk, J.; Sarpong, R. C-C Bond Cleavage Approach to Complex Terpenoids: Development of a Unified Total Synthesis of the Phomactins. *J. Am. Chem. Soc*. **2020**, *142*, 15536–15547.

(3) Mendoza, A.; Ishihara, Y.; Baran, P. S. Scalable Enantioselective Total Synthesis of Taxanes. *Nat. Chem.* **2012**, *4*, 21–25.

(4) Franzoni, I.; Guénée, L.; Mazet, C. Access to Congested Quaternary Centers by Pd-Catalyzed Intermolecular γ-Arylation of Unactivated α,β-Unsaturated Aldehydes. *Chem. Sci*. **2013**, *4*, 2619–2624.

(5) Saini, G.; Mondal, A.; Kapur, M. Palladium-Mediated Remote Functionalization in γ- And ϵ-Arylations and Alkenylations of Unblocked Cyclic Enones. *Org*. *Lett*. **2019**, *21*, 9071–9075.

(6) Kale, A. P.; Pawar, G. G.; Kapur, M. Regioselectivity Switch Achieved in the Palladium Catalyzed α-Arylation of Enones by Employing the Modified Kuwajima-Urabe Conditions. *Org*. *Lett*. **2012**, *14*, 1808–1811.

(7) Mayer, R. J.; Allihn, P. W. A.; Hampel, N.; Mayer, P.; Sieber, S. A.; Ofial, A. R. Electrophilic Reactivities of Cyclic Enones and α,β-Unsaturated Lactones. *Chem*. *Sci*. **2021**, *12*, 4850–4865.

(8) Gilman, H.; Jones, R. G.; Woods, L. A. The Preparation of Methylcopper and Some Observations on the Decomposition of Organocopper Compounds. *J. Org. Chem*. **1952**, *17*, 1930–1934.

(9) House, H.; Respess, W.; Whitesides, G. The Chemistry of Carbanions. XII. The Role of Copper in the Conjugate Addition of Organometallic Reagents. *J. Org. Chem*. **1966**, *31*, 3128–3141.

(10) Munir, R.; Zahoor, A. F.; Nazeer, U.; Saeed, M. A.; Mansha, A.; Irfan, A.; Tariq, M. U. Gilman Reagent toward the Synthesis of Natural Products. *RSC Adv*. **2023**, *13*, 35172–35208.

(11) Nakajima, T.; Yamashita, D.; Suzuki, K.; Nakazaki, A.; Suzuki, T.; Kobayashi, S. Different Modes of Cyclization in Zoanthamine Alkaloid System, Bisaminal versus Spiroketal Formation. *Org. Lett*. **2011**, *13*, 2980–2983.

(12) Kraft, P.; Denizot, N. Synthesis of a Spirocyclic Seco Structure of the Principal Vetiver Odorant Khusimone. *Eur. J. Org. Chem*. **2013**, *2013*, 49–58.

(13) Eriksson, M.; Iliefski, T.; Nilsson, M.; Olsson, T. Iodotrimethylsilane-Promoted 1,4-Addition of Copper Acetylides to α,β-Unsaturated Ketones and Aldehydes. *J. Org. Chem.* **1997**, *62*, 182–187.

(14) Rijs, N. J.; O'Hair, R. A. J. Unimolecular Reactions of Organocuprates and Organoargentates. *Organometallics* **2010**, *29*, 2282–2291.

(15) Morita, K.; Suzuki, Z.; Hirose, H. A Tertiary Phosphine-Catalyzed Reaction of Acrylic Compounds with Aldehydes. *Bull. Chem. Soc. Jpn*. **1968**, *41*, 2815.

(16) Baylis, A. B.; Hillman, M. E. D. German Patent 2155113, 1972.

(17) Luo, S.; Mi, X.; Xu, H.; Wang, P. G.; Cheng, J. P. Efficient Baylis-Hillman Reactions of Cyclic Enones in Methanol as Catalyzed by Methoxide Anion. *J. Org. Chem.* **2004**, *69*, 8413–8422.

(18) Basavaiah, D.; Reddy, B. S.; Badsara, S. S. Recent Contributions from the Baylis - Hillman Reaction to Organic Chemistry. *Chem*. *Rev*. **2010**, *110*, 5447–5674.

(19) Heck, R. F. Palladium-Catalyzed Vinylation of Organic Halides. *Organic Reactions*; Wiley, 1982; pp 345–390.

(20) Kassymbek, A.; José Aguilar Troyano, F.; Dimakos, V.; Canterbury, D. P.; Monfette, S.; Roosen, P. C.; Newman, S. G. Understanding and Controlling the Mizoroki–Heck Reaction of Cyclic Enones. *ACS Catal*. **2024**, *14*, 8193–8202.

(21) Tanaka, D.; Myers, A. G. Heck-Type Arylation of 2-Cycloalken-1-Ones with Arylpalladium Intermediates Formed by Decarboxylative Palladation and by Aryl Iodide Insertion. *Org. Lett*. **2004**, *6*, 433–436.

(22) Kalkman, E. D.; Hartwig, J. F. Direct Observation of Diastereomeric α-C-Bound Enolates during Enantioselective α-Arylations: Synthesis, Characterization, and Reactivity of Arylpalladium Fluorooxindole Complexes. *J. Am. Chem. Soc*. **2021**, *143*, 11741–11750.

(23) Heravi, M. M.; Dehghani, M.; Zadsirjan, V. Rh-Catalyzed Asymmetric 1,4-Addition Reactions to α,β-Unsaturated Carbonyl and Related Compounds: An Update. *Tetrahedron Asymm*. **2016**, *27*, 513–588.

(24) Takaya, Y.; Ogasawara, M.; Hayashi, T.; Sakai, M.; Miyaura, N. Rhodium-Catalyzed Asymmetric 1,4-Addition of Aryl- and Alkenylboronic Acids to Enones. *J. Am. Chem. Soc.* **1998**, *120*, 5579–5580.

(25) Tamura, M.; Ogata, H.; Ishida, Y.; Takahashi, Y. Design and Synthesis of Chiral 1,10-Phenanthroline Ligand, and Application in Palladium Catalyzed Asymmetric 1,4-Addition Reactions. *Tetrahedron Lett.* **2017**, *58*, 3808–3813.

(26) Sandford, C.; Aggarwal, V. K. Stereospecific Functionalizations and Transformations of Secondary and Tertiary Boronic Esters. *Chem. Commun*. **2017**, *53*, 5481–5494.

(27) Ito, H.; Yamanaka, H.; Tateiwa, J. I.; Hosomi, A. Boration of an α,β-Enone Using a Diboron Promoted by a Copper(I) - Phosphine Mixture Catalyst. *Tetrahedron Lett*. **2000**, *41*, 6821–6825.

(28) Takahashi, K.; Ishiyama, T.; Miyaura, N. Addition and Coupling Reactions of Bis(Pinacolato)Diboron Mediated by CuCl in the Presence of Potassium Acetate. *Chem. Lett*. **2000**, *9*, 982–983.

(29) Mun, S.; Lee, J. E.; Yun, J. Copper-Catalyzed β-Boration of α,β-Unsaturated Carbonyl Compounds: Rate Acceleration by Alcohol Additives. *Org. Lett.* **2006**, *8*, 4887–4889.

(30) Lillo, V.; Prieto, A.; Bonet, A.; Dí-Requejo, M. M.; Ramirez, J.; Pérez, P. J.; Fernández, E. Asymmetric β-Boration of α,β-Unsaturated Esters with Chiral (NHC)Cu Catalysts. *Organometallics* **2009**, *28*, 659–662.

(31) Lee, Y.; Hoveyda, A. H. Efficient Boron-Copper Additions to Aryl-Substituted Alkenes Promoted by NHC-Based Catalysts. Enantioselective Cu-Catalyzed Hydroboration Reactions. *J. Am. Chem. Soc.* **2009**, *131*, 3160–3161.

(32) Lee, K. S.; Zhugralin, A. R.; Hoveyda, A. H. Efficient C-B Bond Formation Promoted by n-Heterocyclic Carbenes: Synthesis of Tertiary and Quaternary B-Substituted Carbons through Metal-Free Catalytic Boron Conjugate Additions to Cyclic and Acyclic α,β-Unsaturated Carbonyls. *J. Am. Chem. Soc.* **2009**, *131*, 7253–7255.

(33) Clement, H. A.; Boghi, M.; McDonald, R. M.; Bernier, L.; Coe, J. W.; Farrell, W.; Helal, C. J.; Reese, M. R.; Sach, N. W.; Lee, J. C.; Hall, D. G. High-Throughput Ligand Screening Enables the Enantioselective Conjugate Borylation of Cyclobutenones to Access Synthetically Versatile Tertiary Cyclobutylboronates. *Angew. Chem., Int. Ed*. **2019**, *58*, 18405–18409.

(34) Cui, M.; Zhao, Z. Y.; Oestreich, M. Boosting the Enantioselectivity of Conjugate Borylation of α,β-Disubstituted Cyclobutenones with Monooxides of Chiral C2-Symmetric Bis(Phosphine) Ligands. *Chem. Eur. J.* **2022**, *28*, e202202163.

(35) Zhao, Z. Y.; Cui, M.; Poletti, A. A.; Irran, E.; Oestreich, M. Desymmetrization of Cyclohexadienones Containing a Quaternary γ-Carbon Atom by Conjugate Addition of Boron Nucleophiles. *ACS Catal*. **2024**, *14*, 176–182.

(36) Gu, J.; Rodriguez, K. X.; Kanda, Y.; Yang, S.; Ociepa, M.; Wilke, H.; Abrishami, A. V.; Jørgensen, L.; Skak-Nielsen, T.; Chen, J. S.; Baran, P. S. Convergent Total Synthesis of (+)-Calcipotriol: A Scalable, Modular Approach to Vitamin D Analogs. *Proc. NAS* **2022**, *119*, e2200814119.

(37) Dimakos, V.; Canterbury, D. P.; Monfette, S.; Roosen, P. C.; Newman, S. G. A Morita-Baylis-Hillman Inspired Cross-Coupling Strategy for the Direct α-Arylation of Cyclic Enones. *ACS Catal.* **2022**, *12*, 11557–11562.

(38) Taylor, R. Organocopper Conjugate Addition-Enolate Trapping Reactions. *Synthesis (Stuttg)* **1985**, *4*, 364–392.

(39) Suzuki, M.; Yanagisawa, A.; Noyori, R. The Three-Component Coupling Synthesis of Prostaglandins. *J. Am. Chem. Soc*. **1988**, *110*, 4718–4726.

(40) Bernasconi, S.; Gariboldt, P.; Jommi, G.; Sisti, M. C-Acylation of Enolates from Lithium Dimethylcuprate Addition to α,β-Unsaturated Ketones. *Tetrahedron Lett*. **1980**, *21*, 2237–2340.

(41) Davis, R.; Untch, K. A Convergent Total Synthesis of (±)-Prostaglandin F2α via Conjugate Addition and Regiospecific Enolate Trapping. *J. Org. Chem*. **1979**, *44*, 3755–3759.

(42) Boeckman, R.; Blum, D.; Arthur, S. A Total Synthesis of Gascardic Acid. *J. Am. Chem. Soc*. **1979**, *101*, 5060–5062.

(43) Kurozumi, S.; Toru, T.; Tanaka, T.; Kobayashi, M.; Miura, S.; Ishimoto, S. Prostaglandin Chemistry VII: A Synthesis of New 8-Phenylthio-11-Deoxyprostaglandins. *Tetrahedron Lett.* **1976**, *17*, 4091–4094.

(44) Posner, G. H.; Sterling, J. J.; Whitten, C. E.; Lentz, C. M.; Brunelle, D. J. Alkylation of Enolate Ions Generated Regiospecifically via Organocopper Reactions. Synthesis of Decalin Sesquiterpene Valerane and of Prostaglandin Model Systems. *J. Am. Chem. Soc.* **1975**, *97*, 107–118.

(45) Pan, J. L.; Chen, T.; Zhang, Z. Q.; Li, Y. F.; Zhang, X. M.; Zhang, F. M. A Cu-Mediated One-Pot Michael Addition/α-Arylation Strategy Using a Diaryliodonium Salt: A Direct and Efficient Approach to α-Aryl-β-Substituted Cyclic Ketone Scaffolds. *Chem. Commun*. **2016**, *52*, 2382–2385.

(46) Chen, X. W.; Hou, Z. C.; Chen, C.; Zhang, L. H.; Chen, M. E.; Zhang, F. M. Enantioselective Total Syntheses of Six Natural and Two Proposed Meroterpenoids from Psoralea Corylifolia. *Chem. Sci.* **2023**, *14*, 5699–5704.

(47) Wickham, L. M.; Giri, R. Transition Metal (Ni, Cu, Pd)-Catalyzed Alkene Dicarbofunctionalization Reactions. *Acc. Chem. Res*. **2021**, *54*, 3415–3437.

(48) Derosa, J.; Apolinar, O.; Kang, T.; Tran, V. T.; Engle, K. M. Recent Developments in Nickel-Catalyzed Intermolecular Dicarbofunctionalization of Alkenes. *Chem. Sci.* **2020**, *11*, 4287–4296.

(49) Zhu, S.; Zhao, X.; Li, H.; Chu, L. Catalytic Three-Component Dicarbofunctionalization Reactions Involving Radical Capture by Nickel. *Chem. Soc. Rev.* **2021**, *50*, 10836–10856.

(50) Albéniz, A. C.; Catalina, N. M.; Espinet, P.; Redón, R. Bonding Modes in Palladium(II) Enolates: Consequences for Dynamic Behavior and Reactivity. *Organometallics* **1999**, *18*, 5571–5576.

(51) Huang, Z.; Hartwig, J. F. Copper(I) Enolate Complexes in α-Arylation Reactions: Synthesis, Reactivity, and Mechanism. *Angew. Chem.* **2012**, *124*, 1052–1056.

(52) Hamann, B. C.; Hartwig, J. F. Palladium-Catalyzed Direct α-Arylation of Ketones. Rate Acceleration by Sterically Hindered Chelating Ligands and Reductive Elimination from a Transition Metal Enolate Complex. *J. Am. Chem. Soc*. **1997**, *119*, 12382–12383.

(53) Welle, A.; Cirriez, V.; Riant, O. Copper Catalyzed Tandem Conjugated Borylation-Aldol Reaction. *Tetrahedron* **2012**, *68*, 3435–3443.

(54) Nahra, F.; Macé, Y.; Lambin, D.; Riant, O. Copper/Palladium-Catalyzed 1,4 Reduction and Asymmetric Allylic Alkylation of α,β-Unsaturated Ketones: Enantioselective Dual Catalysis. *Angew. Chem., Int. Ed*. **2013**, *52*, 3208–3212.

(55) Qiqige, Q.; Lundgren, R. J.; Kong, D. Combining Enantioselective Rh-Catalyzed Conjugate Addition and Ir-Catalyzed Allylic Alkylation in Stereodivergent, Multicomponent Coupling Reactions to Form Three Stereocenters. *Chem. Eur. J.* **2023**, *29*, e202300727.

(56) Semba, K.; Ohta, N.; Paulus, F.; Ohata, M.; Nakao, Y. Merging Pd0/PdII Redox and PdII/PdII Non-Redox Catalytic Cycles for the Allylarylation of Electron-Deficient Alkenes. *Chem. Eur. J.* **2021**, *27*, 5035–5040.

(57) Campbell, M. W.; Yuan, M.; Polites, V. C.; Gutierrez, O.; Molander, G. A. Photochemical C-H Activation Enables Nickel-Catalyzed Olefin Dicarbofunctionalization. *J. Am. Chem. Soc*. **2021**, *143*, 3901–3910.

(58) Semba, K.; Nakao, Y. Arylboration of Alkenes by Cooperative Palladium/Copper Catalysis. *J. Am. Chem. Soc.* **2014**, *136*, 7567–7570.

(59) Jensen, K. H.; Sigman, M. S. Mechanistic Approaches to Palladium-Catalyzed Alkene Difunctionalization Reactions. *Org. Biomol. Chem.* **2008**, *6*, 4083–4088.

(60) Liu, Z.; Gao, Y.; Zeng, T.; Engle, K. M. Transition-Metal-Catalyzed 1,2-Carboboration of Alkenes: Strategies, Mechanisms, and Stereocontrol. *Isr. J. Chem.* **2020**, *60*, 219–229.

(61) Manna, S.; Das, K. K.; Nandy, S.; Aich, D.; Paul, S.; Panda, S. A New Avenue for the Preparation of Organoboron Compounds via Nickel Catalysis. *Coord. Chem. Rev.* **2021**, *448*, 214165.

(62) Ye, Y.; Lin, Y.; Mao, N. D.; Yang, H.; Ye, X. Y.; Xie, T. Recent Progress in Nickel-Catalyzed Carboboration of Alkenes. *Org. Biomol. Chem*. **2022**, *20*, 9255–9271.

(63) Dorn, S. K.; Brown, M. K. Cooperative Pd/Cu Catalysis for Alkene Arylboration: Opportunities for Divergent Reactivity. *ACS Catal.* **2022**, *12*, 2058–2063.

(64) Yang, K.; Song, Q. Palladium-Catalyzed Arylboration of Bicyclic Alkenes. *J. Org. Chem.* **2016**, *81*, 1000–1005.

(65) Edelstein, E. K.; Grote, A. C.; Palkowitz, M. D.; Morken, J. P. A Protocol for Direct Stereospecific Amination of Primary, Secondary, and Tertiary Alkylboronic Esters. *Synlett* **2018**, *29*, 1749–1752.

(66) Li, Z.; Wang, Z.; Zhu, L.; Tan, X.; Li, C. Silver-Catalyzed Radical Fluorination of Alkylboronates in Aqueous Solution. *J. Am. Chem. Soc.* **2014**, *136*, 16439–16443.

(67) Pattison, G. Fluorination of Organoboron Compounds. *Org. Biomol. Chem.* **2019**, *17*, 5651–5660.

(68) He, J.; Jiang, H.; Takise, R.; Zhu, R.; Chen, G.; Dai, H.; Dhar, T. G. M.; Shi, J.; Zhang, H.; Cheng, P. T. W.; Yu, J. Ligand-Promoted Borylation of C(sp^3)-H Bonds with Palladium(II) Catalyst. *Angew. Chem.* **2016**, *55*, 785–789.

(69) Nave, S.; Sonawane, R. P.; Elford, T. G.; Aggarwal, V. K. Protodeboronation of Tertiary Boronic Esters: Asymmetric Synthesis of Tertiary Alkyl Stereogenic Centers. *J. Am. Chem. Soc.* **2010**, *132*, 17096–17098.

(70) Speckmeier, E.; Maier, T. C. ART-An Amino Radical Transfer Strategy for C(sp^2)-C(sp^3) Coupling Reactions, Enabled by Dual Photo/Nickel Catalysis. *J. Am. Chem. Soc.* **2022**, *144*, 9997–10005.

(71) Nelson, H. M.; Williams, B. D.; Miró, J.; Toste, F. D. Enantioselective 1,1-Arylborylation of Alkenes: Merging Chiral Anion Phase Transfer with Pd Catalysis. *J. Am. Chem. Soc.* **2015**, *137*, 3213–3216.

(72) Liu, Z.; Chen, J.; Lu, H. X.; Li, X.; Gao, Y.; Coombs, J. R.; Goldfogel, M. J.; Engle, K. M. Palladium(0)-Catalyzed Directed Syn-1,2-Carboboration and -Silylation: Alkene Scope, Applications in Dearomatization, and Stereocontrol by a Chiral Auxiliary. *Angew. Chem., Int. Ed.* **2019**, *58*, 17068–17073.

(73) Sun, C.; Yin, G. Integrating Aryl Chlorides into Nickel-Catalyzed 1,1-Difunctionalization of Alkenes. *Chinese Chem. Lett.* **2022**, *33*, 5096–5100.

(74) Logan, K. M.; Sardini, S. R.; White, S. D.; Brown, M. K. Nickel-Catalyzed Stereoselective Arylboration of Unactivated Alkenes. *J. Am. Chem. Soc*. **2018**, *140*, 159–162.

(75) Chen, L. A.; Lear, A. R.; Gao, P.; Brown, M. K. Nickel-Catalyzed Arylboration of Alkenylarenes: Synthesis of Boron-Substituted Quaternary Carbons and Regiodivergent Reactions. *Angew. Chem., Int. Ed.* **2019**, *58*, 10956–10960.

(76) Sardini, S. R.; Lambright, A. L.; Trammel, G. L.; Omer, H. M.; Liu, P.; Brown, M. K. Ni-Catalyzed Arylboration of Unactivated Alkenes: Scope and Mechanistic Studies. *J. Am. Chem. Soc.* **2019**, *141*, 9391–9400.

(77) Smith, K. B.; Logan, K. M.; You, W.; Brown, M. K. Alkene Carboboration Enabled by Synergistic Catalysis. *Chem. Eur. J.* **2014**, *20*, 12032–12036.

(78) Crook, P. F.; Lear, A. R.; Das, S.; Brown, M. K. Cu/Pd-Catalyzed Arylboration of a 1-Silyl-1,3-Cyclohexadiene for Stereocontrolled and Diverse Cyclohexane/Ene Synthesis. *Chem. Sci.* **2023**, *14*, 10467–10470.

(79) Trammel, G. L.; Kannangara, P. B.; Vasko, D.; Datsenko, O.; Mykhailiuk, P.; Brown, M. K. Arylboration of Enecarbamates for the Synthesis of Borylated Saturated N-Heterocycles. *Angew. Chem., Int. Ed.* **2022**, *61*, e202212117.

(80) Simlandy, A. K.; Lyu, M. Y.; Brown, M. K. Catalytic Arylboration of Spirocyclic Cyclobutenes: Rapid Access to Highly Substituted Spiro[3.n]Alkanes. *ACS Catal.* **2021**, *11*, 12815–12820.

(81) Liao, Y.; Yin, X.; Wang, X.; Yu, W.; Fang, D.; Hu, L.; Wang, M.; Liao, J. Enantioselective Synthesis of Multisubstituted Allenes by Cooperative Cu/Pd-Catalyzed 1,4-Arylboration of 1,3-Enynes. *Angew. Chem., Int. Ed.* **2020**, *59*, 1176-1180.

(82) Logan, K. M.; Brown, M. K. Catalytic Enantioselective Arylboration of Alkenylarenes. *Angew. Chem., Int. Ed.* **2017**, *56*, 851–855.

(83) Sardini, S. R.; Brown, M. K. Catalyst Controlled Regiodivergent Arylboration of Dienes. *J. Am. Chem. Soc*. **2017**, *139*, 9823–9826.

(84) Bergmann, A. M.; Dorn, S. K.; Smith, K. B.; Logan, K. M.; Brown, M. K. Catalyst-Controlled 1,2- and 1,1-Arylboration of α-Alkyl Alkenyl Arenes. *Angew. Chem., Int. Ed.* **2019**, *58*, 1719–1723.

(85) Lee, H.; Lee, S.; Yun, J. Pd-Catalyzed Stereospecific Cross-Coupling of Chiral α-Borylalkylcopper Species with Aryl Bromides. *ACS Catal.* **2020**, *10*, 2069–2073.

(86) Dorn, S. K.; Tharp, A. E.; Brown, M. K. Modular Synthesis of a Versatile Double-Allylation Reagent for Complex Diol Synthesis. *Angew. Chem., Int. Ed.* **2021**, *60*, 16027–16034.

(87) Logan, K. M.; Smith, K. B.; Brown, M. K. Copper/Palladium Synergistic Catalysis for the Syn- and Anti-Selective Carboboration of Alkenes. *Angew. Chem.* **2015**, *127*, 5317–5320.

(88) Smith, K. B.; Kevin Brown, M. Regioselective Arylboration of Isoprene and Its Derivatives by Pd/Cu Cooperative Catalysis. *J. Am. Chem. Soc*. **2017**, *139*, 7721–7724.

(89) Chen, B.; Cao, P.; Yin, X.; Liao, Y.; Jiang, L.; Ye, J.; Wang, M.; Liao, J. Modular Synthesis of Enantioenriched 1,1,2-Triarylethanes by an Enantioselective Arylboration and Cross-Coupling Sequence. *ACS Catal*. **2017**, *7*, 2425–2429.

(90) Wang, W.; Ding, C.; Pang, H.; Yin, G. Nickel-Catalyzed 1,2-Arylboration of Vinylarenes. *Org. Lett.* **2019**, *21*, 3968–3971.

(91) Semba, K.; Ohtagaki, Y.; Nakao, Y. 1,2-Arylboration of Aliphatic Alkenes by Cooperative Palladium/Copper Catalysis. *Tetrahedron Lett.* **2021**, *72*, 153059.

(92) Huang, Y.; Brown, M. K. Synthesis of Bisheteroarylalkanes by Heteroarylboration: Development and Application of a Pyridylidene–Copper Complex. *Angew. Chem., Int. Ed.* **2019**, *58*, 6048–6052.

(93) Das, S.; Reilly, M. A.; Dorn, S. K.; Pearson, A. M.; Brown, M. K. Approach Toward Stereoselective α-Arylation by Pd/Cu-Catalyzed Arylboration of Electron Deficient Alkenes. *Angew. Chem., Int. Ed.* **2025**, *ASAP Article*, e202424073.

(94) Harnedy, J.; Maashi, H. A.; El Gehani, A. A. M. A.; Burns, M.; Morrill, L. C. Deconstructive Functionalization of Unstrained Cycloalkanols via Electrochemically Generated Aromatic Radical Cations. *Org. Lett.* **2023**, *25*, 1486–1490.

(95) Mclachlan, A.; Kekre, N.; Mcnulty, J.; Pandey, S. Pancratistatin: A Natural Anti-Cancer Compound That Targets Mitochondria Specifically in Cancer Cells to Induce Apoptosis. *Apoptosis* **2005**, *10*, 619–630.

(96) Dam, J. H.; Madsen, R. Convergent Synthesis of Pancratistatin from Piperonal and Xylose. *Eur. J. Org. Chem.* **2009**, *2009*, 4666–4673.

(97) Akai, S.; Kojima, M.; Yamauchi, S.; Kohji, T.; Nakamura, Y.; Sato, K. A Concise Total Synthesis of (+)-Pancratistatin from *D*-Glucose Featuring the Henry Reaction. *Asian. J. Org. Chem.* **2013**, *2*, 299–302.

(98) Li, M.; Wu, A.; Zhou, P. A Concise Synthesis of (+)-Pancratistatin Using Pinitol as a Chiral Building Block. *Tetrahedron Lett.* **2006**, *47*, 3707–3710.

(99) Potter, T. J.; Ellman, J. A. Total Synthesis of (+)-Pancratistatin by the Rh(III)-Catalyzed Addition of a Densely Functionalized Benzamide to a Sugar-Derived Nitroalkene. *Org. Lett.* **2017**, *19*, 2985–2988.

(100) Kim, S.; Ko, H.; Kim, E.; Kim, D. Stereocontrolled Total Synthesis of Pancratistatin. *Org. Lett*. **2002**, *4*, 1343–1345.

(101) Hernandez, L. W.; Pospech, J.; Klöckner, U.; Bingham, T. W.; Sarlah, D. Synthesis of (+)-Pancratistatins via Catalytic Desymmetrization of Benzene. *J. Am. Chem. Soc*. **2017**, *139*, 15656–15659.

(102) Cagide-Fagín, F.; Nieto-García, O.; Lago-Santomé, H.; Alonso, R. Enantioselective Synthesis of Protected Nitrocyclohexitols with Five Stereocenters. Total Synthesis of (+)-Pancratistatin. *J. Org. Chem.* **2012**, *77*, 11377–11382.

(103) Rigby, J. H.; Maharoof, U. S. M.; Mateo, M. E. Studies on the Narciclasine Alkaloids: Total Synthesis of (+)-Narciclasine and (+)-Pancratistatin. *J. Am. Chem. Soc*. **2000**, *122*, 6624–6628.

(104) Ding, F.; Liang, L.; Yao, J.; Wang, B.; Xu, C.; Liu, D. Total Synthesis of (+)-Pancratistatin and Its Potent Topo I Inhibition Activity Studies. *Org. Lett.* **2022**, *24*, 9458–9462.

(105) Palau-Lluch, G.; Fernández, E. Synthesis of 2-Aryl-1,3-Cyclopentanediones through Catalytic Borylation as a Key Step. *Asian. J. Org. Chem*. **2015**, *4*, 963–968.

(106) Dang, L.; Lin, Z.; Marder, T. B. DFT Studies on the Borylation of α,β-Unsaturated Carbonyl Compounds Catalyzed by Phosphine Copper(I) Boryl Complexes and Observations on the Interconversions between O- and C-Bound Enolates of Cu, B, and Si. *Organometallics* **2008**, *27*, 4443–4454.

(107) Vandavasi, J. K.; Newman, S. G. A High-Throughput Approach to Discovery: Heck-Type Reactivity with Aldehydes. *Synlett* **2018**, *29*, 2081–2086.

(108) Cook, A.; Clément, R.; Newman, S. G. Reaction Screening in Multiwell Plates: High-Throughput Optimization of a Buchwald–Hartwig Amination. *Nat. Protoc*. **2021**, *16*, 1152–1169.

(109) Yuan, Y.; Wu, F. P.; Xu, J. X.; Wu, X. F. Four-Component Borocarbonylation of Vinylarenes Enabled by Cooperative Cu/Pd Catalysis: Access to β-Boryl Ketones and β-Boryl Vinyl Esters. *Angew. Chem., Int. Ed.* **2020**, *59*, 17055–17061.

(110) Jia, T.; Cao, P.; Wang, B.; Lou, Y.; Yin, X.; Wang, M.; Liao, J. A Cu/Pd Cooperative Catalysis for Enantioselective Allylboration of Alkenes. *J. Am. Chem. Soc.* **2015**, *137*, 13760–13763.

(111) Smith, K. B.; Huang, Y.; Brown, M. K. Copper-Catalyzed Heteroarylboration of 1,3-Dienes with 3-Bromopyridines: A Cine Substitution. *Angew. Chem., Int. Ed.* **2018**, *57*, 6146–6149.

(112) Feng, X.; Yun, J. Catalytic Enantioselective Boron Conjugate Addition to Cyclic Carbonyl Compounds: A New Approach to Cyclic β-Hydroxy Carbonyls. *Chem. Commun.* **2009**, *43*, 6577–6579.

(113) Chen, Z.; Isbrandt, E. S.; Newman, S. G. Regioselective Synthesis of α-Vinyl Boronates via a Pd-Catalyzed Mizoroki–Heck Reaction. *Org. Lett*. **2024**, *26*, 7723–7727.

(114) Isbrandt, E. S.; Chapple, D. E.; Tu, N. T. P.; Dimakos, V.; Beardall, A. M. M.; Boyle, P. D.; Rowley, C. N.; Blacquiere, J. M.; Newman, S. G. Controlling Reactivity and Selectivity in the Mizoroki–Heck Reaction: High Throughput Evaluation of 1,5-Diaza-3,7-Diphosphacyclooctane Ligands. *J. Am. Chem. Soc.* **2024**, *146*, 5650–5660.

(115) Isbrandt, E. S.; Nasim, A.; Zhao, K.; Newman, S. G. Catalytic Aldehyde and Alcohol Arylation Reactions Facilitated by a 1,5-Diaza-3,7-Diphosphacyclooctane Ligand. *J. Am. Chem. Soc.* **2021**, *143*, 14646–14656.

(116) Nasim, A.; Thomas, G. T.; Ovens, J. S.; Newman, S. G. Reductive 1,2-Arylation of Isatins. *Org. Lett.* **2022**, *24*, 7232–7236.

(117) Ariafard, A.; Lin, Z. Understanding the Relative Easiness of Oxidative Addition of Aryl and Alkyl Halides to Palladium(0). *Organometallics* **2006**, *25*, 4030–4033.

(118) MacQueen, P. M.; Holley, R.; Ghorai, S.; Colacot, T. J. Convenient One-Pot Synthesis of $L_2Pd(0)$ Complexes for Cross-Coupling Catalysis. *Organometallics* **2023**, *42*, 2644–2650.

(119) Deangelis, A. J.; Gildner, P. G.; Chow, R.; Colacot, T. J. Generating Active L-Pd(0) via Neutral or Cationic π-Allylpalladium Complexes Featuring

Biaryl/Bipyrazolylphosphines: Synthetic, Mechanistic, and Structure-Activity Studies in Challenging Cross-Coupling Reactions. *J. Org. Chem.* **2015**, *80*, 6794–6813.

(120) Seechurn, C. C. C. J.; Parisel, S. L.; Colacot, T. J. Air-Stable Pd(R-Allyl)LCl (L= Q-Phos, P(*t*-Bu)$_3$, Etc.) Systems for C-C/N Couplings: Insight into the Structure - Activity Relationship and Catalyst Activation Pathway. *J. Org. Chem.* **2011**, *76*, 7918–7932.

(121) Shen, X.; Hyde, A. M.; Buchwald, S. L. Palladium-Catalyzed Conversion of Aryl and Vinyl Triflates to Bromides and Chlorides. *J. Am. Chem. Soc.* **2010**, *132*, 14076–14078.

(122) Huang, L.; Ackerman, L. K. G.; Kang, K.; Parsons, A. M.; Weix, D. J. LiCl-Accelerated Multimetallic Cross-Coupling of Aryl Chlorides with Aryl Triflates. *J. Am. Chem. Soc.* **2019**, *141*, 10978–10983.

(123) Reid, W. B.; Spillane, J. J.; Krause, S. B.; Watson, D. A. Direct Synthesis of Alkenyl Boronic Esters from Unfunctionalized Alkenes: A Boryl-Heck Reaction. *J. Am. Chem. Soc.* **2016**, *138*, 5539–5542.

(124) Becica, J.; Glaze, O. D.; Hruszkewycz, D. P.; Dobereiner, G. E.; Leitch, D. C. The Influence of Additives on Orthogonal Reaction Pathways in the Mizoroki–Heck Arylation of Vinyl Ethers. *React. Chem. Eng*. **2021**, *6*, 1212–1219.

(125) Dang, L.; Zhao, H.; Lin, Z.; Marder, T. B. Understanding the Higher Reactivity of B_2cat_2 versus B_2pin_2 in Copper(I)-Catalyzed Alkene Diboration Reactions. *Organometallics* **2008**, *27*, 1178–1186.

(126) Corey, E. J.; Gross, A. W. Highly Selective, Kinetically Controlled Enolate Formation Using Lithium Dialkylamides in the Presence of Trimethylchlorosilane. *Tetrahedron Lett*. **1984**, *25*, 495–498.

(127) Yoshifuji, M.; Shima, I.; Inamoto, N. A Very Crowded Molecule: Formation of Bis(2,4,6-Tri-*t*-Butylphenyl)Phosphinic Chloride. *Tetrahedron Lett*. **1979**, *20*, 3963–3964.

(128) Yoshifiji, M.; Nakamura, T.; Inamoto, N. 2,4,6-Tri-*t*-Butylphenyllithium as a Base - Kinetic Deprotonation of Benzyl Methyl Ketone. *Tetrahedron Lett*. **1987**, *28*, 6325–6328.

(129) Nicolaou, K. C.; Montagnon, T.; Baran, P. S.; Zhong, Y.-L. Iodine(V) Reagents in Organic Synthesis. Part 4. *o*-Iodoxybenzoic Acid as a Chemospecific Tool for Single Electron Transfer-Based Oxidation Processes. *J. Am. Chem. Soc*. **2002**, *124*, 2245–2258.

(130) Diao, T.; Stahl, S. S. Synthesis of Cyclic Enones via Direct Palladium-Catalyzed Aerobic Dehydrogenation of Ketones. *J. Am. Chem. Soc*. **2011**, *133*, 14566–14569.

(131) Chen, M.; Dong, G. Platinum-Catalyzed α,β-Desaturation of Cyclic Ketones through Direct Metal–Enolate Formation. *Angew. Chem., Int. Ed.* **2021**, *60*, 7956–7961.

(132) Germain, N.; Alexakis, A. Formation of Contiguous Quaternary and Tertiary Stereocenters by Sequential Asymmetric Conjugate Addition of Grignard Reagents to 2-Substituted Enones and Mg-Enolate Trapping. *Chem. Eur. J.* **2015**, *21*, 8597–8606.

(133) Chen, I. H.; Yin, L.; Itano, W.; Kanai, M.; Shibasaki, M. Catalytic Asymmetric Synthesis of Chiral Tertiary Organoboronic Esters through Conjugate Boration of β-Substituted Cyclic Enones. *J. Am. Chem. Soc*. **2009**, *131*, 11664–11665.

(134) Obrien, J. M.; Lee, K. S.; Hoveyda, A. H. Enantioselective Synthesis of Boron-Substituted Quaternary Carbons by NHC-Cu-Catalyzed Boronate Conjugate Additions to Unsaturated Carboxylic Esters, Ketones, or Thioesters. *J. Am. Chem. Soc.* **2010**, *132*, 10630–10633.

(135) Yoshida, K.; Ogasawara, M.; Hayashi, T. Generation of Chiral Boron Enolates by Rhodium-Catalyzed Asymmetric 1,4-Addition of 9-Aryl-9-Borabicyclo[3.3.1]Nonanes (B-Ar-9BBN) to α,β-Unsaturated Ketones. *J. Org. Chem.* **2003**, *68*, 1901–1905.

(136) Busacca, C. A.; Lorenz, J. C.; Grinberg, N.; Haddad, N.; Lee, H.; Li, Z.; Liang, M.; Reeves, D.; Saha, A.; Varsolona, R.; Senanayake, C. H. Asymmetric Hydrogenation of Unsaturated Ureas with the BIPI Ligands. *Org. Lett*. **2008**, *10*, 341–344.

(137) Park, J. K.; Lackey, H. H.; Rexford, M. D.; Kovnir, K.; Shatruk, M.; McQuade, D. T. A Chiral 6-Membered N-Heterocyclic Carbene Copper(I) Complex That Induces High Stereoselectivity. *Org. Lett*. **2010**, *12*, 5008–5011.

(138) Schiffner, J. A.; Müther, K.; Oestreich, M. Enantioselective Conjugate Borylation. *Angew. Chem., Int. Ed.* **2010**, *49*, 1194–1196.

(139) Calow, A. D. J.; Solé, C.; Whiting, A.; Fernández, E. Base-Free β-Boration of α,β-Unsaturated Imines Catalysed by Cu_2O with Concurrent Enhancement of Asymmetric Induction. *ChemCatChem* **2013**, *5*, 2233–2239.

(140) Wang, Y.; Gu, M. The Concept of Spectral Accuracy for MS. *Anal. Chem*. **2010**, *82*, 7055–7062.

(141) Chen, Z.; Isbrandt, E. S.; Newman, S. G. Regioselective Synthesis of α-Vinyl Boronates via a Pd-Catalyzed Mizoroki–Heck Reaction. *Org. Lett.* **2024**, *26*, 7723–7727.

(142) Goossen, L. J.; Rodríguez, N.; Linder, C. Decarboxylative Biaryl Synthesis from Aromatic Carboxylates and Aryl Triflates. *J. Am. Chem. Soc*. **2008**, *130*, 15248–15249.

(143) Santoro, O.; Collado, A.; Slawin, A. M. Z.; Nolan, S. P.; Cazin, C. S. J. A General Synthetic Route to [Cu(X)(NHC)] (NHC = N-Heterocyclic Carbene, X = Cl, Br, I) Complexes. *Chem. Commun.* **2013**, *49*, 10483–10485.

(144) Bruno, N. C.; Tudge, M. T.; Buchwald, S. L. Design and Preparation of New Palladium Precatalysts for C–C and C–N Cross-Coupling Reactions. *Chem. Sci.* **2013**, *4*, 916–920.

(145) Tao, X.; Ma, G.; Song, Y.; Chen, Y.; Qian, Q.; Sun, D.; Gong, H. Alkenylation and Arylation of Peptides via Ni-Catalyzed Reductive Coupling of α-C-Tosyl Peptides with Csp^2 Triflates/Halides. *Org. Lett*. **2021**, *23*, 7418–7422.

(146) Johnson, H. W. B.; Lowe, E.; Anderl, J. L.; Fan, A.; Muchamuel, T.; Bowers, S.; Moebius, D. C.; Kirk, C.; McMinn, D. L. Required Immunoproteasome Subunit Inhibition Profile for Anti-Inflammatory Efficacy and Clinical Candidate KZR-616 ((2S,3R)-N-((S)-3-(Cyclopent-1-En-1-Yl)-1-((R)-2-Methyloxiran-2-Yl)-1-Oxopropan-2-Yl)-3-Hydroxy-3-(4-Methoxyphenyl)-2-((S)-2-(2-Morpholinoacetamido)Propanamido)Propenamide). *J. Med. Chem.* **2018**, *61*, 11127–11143.

(147) Caroff, E.; Meyer, E. A.; Äänismaa, P.; Froidevaux, S.; Keller, M.; Piali, L. Design, Synthesis, and Pharmacological Evaluation of Benzimidazolo-Thiazoles as Potent CXCR3 Antagonists with Therapeutic Potential in Autoimmune Diseases: Discovery of ACT-672125. *J. Med. Chem*. **2022**, *65*, 11533–11549.

(148) Watson, I. D. G.; Yudin, A. K. New Insights into the Mechanism of Palladium-Catalyzed Allylic Amination. *J. Am. Chem. Soc*. **2005**, *127*, 17516–17529.